

**PTN Cooling Canal System**  
**Electromagnetic Conductance Geophysical Survey**

**FINAL REPORT**



**Florida Power and Light (FPL) Turkey Point Power Plant**

**9700 SW 433th Street**

**Homestead, FL 33035**



Prepared by:


**Enercon Services, Inc.**

12906 Tampa Oaks Blvd., Ste. 131

Temple Terrace, FL 33637



		<b>PROJECT REPORT COVER SHEET</b>	
<b>Title:</b>	<b>REPORT NO.:</b> NEE270-REPT-001		
	<b>REVISION:</b> 0		
	<b>Client:</b> NextEra Energy		
	<b>Project Identifier:</b> NEETPX130		
<b>Item</b>	<b>Cover Sheet Items</b>	<b>Yes</b>	<b>No</b>
1	Does this Project Report contain any open assumptions, including preliminary information that require confirmation? (If <b>YES</b> , identify the assumptions.)	<input type="checkbox"/>	<input checked="" type="checkbox"/>
2	Does this Project Report supersede an existing Project Report? (If <b>YES</b> , identify the superseded Project Report.)  <b>Superseded Project Report No.</b> _____	<input type="checkbox"/>	<input checked="" type="checkbox"/>
<b>Scope of Revision:</b> Initial Issue			
<b>Revision Impact on Results:</b>			
Safety-Related <sup>1</sup> <input type="checkbox"/>		Non-Safety-Related <input checked="" type="checkbox"/>	
<i>(Enter Name and Sign)</i>			
<b>Originator:</b> Craig Oural			
<b>Design Verifier <sup>1</sup> (Reviewer for Non-Safety-Related):</b>	Mark Stewart		
<b>Approver:</b> Rick Cowles			
			<b>Date:</b> May 13, 2016

 <i>Excellence—Every project. Every day.</i>		<b>PROJECT REPORT          REVISION STATUS SHEET</b>			
		<b>REPORT NO.:</b> NEE270-REPT-001			
		<b>REVISION:</b> 0			
<b><u>PROJECT REPORT REVISION STATUS</u></b>					
<u>REVISION</u> 0	<u>DATE</u> 5/13/2016	<u>DESCRIPTION</u> Initial Issue			
<b><u>APPENDIX REVISION STATUS</u></b>					
<u>APPENDIX NO.</u>	<u>NO. OF PAGES</u>	<u>REVISION</u>	<u>APPENDIX NO.</u>	<u>NO. OF PAGES</u>	<u>REVISION</u>
A – Geoview Report	116	0			
B – AGF Report	203	0			

## TABLE OF CONTENTS

1.0 EXECUTIVE SUMMARY .....	1
2.0 BACKGROUND .....	2
2.1 Saltwater Interface.....	2
2.2 Natural Occurrence of Hypersaline Water.....	2
3.0 INTRODUCTION .....	3
3.1 Electrical Properties of Earth Materials .....	3
3.2 Project Approach .....	4
3.3 Ground-Based Geophysics .....	4
3.4 Aerial-Based Geophysics .....	4
4.0 GROUND-BASED GEOPHYSICAL METHODS.....	4
4.1 Frequency Domain Electromagnetic Terrain Conductivity .....	5
4.2 Vertical Electrical Soundings .....	5
4.3 Time Domain Electromagnetic Soundings .....	5
5.0 RESULTS OF GROUND BASED GEOPHYSICAL METHODS.....	6
5.1 FDEM - EM34XL.....	6
5.2 Vertical Electrical Soundings .....	6
5.3 Time Domain Sounding Data .....	6
6.0 AERIAL-BASED GEOPHYSICAL METHODS - Airborne Electromagnetic Soundings (AEM) .....	7
6.1 Time Domain Electromagnetic Soundings .....	7
6.2 SkyTEM System .....	7
6.3 SkyTEM Data Inversion .....	8
6.4 Quality Control of 3D AEM Data Inversion .....	8
6.5 Conversion of AEM Resistivity to Estimated Chlorinity of Ground Water .....	9
6.6 Creation of a 3D Chloride Ion Voxel Grid .....	11
7.0 DISCUSSION OF FINDINGS.....	11
7.1 Extent and Estimated Mass of Hypersaline Ground Water .....	11
7.2 Distribution of Chloride Concentrations .....	11
7.3 Possible Controls on Chloride Distribution .....	12
8.0 SUMMARY .....	13
9.0 REFERENCES .....	14



## TABLES

TABLE 1	EM34 FIELD DATA
TABLE 2	THICKNESS AND DEPTH TO BOTTOM FOR EACH LAYER IN THE INVERTED AEM MODELS
TABLE 3	TABLE 3: INDUCTION LOGS USED TO VERIFY THE AEM MODELS
TABLE 4	WATER QUALITY DATA USED FOR CALIBRATION (SEPTEMBER 2015 LABORATORY MEASUREMENTS)

## FIGURES

FIGURE 1	USGS SW INTERFACE
FIGURE 2	RESISTIVITY AT 5-METER DEPTH FROM FIG 40, FITTERMAN ET AL., 2012
FIGURE 3	RESISTIVITY AT 30-METER DEPTH FROM FIG 43, FITTERMAN ET AL., 2012
FIGURE 4	EM 34 SURVEY LINE LOCATIONS
FIGURE 5	VES AND TEM LOCATIONS
FIGURE 6	AIRBORNE ELECTROMAGNETIC SURVEY AREA OF INTEREST
FIGURE 7	EM 34 APPARENT CONDUCTIVITY PROFILES
FIGURE 8	SCHEMATIC OF AEM SURVEY
FIGURE 9	COMPARISONS OF MONITOR WELL INDUCTION LOGS WITH THE AEM RESISTIVITY MODEL
FIGURE 10	FORMATION WATER RESISTIVITIES VS. AEM RESISTIVITY
FIGURE 11	FORMATION WATER RESISTIVITIES VS. LABORATORY CHLORIDE CONCENTRATIONS
FIGURE 12	AEM-DERIVED CHLORIDE CONCENTRATION VS. LABORATORY-DERIVED CHLORIDE CONCENTRATION
FIGURE 13	DEPTH PROFILES SHOWING AEM CHLORIDE VS LABORATORY CHLORIDE AT MONITORING WELLS
FIGURE 14	3D VIEW OF AEM CHLORIDE CONCENTRATIONS GREATER THAN 19,000 MG/L (VIEW TO THE NORTHEAST)
FIGURE 15	CHLORIDE CONCENTRATION DEPTH-SLICE FROM LAYER 12, 65 TO 75 FEET BELOW LAND SURFACE (19.7 TO 22.9M)
FIGURE 16	CHLORIDE CONCENTRATION DEPTH-SLICE FROM LAYER 11, 55 TO 65 FEET BELOW LAND SURFACE (16.8 TO 19.7M)

---

FIGURE 17      CHLORIDE CONCENTRATION DEPTH-SLICE FROM LAYER 14, 87 TO 100 FEET BELOW LAND SURFACE (26.4 TO 30.3M)

#### APPENDICES

APPENDIX A      FINAL REPORT - GEOPHYSICAL INVESTIGATION, PTN COOLING CANAL SYSTEM SITE, MIAMI-DADE COUNTY, FLORIDA; PREPARED BY GEOVIEW, INC. (2016)

APPENDIX B      REPORT ON ADVANCED PROCESSING AND INVERSION OF AEM SURVEY DATA AND DERIVED CHLORIDE CONCENTRATIONS NEAR THE TURKEY POINT POWER PLANT, SOUTHERN FLORIDA; PREPARED BY AQUA GEO FRAMEWORKS, INC. (2016)

---

## DEFINITIONS

CCS	COOLING CANAL SYSTEM
MG/L	MILLIGRAMS PER LITER
PSU	PRACTICAL SALINITY UNITS; A MEASURE OF SALINITY ESSENTIALLY EQUIVALENT TO PARTS PER THOUSAND
CHLORINITY	THE MEASURE OF THE CHLORIDE CONTENT, BY MASS, OF SEAWATER (IN GRAMS PER KILOGRAM)
RESISTIVITY	THE RESISTANCE (EXPRESSED IN OHM-M) OF A UNIT VOLUME OF A MATERIAL TO THE PASSAGE OF ELECTRICITY. RESISTIVITY IS THE RECIPROCAL OF ELECTRICAL CONDUCTIVITY.
CONDUCTIVITY	THE ELECTRICAL CONDUCTANCE (EXPRESSED IN MILLISIEMENS/M) OF A UNIT VOLUME OF MATERIAL. CONDUCTIVITY IS THE RECIPROCAL OF RESISTIVITY.
HYPERSALINITY	FOR THE PURPOSES OF THIS REPORT, HYPERSALINITY IS DEFINED AS WATER WITH A CHLORIDE ION CONTENT (CHLORINITY) GREATER THAN 19,000 MG/L, OR MEASURED SALINITY GREATER THAN 35 PSU.
AOI	AREA OF INTEREST; THE PROJECT AREA TO THE NORTH AND WEST OF THE CCS

## 1.0 EXECUTIVE SUMMARY

A cooling canal system (CCS) operated by Florida Power and Light (FPL) at the Turkey Point Power Station (PTN) has contained surface water salinities greater than that present in Biscayne Bay and in coastal portions of the Biscayne Aquifer. The hypersaline water can migrate from the CCS into the Biscayne Aquifer due to the density difference between the hypersaline water and ambient saline groundwater in the Biscayne Aquifer. A Biscayne Aquifer monitor well system has been used to date, to estimate the extent of hypersaline groundwater migration beyond the CCS. The spatial distribution of the monitoring wells, both vertically and horizontally, introduces significant uncertainty when interpretations are made as to the extent of the hypersaline groundwater. Additional factors confounding the estimation of the hypersaline distribution include uncertainty in the extent of saltwater intrusion that predates the construction and operation of the CCS, and the natural occurrence of hypersaline groundwater along the coast.

In response to a Consent Agreement with Miami-Dade County, Division of Environmental Resource Management (DERM), FPL has conducted an assessment of the location and orientation of hypersaline groundwater (as defined by chloride concentrations above 19,000 milligrams per liter [mg/L]) within the Biscayne Aquifer to the west and north of the CCS using Continuous Surface Electromagnetic (EM) mapping methods. Enercon Services, Inc. (ENERCON) was retained by FPL to conduct a combination of ground-based and airborne geophysical surveys and provide interpretation of the results. ENERCON selected SkyTEM, Inc. and Aqua Geo Frameworks, Inc. (AGF) to conduct the aerial data acquisition and processing, respectively.

The EM methods employed measure the bulk resistivity of aquifer materials and fluids. Chloride is among the most dominant ions in saline groundwater and provides an excellent target for EM resistivity methods. Consequently, in consistent porous aquifer media saturated with saltwater of relatively high ionic strength, bulk resistivity is proportional to chloride ion concentration. The relationship between geophysically-derived bulk resistivity and chloride ion concentration was established following methods used in previous studies by the US Geological Survey. A three dimensional resistivity model was constructed by AGF using the field geophysical data. The resistivity model was favorably compared to electromagnetic borehole induction logs from the monitor well network, and a correlation with water resistivity and chloride concentrations obtained from monitor well samples was derived. A three dimensional chloride concentration model was then developed based on the measured relationship between bulk resistivity and chloride concentrations. The chloride concentration model defined the extent of the hypersaline groundwater in the study area within the Biscayne Aquifer.

The distribution of hypersaline groundwater as defined by chloride concentrations greater than 19,000 mg/L is limited in extent, extending west and north of the CCS approximately 3,300 to 8,200 feet from the boundary of the CCS. The maximum lateral extent of the hypersaline groundwater is at depths of about 55 to 65 feet below land surface, corresponding to a high porosity zone mapped in test wells near the CCS. At the base of the Biscayne Aquifer, at about 100 feet below land surface, the hypersaline groundwater is not present everywhere along the western boundary of the CCS.

Most of the volume of the plume appears to have chloride ion concentrations of 19,000 to 26,000 ppm. The highest concentrations, up to 40,000 ppm, are found within about 3,300 feet of the western and northern boundaries of the CCS. The estimated mass of the chloride concentrations above 19,000 mg/L is calculated to be 3,042,471,451 kg.

## 2.0 BACKGROUND

The Florida Power and Light (FPL) Turkey Point Power Station (PTN) operates a cooling canal system (CCS) covering approximately 5,900 acres adjacent to Biscayne Bay. Average annual CCS salinities have ranged between 40 and 50 practical salinity units (PSU) over the past twenty years as compared to seawater salinity of approximately 35 PSU that is present in Biscayne Bay and in coastal portions of the Biscayne Aquifer. Among other potential influences, the density difference between the hypersaline water (traditionally considered greater than 35 PSU) and ambient saline groundwater has resulted in a density-driven groundwater flow of hypersaline water into the Biscayne Aquifer beyond the CCS. A monitor well system, consisting of 16 monitoring locations with wells screened into the shallow, intermediate and deep sections of the Biscayne Aquifer, and five historic monitor wells, provides water quality information. Historically, the monitor well system has been the primary source of data utilized to evaluate the distribution of salinity impacts associated with the CCS. Complicating this evaluation is: (1) The monitor wells are widely spaced and the region inland of the CCS is large, primarily consisting of protected and inaccessible wetlands, (2) Interpolative methods and assumptions are necessary to generate a distribution of salinity data between monitoring points and vertically within the aquifer as data are obtained from discrete intervals, and (3) the occurrence of saline groundwater in the area is affected by both natural and anthropogenic processes. Consequently, assessing the spatial distribution of CCS groundwater near the PTN facility has been challenging and open to interpretation.

### 2.1 Saltwater Interface

The location of the freshwater / saltwater interface has been mapped by the US Geological Survey (USGS). Figure 1 presents an illustration from Prinos, et al, (2014) showing the location of the saltwater interface for years 1955, 1995, and 2011. The location of the interface near the project area has changed little over the time period and appears to have been predominantly influenced by the construction and management of canals, and groundwater withdrawals from wellfields located to the north and west. Although the CCS has been considered the sole mechanism for the occurrence of hypersaline groundwater in the area, natural processes, as described below, also have a significant contribution.

### 2.2 Natural Occurrence of Hypersaline Water

Saline water contains conductive ions of sodium and chlorine which provide an excellent target for geophysical electromagnetic (EM) methods. In groundwater, these ions constitute the predominant response for methods measuring either resistivity or conductivity. Lower detected resistivities indicate higher salinities. Fitterman et al. (2012) used helicopter electromagnetic surveys (HEM) to map the distribution of saline groundwater in the Model Land area of southeast Miami-Dade County. The HEM data are presented as resistivity-depth profiles. Comparison of geophysically-determined formation resistivity and salinity concentrations from well samples (Fitterman and Prinos 2011) shows that

formation resistivities of 1 to 2 ohm-m represent geologic units saturated with groundwater close to or at normal seawater chloride concentrations (or chlorinity) of 19,000 milligrams per liter (mg/L). Formation resistivities with values of 1 ohm-m or less represent hypersaline groundwater with chlorinity greater than 19,000 mg/L. The HEM data show (Figure 2) that at a depth of approximately 17 feet (5 m), hypersaline groundwater is present between Card Sound Road and US 1 in a coast-parallel band 4,000 to 6,000 feet wide (indicted by orange to red coloring on Figure 2). Hydrologically, it is very unlikely that the hypersaline groundwater in this coastal band is from the CCS, as there is no mechanism for coast-parallel flow of hypersaline groundwater from the CCS southwest past US 1. This hypersaline water corresponds to a coast-parallel zone of lower vegetative density in the coastal wetlands as viewed from satellite images. It is common in coastal wetlands for evaporation of seawater to form hypersaline groundwater that moves downward into the sediments under a density gradient (Prinos et al. 2014). Salinities in shallow groundwater in coastal wetlands can reach 60-100 PSU (Stringer et al. 2010), and will migrate downward due to the increased density as compared to normal seawater. Close to the coast, evaporation of seawater can create a wide band of hypersaline groundwater. The HEM data of Fitterman et al. (2012) suggest that this band of naturally-created hypersaline groundwater extends to the base of the Biscayne Aquifer between Card Sound Road and southwest past US 1 (Figure 3 – see red coloring along costs south of Card Sound Road).

### 3.0 INTRODUCTION

On October 6, 2015, FPL entered a Consent Agreement with Miami-Dade County, Division of Environmental Resource Management (DERM). The Consent Agreement provides monitoring, assessment and remedial requirements associated with the presence of CCS-derived hypersaline groundwater located outside of the CCS. Among the required activities is assessment of the location and orientation of hypersaline groundwater within the Biscayne Aquifer to the west and north of the CCS using Continuous Surface Electromagnetic (EM) Mapping methods. The Biscayne Aquifer in the area west and north of the CCS is the EM survey Area of Interest (AOI).

Enercon Services, Inc. (ENERCON), is the principal contractor for the geophysical surveys. EM field data were collected and processed from January through April 2016. This report presents the EM geophysical data collected during January and February 2016, describes the field procedures, method calibration, data correlation, and interpretation of the geophysical data.

#### 3.1 Electrical Properties of Earth Materials

Bulk resistivity or conductivity represents the combined electrical properties of the earth materials and the saturating pore fluids. Most common earth materials, including the carbonates of the Biscayne Aquifer, have very high bulk resistivities (low bulk conductivities) when saturated with very fresh groundwater. As pore fluid conductivity increases, bulk resistivity decreases. For water saturated materials, bulk resistivity, or its inverse bulk conductivity, is principally determined by pore fluid conductivity and porosity. Porosity has the greatest effect when the earth materials are saturated with fresh waters. When pore water chloride ion content exceeds approximately 1,000 mg/L, bulk conductivity and fluid conductivity have a nearly 1:1 relationship. This allows the measurement of fluid conductivity from bulk resistivity or conductivity values obtained from geophysical surveys, and the high



electrical conductivity of saline groundwater makes it an excellent target for electrical geophysical methods. However, as a result of lithologic effects, the relationship between bulk electrical properties and fluid conductivity must be calibrated with local water quality data. The USGS has established such a relationship for the Biscayne Aquifer in south Florida (Prinos et al., 2014).

### 3.2 Project Approach

Electrical geophysical methods have been used for decades to map the extent of saline groundwater. Geophysical methods can acquire data over large areas at considerably less cost than obtained from monitor well networks. Ground-based electrical methods can determine the vertical variation in water quality at a point. Multiple soundings can be acquired along profiles to obtain information on lateral variations in water quality. Airborne electrical geophysical methods can determine both lateral and vertical variations in electrical resistivity over large areas in a short period of time, can provide data in areas inaccessible to ground surveys, and provide data on spatial scales of a few tens to a few hundred meters. Airborne methods also can provide information on groundwater quality if calibrated with site specific groundwater quality data. A combination of ground-based and airborne geophysical surveys was selected to assess the location and orientation of hypersaline water in the Biscayne Aquifer west and north of the CCS.

### 3.3 Ground-Based Geophysics

An initial phase of the geophysical assessment of CCS groundwater is acquisition of ground-based EM data. The locations of these data acquisition points is limited to existing accessible roadways and paths, and additionally constrained by field conditions and powerline interference. Figures 4 and 5 show the locations of the ground-based data acquisition points. Ground stations also were established near existing monitor wells to provide data to correlate EM response with water-quality parameters at depth. The ground-based geophysical data provide alternative estimates of the electrical resistivity/conductivity of the Biscayne Aquifer for comparison with the airborne data. The ground-based EM methods and results are described in Sections 4 and 5, respectively.

### 3.4 Aerial-Based Geophysics

The final phase of field geophysical data collection was the aerial based EM survey (AEM). The aerial survey area of interest (AOI) selected for data post-processing is presented in Figure 6. A description of the AEM field acquisition procedure, methodology, method calibration, data correlation, and interpretation of the geophysical data is contained in Section 6. The AEM data provide a three dimensional distribution of bulk resistivity/conductivity. With the support of the ground geophysical data, monitor well induction logs and water-quality data, the bulk resistivity distribution can be correlated with salinity and chloride concentrations.

## 4.0 GROUND-BASED GEOPHYSICAL METHODS

Three ground-based EM methods were used to obtain bulk resistivity/conductivity measurements. Frequency domain electromagnetic methods (FDEM), vertical electric soundings (VES), and time-domain electromagnetic soundings (TEM). These methods are described below.

#### 4.1 Frequency Domain Electromagnetic Terrain Conductivity

Frequency domain electromagnetic methods (FDEM) induce currents in the earth by energizing a small (about 1 m) transmitter coil with an alternating current. The amplitude of the induced currents is measured with a receiver coil. The induced current strength is proportional to the bulk conductivity of the earth materials in the vicinity of the transmitter, with the signal, the induced current strength, increasing as pore fluid conductivity increases. For specific combinations of transmitter frequency and spacing between the transmitter and receiver coils, the voltage output of the receiver coil is linearly proportional to terrain conductivity.

The FDEM instrument used in this survey is the Geonics Ltd EM34XL. The EM34 uses three intercoil spacings of 10, 20, and 40 m (33, 66, and 131 feet). The effective depth of exploration for the EM34 with vertical coils is 0.75 times the intercoil spacing, or 7.5, 15, and 30 m (approximately 25, 50, and 100 feet). The earth materials and fluids above the effective depth of investigation contribute a cumulative 70% of the instrument response measured at the surface (Stewart and Bretnall 1986). Field data for the EM34 at a measurement point consist of a station ID, geodetic station coordinates, and the measured terrain conductivity (milliSiemens/m) at each of the three intercoil spacings. At each intercoil spacing, the measured terrain conductivity is an integrated value over the depth of exploration. The resulting data is presented as profiles of terrain conductivity versus distance along each profile.

#### 4.2 Vertical Electrical Soundings

Vertical electrical soundings (VES) introduce direct currents into the ground through metal electrodes driven into the soil. The voltage gradient is measured between two potential electrodes. The bulk resistivity of the earth beneath the electrode array can be calculated with a simple equation based on Ohm's Law and the electrode array geometry. The depth of exploration of VES is proportional to the spacing between the current electrodes, AB. For the Wenner electrode array used in this survey, the effective exploration depth is about 11% of the current electrode spacing, or  $0.11 \cdot AB$  (Stewart and Bretnall 1986).

At a specific sounding site, VES field data consist of a station ID, geodetic station coordinates, and calculated apparent resistivities in ohm-m at each current electrode spacing. For each sounding, apparent resistivity is plotted against current electrode spacing divided by 3 for the Wenner electrode array ( $AB/3$ ). The apparent resistivity versus electrode spacing data can be inverted into layer solutions, with each layer having a specific thickness and resistivity. Saline pore fluids are distinguished by very low layer resistivities, typically a few ohm-m. Hypersaline pore fluids may create bulk resistivities less than 1 ohm-m.

#### 4.3 Time Domain Electromagnetic Soundings

Time domain electromagnetic soundings (TEM) use the time domain to vary exploration depth, in contrast with frequency domain methods that use variations in frequency to obtain different depths of penetration. In time domain soundings, a small single wire loop is energized with a square wave alternating current. The very rapid termination of the transmitter current and its associated magnetic field creates an electromotive force that induces circular eddy currents parallel to the ground under the transmitter coil. The center of maximum current density of the induced eddy currents moves downward

and outward with time after transmitter pulse termination. A very sensitive receiver coil measures the strength of the induced eddy currents at increasing times after the transmitter pulse, with depth of penetration being proportional to the time since termination of the transmitter pulse. The TEM system used in this survey, the Geonics EM47, uses time gates centered at a few microseconds to a few milliseconds, and transmitter waveform cycles of 20 to 30 Hz. Each TEM sounding represents the averaged response of many transmitter on-off cycles.

TEM field data consist of apparent resistivity versus time since transmitter pulse termination. At each sounding station, field data include station/sounding ID, geodetic station coordinates, and the apparent resistivity for each time gate after transmitter pulse termination. TEM field data can be inverted into layer solutions of 3-5 layers with specific layer thicknesses and resistivities. Using local groundwater quality data, TEM resistivities also can be converted into estimated fluid conductivities. A fluid conductivity conversion for TEM data for south Florida is provided by the USGS in Prinos et al., 2014.

## 5.0 RESULTS OF GROUND BASED GEOPHYSICAL METHODS

### 5.1 FDEM - EM34XL

EM34 terrain conductivity data were collected along approximately 26 miles of roads and trails west and north of the CCS (see Figure 4). Field data were acquired approximately every 500 feet along survey lines. Field data are provided as station ID, geodetic station coordinates, and terrain conductivity readings at intercoil spacings of 10 m (33 ft), 20 m (66 ft), and 40 m (131 ft). EM34 field data are tabulated in Table 1. Terrain conductivity data are plotted as conductivity versus distance along a survey line (Figure 7). A review of the east-west profiles shows the EM34 response to more highly conductive materials present near the CCS with a substantially declining trend toward the west.

### 5.2 Vertical Electrical Soundings

VES were collected at 25 sites along roads and trails and at monitor well sites (Figure 5) by GeoView, Inc. (GeoView) VES field data consists of station/sounding ID, geodetic station coordinates, and apparent resistivity for each current electrode spacing. Interpreted VES geo-electrical profiles were developed by GeoView from the individual VES smooth model sounding curves and are presented in the GeoView report contained in Appendix A. The VES data were analyzed using a specialized software program that produced a smooth model of resistivity versus depth at each sounding location. Resistivity profiles were developed by combining the sounding locations into specific cross-sections. GeoView also utilized specific resistivity ranges to characterize broad salinity descriptors for each profile. Where a VES sounding was co-located with an existing monitor well, the measured well salinity was presented in the applicable profile using the same broad salinity descriptors for comparison. The profiles are included in the GeoView report in Appendix A. Generally, the data indicate hypersalinity in some areas at depth near the CCS, with a significant salinity reduction trend to the west.

### 5.3 Time Domain Sounding Data

The TEM soundings require that a 40 m x 40 m or 20 m by 20 m wire transmitter loop be laid on the ground. TEM soundings were co-located with monitoring well to provide an additional independent correlation between acquired instrument response and measured monitor well water quality. The instrument is sensitive to electromagnetic interference, and powerlines located above many of the wells

restricted TEM soundings to one site within the AOI (Figure 5). The data and results for TEM-2 are contained in the GeoView report contained in Appendix A.

## 6.0 AERIAL-BASED GEOPHYSICAL METHODS - Airborne Electromagnetic Soundings (AEM)

The AEM survey utilized two specialized subcontractors uniquely qualified to perform the survey and process the data. SkyTEM, Inc. (SkyTEM), performed the field data acquisition using helicopter based platform equipped with transmitter and receiver as described in the following sections, and performed quality control checks. The SkyTEM data were delivered directly to Aqua Geo Frameworks, Inc., (AGF) for post-processing. AGF conducted the data processing, interpretations, method calibration, data correlations with monitor well induction logs and water quality, and reporting (see AGF report contained in Appendix B). The following discussion of the AEM surveys and results is a summary and condensation of the full AGF report. All figures and tables in this section are reproduced from the AGF report, with the exception of Figure 12, which was created from data in the AGF report.

### 6.1 Time Domain Electromagnetic Soundings

As described in Section 3.3 above, TEM soundings sample the decline in strength of an induced current in the ground with time to vary exploration depth. The airborne TEM system used (SkyTEM) works in the same manner as the ground-based unit. The airborne TEM system, generates a controlled transmitter current, then samples the strength of the induced currents during time intervals centered at a few microseconds to a few milliseconds after transmitter current shut off. The transmitter waveform cycles 30 ('deep' mode) to 270 times per second ('shallow' mode), with each transmitter waveform cycle creating a TEM sounding. For a helicopter flying at 100 knots, this results in a TEM sounding every few feet along a flightline. This high sounding density allows sounding data to be averaged to reduce sounding to sounding noise without compromising spatial resolution.

### 6.2 SkyTEM System

The SkyTEM airborne time domain system uses a multi-turn wire loop suspended under a helicopter for the transmitter coil Figure 8. The receiver coils and power source are also suspended beneath the helicopter. The transmitter coil is about 50 feet in diameter and is typically flown at about 100 feet above the ground surface. For this survey, the distance between the lines flown by the helicopter was 656 feet (200 m) to 1312 feet (400 m). During data acquisition, the altitude of the transmitter coil is continuously recorded, and a GPS receiver logs the geographic position of each data point. The system acquires a TEM sounding every few feet along a flightline. The raw data output from the SkyTEM system is the voltage in the receiver coil at different times after the transmitter current is switched off. Longer times correspond to greater depths of exploration. The sampled receiver coil voltages are converted to apparent earth resistivity versus the sample time. The apparent resistivities are then used to determine the variation of earth resistivity with depth through a process called inversion. A model of the subsurface consisting of 30 resistivity layers is matched to the apparent resistivity field data. The resistivities of the model layers are varied until the calculated response of the model layers closely

matches the field data. The thickness of the model layers increases with depth. For a given survey, the layer thicknesses are held constant and increase with depth.

### 6.3 SkyTEM Data Inversion

The raw field data acquired along flightlines are filtered and processed to improve data quality and reliability. The data are converted to a uniform transmitter coil height above the ground using the helicopter altimeter data, and a geographic GPS location is determined for each data point. An analysis is made of background electromagnetic noise that originates from sources such as thunderstorms and power lines, and data points that are too noisy are 'blanked' and not included in the data inversion. The data are examined for 'spikes' that occur over pipelines and other conductive objects and the spikes are filtered out or blanked. The data are examined to determine the longest sample time at which background noise overwhelms the data signal, and this time is used to determine an effective depth of investigation (DOI). Below the DOI background noise is too large for reliable inversion of the flightline data. In the case of this survey, the DOI was below the base of the Biscayne aquifer as defined in Fish and Stewart, (1991).

The corrected and filtered data are inverted using a forward modeling approach. At each sounding along a flightline, the theoretical field response of a layered earth model is calculated and compared to the actual field data. The forward model has 30 layers, and the resistivities of the model layers are adjusted until the differences between the calculated (model) response and the observed field response are minimized. The inversion program then moves to the next data point along a flightline. In a 2D inversion, the inversion at each data point along a flightline is influenced by adjacent data points along the flightline, with a spatial averaging constant of approximately 300 feet (100 m) along a flightline. This spatial averaging reduces noise in the inverted data and is particularly helpful for saltwater intrusion studies where lateral changes in resistivity are expected to be smooth and not abrupt. In 3D inversion, termed a Spatially Constrained Inversion (SCI) in the AGF (2016) report (Appendix B), the data inversions are constrained by field data both along a flightline and on adjacent flightlines. Again, this spatial averaging is helpful in saltwater intrusion studies where lateral changes in resistivity are expected to be gradual as a result of lateral variations in the salinity of groundwater.

Table 2 lists the thicknesses of the 30 layers used for the 3D inversions. Layer thicknesses increase with depth as AEM resolution decreases. Layer 1 has a thickness of about three feet, while layer 14, with a bottom depth of 100 feet equivalent to the bottom of the Biscayne Aquifer, has a thickness of 13 feet. The data in this AEM survey were inverted first to 2D resistivity sections, then to 3D resistivity versus depth data. Both 2D and 3D inversions were completed using the Aarhus Workbench software (Christensen, Reid, and Halkjaer 2009). The following discussion of the AEM results refers to the 3D data inversions.

### 6.4 Quality Control of 3D AEM Data Inversion

At PTN, borehole induction logs collected from the Turkey Point groundwater monitor network in 2015 were available for the TPGW series monitor wells. These induction logs were acquired with a single frequency electromagnetic logging tool that measures the bulk resistivity of the earth materials outside the well bore. The induction logs provide a continuous record of EM electrical resistivity versus depth at



each well where the induction log data were obtained. The layer inversions from the AEM data can be compared to the induction log data to insure that the parameters chosen in the AEM inversion software are producing layer resistivities that are in close agreement with the borehole induction logs. Not all wells are on flightlines, but several wells are close to flightlines or within a few hundred feet of a flightline.

The 3D AEM resistivity inversions compare very well with the borehole induction logs, indicating that the 3D inversion has produced estimates of the variation of bulk resistivity versus depth comparable to values obtained in observation wells. AEM resistivity sections were compared to induction logs obtained at wells TPGW-1, TPGW-4, TPGW-5, TPGW-7, TPGW-8, and TPGW-12. The wells used for comparisons between the AEM inversions and borehole induction log data are listed in Table 3 and the direct comparisons are shown graphically in Figure 9.

### 6.5 Conversion of AEM Resistivity to Estimated Chlorinity of Ground Water

Quarterly water quality data from the TPGW monitor wells were used to calibrate an equation for conversion of AEM resistivity to equivalent groundwater chloride ion content (chlorinity). Water quality sample results dated September 2015 collected from the TPGW monitor wells were used for this analysis. Normal seawater has a salinity of about 35 PSU and will have a chlorinity of about 19,000 mg/L. In the October 2015 Consent Agreement, DERM delineates 19,000 ppm chloride to be the boundary between normal salinity seawater or brackish waters and hypersaline groundwater. Chloride concentrations greater than 19,000 mg/L traditionally equate to salinity greater than 35 PSU.

The calibration of the AEM data was conducted using a two-step approach as presented in Fitterman and Prinos (2011) and Fitterman et al. (2012). First, a mathematical relationship is established between AEM resistivity and the resistivity of groundwater samples from discrete depth intervals in the TPGW monitor wells (water resistivity is the inverse of specific conductance). For each of the three sampling depths in a TPGW monitor well, the corresponding AEM resistivity at the same depth as each groundwater sample is obtained from the 3D AEM resistivity inversion (Table 4). The data are plotted on a log-log plot with AEM resistivity on the x-axis and groundwater sample resistivity on the y-axis. A regression equation is fitted to the plot to produce a power function of the form

$$\text{Water Resistivity} = 0.0834 \cdot (\text{AEM Resistivity})^{1.239} \quad (1)$$

with  $R^2 = 0.91$ ,  $p < 0.001$ ,  $r = 0.95$  (Figure 10). The  $p$  value measures the probability that the observed relationship is due to random variation,  $R^2$  is the percent of the variance in the dependent variable (water resistivity) explained by the variance of the independent variable (AEM resistivity), and  $r$  is a measure of the correlation between groundwater resistivity and AEM resistivity with 0.95 indicating a very strong, nearly perfect, correlation. This is an expected relationship as the groundwater samples are from one hydrogeologic unit, the Biscayne Aquifer, and bulk resistivity (AEM resistivity) is determined principally by the resistivity of the pore fluids (groundwater) in aquifers saturated with high salinity water.

The second step in the calibration process is to mathematically relate chloride to water resistivity. As chloride concentration increases, water resistivity decreases. In groundwater influenced by seawater,



the dominant and most conductive ions are chloride and sodium, so it is expected that there will be a statistically strong relationship between water resistivity and chlorides. Again, a log-log plot is constructed with water resistivity of well samples on the x-axis, and chloride ion content of well samples on the y-axis. A regression equation is fitted to the data and has the form

$$\text{Chlorinity} = 1893 \cdot (\text{Water Resistivity})^{-1.386} \quad (2)$$

with  $R^2 = 0.98$ ,  $r > 0.99$ , and  $p < 0.001$  (Figure 11). Equations (1) and (2) are combined to form an equation that defines chlorinity as a function of AEM resistivity. This equation is then used to convert AEM 3D inversion resistivity to chlorinity.

The minimum chloride ion content detected in the September 2015 laboratory samples was 21.6 mg/L, from monitor well TPGW-9S, and the maximum, 36,400 mg/L, was from monitor well TPGW-13S. Consequently, application of the calibrated equation was restricted to AEM-derived chlorinity values between 20 and 40,000 ppm estimated chloride ion content.

If a regression equation is fitted to a log-log plot of AEM derived chlorinity (x-axis) and lab-determined chloride ion content (y-axis) for the September, 2015, groundwater samples (Figure 12), a regression equation produces values of  $R^2 = 0.91$ ,  $r = 0.96$ ,  $p < 0.001$ , and  $F$  is 49.7 for an  $F$ -critical value of 4.00. The  $F$  statistic measures the ratio between the variance accounted for by the regression and the error variance. If  $F$  is  $>$   $F$ -critical, the regression passes the  $F$ -test for statistical significance. The  $p$  value measures the probability that the observed relationship is due to random variation,  $R^2$  is the percent of the variance in the dependent variable explained by the variance of the independent variable, and  $r$  measures the strength of the correlation between AEM determined chlorinity and lab-determined chloride ion content, with an  $r$  of 1.0 being a perfect correlation (1:1).

The correspondence of chlorinity calculated from AEM resistivity and lab-derived values of chloride ion content from TPGW wells can be graphically illustrated by superimposing the TPGW-well derived chloride values on AEM-derived chlorinity versus depth profiles, using the same color-coded contour intervals. The relationship at monitor well TPGW-1 is illustrated in Figure 13, and the relationship at monitor well TPGW-2 also is illustrated in Figure 13. Note that monitor well TPGW-2 is more than 200 m from the flightline where the AEM data were acquired, but that the correspondence of AEM chlorinity and lab-derived chloride ion content is excellent. Similar figures for other TPGW wells are included in the AGF (2016) report in Appendix B.

It should be noted that because the TPGW monitor well data are from the Biscayne Aquifer only, the calibrated equation relating AEM resistivity to groundwater chlorinity is valid only for the Biscayne Aquifer. For this reason, mapping of the AEM derived groundwater chlorinity was restricted to the Biscayne Aquifer, as defined by Fish and Stewart (1991). AEM resistivity values were obtained for hydrostratigraphic units below the base of the Biscayne, but these resistivity values cannot be reliably converted to chlorinity values without depth specific water quality data from those units.

## 6.6 Creation of a 3D Chloride Ion Voxel Grid

A voxel is a three dimensional grid cell, a “volume element”. The AEM derived chlorinity values were interpolated to a uniform voxel grid to allow for more effective graphical visualization of the chloride ion distribution. Each voxel has lateral (x, y) dimensions of 328 x 328 feet (100 x 100 m) and a thickness equivalent a layer in the 3D AEM resistivity inversion (Table 1-4). The voxel grid is restricted to the thickness of the Biscayne Aquifer, derived from Fish and Stewart (1991) and utilizes layers 1 through 14 of the AEM 3D inversion. The bottom of layer 14 is at a depth of about 100 feet below land surface (30.3 m).

An example of a 3D voxel view of the AEM-derived chloride concentrations greater than 19,000 mg/L is presented in Figure 14. The chloride concentration data in Figure 14 are presented down to the base of the Biscayne Aquifer, as determined by Fish and Stewart (1991), and for chloride concentrations greater than 19,000 mg/L. An example of a voxel-derived, chloride concentration depth-slice from layer 12, 65 to 75 feet below land surface (19.7 to 22.9 m), is presented in Figure 15. Depth-slices of chloride ion concentration are presented for layers 1-14 in Appendix B.

## 7.0 DISCUSSION OF FINDINGS

### 7.1 Extent and Estimated Mass of Hypersaline Ground Water

The maximum extent of hypersaline groundwater westward from the CCS is illustrated as a solid volume in Figure 14, and for layer 11, in Figure 16. On average, in layer 11 the hypersaline plume extends 3,300 to 8,200 feet (1,000-2,500 m) west from the west margin of the CCS, and is present along the entire westward margin of the CCS. The maximum westward extent is at a depth of about 55 to 65 feet. The hypersaline plume is wedge shaped, with the tip of the wedge at about 55 to 65 feet below land surface. At both shallower and deeper depths, the plume does not extend as far west. At the base of the Biscayne Aquifer, represented by layer 14 (Figure 17), the plume extends about 3,300 feet westward (1,000 m) from the CCS, and is not present everywhere along the western margin of the CCS.

To the north of the CCS, hypersaline groundwater extends about 7,200 feet (2,200 m) north of the CCS. The maximum lateral extent is in layer 11, at a depth of 55 to 65 feet below land surface.

The volume and mass of the material with chloride concentrations greater than 19,000 mg/L within the AOI was estimated by AGF using assumptions related to the average porosity of the Biscayne Aquifer in the AOI. The procedure, described in Appendix B, uses a calculation of the volume of each model cell, and the estimated mass of chloride in each cell of the AOI greater than 19,000 mg/L. The mass of each cell was then summed. The estimated mass of chloride in those zones with chloride concentrations greater than 19,000 mg/L is approximately 3,042,471,451 kg.

### 7.2 Distribution of Chloride Concentrations

At the westward and northern boundaries of the hypersaline plume (layer 11, Figure 16), the chloride concentrations are between 19,000 mg/L and 23,000 mg/L. The largest volume of the plume has concentrations between about 23,000 and 26,000 mg/L. The highest chloride concentrations, up to 40,000 mg/L, occur generally within 3,300 feet (1,000 m) of the western and northern boundaries of the

CCS. The highest chloride concentrations are not evenly distributed along the margins of the CCS, but are concentrated along shorter sections of the CCS margin close to the western boundary of L-31E.

### 7.3 Possible Controls on Chloride Distribution

The driving force for downward and lateral migration of high chloride groundwater from the CCS is the density difference between saline water in the Biscayne Aquifer and the higher salinity CCS groundwater. Fresh water has a density of 1,000 kilograms per cubic meter ( $\text{kg}/\text{m}^3$ ). Seawater has a salinity equivalent to 35 kg of dissolved solids per  $\text{m}^3$ , so seawater is 1.035 times the density of freshwater, at the same temperature. The average salinity of the CCS is about 60 PSU, or 60 kg of dissolved solids per  $\text{m}^3$ . CCS waters should be about 1.024 times as dense as seawater, the value of the ratio ( $1.060/1.035$ ). The actual density of seawater and the CCS groundwater will vary with temperature, with the actual CCS/seawater ratio somewhat less than 1.024 as the CCS waters are warmer than Biscayne Bay waters. However, Biscayne Bay water has less than normal seawater salinity, about 25 to 30 PSU. The result is that the density difference between higher salinity CCS groundwater and the saline groundwater in the Biscayne Aquifer in the vicinity of the CCS is roughly equivalent to the density difference between fresh water and seawater. It is expected that migration of the hypersaline surface water from the CCS under the imposed density gradient will be similar in rate to natural seawater intrusion driven by the density difference between seawater and fresh water. The principal conditions that have influenced the migration of high salinity CCS water into the underlying aquifer have been operating for years or decades. Recent salinity events or conditions within the CCS have had relatively little effect on the present configuration of the hypersaline plume west and north of the CCS. The current general configuration of the hypersaline plume is the result of the long-term average density difference between the CCS water and the saline groundwater in the Biscayne Aquifer, variations in the degree of communication between the CCS and the aquifer in different parts of the CCS, and vertical and lateral variations in the hydraulic conductivity of the Biscayne Aquifer adjacent to and below the CCS.

For example, along the western boundary of the CCS, the lithologic log for USGS well G-3321 (Fish and Stewart 1991) indicates that the contact between the Ft Thompson Formation and the underlying Tamiami Formation is at about 55 to 60 feet below land surface. This corresponds to a high porosity zone encountered in a test well drilled at the north end of the CCS between the interceptor ditch and L-31E (Biscayne Aquifer Performance Testing, Turkey Point, April 2016). This high porosity zone and the contact between upper Tamiami and Ft Thompson Formations is likely the cause of the maximum lateral extent of the hypersaline plume to be at depths of about 55 to 65 feet below land surface (layer 11, Figure 16). In addition, testing results from two wells (Biscayne Aquifer Performance Testing, Turkey Point, April 2016) drilled several hundred feet apart near the northern boundary of the CCS suggest that significant variations can occur in the hydraulic conductivity of the Upper Tamiami Clastic Unit (Fish and Stewart 1991) near the CCS. Lateral variations in hydraulic conductivity within the Biscayne Aquifer north and west of the CCS, and particularly in the Upper Tamiami unit, may be the reason for the uneven distribution of elevated concentrations of chloride in groundwater near L-31E along the western boundary of the CCS.

The western and northern boundaries between the >19,000 mg/L chloride groundwater and <19,000 mg/L groundwater in the Biscayne Aquifer mapped by the AEM resistivity (Figure 13) are sharp and well defined. This is the expected configuration for the boundary between two groundwater masses with different densities. There is likely some mixing within a narrow transition zone between ambient saline groundwater and the hypersaline waters, but at the scale of Figure 13, this mixing or transition zone is not apparent. In addition, the sharp transition in Figure 13 between groundwater delineated as >19,000 mg/L chloride and less saline groundwater indicates that the AEM method can reliably locate the hypersaline boundary. If the AEM resistivity relationship to chloride ion content was poorly determined or 'noisy', the AEM mapped boundary would be transitional, with many isolated colored voxels west and north of the main boundary. However, this is not the case, indicating that the AEM defined hypersaline boundary of >19,000 mg/L chloride groundwater is mapping an actual physical boundary.

## 8.0 SUMMARY

1. The AEM methodology and data used to map the extent of >19,000 mg/L chloride groundwater in the Biscayne Aquifer near the CCS provide valid, defensible and statistically significant results.
2. The AEM resistivity and chloride ion concentration data correlate very well with geologic data, ground-based geophysics, and laboratory water-quality data from the monitoring well system.
3. The location of the hypersaline groundwater in the Biscayne Aquifer near the CCS is well defined by the geophysical methodologies employed.
4. The geophysically-mapped boundary between groundwater having greater than 19,000 mg/L chloride and that having less than 19,000 mg/L chloride is sharp and well defined.
5. The hypersaline plume extends west and north of the CCS approximately 3,300 to 8,200 feet from the boundary of the CCS.
6. The maximum lateral extent of the hypersaline plume is at depths of about 55 to 65 feet below land surface, corresponding to a high porosity zone mapped in test wells near the CCS.
7. At the base of the Biscayne Aquifer, at about 100 feet below land surface, the hypersaline plume does not extend as far from the CCS as it does in the layer between 55 to 65 feet, and is not present everywhere along the L-31E canal west of the CCS.
8. Most of the volume of the plume appears to have chloride ion concentrations of 19,000 to 26,000 ppm. The highest concentrations, up to 40,000 ppm, are found within about 3,300 feet of the western and northern boundaries of the CCS.

## 9.0 REFERENCES

- Christensen, N. B., Reid, J. E., and Halkjaer, M., 2009, Fast, laterally smooth inversion of airborne time-domain electromagnetic data. *Near Surface Geophysics*, 7, p. 599-612
- Fish, J. E., and M. Stewart, 1991. Hydrogeology, aquifer characteristics, and ground-water flow of the surficial aquifer system, Dade County, Florida. U.S. Geological Survey, Water Resources Inv. 91-4000.
- Fitterman, David V.; Prinos, Scott T., 2011. Results of time-domain electromagnetic soundings in Miami-Dade and southern Broward Counties, Florida. U.S. Geological Society Open-File Report 2011-1299, ix, 42 p.
- Fitterman, David V.; Deszcz-Pan, Maria; Prinos, Scott T., 2012. Helicopter Electromagnetic Survey of the Model Land Area, Southeastern Miami-Dade County, Florida. U.S. Geological Society Open-File Report 2012-1176, 77 p.
- Prinos, Scott T.; Wacker, Michael A.; Cunningham, Kevin J.; Fitterman, David V., 2014. Origins and delineation of saltwater intrusion in the Biscayne aquifer and changes in the distribution of saltwater in Miami-Dade County, Florida. U.S. Geological Survey Scientific Investigations Report 2014-5025, Report: xi, 101 p.
- Prinos, S., Wacker, M., Cunningham, K., and D. Fitterman, 2014. Origins and Delineation of Saltwater Intrusion in the Biscayne Aquifer and Changes in the Distribution of Saltwater in Miami-Dade County, Florida. U.S. Geological Survey Scientific Investigations Report 2014-5025, 101 p.
- Stewart, M., and R. Bretnall, 1986. Interpretation of VLF resistivity data for ground water contamination studies: *Ground Water Monitoring Review*, v. 6, no. 1, p. 71-75.
- Stringer, Christina E; Rains, Mark C; Kruse, Sarah; and Dennis Whigham, 2010. Controls on Water Levels and Salinity in a Barrier Island Mangrove, Indian River Lagoon, Florida. *Wetlands Journal* No. 30, p. 725-734



TABLES



Table 1: M34 FIELD DATA

Date	Line Designation	Station #	Distance Along Profile (ft)	GPS Location		Direction of Survey	Coil Spacing (Meters)	Terrain Conductivity (mS/m)
				N	W			
1/19/2016	LN-1	1	0	25.44844	80.35009	W	10	61.4
1/19/2016	LN-1	1	0	25.44844	80.35009	W	20	104.0
1/19/2016	LN-1	1	0	25.44844	80.35009	W	40	111.0
1/19/2016	LN-1	2	500	25.44843	80.35159	W	10	58.0
1/19/2016	LN-1	2	500	25.44843	80.35159	W	20	99.9
1/19/2016	LN-1	2	500	25.44843	80.35159	W	40	173.0
1/19/2016	LN-1	3	1000	25.4484	80.3531	W	10	64.3
1/19/2016	LN-1	3	1000	25.4484	80.3531	W	20	91.4
1/19/2016	LN-1	3	1000	25.4484	80.3531	W	40	161.0
1/19/2016	LN-1	4	1500	25.44842	80.35462	W	10	46.2
1/19/2016	LN-1	4	1500	25.44842	80.35462	W	20	83.8
1/19/2016	LN-1	4	1500	25.44842	80.35462	W	40	150.0
1/19/2016	LN-1	5	2000	25.44841	80.35616	W	10	48.1
1/19/2016	LN-1	5	2000	25.44841	80.35616	W	20	91.6
1/19/2016	LN-1	5	2000	25.44841	80.35616	W	40	149.0
1/19/2016	LN-1	6	2500	25.4484	80.35768	W	10	43.8
1/19/2016	LN-1	6	2500	25.4484	80.35768	W	20	82.9
1/19/2016	LN-1	6	2500	25.4484	80.35768	W	40	156.0
1/19/2016	LN-1	7	3000	25.44839	80.35919	W	10	48.3
1/19/2016	LN-1	7	3000	25.44839	80.35919	W	20	84.2
1/19/2016	LN-1	7	3000	25.44839	80.35919	W	40	148.0
1/19/2016	LN-1	8	3500	25.4484	80.36071	W	10	51.0
1/19/2016	LN-1	8	3500	25.4484	80.36071	W	20	85.1
1/19/2016	LN-1	8	3500	25.4484	80.36071	W	40	145.0
1/19/2016	LN-1	9	4000	25.44838	80.36224	W	10	50.5
1/19/2016	LN-1	9	4000	25.44838	80.36224	W	20	86.4
1/19/2016	LN-1	9	4000	25.44838	80.36224	W	40	153.0
1/19/2016	LN-1	10	4500	25.44838	80.36375	W	10	42.5
1/19/2016	LN-1	10	4500	25.44838	80.36375	W	20	73.8
1/19/2016	LN-1	10	4500	25.44838	80.36375	W	40	128.0
1/19/2016	LN-1	11	5000	25.44835	80.36525	W	10	30.1
1/19/2016	LN-1	11	5000	25.44835	80.36525	W	20	54.2
1/19/2016	LN-1	11	5000	25.44835	80.36525	W	40	110.0
1/19/2016	LN-1	12	5500	25.44835	80.36678	W	10	31.3
1/19/2016	LN-1	12	5500	25.44835	80.36678	W	20	61.1
1/19/2016	LN-1	12	5500	25.44835	80.36678	W	40	125.0
1/19/2016	LN-1	13	6000	25.44836	80.36827	W	10	35.2
1/19/2016	LN-1	13	6000	25.44836	80.36827	W	20	62.0
1/19/2016	LN-1	13	6000	25.44836	80.36827	W	40	117.0
1/19/2016	LN-1	14	6500	25.44838	80.36979	W	10	36.0
1/19/2016	LN-1	14	6500	25.44838	80.36979	W	20	65.6
1/19/2016	LN-1	14	6500	25.44838	80.36979	W	40	116.0
1/19/2016	LN-1	15	7000	25.44838	80.3713	W	10	36.6
1/19/2016	LN-1	15	7000	25.44838	80.3713	W	20	68.9
1/19/2016	LN-1	15	7000	25.44838	80.3713	W	40	123.0
1/19/2016	LN-1	16	7500	25.44836	80.37283	W	10	31.0
1/19/2016	LN-1	16	7500	25.44836	80.37283	W	20	61.2
1/19/2016	LN-1	16	7500	25.44836	80.37283	W	40	110.0
1/20/2016	LN-1	17	8000	25.44835	80.37437	W	10	33.0
1/20/2016	LN-1	17	8000	25.44835	80.37437	W	20	62.6
1/20/2016	LN-1	17	8000	25.44835	80.37437	W	40	100.0
1/20/2016	LN-1	18	8500	25.44834	80.37589	W	10	34.7

Table 1 - ELD DATA (Continued)

Date	Line Designation	Station #	Distance Along Profile (ft)	GPS Location		Direction of Survey	Coil Spacing (Meters)	Terrain Conductivity (mS/m)
				N	W			
1/20/2016	LN-1	18	8500	25.44834	80.37589	W	20	61.8
1/20/2016	LN-1	18	8500	25.44834	80.37589	W	40	98.0
1/20/2016	LN-1	19	9000	25.44835	80.37737	W	10	31.9
1/20/2016	LN-1	19	9000	25.44835	80.37737	W	20	57.8
1/20/2016	LN-1	19	9000	25.44835	80.37737	W	40	99.0
1/20/2016	LN-1	20	9500	25.44832	80.37889	W	10	31.4
1/20/2016	LN-1	20	9500	25.44832	80.37889	W	20	55.9
1/20/2016	LN-1	20	9500	25.44832	80.37889	W	40	85.0
1/20/2016	LN-1	20	9500	25.44832	80.37889	W	10	18.1
1/20/2016	LN-1	20	9500	25.44832	80.37889	W	20	38.8
1/20/2016	LN-1	20	9500	25.44832	80.37889	W	40	73.0
1/20/2016	LN-1	22	9750	25.44831	80.3796	W	10	31.0
1/20/2016	LN-1	22	9750	25.44831	80.3796	W	20	46.1
1/20/2016	LN-1	22	9750	25.44831	80.3796	W	40	74.0
1/20/2016	LN-1	23	10500	25.4483	80.38186	W	10	17.8
1/20/2016	LN-1	23	10500	25.4483	80.38186	W	20	37.0
1/20/2016	LN-1	23	10500	25.4483	80.38186	W	40	66.0
1/20/2016	LN-1	24	11000	25.44835	80.38334	W	10	18.6
1/20/2016	LN-1	24	11000	25.44835	80.38334	W	20	37.4
1/20/2016	LN-1	24	11000	25.44835	80.38334	W	40	60.0
1/20/2016	LN-1	25	11500	25.44831	80.38486	W	10	18.9
1/20/2016	LN-1	25	11500	25.44831	80.38486	W	20	36.3
1/20/2016	LN-1	25	11500	25.44831	80.38486	W	40	62.0
1/20/2016	LN-1	26	12000	25.44827	80.38634	W	10	17.6
1/20/2016	LN-1	26	12000	25.44827	80.38634	W	20	34.7
1/20/2016	LN-1	26	12000	25.44827	80.38634	W	40	61.0
1/20/2016	LN-1	27	12500	25.44825	80.38788	W	10	18.8
1/20/2016	LN-1	27	12500	25.44825	80.38788	W	20	33.9
1/20/2016	LN-1	27	12500	25.44825	80.38788	W	40	53.0
1/20/2016	LN-1	28	13000	25.44825	80.38937	W	10	17.3
1/20/2016	LN-1	28	13000	25.44825	80.38937	W	20	31.5
1/20/2016	LN-1	28	13000	25.44825	80.38937	W	40	55.0
1/20/2016	LN-1	29	13500	25.44828	80.39087	W	10	15.9
1/20/2016	LN-1	29	13500	25.44828	80.39087	W	20	28.9
1/20/2016	LN-1	29	13500	25.44828	80.39087	W	40	49.0
1/20/2016	LN-1	30	14000	25.44826	80.39237	W	10	15.3
1/20/2016	LN-1	30	14000	25.44826	80.39237	W	20	27.6
1/20/2016	LN-1	30	14000	25.44826	80.39237	W	40	48.0
1/20/2016	LN-1	31	14500	25.44828	80.39389	W	10	15.5
1/20/2016	LN-1	31	14500	25.44828	80.39389	W	20	25.7
1/20/2016	LN-1	31	14500	25.44828	80.39389	W	40	47.0
1/20/2016	LN-1	32	15000	25.44825	80.39534	W	10	19.3
1/20/2016	LN-1	32	15000	25.44825	80.39534	W	20	27.4
1/20/2016	LN-1	32	15000	25.44825	80.39534	W	40	49.0
1/20/2016	LN-1	33	15500	25.44824	80.39685	W	10	15.3
1/20/2016	LN-1	33	15500	25.44824	80.39685	W	20	26.5
1/20/2016	LN-1	33	15500	25.44824	80.39685	W	40	50.0
1/20/2016	LN-1	34	16000	25.44823	80.39836	W	10	14.3
1/20/2016	LN-1	34	16000	25.44823	80.39836	W	20	27.2
1/20/2016	LN-1	34	16000	25.44823	80.39836	W	40	54.0
1/20/2016	LN-1	35	16500	25.44823	80.39984	W	10	12.5
1/20/2016	LN-1	35	16500	25.44823	80.39984	W	20	25.2

Table 25 - FIELD DATA (Continued)

Date	Line Designation	Station #	Distance Along Profile (ft)	GPS Location		Direction of Survey	Coil Spacing (Meters)	Terrain Conductivity (mS/m)
				N	W			
1/20/2016	LN-1	35	16500	25.44823	80.39984	W	40	55.6
1/20/2016	LN-1	36	17000	25.44824	80.40135	W	10	12.5
1/20/2016	LN-1	36	17000	25.44824	80.40135	W	20	25.1
1/20/2016	LN-1	36	17000	25.44824	80.40135	W	40	52.0
1/20/2016	LN-1	37	17500	25.44822	80.40284	W	10	12.0
1/20/2016	LN-1	37	17500	25.44822	80.40284	W	20	23.1
1/20/2016	LN-1	37	17500	25.44822	80.40284	W	40	50.0
1/20/2016	LN-7	38	0	25.4488	80.34934	NE	10	56.5
1/20/2016	LN-7	38	0	25.4488	80.34934	NE	20	103.5
1/20/2016	LN-7	38	0	25.4488	80.34934	NE	40	164.0
1/20/2016	LN-7	39	500	25.44977	80.34825	NE	10	97.4
1/20/2016	LN-7	39	500	25.44977	80.34825	NE	20	121.0
1/20/2016	LN-7	39	500	25.44977	80.34825	NE	40	178.0
1/20/2016	LN-7	40	1000	25.45097	80.34776	N	10	65.5
1/20/2016	LN-7	40	1000	25.45097	80.34776	N	20	108.5
1/20/2016	LN-7	40	1000	25.45097	80.34776	N	40	171.0
1/20/2016	LN-7	41	1500	25.45232	80.34778	N	10	78.8
1/20/2016	LN-7	41	1500	25.45232	80.34778	N	20	127.2
1/20/2016	LN-7	41	1500	25.45232	80.34778	N	40	195.0
1/20/2016	LN-7	42	2000	25.45368	80.34776	N	10	99.7
1/20/2016	LN-7	42	2000	25.45368	80.34776	N	20	126.1
1/20/2016	LN-7	42	2000	25.45368	80.34776	N	40	181.0
1/20/2016	LN-7	43	2500	25.45506	80.34776	N	10	81.2
1/20/2016	LN-7	43	2500	25.45506	80.34776	N	20	118.5
1/20/2016	LN-7	43	2500	25.45506	80.34776	N	40	163.0
1/20/2016	LN-7	44	3000	25.45644	80.34779	N	10	108.0
1/20/2016	LN-7	44	3000	25.45644	80.34779	N	20	125.6
1/20/2016	LN-7	44	3000	25.45644	80.34779	N	40	168.0
1/20/2016	LN-7	45	3500	25.45782	80.34779	N	10	102.8
1/20/2016	LN-7	45	3500	25.45782	80.34779	N	20	117.7
1/20/2016	LN-7	45	3500	25.45782	80.34779	N	40	168.0
1/20/2016	LN-7	46	4000	25.45781	80.34781	N	10	102.2
1/20/2016	LN-7	46	4000	25.45781	80.34781	N	20	117.7
1/20/2016	LN-7	46	4000	25.45781	80.34781	N	40	167.0
1/20/2016	LN-7	47	4500	25.46056	80.34782	N	10	96.9
1/20/2016	LN-7	47	4500	25.46056	80.34782	N	20	121.4
1/20/2016	LN-7	47	4500	25.46056	80.34782	N	40	173.0
1/20/2016	LN-7	48	5000	25.46173	80.34718	N	10	69.9*
1/20/2016	LN-7	48	5000	25.46173	80.34718	N	20	130*
1/20/2016	LN-7	48	5000	25.46173	80.34718	N	40	-1*
1/20/2016	LN-7	49	5425	25.46274	80.34658	N	10	85.0
1/20/2016	LN-7	49	5425	25.46274	80.34658	N	20	NA
1/20/2016	LN-7	49	5425	25.46274	80.34658	N	40	NA
1/21/2016	LN-7	70	10000	25.35576	80.38586	NE	10	52.4
1/21/2016	LN-7	70	10000	25.35576	80.38586	NE	20	111.8
1/21/2016	LN-7	70	10000	25.35576	80.38586	NE	40	172.0
1/21/2016	LN-7	71	10500	25.35647	80.38455	NE	10	57.1
1/21/2016	LN-7	71	10500	25.35647	80.38455	NE	20	106.5
1/21/2016	LN-7	71	10500	25.35647	80.38455	NE	40	189.0
1/21/2016	LN-7	72	11000	25.35716	80.38324	NE	10	60.1
1/21/2016	LN-7	72	11000	25.35716	80.38324	NE	20	113.0
1/21/2016	LN-7	72	11000	25.35716	80.38324	NE	40	189.0

\* - Indicates potential interference from powerlines

Table 1 - EMLD DATA (Continued)

Date	Line Designation	Station #	Distance Along Profile (ft)	GPS Location		Direction of Survey	Coil Spacing (Meters)	Terrain Conductivity (mS/m)
				N	W			
1/21/2016	LN-7	73	11500	25.35785	80.38196	NE	10	55.3
1/21/2016	LN-7	73	11500	25.35785	80.38196	NE	20	107.3
1/21/2016	LN-7	73	11500	25.35785	80.38196	NE	40	179.0
1/21/2016	LN-7	74	12000	25.35856	80.38062	NE	10	54.3
1/21/2016	LN-7	74	12000	25.35856	80.38062	NE	20	111.6
1/21/2016	LN-7	74	12000	25.35856	80.38062	NE	40	180.0
1/21/2016	LN-7	75	12500	25.35927	80.37936	NE	10	53.3
1/21/2016	LN-7	75	12500	25.35927	80.37936	NE	20	99.4
1/21/2016	LN-7	75	12500	25.35927	80.37936	NE	40	157.0
1/21/2016	LN-7	76	13000	25.36056	80.37885	N-NE	10	53.7
1/21/2016	LN-7	76	13000	25.36056	80.37885	N-NE	20	122.4
1/21/2016	LN-7	76	13000	25.36056	80.37885	N-NE	40	201.0
1/21/2016	LN-7	77	13500	25.36184	80.37838	N-NE	10	52.5
1/21/2016	LN-7	77	13500	25.36184	80.37838	N-NE	20	122.0
1/21/2016	LN-7	77	13500	25.36184	80.37838	N-NE	40	199.0
1/21/2016	LN-7	78	14000	25.36315	80.37792	N-NE	10	51.2
1/21/2016	LN-7	78	14000	25.36315	80.37792	N-NE	20	121.8
1/21/2016	LN-7	78	14000	25.36315	80.37792	N-NE	40	203.0
1/21/2016	LN-7	79	14500	25.36443	80.37743	N-NE	10	47.7
1/21/2016	LN-7	79	14500	25.36443	80.37743	N-NE	20	112.5
1/21/2016	LN-7	79	14500	25.36443	80.37743	N-NE	40	195.0
1/21/2016	LN-7	80	15000	25.36525	80.37701	N-NE	10	51.3
1/21/2016	LN-7	80	15000	25.36525	80.37701	N-NE	20	122.4
1/21/2016	LN-7	80	15000	25.36525	80.37701	N-NE	40	200.0
1/21/2016	LN-7	81	15500	25.367	80.37645	N-NE	10	29.0
1/21/2016	LN-7	81	15500	25.367	80.37645	N-NE	20	58.0
1/21/2016	LN-7	81	15500	25.367	80.37645	N-NE	40	233.0
1/21/2016	LN-7	82	16000	25.36831	80.3761	N-NE	10	44.2
1/21/2016	LN-7	82	16000	25.36831	80.3761	N-NE	20	105.1
1/21/2016	LN-7	82	16000	25.36831	80.3761	N-NE	40	173.0
1/21/2016	LN-7	83	16500	25.36965	80.37562	N-NE	10	45.1
1/21/2016	LN-7	83	16500	25.36965	80.37562	N-NE	20	105.3
1/21/2016	LN-7	83	16500	25.36965	80.37562	N-NE	40	174.0
1/21/2016	LN-7	84	17000	25.37095	80.37515	N-NE	10	43.2
1/21/2016	LN-7	84	17000	25.37095	80.37515	N-NE	20	107.1
1/21/2016	LN-7	84	17000	25.37095	80.37515	N-NE	40	175.0
1/21/2016	LN-7	85	17500	25.37228	80.37469	N-NE	10	46.1
1/21/2016	LN-7	85	17500	25.37228	80.37469	N-NE	20	107.0
1/21/2016	LN-7	85	17500	25.37228	80.37469	N-NE	40	168.0
1/21/2016	LN-7	86	18000	25.37359	80.37421	N-NE	10	44.5
1/21/2016	LN-7	86	18000	25.37359	80.37421	N-NE	20	108.3
1/21/2016	LN-7	86	18000	25.37359	80.37421	N-NE	40	171.0
1/21/2016	LN-7	87	18500	25.37493	80.37373	N-NE	10	46.5
1/21/2016	LN-7	87	18500	25.37493	80.37373	N-NE	20	116.1
1/21/2016	LN-7	87	18500	25.37493	80.37373	N-NE	40	185.0
1/21/2016	LN-7	88	19000	25.37624	80.37327	N-NE	10	49.6
1/21/2016	LN-7	88	19000	25.37624	80.37327	N-NE	20	121.6
1/21/2016	LN-7	88	19000	25.37624	80.37327	N-NE	40	185.0
1/25/2016	LN-7	89	19500	25.37754	80.3728	N-NE	10	45.0
1/25/2016	LN-7	89	19500	25.37754	80.3728	N-NE	20	107.5
1/25/2016	LN-7	89	19500	25.37754	80.3728	N-NE	40	160.0
1/25/2016	LN-7	90	20000	25.37786	80.37234	N-NE	10	46.9

**Florida Power & Light Company; Docket No. 20170007-EI  
Staff's Second Set of Interrogatories; Interrogatory No. 39  
Attachment No. 1, Page 27 of 200**

Table 1 - EMI FIELD DATA (Continued)

Date	Line Designation	Station #	Distance Along Profile (ft)	GPS Location		Direction of Survey	Coil Spacing (Meters)	Terrain Conductivity (mS/m)
				N	W			
1/25/2016	LN-7	90	20000	25.37786	80.37234	N-NE	20	116.5
1/25/2016	LN-7	90	20000	25.37786	80.37234	N-NE	40	182.0
1/25/2016	LN-7	91	20500	25.38017	80.37186	N-NE	10	48.8
1/25/2016	LN-7	91	20500	25.38017	80.37186	N-NE	20	121.9
1/25/2016	LN-7	91	20500	25.38017	80.37186	N-NE	40	183.0
1/25/2016	LN-7	92	21000	25.38147	80.37141	N-NE	10	48.5
1/25/2016	LN-7	92	21000	25.38147	80.37141	N-NE	20	116.8
1/25/2016	LN-7	92	21000	25.38147	80.37141	N-NE	40	177.0
1/25/2016	LN-7	93	21500	25.38278	80.37093	N-NE	10	45.7
1/25/2016	LN-7	93	21500	25.38278	80.37093	N-NE	20	115.6
1/25/2016	LN-7	93	21500	25.38278	80.37093	N-NE	40	181.0
1/25/2016	LN-7	94	22000	25.38408	80.3705	N-NE	10	47.4
1/25/2016	LN-7	94	22000	25.38408	80.3705	N-NE	20	114.8
1/25/2016	LN-7	94	22000	25.38408	80.3705	N-NE	40	174.0
1/25/2016	LN-7	95	22500	25.38536	80.37001	N-NE	10	48.9
1/25/2016	LN-7	95	22500	25.38536	80.37001	N-NE	20	121.1
1/25/2016	LN-7	95	22500	25.38536	80.37001	N-NE	40	180.0
1/25/2016	LN-7	96	23000	25.38669	80.36955	N-NE	10	46.5
1/25/2016	LN-7	96	23000	25.38669	80.36955	N-NE	20	108.8
1/25/2016	LN-7	96	23000	25.38669	80.36955	N-NE	40	165.0
1/25/2016	LN-7	97	23500	25.38798	80.36911	N-NE	10	41.0
1/25/2016	LN-7	97	23500	25.38798	80.36911	N-NE	20	100.9
1/25/2016	LN-7	97	23500	25.38798	80.36911	N-NE	40	172.0
1/25/2016	LN-7	98	24000	25.38928	80.36862	N-NE	10	39.5
1/25/2016	LN-7	98	24000	25.38928	80.36862	N-NE	20	104.1
1/25/2016	LN-7	98	24000	25.38928	80.36862	N-NE	40	169.0
1/25/2016	LN-7	99	24500	25.39059	80.36817	N-NE	10	41.0
1/25/2016	LN-7	99	24500	25.39059	80.36817	N-NE	20	101.8
1/25/2016	LN-7	99	24500	25.39059	80.36817	N-NE	40	163.0
1/25/2016	LN-7	100	25000	25.39189	80.36771	N-NE	10	39.7
1/25/2016	LN-7	100	25000	25.39189	80.36771	N-NE	20	106.4
1/25/2016	LN-7	100	25000	25.39189	80.36771	N-NE	40	178.0
1/25/2016	LN-7	101	25500	25.39318	80.36726	N-NE	10	47.7
1/25/2016	LN-7	101	25500	25.39318	80.36726	N-NE	20	115.2
1/25/2016	LN-7	101	25500	25.39318	80.36726	N-NE	40	181.0
1/25/2016	LN-7	102	26000	25.39444	80.36681	N-NE	10	40.5
1/25/2016	LN-7	102	26000	25.39444	80.36681	N-NE	20	110.5
1/25/2016	LN-7	102	26000	25.39444	80.36681	N-NE	40	181.0
1/25/2016	LN-7	103	26500	25.39573	80.36633	N-NE	10	40.9
1/25/2016	LN-7	103	26500	25.39573	80.36633	N-NE	20	111.8
1/25/2016	LN-7	103	26500	25.39573	80.36633	N-NE	40	176.0
1/25/2016	LN-7	104	27000	25.39704	80.36588	N-NE	10	46.0
1/25/2016	LN-7	104	27000	25.39704	80.36588	N-NE	20	101.9
1/25/2016	LN-7	104	27000	25.39704	80.36588	N-NE	40	172.0
1/25/2016	LN-7	105	27500	25.39832	80.36542	N-NE	10	38.2
1/25/2016	LN-7	105	27500	25.39832	80.36542	N-NE	20	101.4
1/25/2016	LN-7	105	27500	25.39832	80.36542	N-NE	40	173.0
1/25/2016	LN-7	106	28000	25.39958	80.36497	N-NE	10	43.1
1/25/2016	LN-7	106	28000	25.39958	80.36497	N-NE	20	98.5
1/25/2016	LN-7	106	28000	25.39958	80.36497	N-NE	40	159.0
1/26/2016	LN-7	107	28500	25.40087	80.36452	N-NE	10	43.7
1/26/2016	LN-7	107	28500	25.40087	80.36452	N-NE	20	98.0

\* - Indicates potential interference from powerlines

**Florida Power & Light Company; Docket No. 20170007-EI  
Staff's Second Set of Interrogatories; Interrogatory No. 39  
Attachment No. 1, Page 28 of 200**

Table 25 - ELD DATA (Continued)

Date	Line Designation	Station #	Distance Along Profile (ft)	GPS Location		Direction of Survey	Coil Spacing (Meters)	Terrain Conductivity (mS/m)
				N	W			
1/26/2016	LN-7	107	28500	25.40087	80.36452	N-NE	40	162.0
1/26/2016	LN-7	108	29000	25.40216	80.36405	N-NE	10	42.1
1/26/2016	LN-7	108	29000	25.40216	80.36405	N-NE	20	98.9
1/26/2016	LN-7	108	29000	25.40216	80.36405	N-NE	40	157.0
1/26/2016	LN-7	109	29500	25.40346	80.36358	N-NE	10	42.6
1/26/2016	LN-7	109	29500	25.40346	80.36358	N-NE	20	100.4
1/26/2016	LN-7	109	29500	25.40346	80.36358	N-NE	40	169.0
1/26/2016	LN-7	110	30000	25.40474	80.36313	N-NE	10	40.3
1/26/2016	LN-7	110	30000	25.40474	80.36313	N-NE	20	96.4
1/26/2016	LN-7	110	30000	25.40474	80.36313	N-NE	40	157.0
1/26/2016	LN-7	111	30500	25.40602	80.36267	N-NE	10	44.1
1/26/2016	LN-7	111	30500	25.40602	80.36267	N-NE	20	100.8
1/26/2016	LN-7	111	30500	25.40602	80.36267	N-NE	40	158.0
1/26/2016	LN-7	112	31000	25.40733	80.36221	N-NE	10	42.2
1/26/2016	LN-7	112	31000	25.40733	80.36221	N-NE	20	100.4
1/26/2016	LN-7	112	31000	25.40733	80.36221	N-NE	40	167.0
1/26/2016	LN-7	113	31500	25.40864	80.36174	N-NE	10	40.2
1/26/2016	LN-7	113	31500	25.40864	80.36174	N-NE	20	101.5
1/26/2016	LN-7	113	31500	25.40864	80.36174	N-NE	40	172.0
1/26/2016	LN-7	114	32000	25.40993	80.36128	N-NE	10	39.6
1/26/2016	LN-7	114	32000	25.40993	80.36128	N-NE	20	98.7
1/26/2016	LN-7	114	32000	25.40993	80.36128	N-NE	40	177.0
1/26/2016	LN-7	115	32500	25.4112	80.36082	N-NE	10	42.6
1/26/2016	LN-7	115	32500	25.4112	80.36082	N-NE	20	108.8
1/26/2016	LN-7	115	32500	25.4112	80.36082	N-NE	40	183.0
1/26/2016	LN-7	116	33000	25.41249	80.36035	N-NE	10	44.3
1/26/2016	LN-7	116	33000	25.41249	80.36035	N-NE	20	105.8
1/26/2016	LN-7	116	33000	25.41249	80.36035	N-NE	40	183.0
1/26/2016	LN-7	117	33500	25.41378	80.3599	N-NE	10	40.0
1/26/2016	LN-7	117	33500	25.41378	80.3599	N-NE	20	100.1
1/26/2016	LN-7	117	33500	25.41378	80.3599	N-NE	40	179.0
1/26/2016	LN-7	118	34000	25.41509	80.35944	N-NE	10	47.6
1/26/2016	LN-7	118	34000	25.41509	80.35944	N-NE	20	106.2
1/26/2016	LN-7	118	34000	25.41509	80.35944	N-NE	40	185.0
1/26/2016	LN-7	119	34500	25.4164	80.35896	N-NE	10	45.5
1/26/2016	LN-7	119	34500	25.4164	80.35896	N-NE	20	103.0
1/26/2016	LN-7	119	34500	25.4164	80.35896	N-NE	40	190.0
1/26/2016	LN-7	120	35000	25.4177	80.35851	N-NE	10	42.6
1/26/2016	LN-7	120	35000	25.4177	80.35851	N-NE	20	98.9
1/26/2016	LN-7	120	35000	25.4177	80.35851	N-NE	40	187.0
1/26/2016	LN-7	121	35500	25.41897	80.35806	N-NE	10	48.6
1/26/2016	LN-7	121	35500	25.41897	80.35806	N-NE	20	103.7
1/26/2016	LN-7	121	35500	25.41897	80.35806	N-NE	40	190.0
1/26/2016	LN-7	122	36000	25.42026	80.3576	N-NE	10	49.1
1/26/2016	LN-7	122	36000	25.42026	80.3576	N-NE	20	116.1
1/26/2016	LN-7	122	36000	25.42026	80.3576	N-NE	40	248.0
1/26/2016	LN-7	123	36500	25.42156	80.35714	N-NE	10	46.8
1/26/2016	LN-7	123	36500	25.42156	80.35714	N-NE	20	101.5
1/26/2016	LN-7	123	36500	25.42156	80.35714	N-NE	40	228.0
1/26/2016	LN-7	124	37000	25.42286	80.35667	N-NE	10	45.2
1/26/2016	LN-7	124	37000	25.42286	80.35667	N-NE	20	107.6
1/26/2016	LN-7	124	37000	25.42286	80.35667	N-NE	40	250.6

\* - Indicates potential interference from powerlines



Table 25 - FIELD DATA (Continued)

Date	Line Designation	Station #	Distance Along Profile (ft)	GPS Location		Direction of Survey	Coil Spacing (Meters)	Terrain Conductivity (mS/m)
				N	W			
1/26/2016	LN-7	125	37500	25.42415	80.35621	N-NE	10	49.4
1/26/2016	LN-7	125	37500	25.42415	80.35621	N-NE	20	101.1
1/26/2016	LN-7	125	37500	25.42415	80.35621	N-NE	40	219.0
1/26/2016	LN-7	126	38000	25.42545	80.35574	N-NE	10	45.1
1/26/2016	LN-7	126	38000	25.42545	80.35574	N-NE	20	110.2
1/26/2016	LN-7	126	38000	25.42545	80.35574	N-NE	40	231.0
1/26/2016	LN-7	127	38500	25.42677	80.35528	N-NE	10	48.9
1/26/2016	LN-7	127	38500	25.42677	80.35528	N-NE	20	86.6
1/26/2016	LN-7	127	38500	25.42677	80.35528	N-NE	40	188.0
1/26/2016	LN-7	128	39000	25.42806	80.35482	N-NE	10	52.1
1/26/2016	LN-7	128	39000	25.42806	80.35482	N-NE	20	123.4
1/26/2016	LN-7	128	39000	25.42806	80.35482	N-NE	40	236.8
1/26/2016	LN-7	129	39500	25.42936	80.35435	N-NE	10	50.8
1/26/2016	LN-7	129	39500	25.42936	80.35435	N-NE	20	116.1
1/26/2016	LN-7	129	39500	25.42936	80.35435	N-NE	40	240.0
1/26/2016	LN-7	130	40000	25.43066	80.35388	N-NE	10	49.5
1/26/2016	LN-7	130	40000	25.43066	80.35388	N-NE	20	105.6
1/26/2016	LN-7	130	40000	25.43066	80.35388	N-NE	40	240.0
1/26/2016	LN-7	131	40500	25.43196	80.35342	N-NE	10	42.0
1/26/2016	LN-7	131	40500	25.43196	80.35342	N-NE	20	96.5
1/26/2016	LN-7	131	40500	25.43196	80.35342	N-NE	40	229.0
1/26/2016	LN-7	132	41000	25.43326	80.35297	N-NE	10	45.6
1/26/2016	LN-7	132	41000	25.43326	80.35297	N-NE	20	110.2
1/26/2016	LN-7	132	41000	25.43326	80.35297	N-NE	40	242.0
1/26/2016	LN-7	133	41500	25.43408	80.35268	N-NE	10	46.5
1/26/2016	LN-7	133	41500	25.43408	80.35268	N-NE	20	110.4
1/26/2016	LN-7	133	41500	25.43408	80.35268	N-NE	40	265.0
1/26/2016	LN-7	134	42000	25.43585	80.35207	N-NE	10	57.3
1/26/2016	LN-7	134	42000	25.43585	80.35207	N-NE	20	121.9
1/26/2016	LN-7	134	42000	25.43585	80.35207	N-NE	40	193.0
1/26/2016	LN-7	135	42500	25.43713	80.35161	N-NE	10	46.7
1/26/2016	LN-7	135	42500	25.43713	80.35161	N-NE	20	108.2
1/26/2016	LN-7	135	42500	25.43713	80.35161	N-NE	40	268.0
1/26/2016	LN-7	136	43000	25.43846	80.35114	N-NE	10	47.0
1/26/2016	LN-7	136	43000	25.43846	80.35114	N-NE	20	114.0
1/26/2016	LN-7	136	43000	25.43846	80.35114	N-NE	40	216.0
1/26/2016	LN-7	137	43500	25.43976	80.35069	N-NE	10	45.7
1/26/2016	LN-7	137	43500	25.43976	80.35069	N-NE	20	103.6
1/26/2016	LN-7	137	43500	25.43976	80.35069	N-NE	40	236.0
1/26/2016	LN-7	138	44000	25.44100	80.35023	N-NE	10	40.2
1/26/2016	LN-7	138	44000	25.44100	80.35023	N-NE	20	96.3
1/26/2016	LN-7	138	44000	25.44100	80.35023	N-NE	40	198.0
1/26/2016	LN-7	139	44500	25.44229	80.34978	N-NE	10	41.5
1/26/2016	LN-7	139	44500	25.44229	80.34978	N-NE	20	88.9
1/26/2016	LN-7	139	44500	25.44229	80.34978	N-NE	40	189.0
1/26/2016	LN-7	140	45000	25.44363	80.34959	N	10	38.0
1/26/2016	LN-7	140	45000	25.44363	80.34959	N	20	84.2
1/26/2016	LN-7	140	45000	25.44363	80.34959	N	40	192.0
1/26/2016	LN-7	141	45500	25.44498	80.34959	N	10	35.9
1/26/2016	LN-7	141	45500	25.44498	80.34959	N	20	81.6
1/26/2016	LN-7	141	45500	25.44498	80.34959	N	40	192.0
1/26/2016	LN-7	142	46000	25.44632	80.34959	N	10	31.2

Florida Power & Light Company; Docket No. 20170007-EI  
 Staff's Second Set of Interrogatories; Interrogatory No. 39  
 Attachment No. 1, Page 38 of 200

Table 1 - FIELD DATA (Continued)

Date	Line Designation	Station #	Distance Along Profile (ft)	GPS Location		Direction of Survey	Coil Spacing (Meters)	Terrain Conductivity (mS/m)
				N	W			
1/26/2016	LN-7	142	46000	25.44632	80.34959	N	20	75.5
1/26/2016	LN-7	142	46000	25.44632	80.34959	N	40	177.0
1/26/2016	LN-7	143	46500	25.44767	80.34957	N	10	43.3
1/26/2016	LN-7	143	46500	25.44767	80.34957	N	20	87.7
1/26/2016	LN-7	143	46500	25.44767	80.34957	N	40	174.0
1/26/2016	LN-2	144	47000	25.43458	80.45203	E	10	23.9*
1/26/2016	LN-2	144	47000	25.43458	80.45203	E	20	22.6*
1/26/2016	LN-2	144	47000	25.43458	80.45203	E	40	-0.004*
1/26/2016	LN-2	145	47500	25.43461	80.45053	E	10	-42.6*
1/26/2016	LN-2	145	47500	25.43461	80.45053	E	20	20*
1/26/2016	LN-2	145	47500	25.43461	80.45053	E	40	686*
1/27/2016	LN-6	146	0	25.44759	80.41199	S	10	8.7
1/27/2016	LN-6	146	0	25.44759	80.41199	S	20	19.7
1/27/2016	LN-6	146	0	25.44759	80.41199	S	40	48.0
1/27/2016	LN-6	147	500	25.44626	80.41191	S	10	10.1
1/27/2016	LN-6	147	500	25.44626	80.41191	S	20	19.2
1/27/2016	LN-6	147	500	25.44626	80.41191	S	40	46.0
1/27/2016	LN-6	148	1000	25.44488	80.4119	S	10	9.0
1/27/2016	LN-6	148	1000	25.44488	80.4119	S	20	18.4
1/27/2016	LN-6	148	1000	25.44488	80.4119	S	40	45.0
1/27/2016	LN-6	149	1500	25.44353	80.4119	S	10	8.1
1/27/2016	LN-6	149	1500	25.44353	80.4119	S	20	16.7
1/27/2016	LN-6	149	1500	25.44353	80.4119	S	40	41.0
1/27/2016	LN-6	150	2000	25.44216	80.4119	S	10	8.5
1/27/2016	LN-6	150	2000	25.44216	80.4119	S	20	18.0
1/27/2016	LN-6	150	2000	25.44216	80.4119	S	40	42.0
1/27/2016	LN-6	151	2500	25.44082	80.4119	S	10	8.9
1/27/2016	LN-6	151	2500	25.44082	80.4119	S	20	15.5
1/27/2016	LN-6	151	2500	25.44082	80.4119	S	40	35.0
1/27/2016	LN-6	152	3000	25.43945	80.41192	S	10	7.3
1/27/2016	LN-6	152	3000	25.43945	80.41192	S	20	16.2
1/27/2016	LN-6	152	3000	25.43945	80.41192	S	40	36.0
1/27/2016	LN-6	153	3500	25.43813	80.4119	S	10	6.7
1/27/2016	LN-6	153	3500	25.43813	80.4119	S	20	15.9
1/27/2016	LN-6	153	3500	25.43813	80.4119	S	40	34.0
1/27/2016	LN-6	154	4000	25.43675	80.41192	S	10	5.6
1/27/2016	LN-6	154	4000	25.43675	80.41192	S	20	14.9
1/27/2016	LN-6	154	4000	25.43675	80.41192	S	40	33.0
1/27/2016	LN-6	155	4500	25.4354	80.41193	S	10	4.6
1/27/2016	LN-6	155	4500	25.4354	80.41193	S	20	12.3
1/27/2016	LN-6	155	4500	25.4354	80.41193	S	40	29.0
1/27/2016	LN-2	156	50' from powerline	25.43454	80.44416	S	10	9.6
1/27/2016	LN-2	156	50' from powerline	25.43454	80.44416	S	20	9.8
1/27/2016	LN-2	156	50' from powerline	25.43454	80.44416	S	40	13.0
1/27/2016	LN-2	157	20' off road	25.43462	80.43615	S	10	9.8
1/27/2016	LN-2	157	20' off road	25.43462	80.43615	S	20	10.5
1/27/2016	LN-2	157	20' off road	25.43462	80.43615	S	40	15.0
1/27/2016	LN-2	158	20' off road	25.43464	80.42801	S	10	11.5
1/27/2016	LN-2	158	20' off road	25.43464	80.42801	S	20	12.6
1/27/2016	LN-2	158	20' off road	25.43464	80.42801	S	40	18.0
1/27/2016	LN-2	159	side of road	25.43465	80.35427	S	10	48.9
1/27/2016	LN-2	159	side of road	25.43465	80.35427	S	20	86.0

\* - Indicates potential interference from powerlines

Table 1 - FIELD DATA (Continued)

Date	Line Designation	Station #	Distance Along Profile (ft)	GPS Location		Direction of Survey	Coil Spacing (Meters)	Terrain Conductivity (mS/m)
				N	W			
1/27/2016	LN-2	159	side of road	25.43465	80.35427	S	40	154.0
1/27/2016	LN-2	160	500' from STA #159	25.43469	80.35576	W	10	NM*
1/27/2016	LN-2	160	500' from STA #159	25.43469	80.35576	W	20	NM*
1/27/2016	LN-2	160	500' from STA #159	25.43469	80.35576	W	40	NM*
1/27/2016	LN-2	161	75' north of road	25.43509	80.37942	N	10	29.3
1/27/2016	LN-2	161	75' north of road	25.43509	80.37942	N	20	52.3
1/27/2016	LN-2	161	75' north of road	25.43509	80.37942	N	40	84.0
1/27/2016	LN-2	162	00' north of STA #16	25.43643	80.37944	N	10	31.8
1/27/2016	LN-2	162	00' north of STA #16	25.43643	80.37944	N	20	51.7
1/27/2016	LN-2	162	00' north of STA #16	25.43643	80.37944	N	40	75.0
1/27/2016	LN-2	163	20' south of road	25.43479	80.38759	S	10	21.6
1/27/2016	LN-2	163	20' south of road	25.43479	80.38759	S	20	41.3
1/27/2016	LN-2	163	20' south of road	25.43479	80.38759	S	40	68.0
1/27/2016	LN-2	164	12' south of road	25.43477	80.39567	S	10	17.6
1/27/2016	LN-2	164	12' south of road	25.43477	80.39567	S	20	32.0
1/27/2016	LN-2	164	12' south of road	25.43477	80.39567	S	40	60.0
1/27/2016	LN-2	165	15' south of road	25.43469	80.40379	S	10	14.8
1/27/2016	LN-2	165	15' south of road	25.43469	80.40379	S	20	26.5
1/27/2016	LN-2	165	15' south of road	25.43469	80.40379	S	40	50.0
1/27/2016	LN-6	166	5000	25.43403	80.41195	S	10	14.8
1/27/2016	LN-6	166	5000	25.43403	80.41195	S	20	26.5
1/27/2016	LN-6	166	5000	25.43403	80.41195	S	40	50.0
1/27/2016	LN-6	167	5500	25.43269	80.41195	S	10	9.7
1/27/2016	LN-6	167	5500	25.43269	80.41195	S	20	18.2
1/27/2016	LN-6	167	5500	25.43269	80.41195	S	40	33.0
1/27/2016	LN-6	168	6000	25.43132	80.41198	S	10	9.3
1/27/2016	LN-6	168	6000	25.43132	80.41198	S	20	19.0
1/27/2016	LN-6	168	6000	25.43132	80.41198	S	40	36.0
1/27/2016	LN-6	169	6500	25.42997	80.41196	S	10	6.4
1/27/2016	LN-6	169	6500	25.42997	80.41196	S	20	14.7
1/27/2016	LN-6	169	6500	25.42997	80.41196	S	40	30.0
1/27/2016	LN-6	170	7000	25.42859	80.41194	S	10	9.2
1/27/2016	LN-6	170	7000	25.42859	80.41194	S	20	20.0
1/27/2016	LN-6	170	7000	25.42859	80.41194	S	40	40.0
1/27/2016	LN-6	171	7500	25.42721	80.41198	S	10	6.0
1/27/2016	LN-6	171	7500	25.42721	80.41198	S	20	16.8
1/27/2016	LN-6	171	7500	25.42721	80.41198	S	40	36.0
1/27/2016	LN-6	172	8000	25.42586	80.41195	S	10	9.9
1/27/2016	LN-6	172	8000	25.42586	80.41195	S	20	23.7
1/27/2016	LN-6	172	8000	25.42586	80.41195	S	40	45.0
1/27/2016	LN-6	173	8500	25.42452	80.41198	S	10	9.7
1/27/2016	LN-6	173	8500	25.42452	80.41198	S	20	23.9
1/27/2016	LN-6	173	8500	25.42452	80.41198	S	40	46.0
1/27/2016	LN-6	174	9000	25.42317	80.41199	S	10	8.2
1/27/2016	LN-6	174	9000	25.42317	80.41199	S	20	25.2
1/27/2016	LN-6	174	9000	25.42317	80.41199	S	40	52.0
1/27/2016	LN-6	175	9500	25.42183	80.41199	S	10	10.9
1/27/2016	LN-6	175	9500	25.42183	80.41199	S	20	29.8
1/27/2016	LN-6	175	9500	25.42183	80.41199	S	40	61.0
1/27/2016	LN-6	176	10000	25.42046	80.41202	S	10	10.5
1/27/2016	LN-6	176	10000	25.42046	80.41202	S	20	32.0
1/27/2016	LN-6	176	10000	25.42046	80.41202	S	40	68.0

\* - Indicates potential interference from powerlines

Table 35 - FIELD DATA (Continued)

Date	Line Designation	Station #	Distance Along Profile (ft)	GPS Location		Direction of Survey	Coil Spacing (Meters)	Terrain Conductivity (mS/m)
				N	W			
1/28/2016	LN-6	177	10500	25.41909	80.41202	S	10	13.4
1/28/2016	LN-6	177	10500	25.41909	80.41202	S	20	34.5
1/28/2016	LN-6	177	10500	25.41909	80.41202	S	40	62.0
1/28/2016	LN-6	178	11000	25.41769	80.41202	S	10	15*
1/28/2016	LN-6	178	11000	25.41769	80.41202	S	20	40.3*
1/28/2016	LN-6	178	11000	25.41769	80.41202	S	40	131*
1/28/2016	LN-6	179	11500	25.41633	80.41203	S	10	16*
1/28/2016	LN-6	179	11500	25.41633	80.41203	S	20	43.5*
1/28/2016	LN-6	179	11500	25.41633	80.41203	S	40	194*
1/28/2016	LN-6	180	12000	25.41495	80.41206	S	10	14.5*
1/28/2016	LN-6	180	12000	25.41495	80.41206	S	20	41.2*
1/28/2016	LN-6	180	12000	25.41495	80.41206	S	40	140*
1/28/2016	LN-6	181	12500	25.41359	80.41206	S	10	13.4*
1/28/2016	LN-6	181	12500	25.41359	80.41206	S	20	43.1*
1/28/2016	LN-6	181	12500	25.41359	80.41206	S	40	189*
1/28/2016	LN-6	182	At SW 384 opening	25.41124	80.41208	S	10	16.2*
1/28/2016	LN-6	182	At SW 384 opening	25.41124	80.41208	S	20	52.6*
1/28/2016	LN-6	182	At SW 384 opening	25.41124	80.41208	S	40	154*
1/28/2016	LN-8	183	bad at opening of SW	25.41126	80.41207	W	10	14.9
1/28/2016	LN-8	183	bad at opening of SW	25.41126	80.41207	W	20	54.2
1/28/2016	LN-8	183	bad at opening of SW	25.41126	80.41207	W	40	80.0
1/28/2016	LN-8	184	500	25.41125	80.4136	W	10	17.6
1/28/2016	LN-8	184	500	25.41125	80.4136	W	20	47.6
1/28/2016	LN-8	184	500	25.41125	80.4136	W	40	89.0
1/28/2016	LN-8	185	1000	25.41127	80.41512	W	10	18.1
1/28/2016	LN-8	185	1000	25.41127	80.41512	W	20	43.8
1/28/2016	LN-8	185	1000	25.41127	80.41512	W	40	81.0
1/28/2016	LN-8	186	1500	25.41128	80.41663	W	10	18.7
1/28/2016	LN-8	186	1500	25.41128	80.41663	W	20	44.3
1/28/2016	LN-8	186	1500	25.41128	80.41663	W	40	78.0
1/28/2016	LN-8	187	2000	25.41127	80.41812	W	10	17.1
1/28/2016	LN-8	187	2000	25.41127	80.41812	W	20	38.0
1/28/2016	LN-8	187	2000	25.41127	80.41812	W	40	78.0
1/28/2016	LN-8	188	2500	25.41128	80.41965	W	10	18.7
1/28/2016	LN-8	188	2500	25.41128	80.41965	W	20	39.3
1/28/2016	LN-8	188	2500	25.41128	80.41965	W	40	70.0
1/29/2016	LN-3	189	0	25.38177	80.37197	W	10	62.4
1/29/2016	LN-3	189	0	25.38177	80.37197	W	20	123.8
1/29/2016	LN-3	189	0	25.38177	80.37197	W	40	181.0
1/29/2016	LN-3	190	500	25.38178	80.3735	W	10	61.7
1/29/2016	LN-3	190	500	25.38178	80.3735	W	20	136.6
1/29/2016	LN-3	190	500	25.38178	80.3735	W	40	214.0
1/29/2016	LN-3	191	1000	25.38179	80.37498	W	10	60.1
1/29/2016	LN-3	191	1000	25.38179	80.37498	W	20	124.8
1/29/2016	LN-3	191	1000	25.38179	80.37498	W	40	212.0
1/29/2016	LN-3	192	1500	25.38179	80.37647	W	10	57.5
1/29/2016	LN-3	192	1500	25.38179	80.37647	W	20	115.4
1/29/2016	LN-3	192	1500	25.38179	80.37647	W	40	187.0
1/29/2016	LN-3	193	2000	25.38181	80.378	W	10	56.3
1/29/2016	LN-3	193	2000	25.38181	80.378	W	20	117.4
1/29/2016	LN-3	193	2000	25.38181	80.378	W	40	174.0
1/29/2016	LN-3	194	2500	25.38179	80.37946	W	10	56.7

\* - Indicates potential interference from powerlines

Table 35 - FIELD DATA (Continued)

Date	Line Designation	Station #	Distance Along Profile (ft)	GPS Location		Direction of Survey	Coil Spacing (Meters)	Terrain Conductivity (mS/m)
				N	W			
1/29/2016	LN-3	194	2500	25.38179	80.37946	W	20	109.6
1/29/2016	LN-3	194	2500	25.38179	80.37946	W	40	170.0
1/29/2016	LN-3	195	3000	25.38181	80.38096	W	10	54.6
1/29/2016	LN-3	195	3000	25.38181	80.38096	W	20	110.4
1/29/2016	LN-3	195	3000	25.38181	80.38096	W	40	167.0
1/29/2016	LN-3	196	3500	25.38181	80.38247	W	10	54.0
1/29/2016	LN-3	196	3500	25.38181	80.38247	W	20	101.5
1/29/2016	LN-3	196	3500	25.38181	80.38247	W	40	170.0
1/29/2016	LN-3	197	4000	25.38181	80.38399	W	10	49.6
1/29/2016	LN-3	197	4000	25.38181	80.38399	W	20	99.5
1/29/2016	LN-3	197	4000	25.38181	80.38399	W	40	171.0
1/29/2016	LN-3	198	4500	25.38181	80.3855	W	10	52.2
1/29/2016	LN-3	198	4500	25.38181	80.3855	W	20	108.5
1/29/2016	LN-3	198	4500	25.38181	80.3855	W	40	177.0
1/29/2016	LN-3	199	5000	25.38181	80.387	W	10	48.3
1/29/2016	LN-3	199	5000	25.38181	80.387	W	20	94.3
1/29/2016	LN-3	199	5000	25.38181	80.387	W	40	157.0
1/29/2016	LN-3	200	5500	25.38181	80.3885	W	10	42.5
1/29/2016	LN-3	200	5500	25.38181	80.3885	W	20	93.6
1/29/2016	LN-3	200	5500	25.38181	80.3885	W	40	158.0
1/29/2016	LN-3	201	6000	25.38177	80.39005	W	10	51.8
1/29/2016	LN-3	201	6000	25.38177	80.39005	W	20	95.7
1/29/2016	LN-3	201	6000	25.38177	80.39005	W	40	157.0
1/29/2016	LN-3	202	6500	25.38179	80.39158	W	10	51.4
1/29/2016	LN-3	202	6500	25.38179	80.39158	W	20	92.6
1/29/2016	LN-3	202	6500	25.38179	80.39158	W	40	156.0
1/29/2016	LN-3	203	7000	25.3818	80.39307	W	10	45.6
1/29/2016	LN-3	203	7000	25.3818	80.39307	W	20	91.9
1/29/2016	LN-3	203	7000	25.3818	80.39307	W	40	145.0
1/29/2016	LN-3	204	7500	25.38181	80.39454	W	10	47.1
1/29/2016	LN-3	204	7500	25.38181	80.39454	W	20	93.6
1/29/2016	LN-3	204	7500	25.38181	80.39454	W	40	163.0
1/29/2016	LN-3	205	8000	25.38178	80.39608	W	10	42.7
1/29/2016	LN-3	205	8000	25.38178	80.39608	W	20	84.6
1/29/2016	LN-3	205	8000	25.38178	80.39608	W	40	148.0
1/29/2016	LN-3	206	8500	25.38181	80.39759	W	10	41.0
1/29/2016	LN-3	206	8500	25.38181	80.39759	W	20	78.0
1/29/2016	LN-3	206	8500	25.38181	80.39759	W	40	141.0
1/29/2016	LN-3	207	9000	25.3818	80.39906	W	10	48.0
1/29/2016	LN-3	207	9000	25.3818	80.39906	W	20	89.7
1/29/2016	LN-3	207	9000	25.3818	80.39906	W	40	146.0
1/29/2016	LN-3	208	9500	25.38181	80.40055	W	10	50.8
1/29/2016	LN-3	208	9500	25.38181	80.40055	W	20	92.0
1/29/2016	LN-3	208	9500	25.38181	80.40055	W	40	139.0
1/29/2016	LN-3	209	10000	25.38179	80.40207	W	10	44.7
1/29/2016	LN-3	209	10000	25.38179	80.40207	W	20	82.1
1/29/2016	LN-3	209	10000	25.38179	80.40207	W	40	124.0
1/29/2016	LN-3	210	10500	25.38183	80.40351	W	10	43.6
1/29/2016	LN-3	210	10500	25.38183	80.40351	W	20	80.0
1/29/2016	LN-3	210	10500	25.38183	80.40351	W	40	127.0
1/29/2016	LN-3	211	11000	25.38181	80.40504	W	10	32.8
1/29/2016	LN-3	211	11000	25.38181	80.40504	W	20	67.3

**Florida Power & Light Company; Docket No. 20170007-EI  
Staff's Second Set of Interrogatories; Interrogatory No. 39  
Attachment No. 1, Page 34 of 200**

Table 1 - FIELD DATA (Continued)

Date	Line Designation	Station #	Distance Along Profile (ft)	GPS Location		Direction of Survey	Coil Spacing (Meters)	Terrain Conductivity (mS/m)
				N	W			
1/29/2016	LN-3	211	11000	25.38181	80.40504	W	40	112.0
1/29/2016	LN-3	212	11500	25.38181	80.40655	W	10	33.6
1/29/2016	LN-3	212	11500	25.38181	80.40655	W	20	62.5
1/29/2016	LN-3	212	11500	25.38181	80.40655	W	40	97.0
1/29/2016	LN-3	213	12000	25.38182	80.40804	W	10	30.7
1/29/2016	LN-3	213	12000	25.38182	80.40804	W	20	62.6
1/29/2016	LN-3	213	12000	25.38182	80.40804	W	40	106.0
1/29/2016	LN-3	214	12500	25.38181	80.40996	W	10	27.5
1/29/2016	LN-3	214	12500	25.38181	80.40996	W	20	58.4
1/29/2016	LN-3	214	12500	25.38181	80.40996	W	40	100.0
1/29/2016	LN-3	215	12950	25.38178	80.4113	W	10	25.9
1/29/2016	LN-3	215	12950	25.38178	80.4113	W	20	60.3
1/29/2016	LN-3	215	12950	25.38178	80.4113	W	40	106.0
1/29/2016	LN-4	216	0	25.36711	80.41177	E	10	34.1
1/29/2016	LN-4	216	0	25.36711	80.41177	E	20	67.5
1/29/2016	LN-4	216	0	25.36711	80.41177	E	40	104.0
1/29/2016	LN-4	217	500	25.36709	80.41024	E	10	33.0
1/29/2016	LN-4	217	500	25.36709	80.41024	E	20	72.0
1/29/2016	LN-4	217	500	25.36709	80.41024	E	40	123.0
1/29/2016	LN-4	218	1000	25.36708	80.40872	E	10	32.9
1/29/2016	LN-4	218	1000	25.36708	80.40872	E	20	76.4
1/29/2016	LN-4	218	1000	25.36708	80.40872	E	40	126.0
1/29/2016	LN-4	219	1500	25.36711	80.40721	E	10	30.1
1/29/2016	LN-4	219	1500	25.36711	80.40721	E	20	70.0
1/29/2016	LN-4	219	1500	25.36711	80.40721	E	40	117.0
1/29/2016	LN-4	220	2000	25.36713	80.40573	E	10	34.8
1/29/2016	LN-4	220	2000	25.36713	80.40573	E	20	82.3
1/29/2016	LN-4	220	2000	25.36713	80.40573	E	40	140.0
1/30/2016	LN-4	221	2750	25.3671	80.4042	W	10	36.3
1/30/2016	LN-4	221	2750	25.3671	80.4042	W	20	79.0
1/30/2016	LN-4	221	2750	25.3671	80.4042	W	40	136.0
1/30/2016	LN-4	222	3000	25.36711	80.40345	W	10	38.1
1/30/2016	LN-4	222	3000	25.36711	80.40345	W	20	80.6
1/30/2016	LN-4	222	3000	25.36711	80.40345	W	40	141.0
1/30/2016	LN-4	223	3500	25.36711	80.40195	W	10	37.9
1/30/2016	LN-4	223	3500	25.36711	80.40195	W	20	82.9
1/30/2016	LN-4	223	3500	25.36711	80.40195	W	40	147.0
1/30/2016	LN-4	224	4000	25.36713	80.40044	W	10	44.8
1/30/2016	LN-4	224	4000	25.36713	80.40044	W	20	86.1
1/30/2016	LN-4	224	4000	25.36713	80.40044	W	40	140.0
1/30/2016	LN-4	225	4500	25.36711	80.39898	W	10	45.7
1/30/2016	LN-4	225	4500	25.36711	80.39898	W	20	85.2
1/30/2016	LN-4	225	4500	25.36711	80.39898	W	40	141.6
1/30/2016	LN-4	226	5000	25.36709	80.39746	W	10	47.3
1/30/2016	LN-4	226	5000	25.36709	80.39746	W	20	93.2
1/30/2016	LN-4	226	5000	25.36709	80.39746	W	40	149.0
1/30/2016	LN-4	227	5500	25.36708	80.39597	W	10	50.1
1/30/2016	LN-4	227	5500	25.36708	80.39597	W	20	93.6
1/30/2016	LN-4	227	5500	25.36708	80.39597	W	40	164.0
1/30/2016	LN-4	228	6000	25.36711	80.39444	W	10	59.4
1/30/2016	LN-4	228	6000	25.36711	80.39444	W	20	102.0
1/30/2016	LN-4	228	6000	25.36711	80.39444	W	40	173.0

\* - Indicates potential interference from powerlines

Table 1 - EMP FIELD DATA (Continued)

Date	Line Designation	Station #	Distance Along Profile (ft)	GPS Location		Direction of Survey	Coil Spacing (Meters)	Terrain Conductivity (mS/m)
				N	W			
1/30/2016	LN-4	229	6500	25.36711	80.39289	W	10	59.3
1/30/2016	LN-4	229	6500	25.36711	80.39289	W	20	108.0
1/30/2016	LN-4	229	6500	25.36711	80.39289	W	40	181.6
1/30/2016	LN-4	230	7000	25.36714	80.39138	W	10	49.8
1/30/2016	LN-4	230	7000	25.36714	80.39138	W	20	98.0
1/30/2016	LN-4	230	7000	25.36714	80.39138	W	40	175.0
1/30/2016	LN-4	231	7500	25.36714	80.38988	W	10	53.7
1/30/2016	LN-4	231	7500	25.36714	80.38988	W	20	103.5
1/30/2016	LN-4	231	7500	25.36714	80.38988	W	40	183.0
1/30/2016	LN-4	232	8000	25.36711	80.38836	W	10	52.0
1/30/2016	LN-4	232	8000	25.36711	80.38836	W	20	96.9
1/30/2016	LN-4	232	8000	25.36711	80.38836	W	40	177.0
1/30/2016	LN-4	233	8500	25.36712	80.38684	W	10	65.6
1/30/2016	LN-4	233	8500	25.36712	80.38684	W	20	113.8
1/30/2016	LN-4	233	8500	25.36712	80.38684	W	40	175.0

\* - Indicates potential interference from powerlines



Table 2. Thickness and Depth to Bottom for each layer in the inverted AEM models

Layer	Depth to Bottom (m)	Thickness (m)	Layer	Depth to Bottom (m)	Thickness (m)
1	1.0	1	16	39.4	4.8
2	2.1	1.1	17	44.7	5.3
3	3.3	1.2	18	50.6	5.9
4	4.7	1.4	19	57.2	6.6
5	6.2	1.5	20	64.5	7.3
6	7.9	1.7	21	72.6	8.1
7	9.8	1.9	22	81.6	9.0
8	11.9	2.1	23	91.6	10.0
9	14.2	2.3	24	103.0	11.1
10	16.8	2.6	25	115.0	12.4
11	19.7	2.9	26	129.0	13.7
12	22.9	3.2	27	144.0	15.3
13	26.4	3.5	28	161.0	16.9
14	30.3	3.9	29	180.0	18.8
15	34.6	4.3	30	201.0	20.7

Table 3: Induction Logs Used to Verify the AEM Models  
Attachment No. 1, page 37 of 200

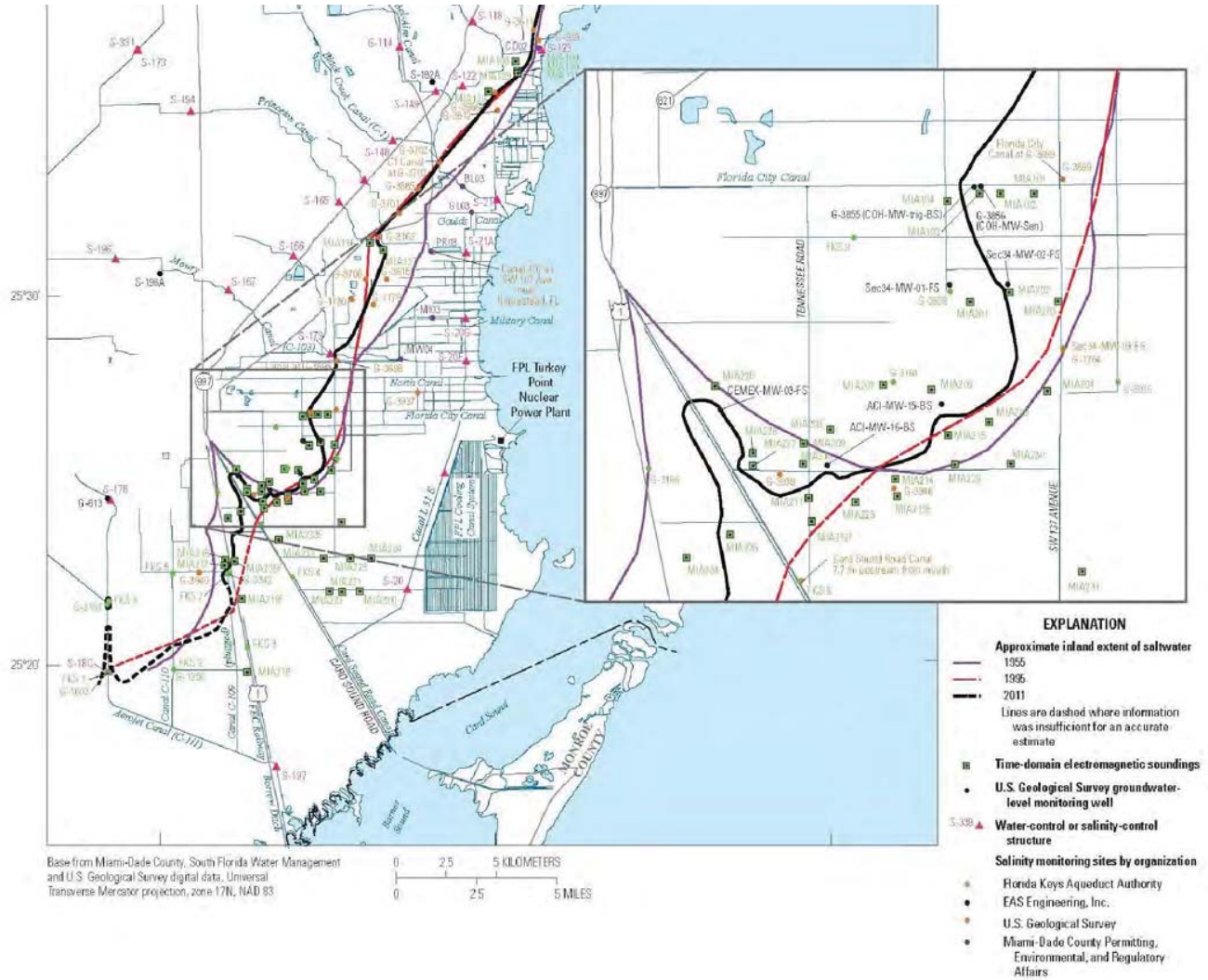
Well ID	Logging Date	AEM Line	Position of AEM Line in Reference to Well Location
TPGW-1	03-25-2013	101101	Off Line
TPGW-4	03-27-2013	200301	Off Line
TPGW-5	03-26-2013	101701	Within 200 m
TPGW-7	03-26-2013	301201	Within 200 m
TPGW-8	03-26-2013	302401	Off Line
TPGW-12	03-25-2013	100501	Within Line Break due to Coupling

Table 4. Water Quality Data Used for Calibration (September 2015 Laboratory Measurements)

Well ID	Screen		CL (mg/L)	NA (mg/L)	TDS (mg/L)	Salinity (PSU)	Specific Conductance (μS/cm)
	From (m)	To (m)					
TPGW-1S	8.23	8.84	21200	11800	37200	38.909	58381
TPGW-1M	14.63	15.24	26700	14500	39600	48.97	71423
TPGW-1D	24.38	25.6	27000	14800	48200	50.08	72806
TPGW-4S	6.86	7.47	487	244	1150	1.12	2195
TPGW-4M	11.58	13.1	12900	7530	24500	25.8	40457
TPGW-4D	18.89	20.12	15500	8250	26600	27.52	42850
TPGW-5S	7.32	8.53	151	74.4	526	0.49	999
TPGW-5M	13.72	15.24	10700	5870	18000	19.7	31646
TPGW-5D	19.05	20.57	11800	6700	21100	22.71	35991
TPGW-7S	6.71	7.92	36.7	21.1	298	0.28	572
TPGW-7M	14.63	15.84	37.799	21.2	314	0.28	584
TPGW-7D	24.38	25.6	2130	876	5100	3.75	6840
TPGW-8S	5.18	6.4	31.8	17.1	216	0.21	444
TPGW-8M	10.67	11.28	31.8	17.6	360	0.31	643
TPGW-8D	15.09	16.31	43	25.2	382	0.34	705
TPGW-12S	6.71	7.31	16300	9480	29200	30.93	47659
TPGW-12M	17.07	18.29	23000	12800	41200	41.99	62472
TPGW-12D	27.43	28.65	23700	14100	41500	44.4	65603



FIGURES



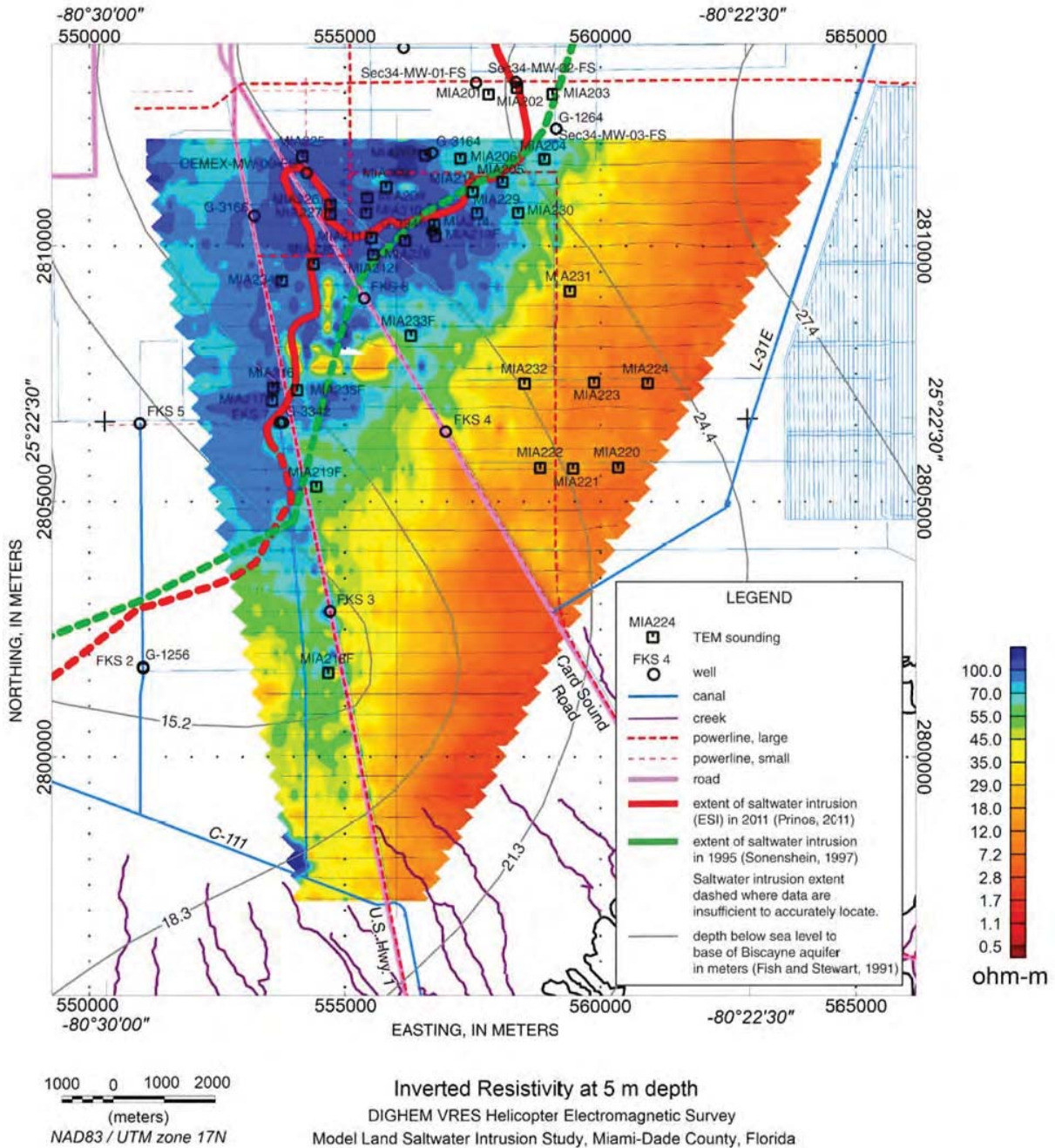
Caption:  
 Map showing the locations of salinity monitoring sites, time-domain electromagnetic soundings, water-level monitoring sites, and the mapped approximations of the inland extent of saltwater in the Biscayne aquifer in Miami-Dade and southern Broward Counties 1955, 1995, and 2011.

Prepared for:  
**Florida Power & Light**

**Subject Property:**  
 Turkey Point Nuclear Generating Station  
 Homestead, Florida



**Figure 1: USGS SW Interface**  
 Source: Prinos, Scott T.; Wacker, Michael A.; Cunningham, Kevin J.; Fitterman, David V., 2014. Origins and delineation of saltwater intrusion in the Biscayne aquifer and changes in the distribution of saltwater in Miami-Dade County, Florida. U.S. Geological Survey Scientific Investigations Report 2014-5025, Report: xi, 101 p.  
 Prepared by: E. Dare; April 29, 2016



Caption:  
 Resistivity at 5-meter depth from Fig 40, Fitterman et al., 2012.

Prepared for:  
**Florida Power & Light**

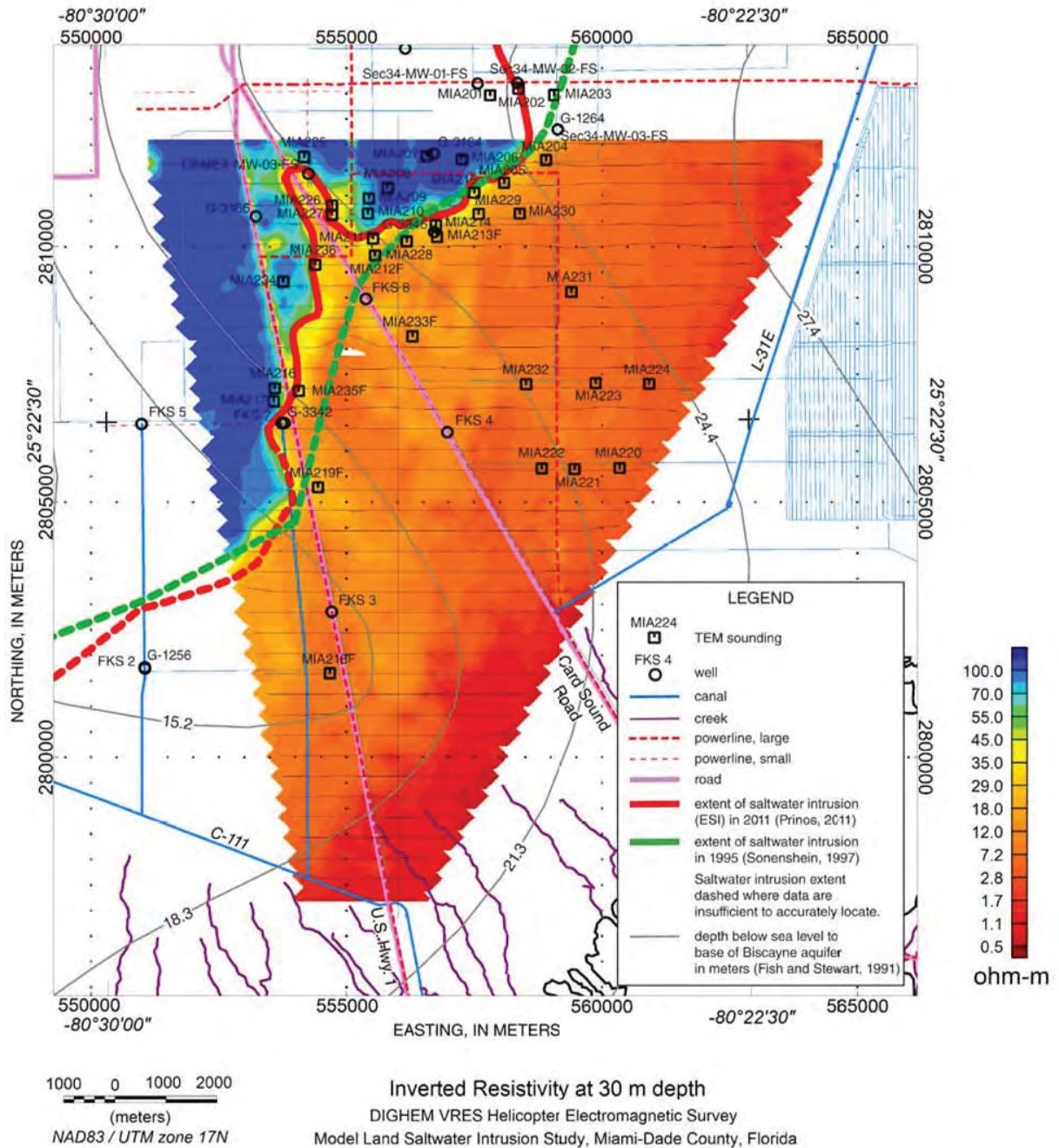
**Subject Property:**  
 Turkey Point Nuclear Generating Station  
 Homestead, Florida



**Figure 2: Fitterman et al 2012 Fig 40**

Source: Fitterman D.; Deszcz-Pan M.; Prinos S., 2012.  
 Helicopter Electromagnetic Survey of the Model Land Area,  
 Southeastern Miami-Dade County, Florida, U.S.  
 Geological Survey Open-File Report 2012-1176.





Caption:  
 Resistivity at 30-meter depth from Fig 43, Fitterman et al., 2012

Prepared for:  
**Florida Power & Light**

**Subject Property:**  
 Turkey Point Nuclear Generating Station  
 Homestead, Florida



**Figure 3: Fitterman et al 2012 Fig 43**

Source: Fitterman D.; Deszcz-Pan M.; Prinos S., 2012.  
 Helicopter Electromagnetic Survey of the Model Land Area,  
 Southeastern Miami-Dade County, Florida, U.S. Geological  
 Survey Open-File Report 2012-1176





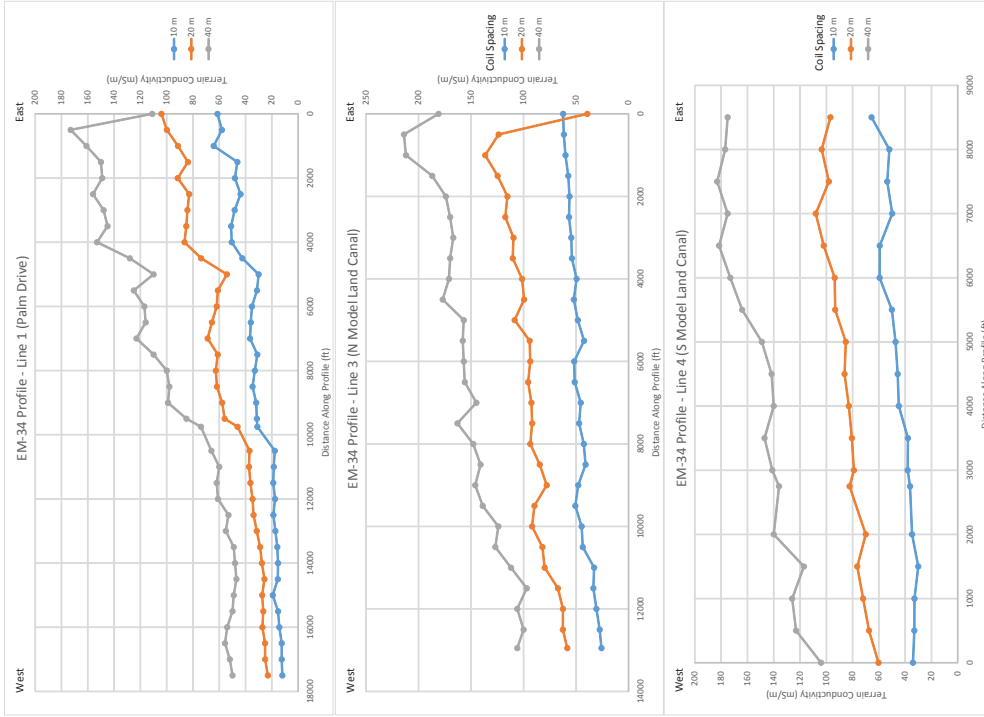
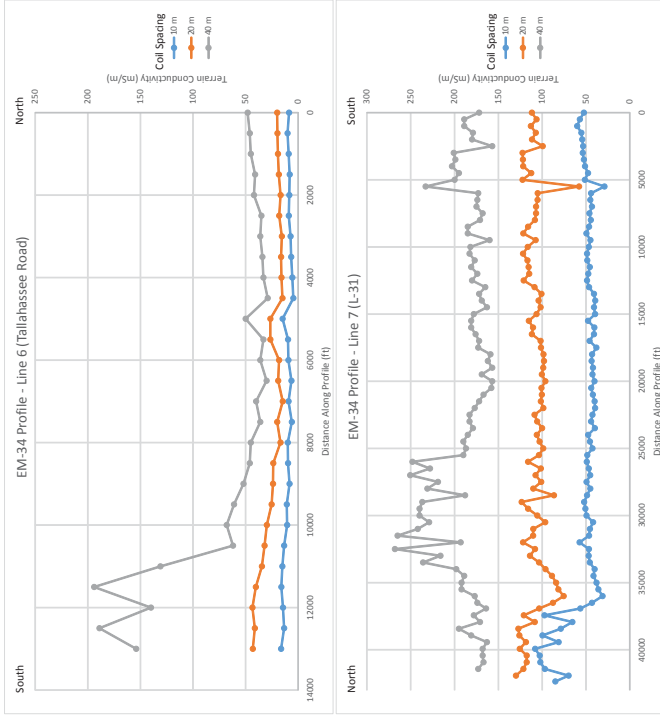
<p><b>Prepared for: Florida Power &amp; Light</b></p>	<p><b>ENERCON</b></p>
<p><b>Subject Property:</b>          Turkey Point Nuclear Generating Station          Homestead, Florida</p>	<p><b>Figure 4: EM-34 Survey Line Locations</b>          Source: Enercon Services, Inc;          ESRI World Imagery Basemap          Prepared by: E. Dare; April 28, 2016</p>
<p>1:80,000</p> <p>0 1.5 3 Miles</p>	<p>0 1.5 3 Miles</p>









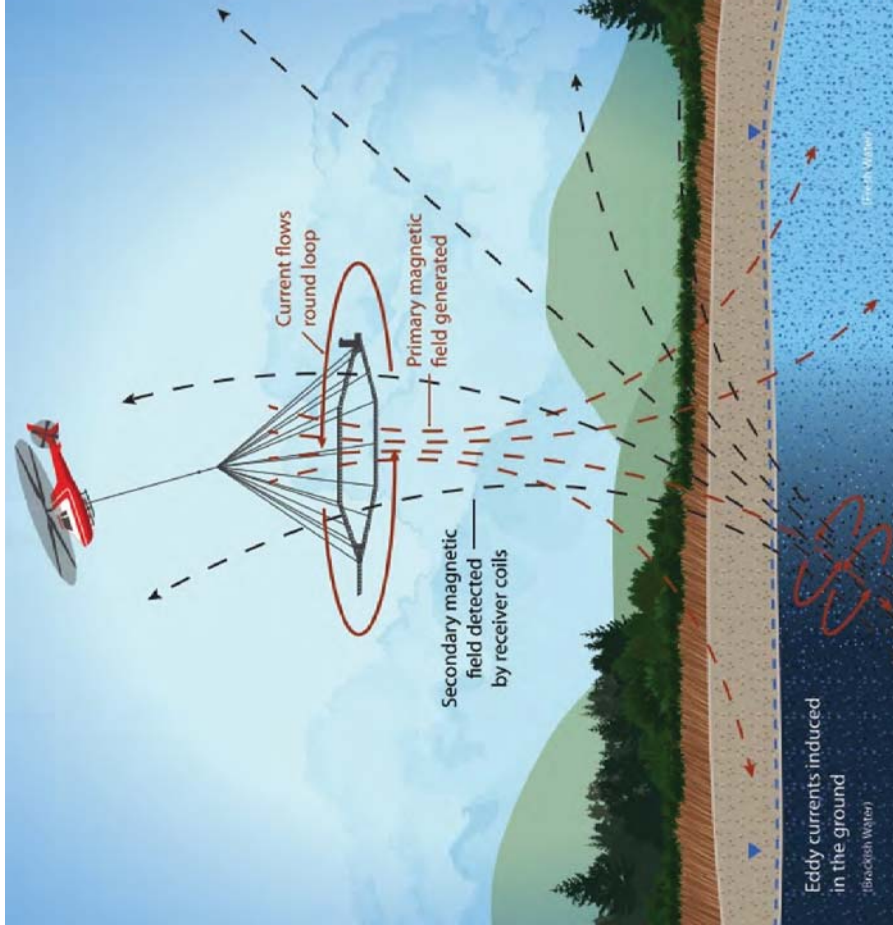


**Figure 7: EM 34 Apparent Conductivity Profiles**

Source: Enercon Services, Inc.; GeoView, Inc.  
 Prepared by: E. Dare; April 28, 2016

**Prepared for: Florida Power & Light**

**Subject Property:**  
 Turkey Point Nuclear Generating Station  
 Homestead, Florida



**Figure 8: Schematic of AEM Survey**

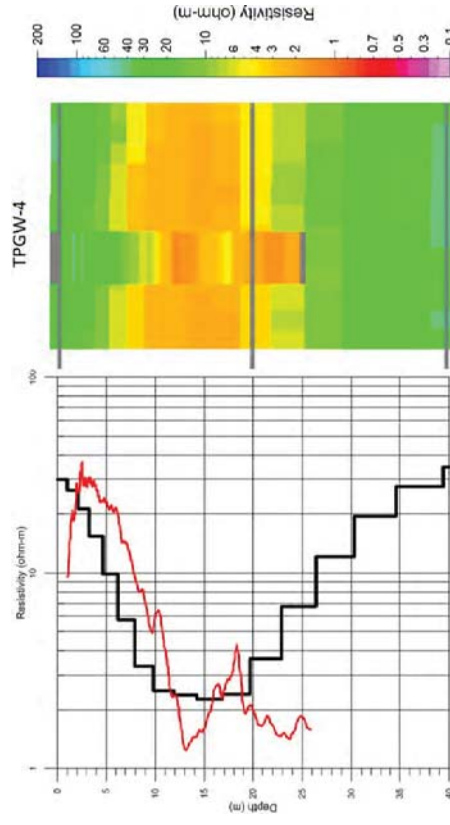
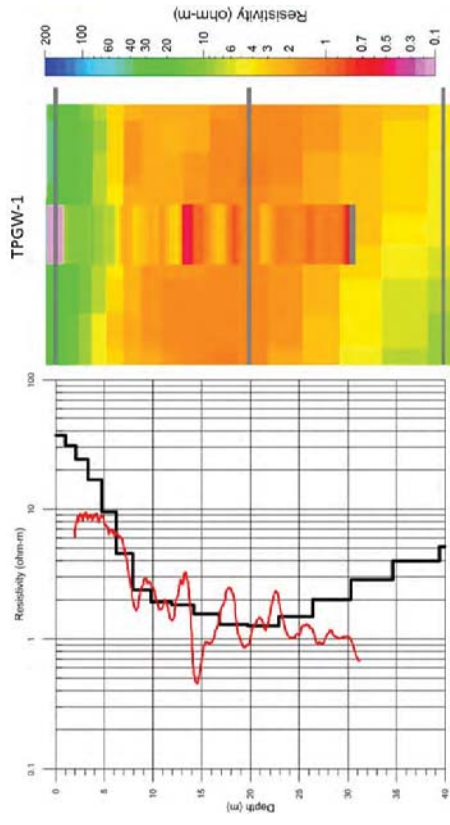
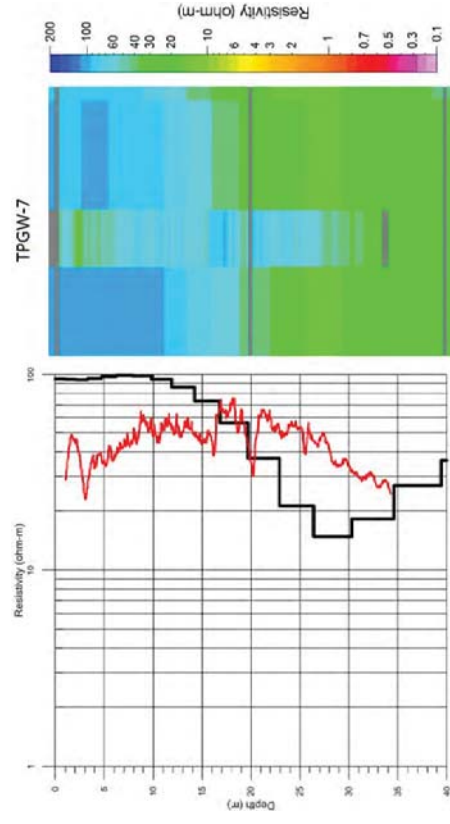
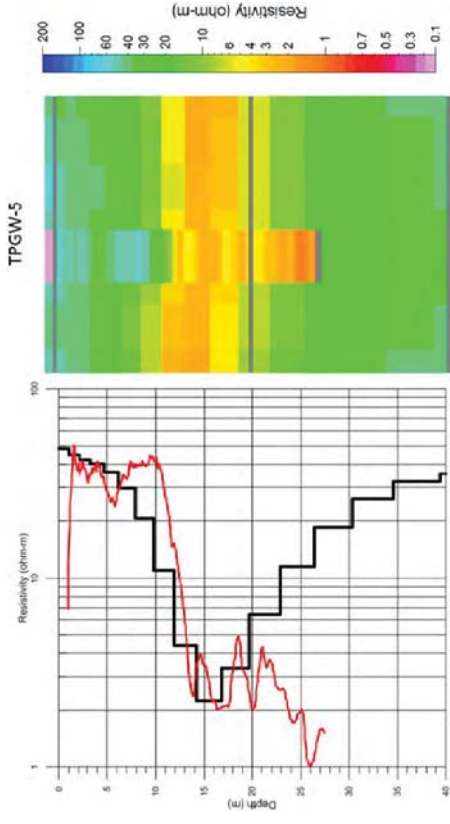
Reproduced from: "Report on Advanced Processing and Inversion of AEM Survey Data and Derived Chloride Concentrations near the Turkey Point Power Plant - Southern Florida. Aqua Geo Frameworks, Inc. 2016".  
Prepared by: E. Dare, April 28, 2016.

**Prepared for: Florida Power & Light**

**Subject Property:**

Turkey Point Nuclear Generating Station  
Homesstead, Florida





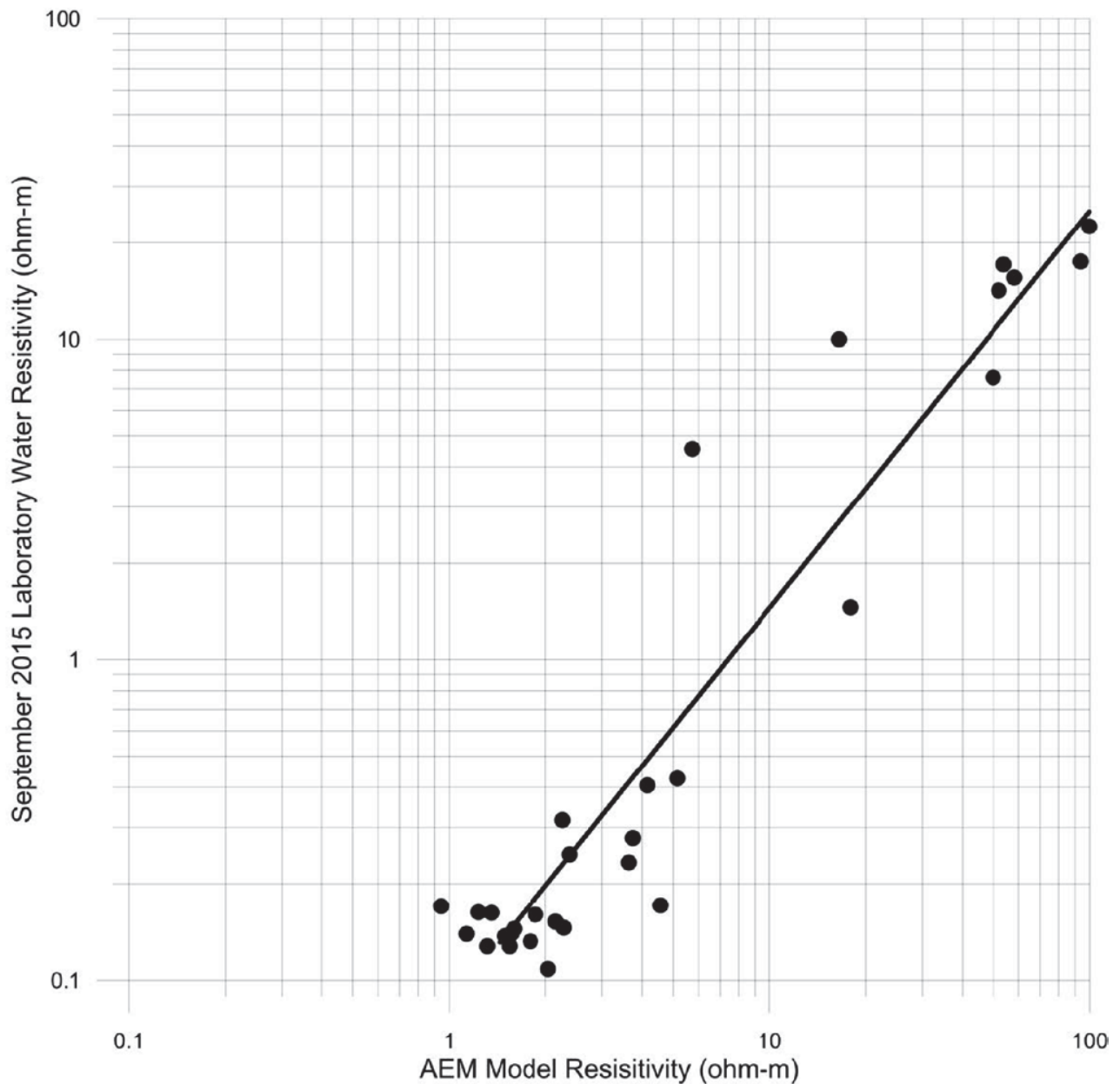
**Figure 9: Comparisons of Monitor Well Induction Logs with the AEM Resistivity Model**  
 Reproduced from: "Report on Advanced Processing and Inversion of AEM Survey Data and Derived Chloride Concentrations near the Turkey Point Power Plant, Southern Florida, Aqua Geo Frameworks, Inc. 2016"  
 Prepared by: E. Darr; April 28, 2016.

Prepared for: Florida Power & Light

**Subject Property:**  
 Turkey Point Nuclear Generating Station  
 Homestead, Florida



2016 AEM Water Resistivity = 0.08378(AEM Model Resistivity)<sup>1.2387</sup>  
 R<sup>2</sup>= 0.91



**Prepared for:**  
**Florida Power & Light**

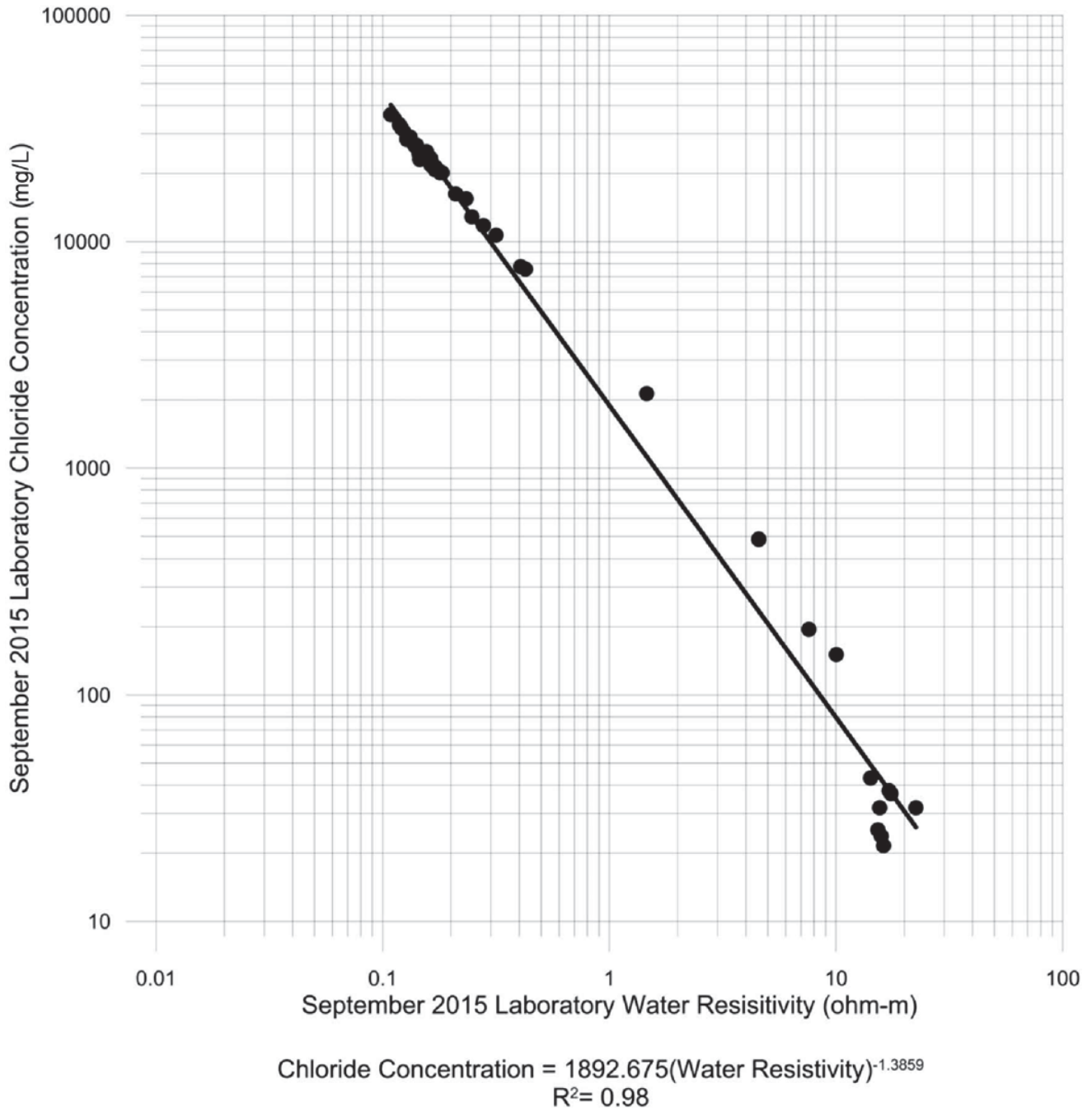
**Subject Property:**  
 Turkey Point Nuclear Generating Station  
 Homestead, Florida



**Figure 10: Formation Water Resistivities vs. AEM Resistivity**

Reproduced from: "Report on Advanced Processing and Inversion of AEM Survey Data and Derived Chloride Concentrations near the TurkeyPoint Power Plant, Southern Florida. Aqua Geo Frameworks, Inc. 2016"

Prepared by: E. Dare; April 28, 2016



**Prepared for:**  
 Florida Power & Light

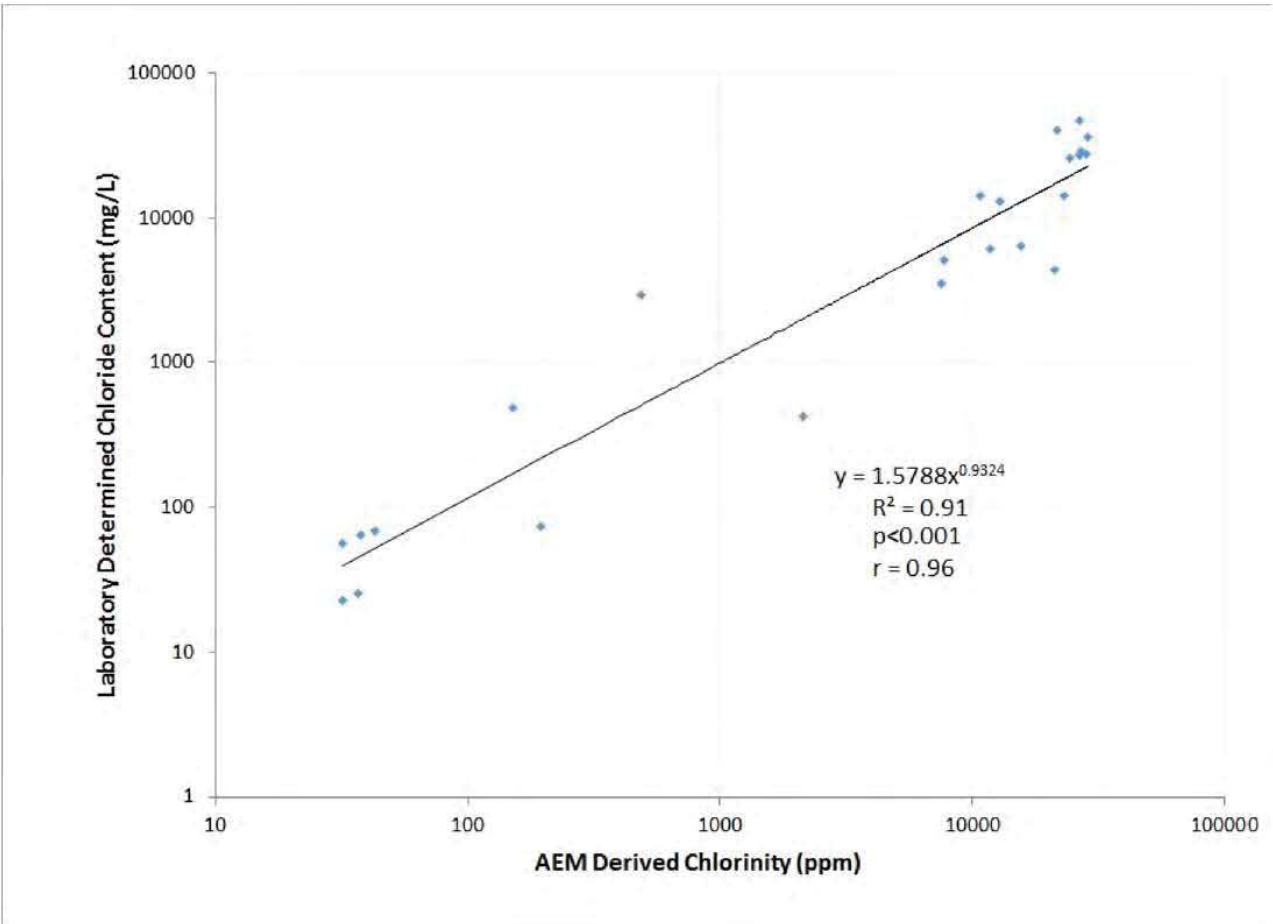
**Subject Property:**  
 Turkey Point Nuclear Generating Station  
 Homestead, Florida



**Figure 11: Formation Water Resistivities vs. Laboratory Chloride Concentrations**

Reproduced from: "Report on Advanced Processing and Inversion of AEM Survey Data and Derived Chloride Concentrations near the TurkeyPoint Power Plant, Southern Florida. Aqua Geo Frameworks, Inc. 2016"

Prepared by: E. Dare; April 28, 2016



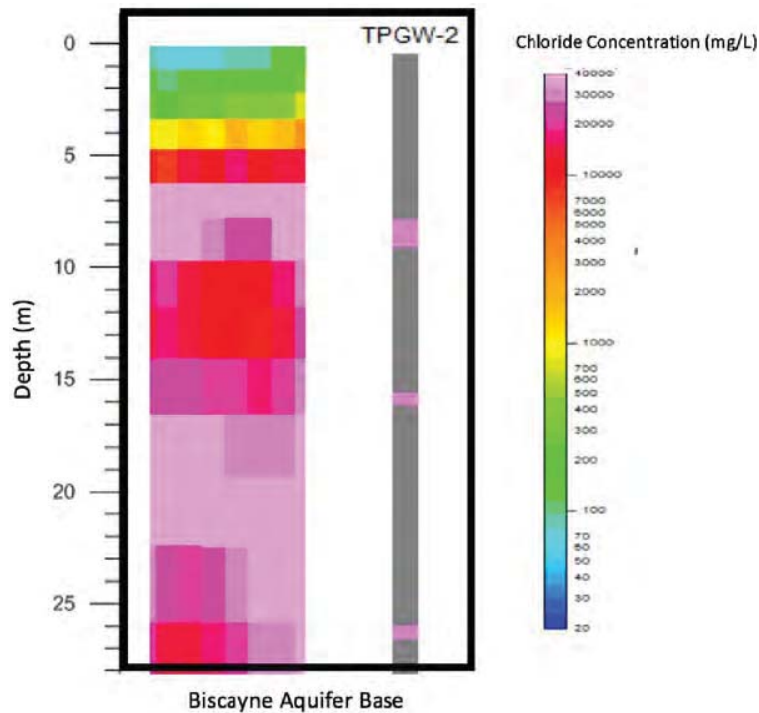
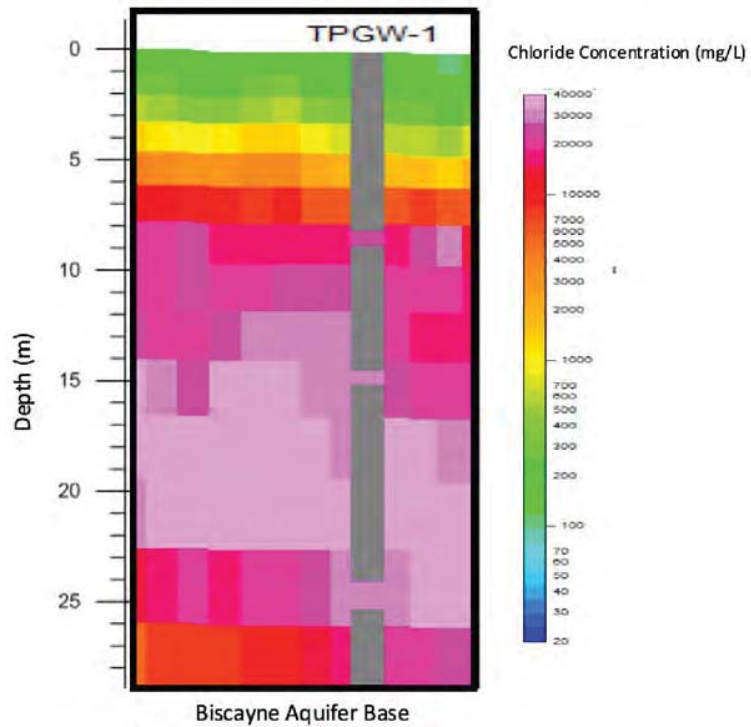
**Prepared for:**  
Florida Power & Light

**Subject Property:**  
Turkey Point Nuclear Generating Station  
Homestead, Florida



**Figure 12: AEM-Derived Chloride Concentration vs. Laboratory-Derived Chloride Concentration**

Prepared by: E. Dare; April 28, 2016



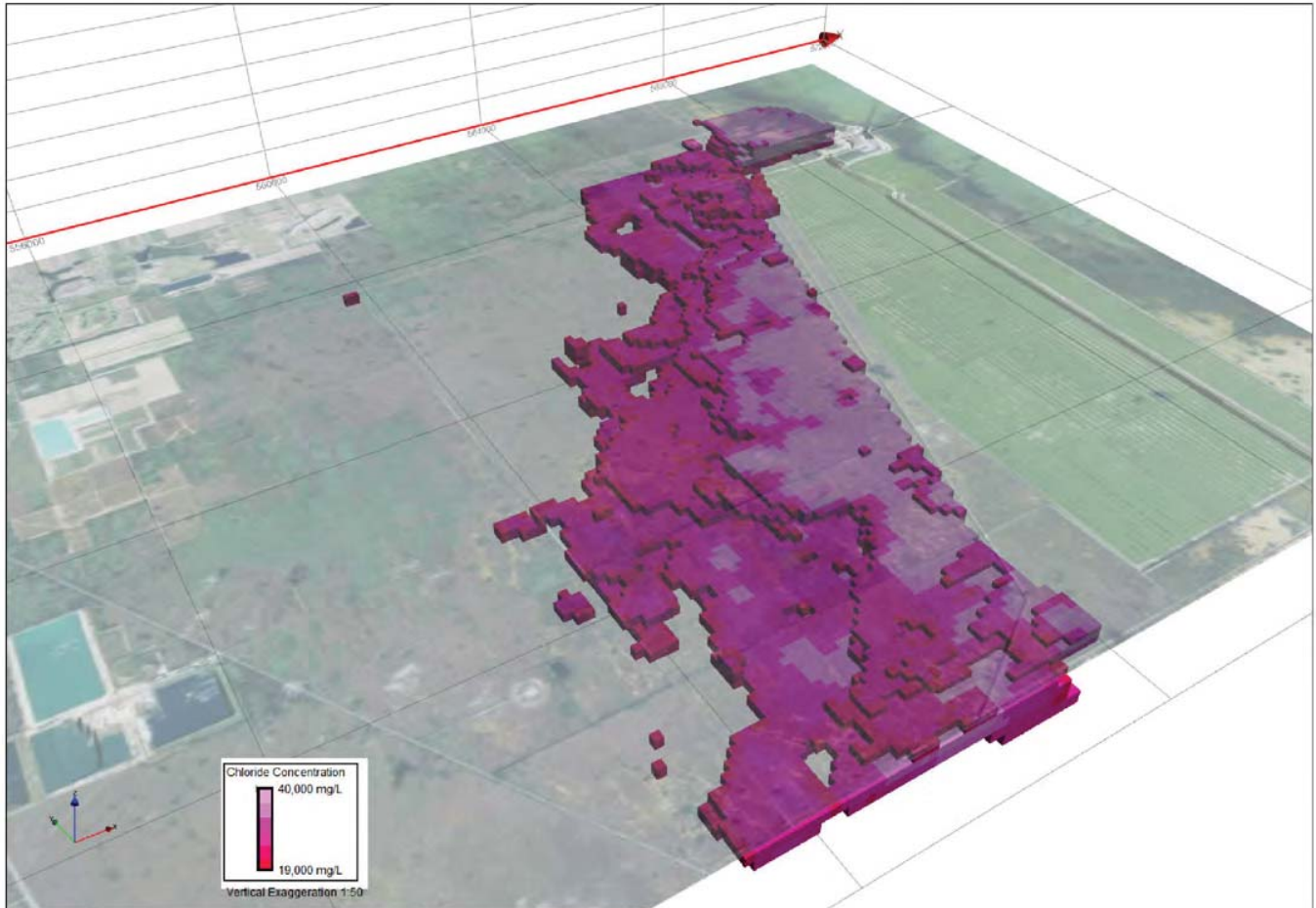
**Prepared for:**  
 Florida Power & Light

**Subject Property:**  
 Turkey Point Nuclear Generating Station  
 Homestead, Florida



**Figure 13: Depth Profiles Showing AEM Chloride vs Laboratory Chloride at Monitoring Wells**

Reproduced from: "Report on Advanced Processing and Inversion of AEM Survey Data and Derived Chloride Concentrations near the TurkeyPoint Power Plant, Southern Florida. Aqua Geo Frameworks, Inc. 2016"



**Prepared for:**  
**Florida Power & Light**

**Subject Property:**  
Turkey Point Nuclear Generating Station  
Homestead, Florida

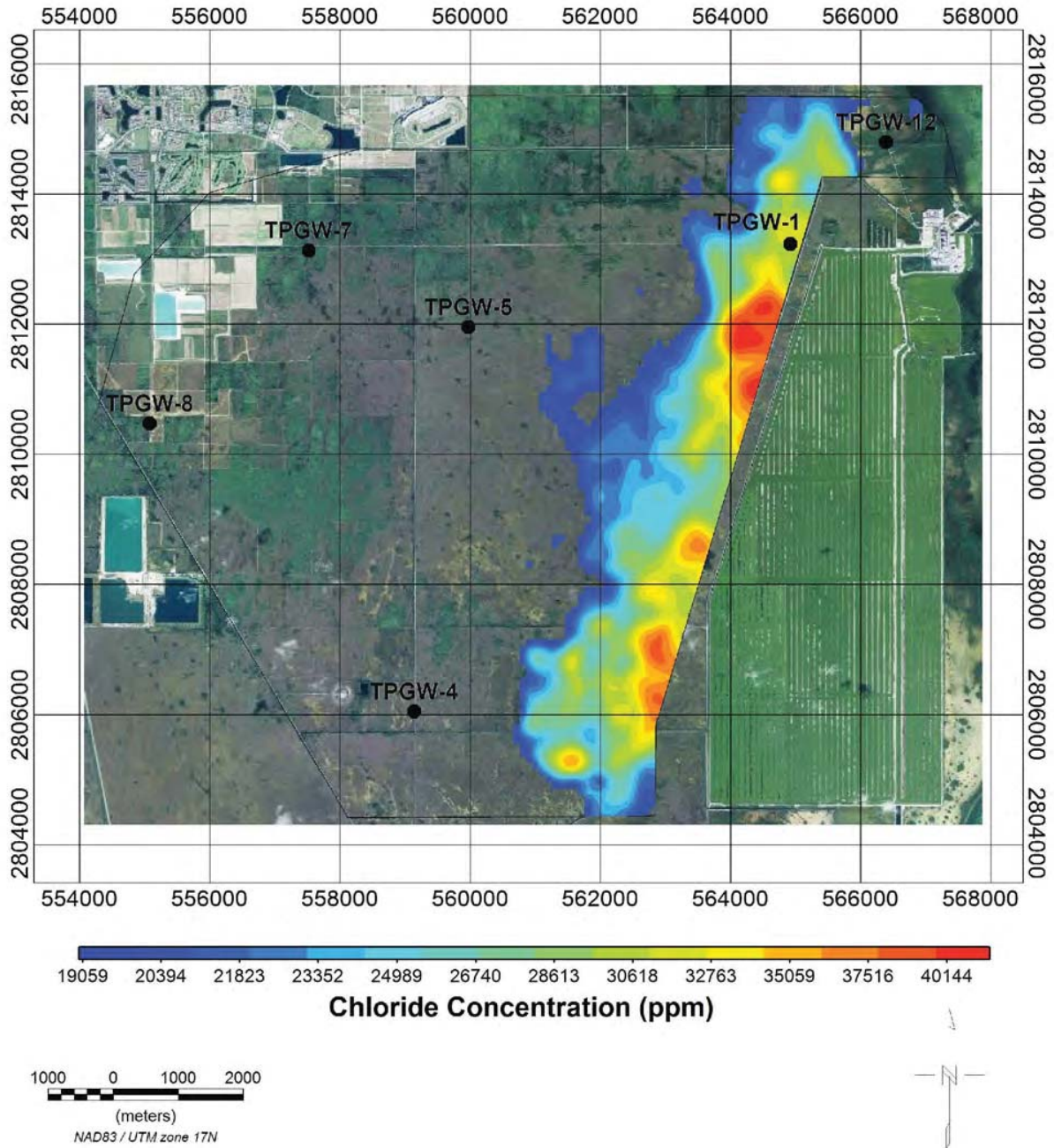


**Figure 14: 3D View of AEM Chloride Concentrations Greater than 19,000 mg/L (View to the Northeast)**

Reproduced from: "Report on Advanced Processing and Inversion of AEM Survey Data and Derived Chloride Concentrations near the TurkeyPoint Power Plant, Southern Florida. Aqua Geo Frameworks, Inc. 2016"

Prepared by: E. Dare; April 28, 2016





19059 20394 21823 23352 24989 26740 28613 30618 32763 35059 37516 40144  
**Chloride Concentration (ppm)**

1000 0 1000 2000  
 (meters)  
 NAD83 / UTM zone 17N

**Prepared for:**  
**Florida Power & Light**

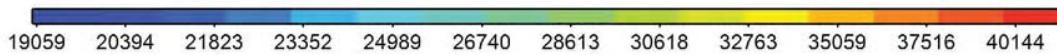
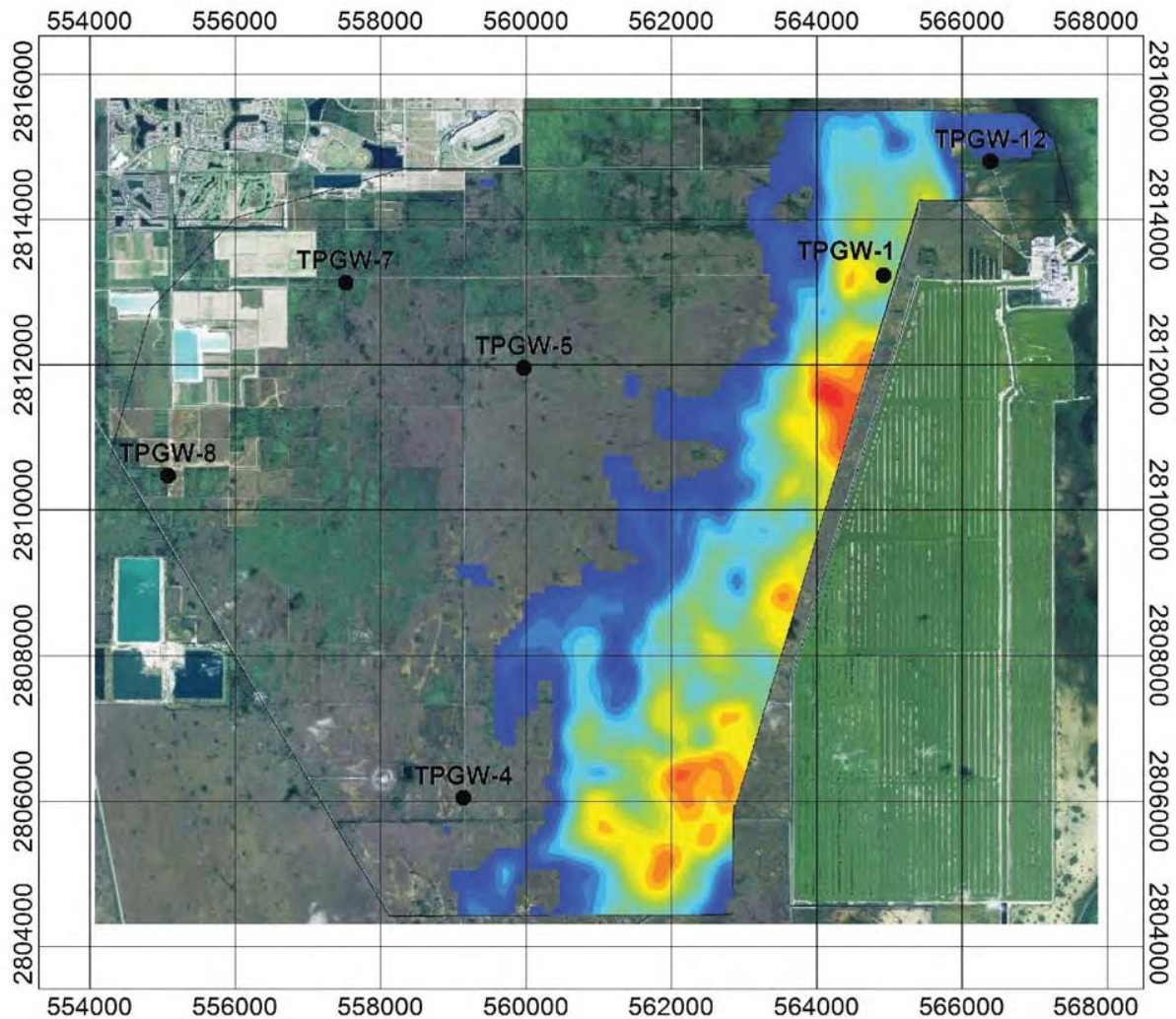
**Subject Property:**  
 Turkey Point Nuclear Generating Station  
 Homestead, Florida



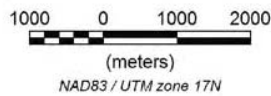
**Figure 15: Chloride Concentration Depth-Slice from Layer 12, 65 to 75 feet below land surface (19.7 to 22.9m)**

Reproduced from: "Report on Advanced Processing and Inversion of AEM Survey Data and Derived Chloride Concentrations near the TurkeyPoint Power Plant, Southern Florida. Aqua Geo Frameworks, Inc. 2016"  
 Prepared by: E. Dare; April 28, 2016





**Chloride Concentration (ppm)**



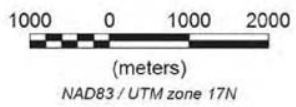
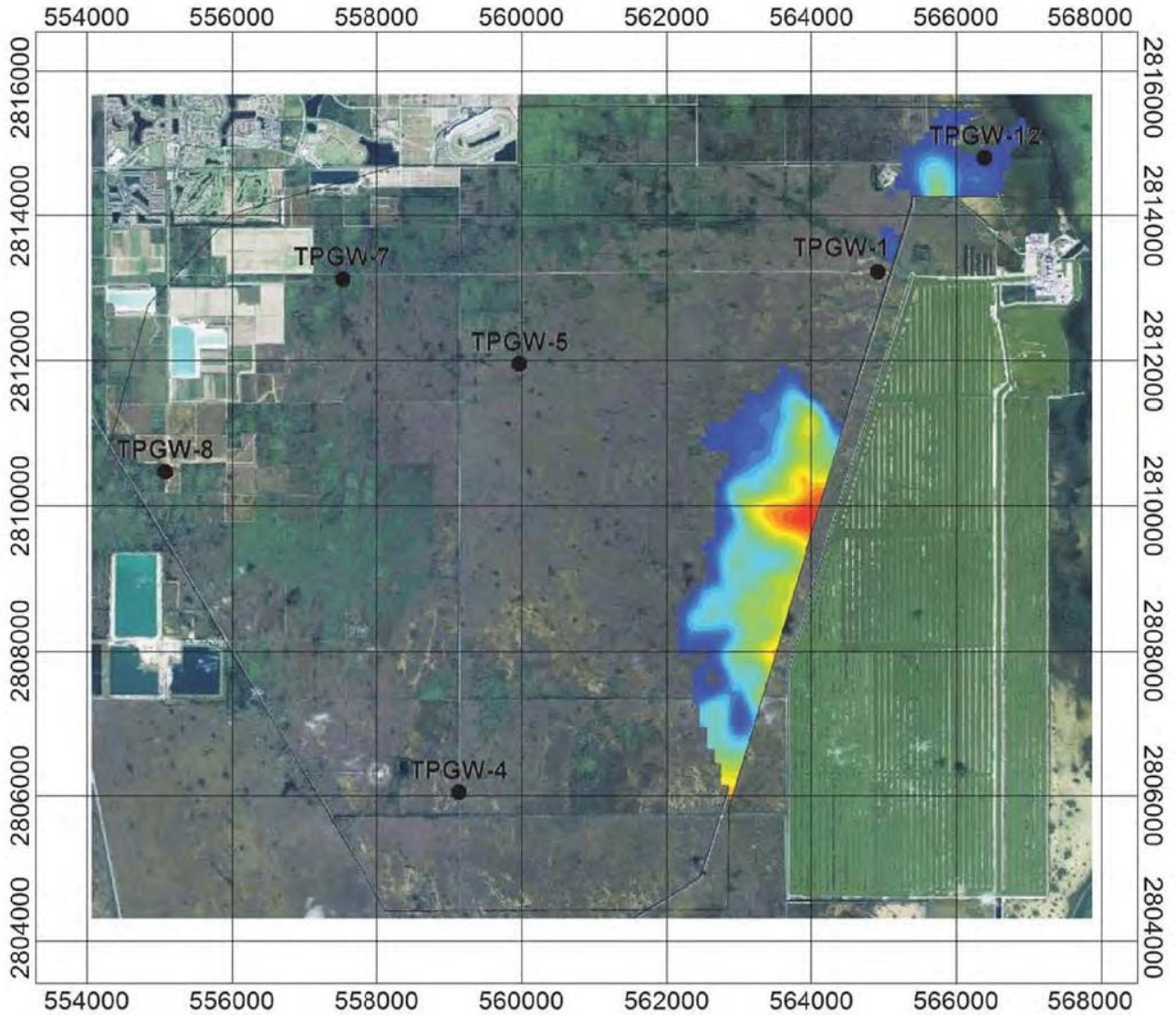
**Prepared for:**  
**Florida Power & Light**

**Subject Property:**  
 Turkey Point Nuclear Generating Station  
 Homestead, Florida



**Figure 16: Chloride Concentration Depth-Slice from Layer 11, 55 to 65 feet below land surface (16.8 to 19.7m)**

Reproduced from: "Report on Advanced Processing and Inversion of AEM Survey Data and Derived Chloride Concentrations near the TurkeyPoint Power Plant, Southern Florida. Aqua Geo Frameworks, Inc. 2016"  
 Prepared by: E. Dare; April 28, 2016



**Prepared for:**  
**Florida Power & Light**

**Subject Property:**  
 Turkey Point Nuclear Generating Station  
 Homestead, Florida



**Figure 17: Chloride Concentration Depth-Slice from Layer 14, 87 to 100 feet below land surface (26.4 to 30.3m)**

Reproduced from: "Report on Advanced Processing and Inversion of AEM Survey Data and Derived Chloride Concentrations near the TurkeyPoint Power Plant, Southern Florida. Aqua Geo Frameworks, Inc. 2016"  
 Prepared by: E. Dare; April 28, 2016



APPENDIX A  
GEOVIEW REPORT

- 03(1 6 ,5468  
. ,45/=70\*(1 03:,780.(8043  
583 \* 44103. \* (3(1 7=78,2 708,  
2 0(20 + (+, \* 4938= Ä -1460+(

Prepared for Enercon Services, Inc.  
Tampa, Florida

Prepared by GeoView, Inc.  
St. Petersburg, FL





April 14, 2016

Mr. Craig R. Oural  
Enercon Services, Inc.  
12906 Tampa Oaks Blvd., Suite 131  
Tampa, FL 33637

7P?GB@O8 M J N IOO>HÄHJ>HÄGÜMÄ.BLESNF@>HÄNDQKJ  
583 Ä KKHÄ>J>HÄSNBI ÄFOB ÈI F +>ABÄ KEJGÄ HKMF  
.BK:FBR 5MKGBÄ3PPBM\$%\$&%

Dear Mr. Oural,

GeoView, Inc. (GeoView) is pleased to submit the final report that summarizes and presents the results of the geophysical investigation performed at the above referenced site. GeoView appreciates the opportunity to have assisted you on this project. If you have any questions or comments about the report, please contact us.

Sincerely,

. ,4 : 0; ÄÖ!

A handwritten signature in black ink, appearing to read "Michael J. Wightman".

Michael J. Wightman, P.G.  
President  
Florida Professional Geologist  
Number 1423

*A Geophysical Services Company*

4610 Central Avenue  
St. Petersburg, FL 33711

Tel.: (727) 209-2334  
Fax: (727) 328-2477

**801, A4-A\*438,387**

1.0	INTRODUCTION .....	1
2.0	DESCRIPTION OF GEOPHYSICAL INVESTIGATION	
2.1	Electrical Resistivity Testing .....	1
2.2	Transient Electromagnetic Domain Testing .....	2
2.3	Analysis of VES and TEM Data.....	3
3.0	SURVEY RESULTS .....	3
3.1	Electrical Resistivity Testing .....	3
3.2	Transient Electromagnetic Domain Testing .....	3
4.0	LIMITATIONS.....	4

APPENDIX 1-Figures

- Figure 1 Site Map Showing Locations of Geophysical Test Sites
- Figures 2-9: West to East and North to South VES Geo-Electrical Profiles
- Figure 10: Comparison of VES 12 and TEM 2 Results

APPENDIX 2-Electrical Resistivity Testing Results

APPENDIX 3- Transient Electromagnetic Domain Testing Results



#!" AJOMP@KJ

A geophysical and hydrogeological investigation was performed as part of a study to assess the vertical and lateral extent of groundwater impacts associated with the hypersaline waters contained within the cooling canal system for the Turkey Point power plant located east of Homestead, FL. GeoView performed vertical electrical soundings (VES) and time domain electromagnetic (TEM) soundings as part of the investigation.

\$!" A BN@FKJ KC BKESN @HQBND>OK

The geophysical investigation was conducted over a period of eleven field days between the dates of January 20-February 3, 2016. The location of the VES and TEM testing sites are provided on Figure 1. The investigation was conducted under the supervision of Mr. Michael J. Wightman, P.G., President, GeoView, Inc. A brief description of scope and field procedures associated with each of the geophysical methods is as follows:

### 2.1 DC Electrical Resistivity Testing

The DC electrical resistivity testing was done to determine a vertical profile of electrical resistance of earth materials at various locations throughout the project site. The resistance of the earth materials was measured by passing an electrical current between two-electrodes placed in the earth and measuring the resultant induced voltage potential between two other electrodes. By taking into account the geometry of the electrodes and by increasing the spacing between the electrodes, the induced voltage reading was converted into the electrical resistivity of the earth materials at various depth intervals.

The resistivity testing was done using a Wenner four-point array. In such an array there are total of four electrodes that are spaced an equal distance apart. A collection of resistivity measurements were gathered from a common center point using a range of distances between electrodes (commonly referred to as “a-spacings”). The collection of resistivity measurements at various “a spacings” about a center point is referred to as a vertical electrical sounding (VES).

The “a spacings” used for the investigation ranged from 2.5 to 200 ft. Additional readings were collected at some VES locations using electrode spacing’s of 250, 300 and 400 ft. An increased “a spacing” was used at these locations in order to provide an increased depth of exploration. A R8 Super Sting resistivity system, manufactured by Advanced Geosciences, Inc. was used for the investigation. This equipment was calibrated per manufacturer’s recommendations prior to the investigation.

The VES testing was performed at a total of 24 locations throughout the project site. Seventeen of the VES's were performed at the locations specified in original project proposal. The additional seven VES's were performed in areas where TEM soundings could not be performed due to the interference effects caused by proximate high-tension power lines (further discussion in Section 2.2).

## 2.2 Time Domain Electromagnetics

Similar to the VES testing, the TEM soundings were done to determine a vertical profile of electrical resistance of earth materials at various locations throughout the project site. The TEM method operates on a completely different principle than the DC electrical resistivity (VES) method. In the TEM method, a primary electrical field is created within a large current loop (transmitter loop) placed on the ground surface. This primary electrical field is very rapidly shut off. The resultant change in the EMF field created by the termination of the transmitter loop current creates a high-amplitude current field which radiates down into the ground. This current field creates a secondary field in the subsurface earth materials. By sampling the associated voltage response of this secondary field at discrete time intervals, a vertical profile earth resistivity is obtained.

The TEM method is sensitive to the presence of ambient high-strength electrical fields as those that are created by high-tension power lines. These background electrical fields overwhelm the response associated with the secondary electrical fields and make the data non interpretable.

The TEM survey was performed using a Geonics TEM47 system. The transmitter loop consisted of a 16-gauge copper wire that was laid out in a 20 by 20 meter (m) square. The high-frequency receiver coil was placed 20 m outside of the outer edge of the transmitter wire. The data was collected over a 30-gate time period at a frequency of 30 Hz.

It was originally proposed that a TEM survey be conducted at 20 locations across the project site. The majority of the TEM locations were either directly under or very close to high-tension power lines associated with the power plant. Prior to the performance of a TEM survey at a given location, the TEM receiver coil was set up and the effect of the ambient electrical fields created by the high-tension powerlines upon the TEM equipment was evaluated. It was determined that the interference effect from the powerlines overwhelmed the TEM instrument response in all but one of the 20 proposed locations. The location of the TEM test site (TEM 2) is provided on Figure 1.

### 2.3 Analysis of VES and TEM Data

The VES and TEM data was analyzed using IX1D TEM, a software program developed by Interpex, Inc. The following information was provided in the analysis:

- A 3-6 layer hydrogeological model of conditions at each of the study sites.
- An equivalence analysis of the layered model solution showing the quality and uniqueness of the individual layer resistivity's and thicknesses.
- A smooth model in which resistivity values were assigned for each data point at a calculated depth range.

### 3.1 Electrical Resistivity Testing

Geo-Electrical profiles developed from the individual VES smooth model results are presented as Figures 2-9 (Appendix 1). These ten profiles are labeled as A-A' to H-H' and are shown on Figure 1. The VES profiles A-A' to D-D' (Figures 2-5) trend west to east while VES Profiles E-E' to H-H' (Figures 6-9) trend north to south. The following resistivity ranges were used for estimating water quality:

- Fresh: < 100 Ohm-m
- Brackish: 100-10 Ohm-m
- Saline: 10-2 Ohm-m
- Hypersaline: < 2 Ohm-m

Modeling results presenting the 3-5 layer hydrogeological model, equivalence analysis and smooth model for each of the VES sites are provided in Appendix 2.

### 3.2 Time Domain Electromagnetics

A comparison of the modeling results between the TEM 2 and VES 12 (which conducted at the same location) is provided on Figure 10. The results do not compare well. The reason for this poor correlation are not known. It is possible that the instrumentation platform created some type of interference effect. However, the transmitter loop was set up approximately 50 meters away from the platform. Based on the water quality information from Monitor Well TPGW-5, it appears that the results from the VES sounding are the best representation of conditions at the site. The modeling results presenting the 4-6 layer hydrogeological models, equivalence analysis and smooth model for the TEM 2 site is provided in Appendix 3.

Page 4

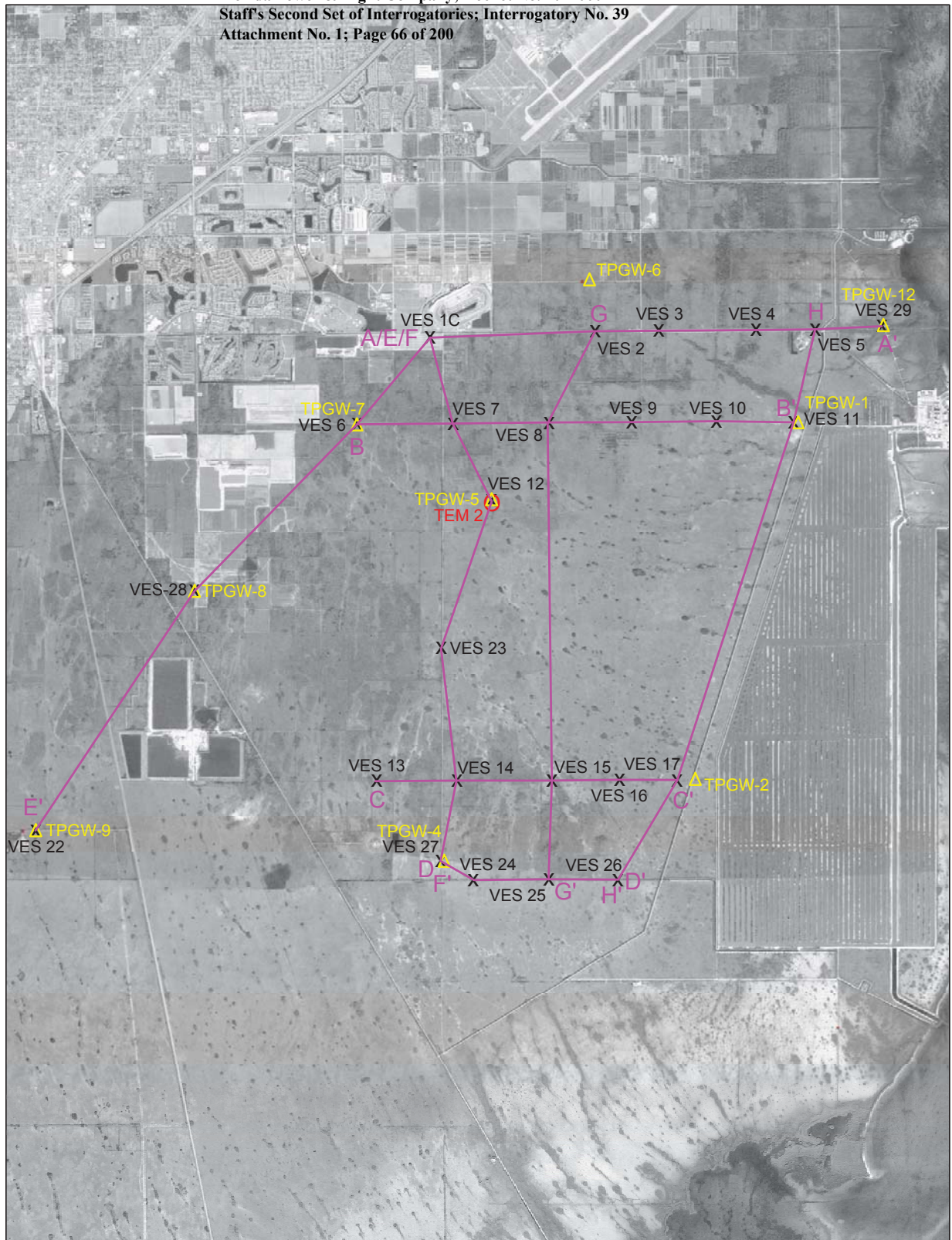
**&!Ā H IO>B.N**

The results of the VES and TEM survey are based on our professional evaluation of the data and our experience with such investigations in the State of Florida. The VES survey was performed in general accordance to ASTM Standards G57-95a entitled "Standard Test Method for Field Measurement of Soil Resistivity Using the Wenner Four-Electrode Method". The TEM survey was conducted in accordance with the manufacturer's guidelines. The results provided in this report meet the standards of care for our profession. No other warranty or representation, either expressed or implied, is included or intended.

( 55,3+ 0< #  
- 0.96 ,7



Florida Power & Light Company; Docket No. 20170007-E1  
Staff's Second Set of Interrogatories; Interrogatory No. 39  
Attachment No. 1; Page 66 of 200



**EXPLANATION (GEOVIEW)**

- VES 20 x LOCATION OF VERTICAL ELECTRICAL SOUNDING
- TEM 2 O LOCATION OF TEM SOUNDING
- TPGW-5 Δ LOCATION OF MONITOR WELLS
- A—A' GEO-ELECTRICAL CROSS-SECTION WITH DESIGNATION (FIGURES 2-9)

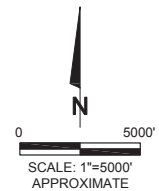


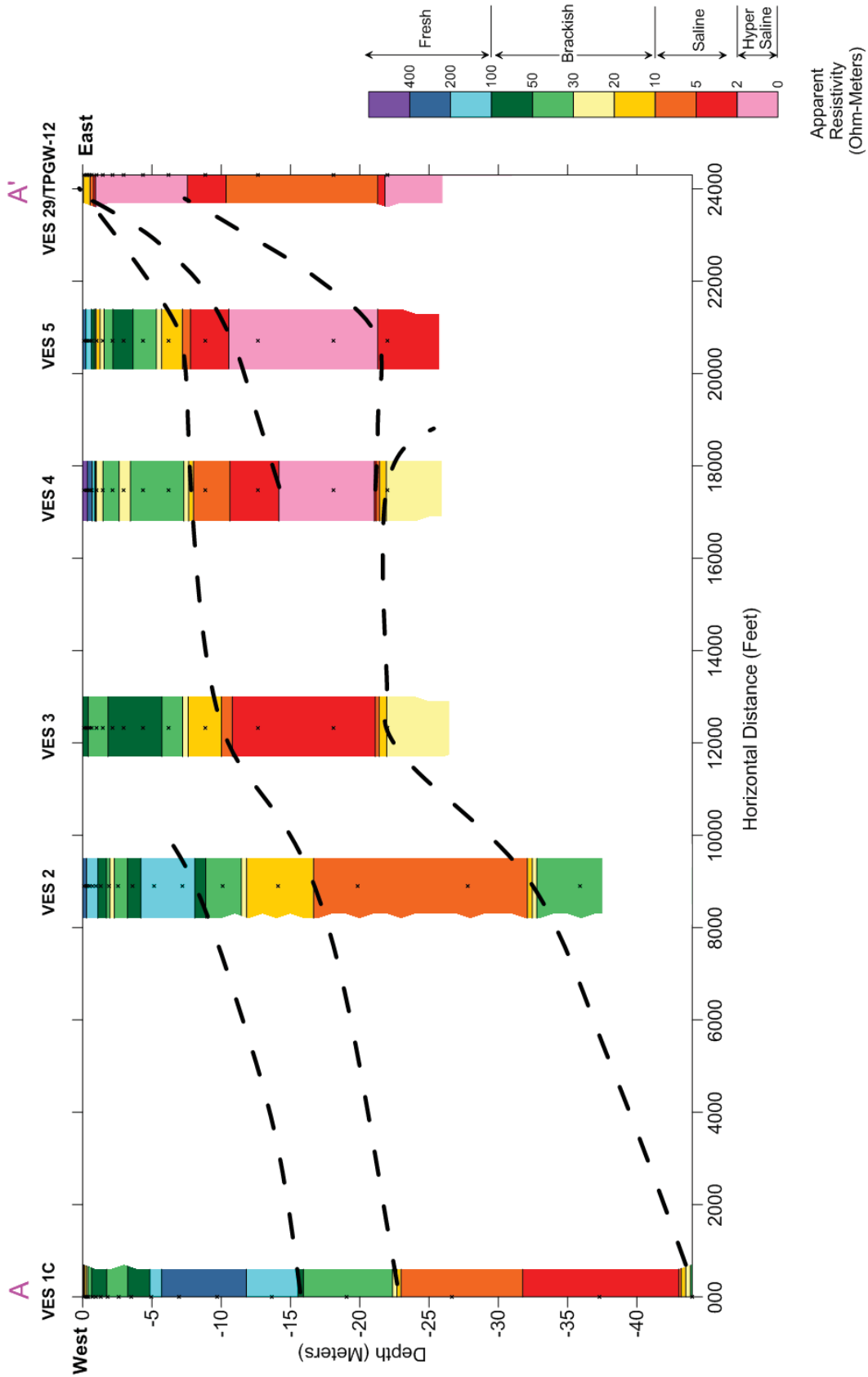
FIGURE 1  
SITE MAP  
SHOWING LOCATION OF  
GEOPHYSICAL TEST SITES

PTN COOLING CANAL SYSTEM  
HOMESTEAD, FLORIDA

ENERCON SERVICES, INC.  
TAMPA, FLORIDA

PROJECT:  
23243  
DATE:  
04/11/16





**FIGURE 2**

**GEO-ELECTRICAL CROSS-SECTION  
 VES PROFILE 1C-2-3-4-5-29**

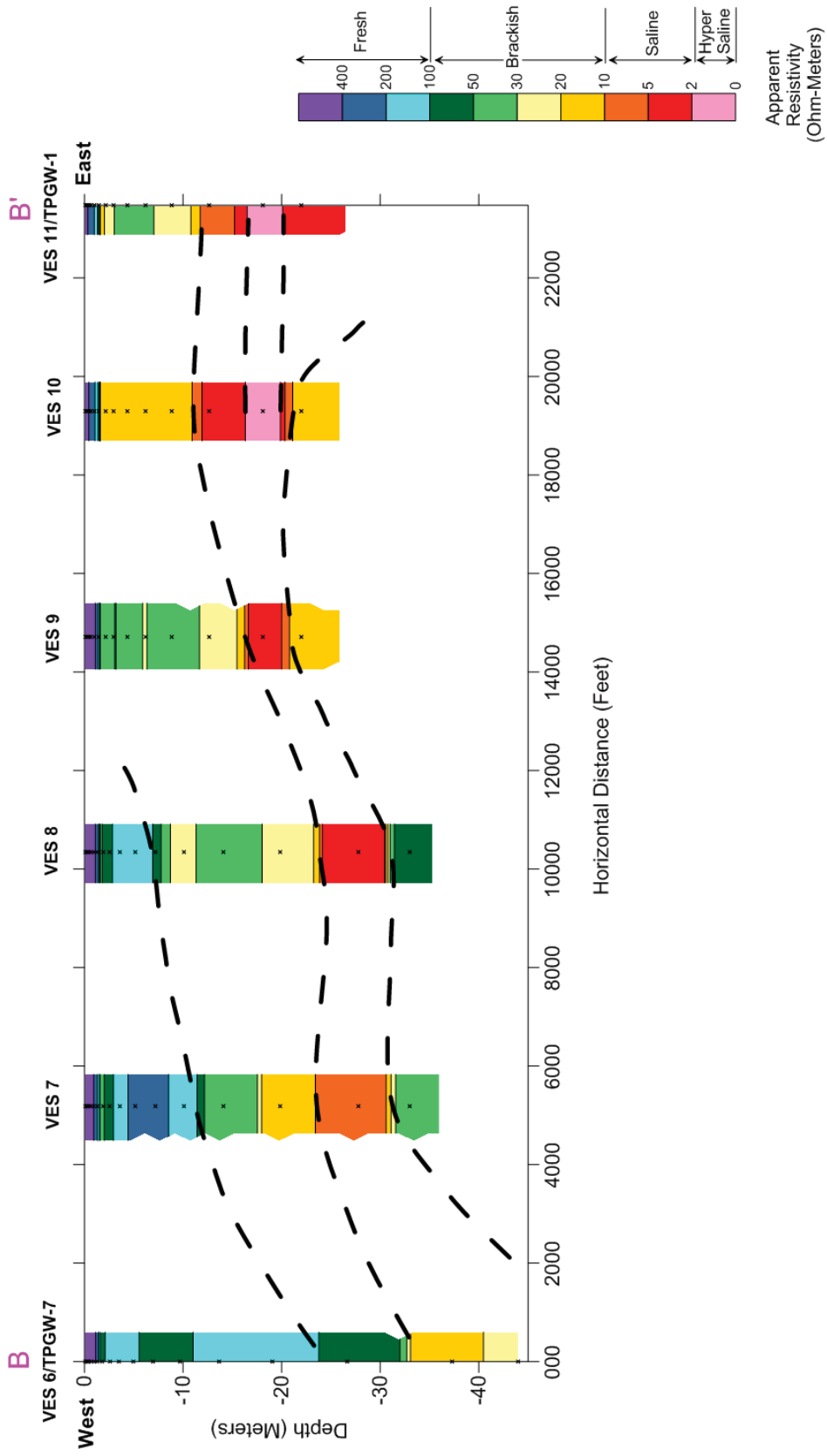
**PTN COOLING CANAL SYSTEM SITE  
 HOMESTEAD, FLORIDA**

**ENERCON SERVICES, INC.  
 TAMPA, FLORIDA**

**PROJECT:  
 23243**

**DATE:  
 04/11/16**





**FIGURE 3**

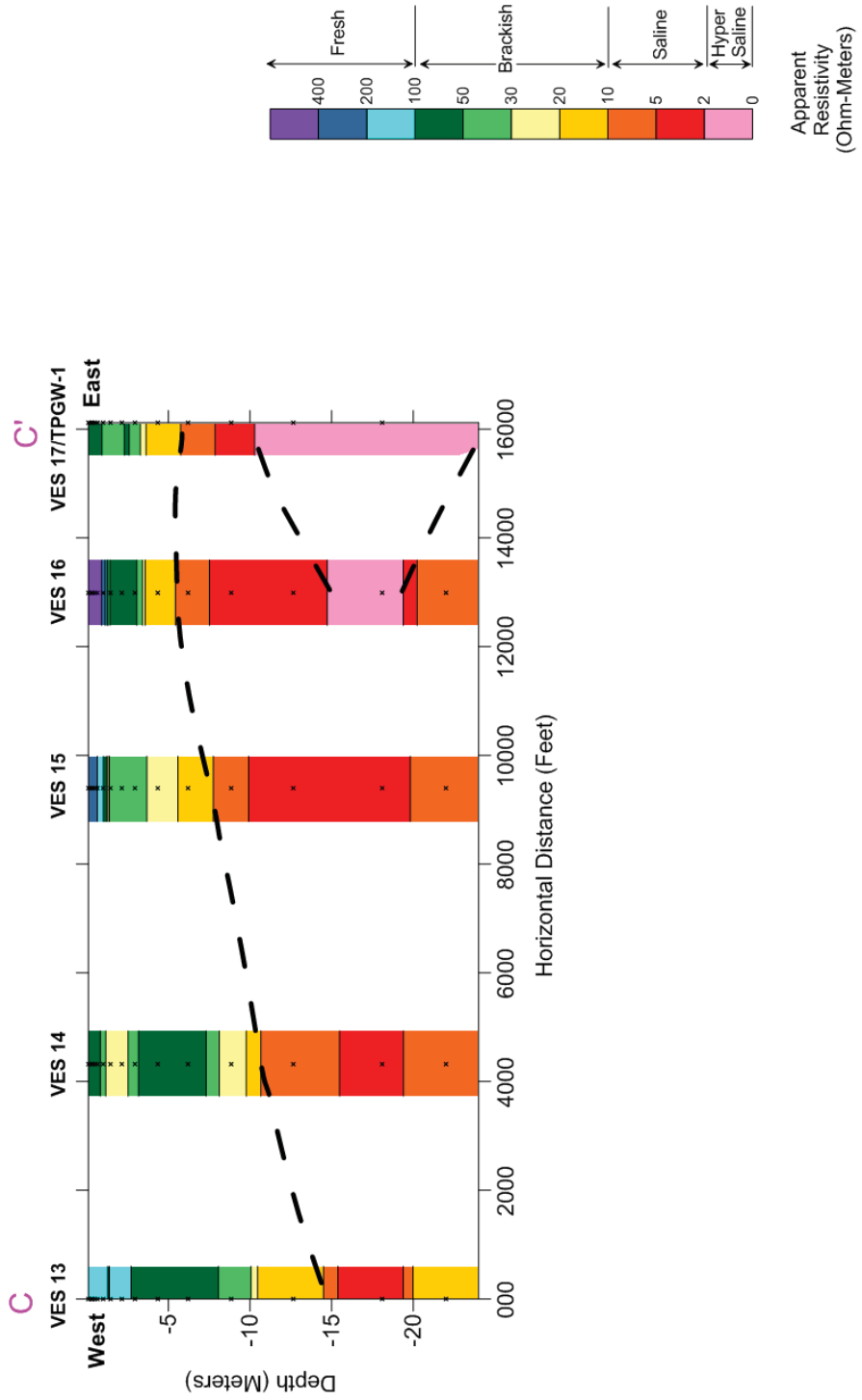
PTN COOLING CANAL SYSTEM SITE  
 HOMESTEAD, FLORIDA

PROJECT:  
 23243  
 DATE:  
 04/11/16

ENERCON SERVICES, INC.  
 TAMPA, FLORIDA

GEO-ELECTRICAL CROSS-SECTION  
 VES PROFILE 6-7-8-9-10-11






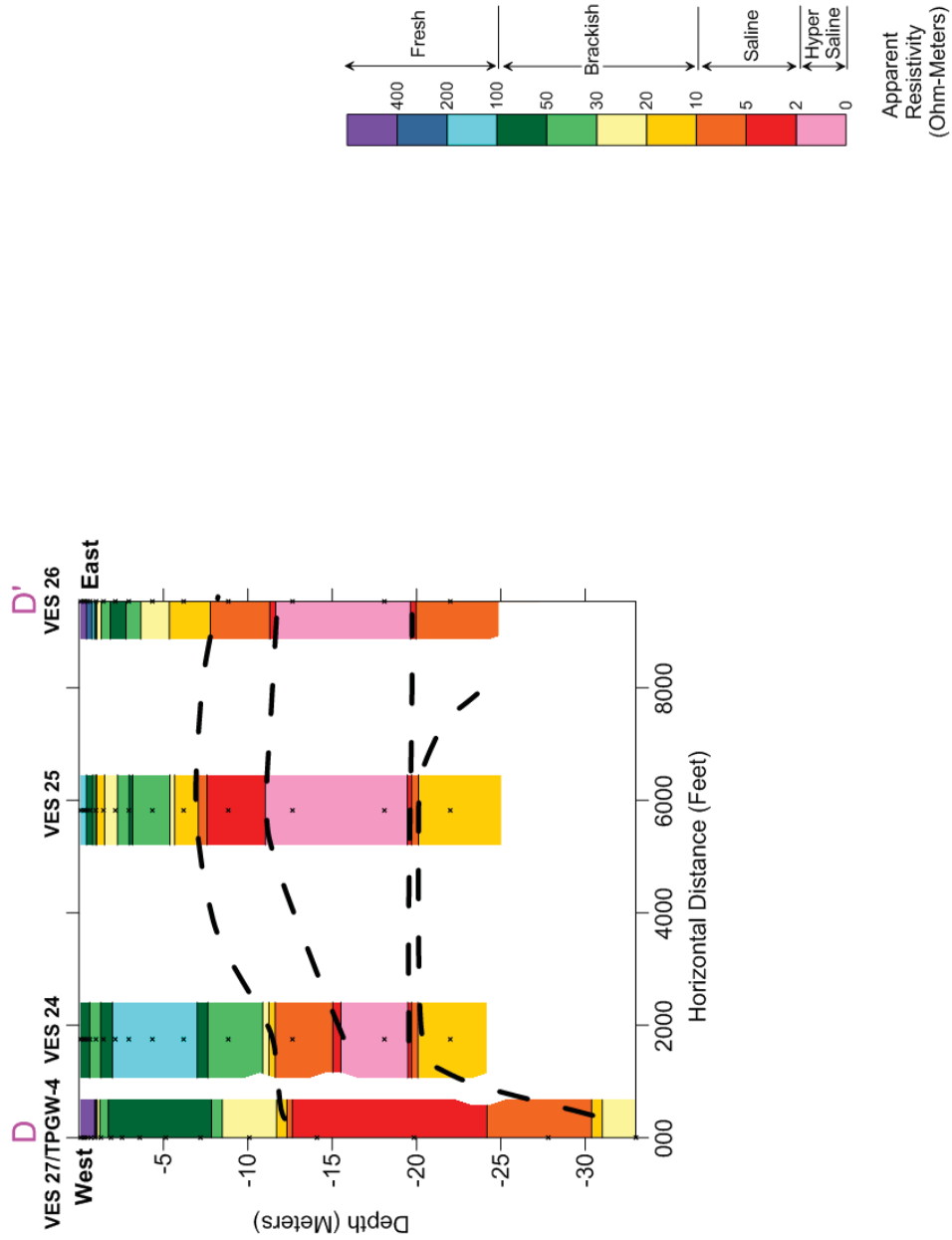
**FIGURE 4**  
 GEO-ELECTRICAL CROSS-SECTION  
 VES PROFILE 13-14-15-16-17

PTN COOLING CANAL SYSTEM SITE  
 HOMESTEAD, FLORIDA

PROJECT:  
 23243  
 DATE:  
 04/11/16

ENERCON SERVICES, INC.  
 TAMPA, FLORIDA





**FIGURE 5**

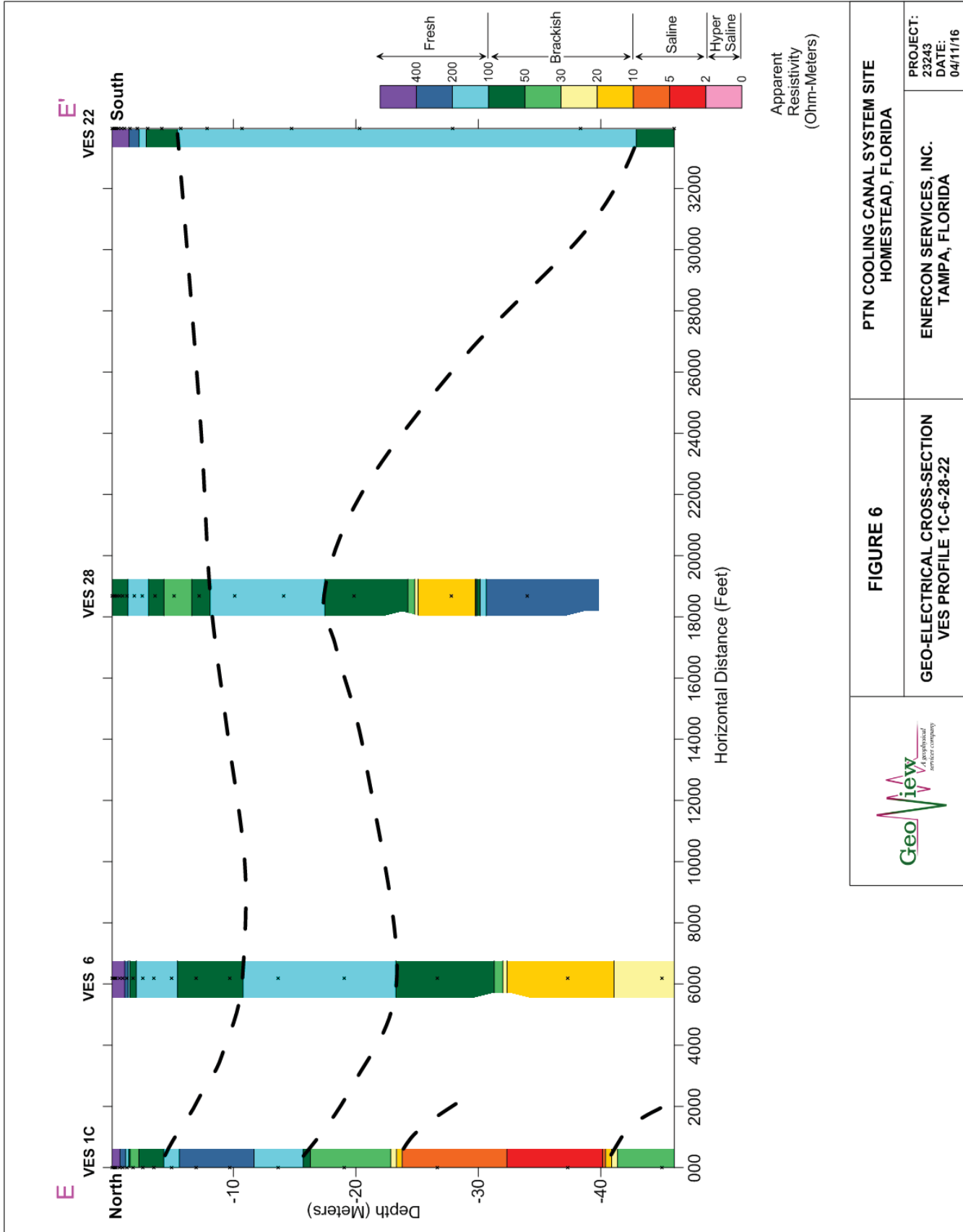
PTN COOLING CANAL SYSTEM SITE  
 HOMESTEAD, FLORIDA

PROJECT:  
 23243  
 DATE:  
 04/11/16

GEO-ELECTRICAL CROSS-SECTION  
 VES PROFILE 27-24-25-26

ENERCON SERVICES, INC.  
 TAMPA, FLORIDA





**FIGURE 6**

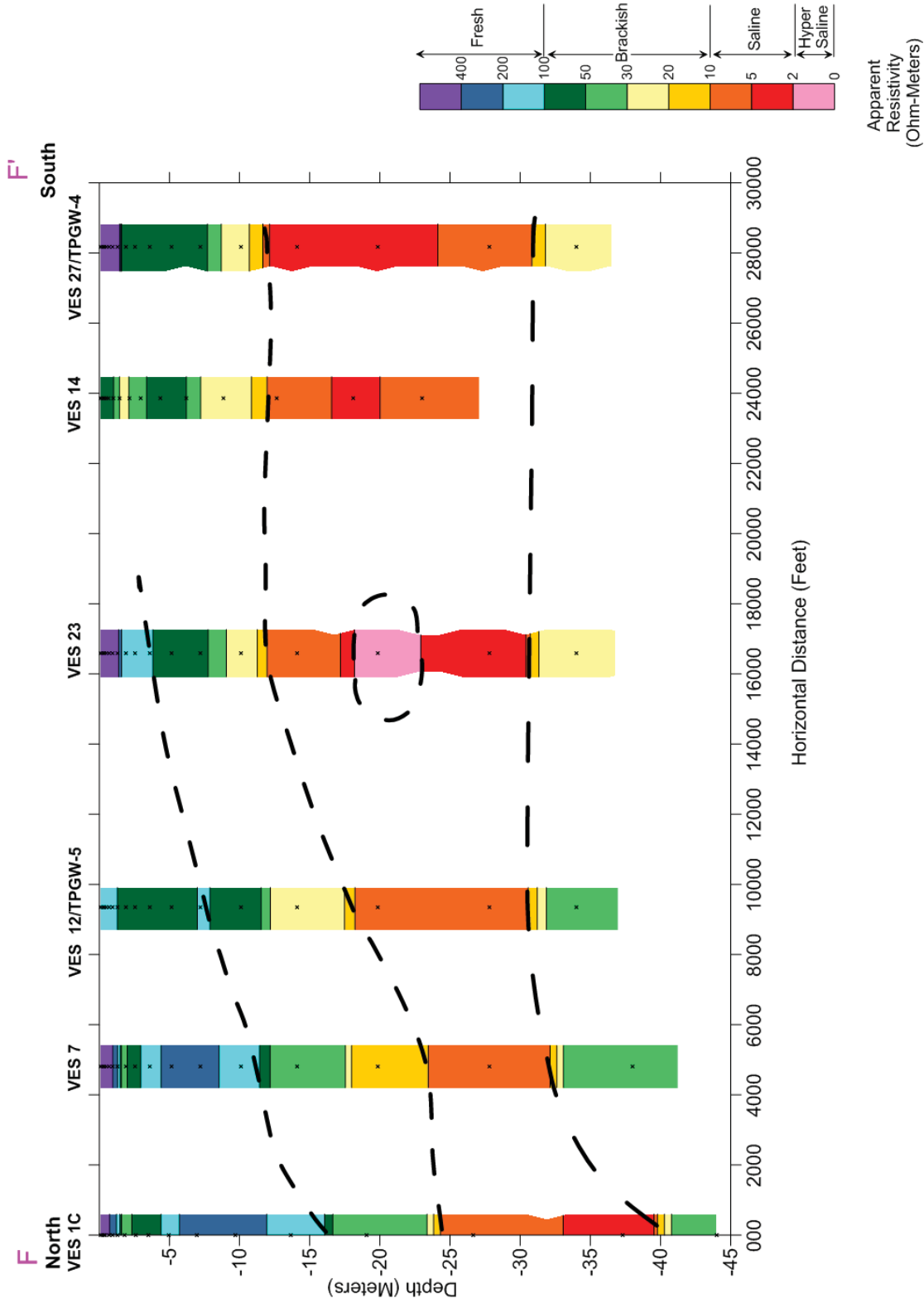
**GEO-ELECTRICAL CROSS-SECTION  
 VES PROFILE 1C-6-28-22**

**PTN COOLING CANAL SYSTEM SITE  
 HOMESTEAD, FLORIDA**

**ENERCON SERVICES, INC.  
 TAMPA, FLORIDA**

**PROJECT:  
 23243**

**DATE:  
 04/11/16**



**FIGURE 7**

**PTN COOLING CANAL SYSTEM SITE  
 HOMESTEAD, FLORIDA**

**GEO-ELECTRICAL CROSS-SECTION  
 VES PROFILE 1C-7-12-23-14-27**

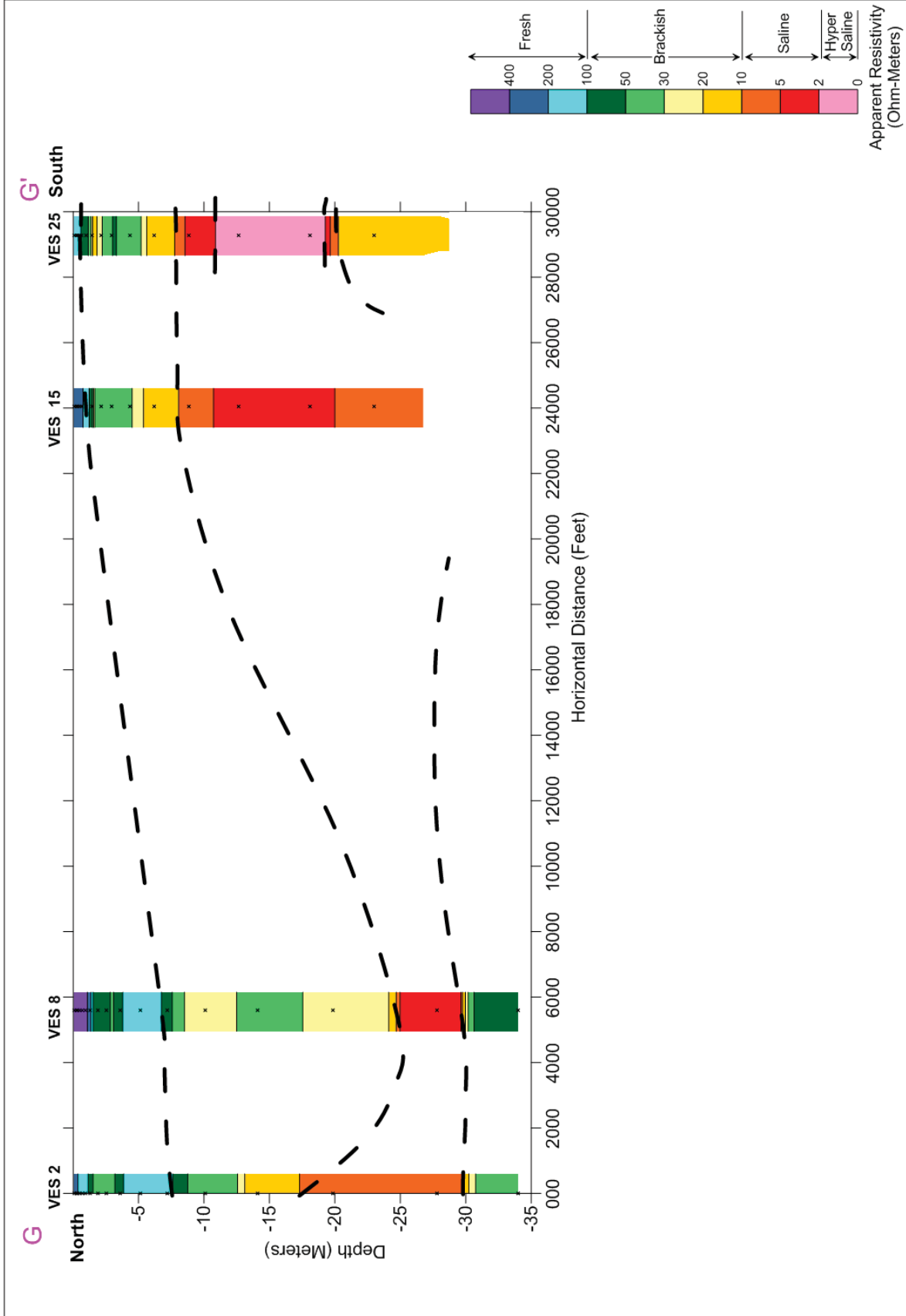
**ENERCON SERVICES, INC.  
 TAMPA, FLORIDA**


**PROJECT:  
 23243**

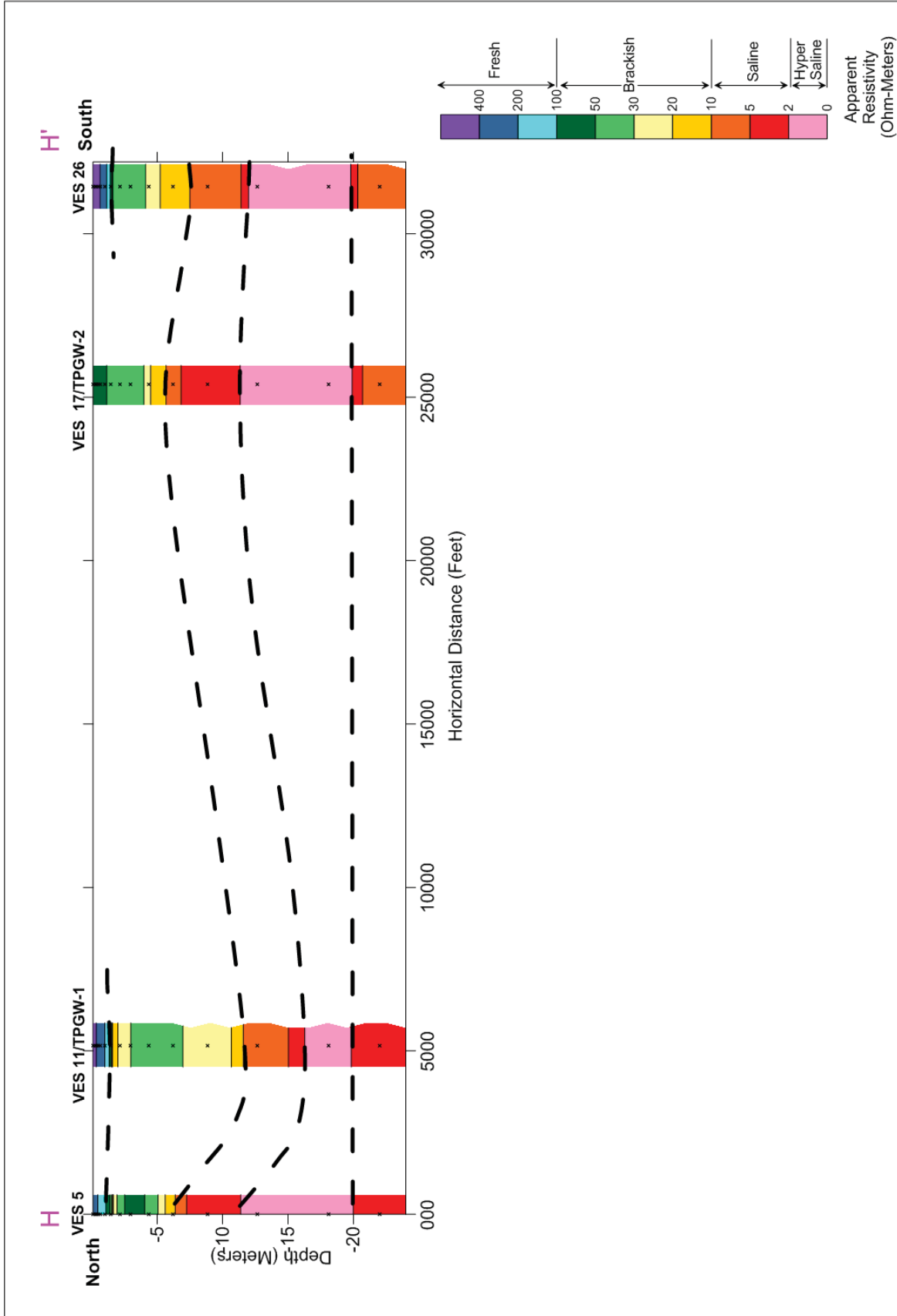
**DATE:  
 04/11/16**







	<b>FIGURE 8</b>	<b>PTN COOLING CANAL SYSTEM SITE HOMESTEAD, FLORIDA</b>
	<b>GEO-ELECTRICAL CROSS-SECTION VES PROFILE 2-8-15-25</b>	<b>ENERCON SERVICES, INC. TAMPA, FLORIDA</b>
		PROJECT: 23243 DATE: 04/11/16



**FIGURE 9**

**GEO-ELECTRICAL CROSS-SECTION  
 VES PROFILE 5-11-17-26**

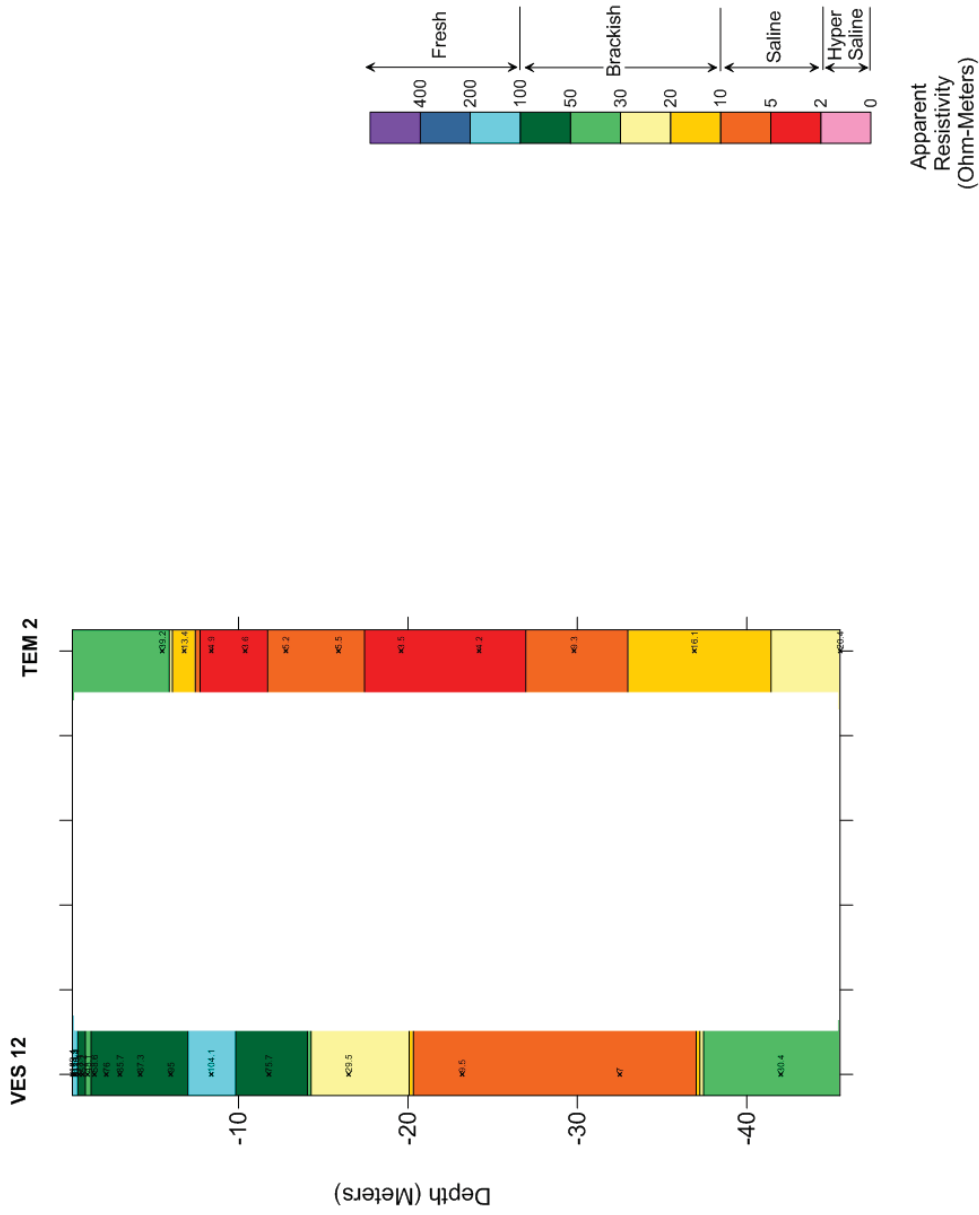
**PTN COOLING CANAL SYSTEM SITE  
 HOMESTEAD, FLORIDA**

**ENERCON SERVICES, INC.  
 TAMPA, FLORIDA**

**PROJECT:  
 23243**

**DATE:  
 04/11/16**





**FIGURE 10**

**GEO-ELECTRICAL COMPARISON  
 VES12 AND TEM2**

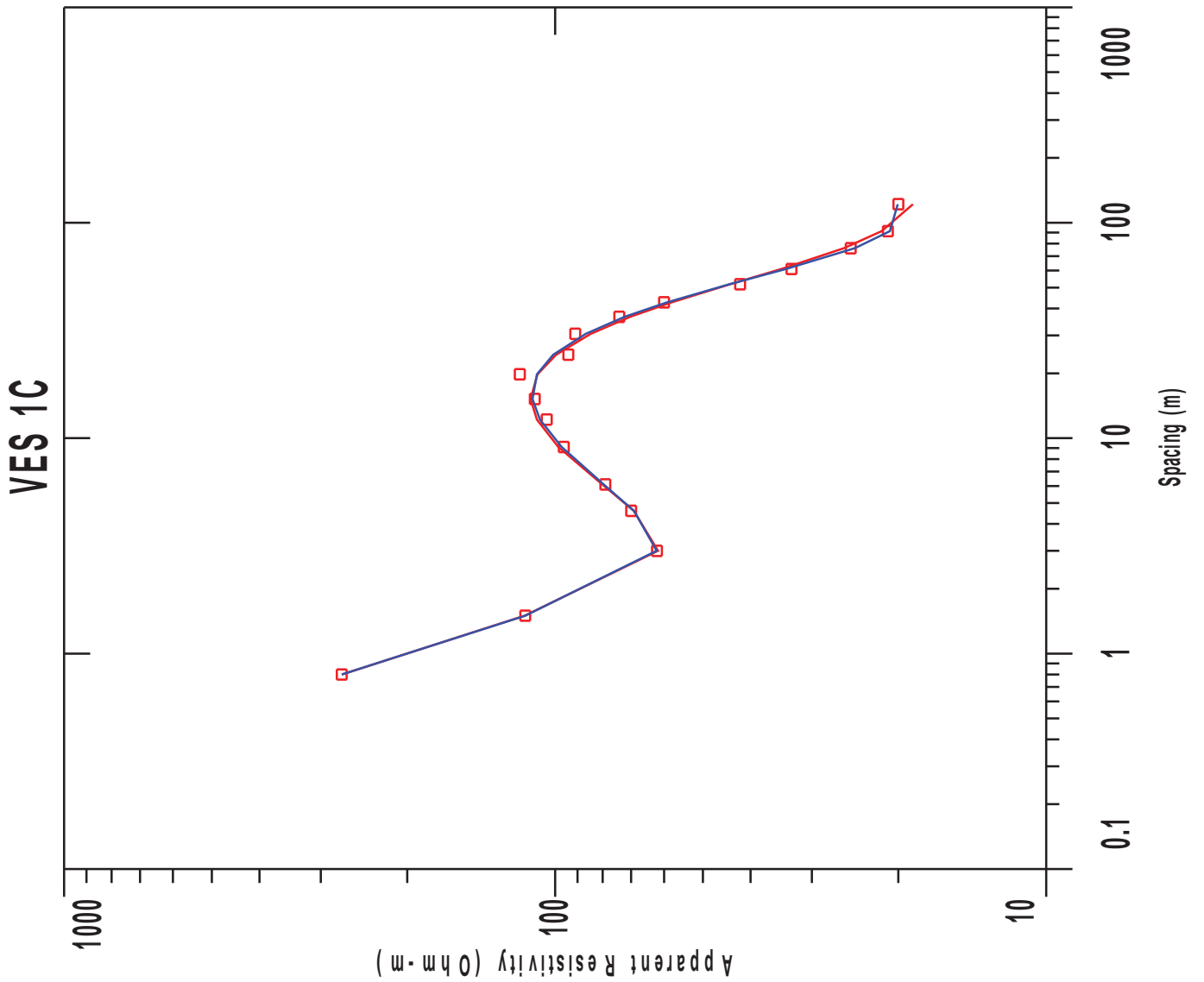
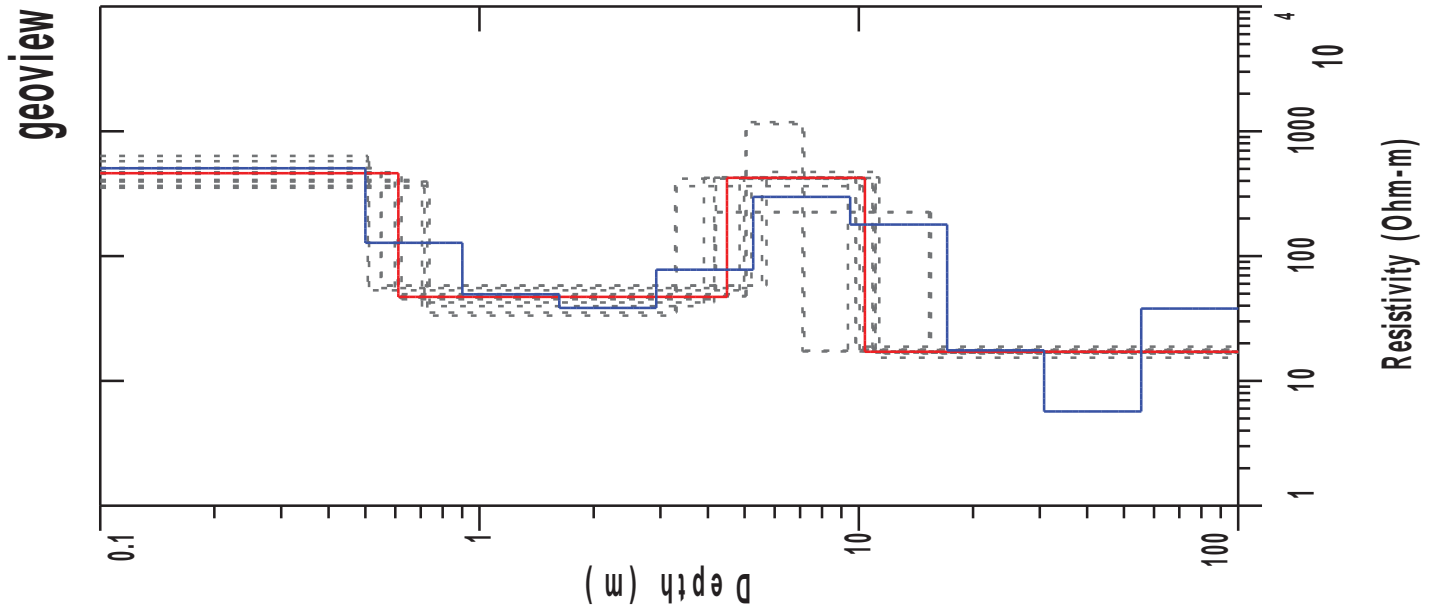
**PTN COOLING CANAL SYSTEM SITE  
 HOMESTEAD, FLORIDA**

**ENERCON SERVICES, INC.  
 TAMPA, FLORIDA**

**PROJECT:  
 23243  
 DATE:  
 04/11/16**



( 55,3+ 0< \$  
, 1,\*860 \* (1 6,7 0780:0 8= 8,7 803. 6,791 87





# VES 1C

## Wenner Array

Northing: 0.0 Easting: 0.0 Elevation: 0.0

No.	Spacing (meters)	Layered Model:			Smooth Model:	
		Data Resistivity	Synthetic Resistivity	DIFFERENCE (percent)	Synthetic Resistivity	DIFFERENCE (percent)
1	0.800	272.0	271.6	0.118	272.0	-0.00377
2	1.50	115.0	115.2	-0.213	114.9	0.0143
3	3.00	62.00	61.73	0.434	62.13	-0.216
4	4.60	70.00	69.12	1.24	69.07	1.32
5	6.10	79.00	80.17	-1.48	79.64	-0.810
6	9.10	96.00	98.47	-2.57	96.98	-1.02
7	12.20	104.0	108.9	-4.71	107.3	-3.20
8	15.20	110.0	112.1	-1.95	111.1	-1.07
9	19.80	118.0	108.6	7.96	108.9	7.69
10	24.40	94.00	99.50	-5.85	100.8	-7.31
11	30.50	91.00	84.65	6.96	86.65	4.77
12	36.60	74.00	70.27	5.02	72.12	2.52
13	42.70	60.00	57.97	3.37	59.22	1.28
14	51.80	42.00	44.06	-4.90	44.20	-5.25
15	61.00	33.00	34.61	-4.90	33.87	-2.64
16	76.20	25.00	25.79	-3.18	24.51	1.93
17	91.40	21.00	21.63	-3.04	20.80	0.935
18	121.9	20.00	18.68	6.59	20.04	-0.240

NO DATA ARE MASKED

### Layered Model

L #	RESISTIVITY	THICKNESS (meters)	DEPTH	ELEVATION (meters)	LONG. COND. (Siemens)	TRANS. RES. (Ohm-m <sup>2</sup> )
				0.0		
1	461.9	0.611	0.611	-0.611	0.00132	282.2
2	47.12	3.88	4.49	-4.49	0.0823	182.9
3	423.1	5.88	10.37	-10.37	0.0139	2490.3
4	17.10					

ALL PARAMETERS ARE FREE

VES 1C

Page 2

Parameter Bounds from Equivalence Analysis

LAYER		MINIMUM	BEST	MAXIMUM
RHO	1	352.75	461.98	634.52
	2	33.36	47.13	58.11
	3	223.89	423.14	1183.31
	4	15.36	17.11	18.83
THICK	1	0.51	0.61	0.74
	2	2.55	3.88	5.16
	3	2.08	5.89	11.33

PARAMETER RESOLUTION MATRIX:  
 "FIX" INDICATES FIXED PARAMETER

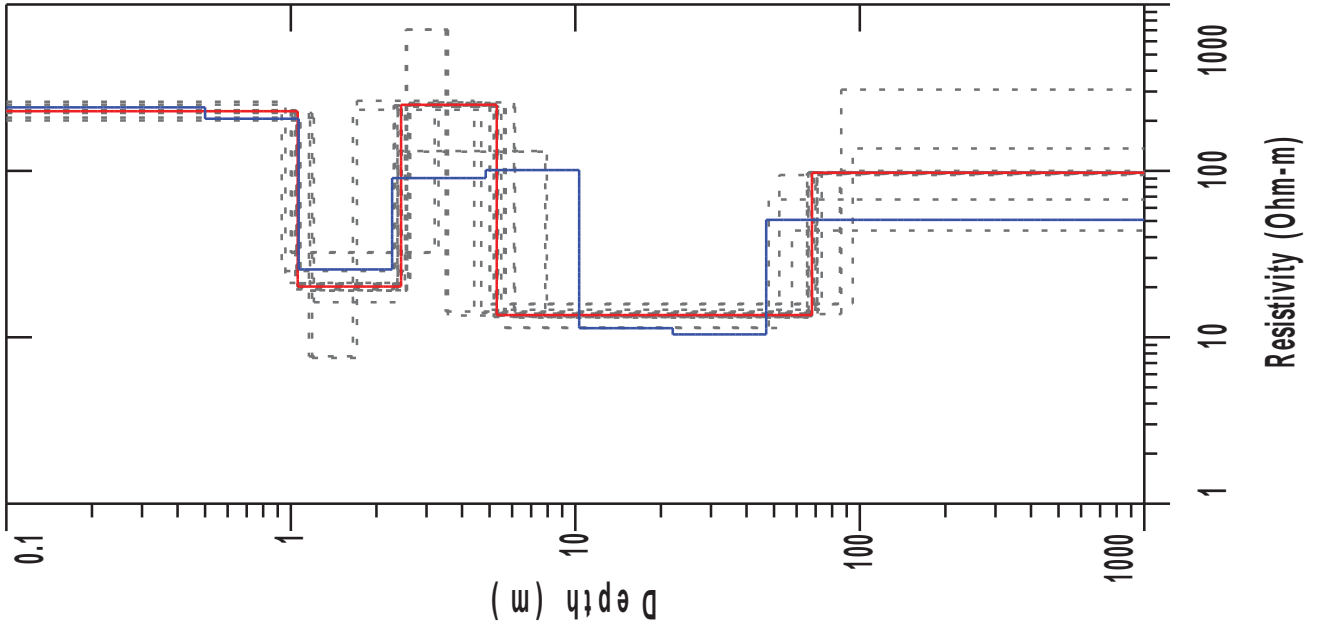
RHO	1	0.89						
RHO	2	-0.04	0.91					
RHO	3	0.00	0.00	0.51				
RHO	4	0.00	0.01	0.00	0.98			
THK	1	0.07	0.05	0.00	0.00	0.95		
THK	2	-0.05	-0.12	-0.06	0.02	0.06	0.84	
THK	3	0.00	0.01	0.49	0.01	0.00	0.07	0.50
	R	1	R	2	R	3	R	4
	T	1	T	2	T	3		

Smooth Model: Ridge Regression

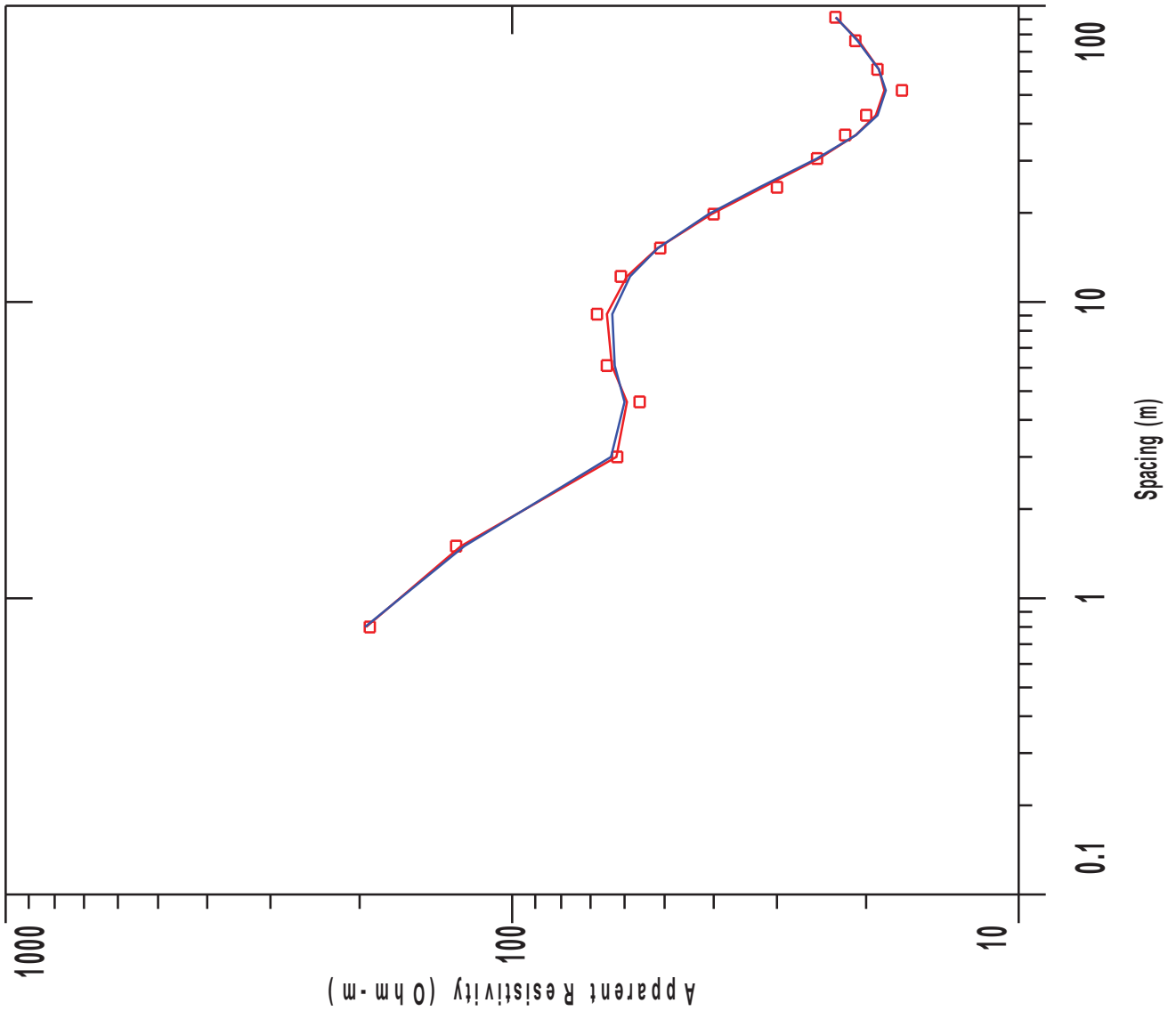
L #	RESISTIVITY	THICKNESS (meters)	DEPTH	ELEVATION (meters)	LONG. COND. (Siemens)	TRANS. RES. (Ohm-m <sup>2</sup> )
				0.0		
1	505.6	0.500	0.500 *	-0.500	0.0	252.8
2	127.8	0.400	0.900 *	-0.900	0.00313	51.24
3	49.41	0.722	1.62 *	-1.62	0.0146	35.68
4	38.43	1.30	2.92 *	-2.92	0.0338	50.00
5	77.75	2.34	5.26 *	-5.26	0.0301	182.2
6	297.6	4.22	9.49 *	-9.49	0.0141	1256.8
7	179.0	7.60	17.09 *	-17.09	0.0424	1362.5
8	17.60	13.70	30.80 *	-30.80	0.778	241.2
9	5.69	24.69	55.50 *	-55.50	4.33	140.6
10	38.02					

"\*" INDICATES FIXED PARAMETER

geoview



VES 2



# VES 2

## Wenner Array

Northing: 0.0 Easting: 0.0 Elevation: 0.0

No.	Spacing (meters)	Layered Model:			Smooth Model:	
		Data Resistivity	Synthetic Resistivity	DIFFERENCE (percent)	Synthetic Resistivity	DIFFERENCE (percent)
1	0.800	191.0	194.1	-1.63	195.0	-2.14
2	1.50	129.0	126.1	2.22	124.1	3.74
3	3.00	62.00	62.22	-0.360	63.79	-2.89
4	4.60	56.00	59.33	-5.95	59.97	-7.09
5	6.10	65.00	63.53	2.25	62.72	3.50
6	9.10	68.00	64.97	4.44	63.41	6.73
7	12.20	61.00	59.31	2.76	58.46	4.15
8	15.20	51.00	51.61	-1.21	51.53	-1.04
9	19.80	40.00	40.41	-1.02	40.92	-2.30
10	24.40	30.00	31.92	-6.41	32.45	-8.19
11	30.50	25.00	24.78	0.854	25.03	-0.122
12	36.60	22.00	20.96	4.70	20.93	4.82
13	42.70	20.00	19.14	4.27	18.99	5.03
14	51.80	17.00	18.41	-8.33	18.29	-7.61
15	61.00	19.00	18.86	0.685	18.87	0.647
16	76.20	21.00	20.68	1.51	20.80	0.945
17	91.40	23.00	22.98	0.0623	22.95	0.209

NO DATA ARE MASKED

### Layered Model

L #	RESISTIVITY	THICKNESS (meters)	DEPTH	ELEVATION (meters)	LONG. COND. (Siemens)	TRANS. RES. (Ohm-m <sup>2</sup> )
				0.0		
1	228.4	1.05	1.05	-1.05	0.00463	241.6
2	20.16	1.38	2.44	-2.44	0.0686	27.91
3	249.2	2.85	5.30	-5.30	0.0114	712.6
4	13.60	62.65	67.95	-67.95	4.60	852.7
5	97.39					

ALL PARAMETERS ARE FREE

Parameter Bounds from Equivalence Analysis

LAYER	MINIMUM	BEST	MAXIMUM	
RHO	1	200.96	228.46	259.96
	2	7.52	20.17	32.47
	3	130.53	249.28	706.32
	4	11.37	13.61	15.92
	5	43.74	97.40	308.00
THICK	1	0.93	1.06	1.21
	2	0.50	1.38	2.30
	3	0.97	2.86	5.56
	4	42.25	62.66	89.52

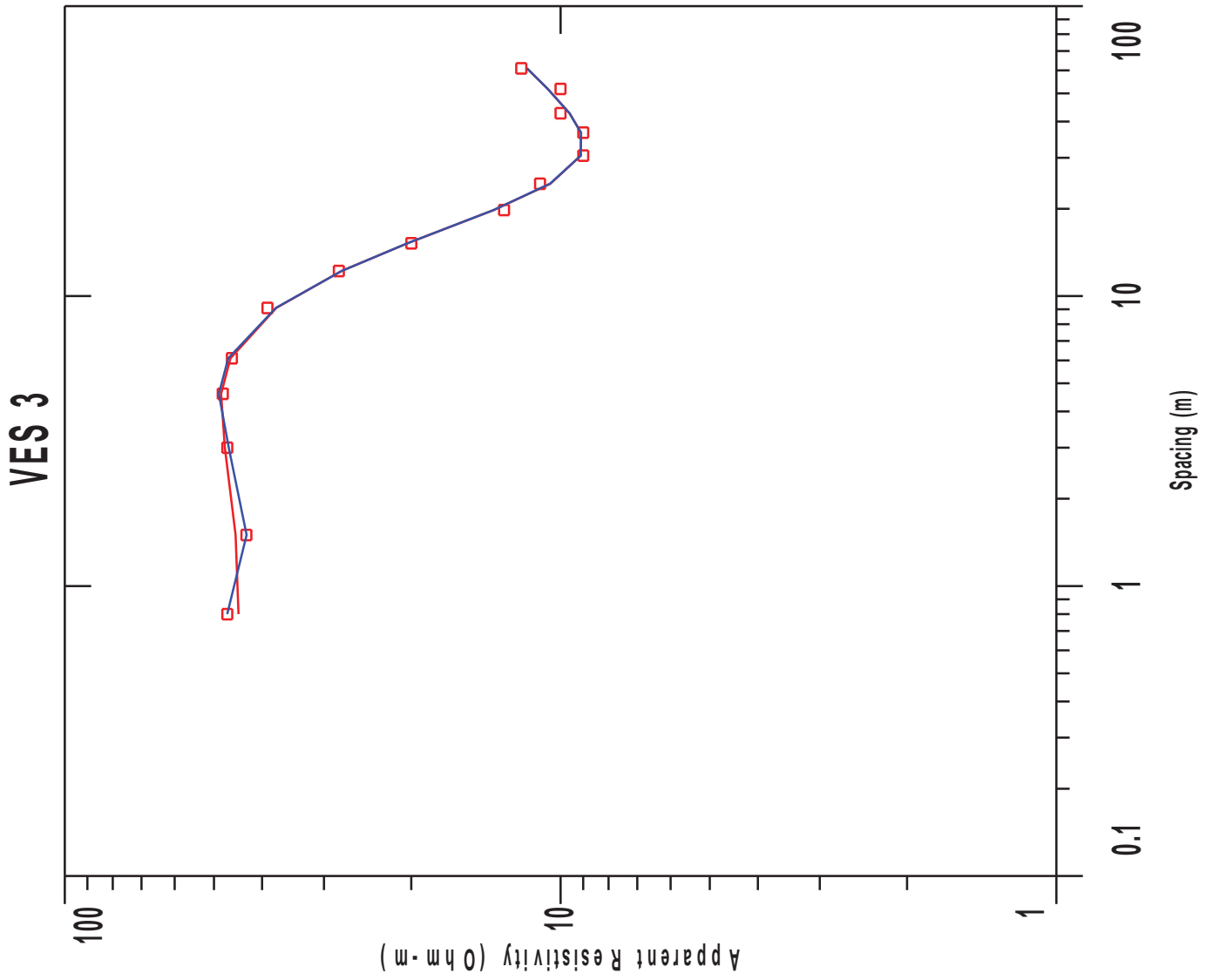
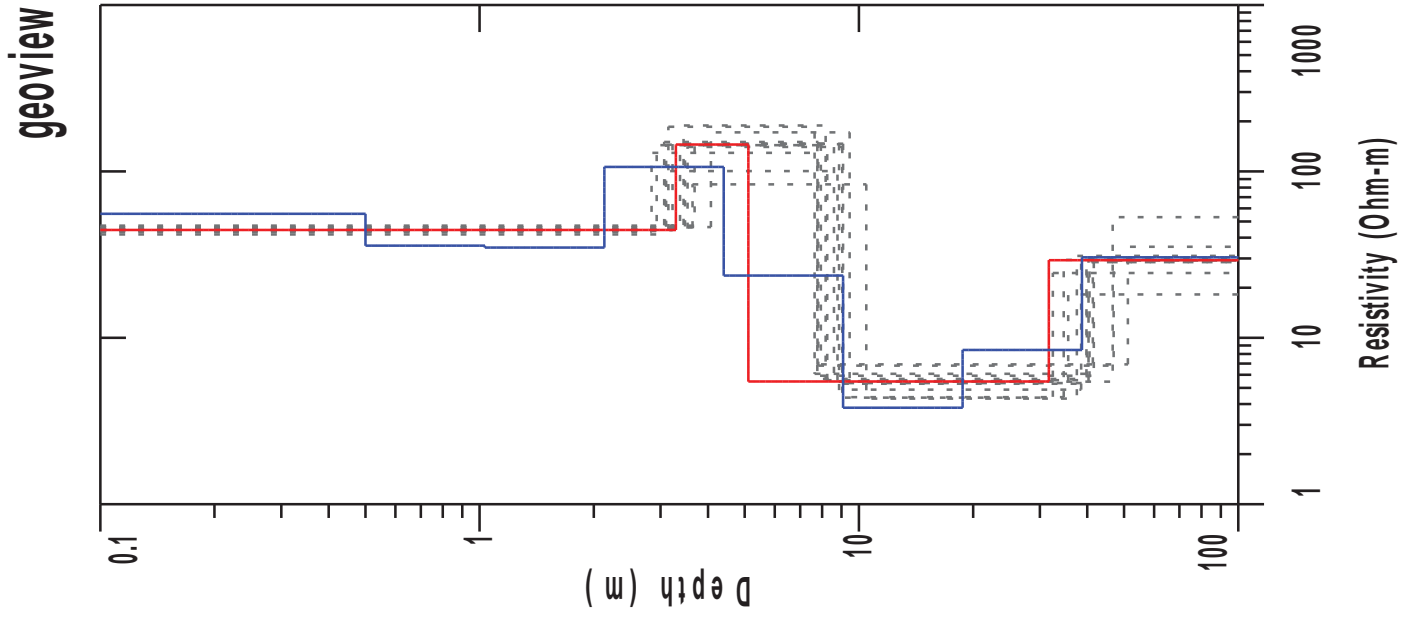
PARAMETER RESOLUTION MATRIX:  
 "FIX" INDICATES FIXED PARAMETER

RHO	1	0.97									
RHO	2	-0.01	0.51								
RHO	3	0.00	0.03	0.51							
RHO	4	0.00	0.02	0.00	0.94						
RHO	5	0.00	-0.01	0.00	-0.01	0.06					
THK	1	0.02	0.06	-0.01	0.01	0.00	0.97				
THK	2	-0.01	-0.48	-0.03	0.04	-0.01	0.05	0.48			
THK	3	0.00	-0.03	0.49	0.02	0.00	0.01	0.03	0.49		
THK	4	-0.01	0.02	0.01	-0.10	-0.21	0.01	0.05	0.03	0.78	
		R	1 R	2 R	3 R	4 R	5 T	1 T	2 T	3 T	4

Smooth Model: Ridge Regression

L #	RESISTIVITY	THICKNESS (meters)	DEPTH	ELEVATION (meters)	LONG. COND. (Siemens)	TRANS. RES. (Ohm-m <sup>2</sup> )
				0.0		
1	240.7	0.500	0.500 *	-0.500	0.00208	120.3
2	205.5	0.565	1.06 *	-1.06	0.00275	116.2
3	25.56	1.20	2.27 *	-2.27	0.0471	30.83
4	90.41	2.57	4.84 *	-4.84	0.0284	232.4
5	100.9	5.48	10.32 *	-10.32	0.0542	553.5
6	11.35	11.68	22.00 *	-22.00	1.02	132.6
7	10.40	24.90	46.91 *	-46.91	2.39	259.1
8	50.83					





# VES 3

## Wenner Array

Northing: 0.0 Easting: 0.0 Elevation: 0.0

No.	Spacing (meters)	Layered Model:			Smooth Model:	
		Data Resistivity	Synthetic Resistivity	DIFFERENCE (percent)	Synthetic Resistivity	DIFFERENCE (percent)
1	0.800	47.00	44.61	5.08	47.02	-0.0453
2	1.50	43.00	45.22	-5.18	42.95	0.101
3	3.00	47.00	47.55	-1.17	46.69	0.649
4	4.60	48.00	48.37	-0.771	48.87	-1.81
5	6.10	46.00	46.30	-0.670	46.81	-1.76
6	9.10	39.00	37.43	4.01	37.51	3.81
7	12.20	28.00	27.64	1.27	27.62	1.34
8	15.20	20.00	20.37	-1.85	20.37	-1.88
9	19.80	13.00	13.62	-4.83	13.65	-5.02
10	24.40	11.00	10.48	4.70	10.49	4.56
11	30.50	9.00	9.10	-1.11	9.10	-1.19
12	36.60	9.00	9.08	-0.970	9.09	-1.03
13	42.70	10.00	9.58	4.15	9.58	4.10
14	51.80	10.00	10.61	-6.10	10.60	-6.09
15	61.00	12.00	11.69	2.54	11.68	2.60

NO DATA ARE MASKED

### Layered Model

L #	RESISTIVITY	THICKNESS (meters)	DEPTH	ELEVATION (meters)	LONG. COND. (Siemens)	TRANS. RES. (Ohm-m <sup>2</sup> )
				0.0		
1	44.48	3.29	3.29	-3.29	0.0739	146.3
2	145.1	1.81	5.10	-5.10	0.0125	264.0
3	5.47	26.56	31.67	-31.67	4.85	145.3
4	29.25					

ALL PARAMETERS ARE FREE

Parameter Bounds from Equivalence Analysis

LAYER		MINIMUM	BEST	MAXIMUM
RHO	1	41.82	44.48	47.26
	2	83.52	145.15	188.82
	3	4.31	5.47	6.93
	4	18.23	29.25	53.03
DEPTH	1	2.84	3.29	4.07
	2	4.50	5.11	6.81
	3	23.59	31.68	43.22

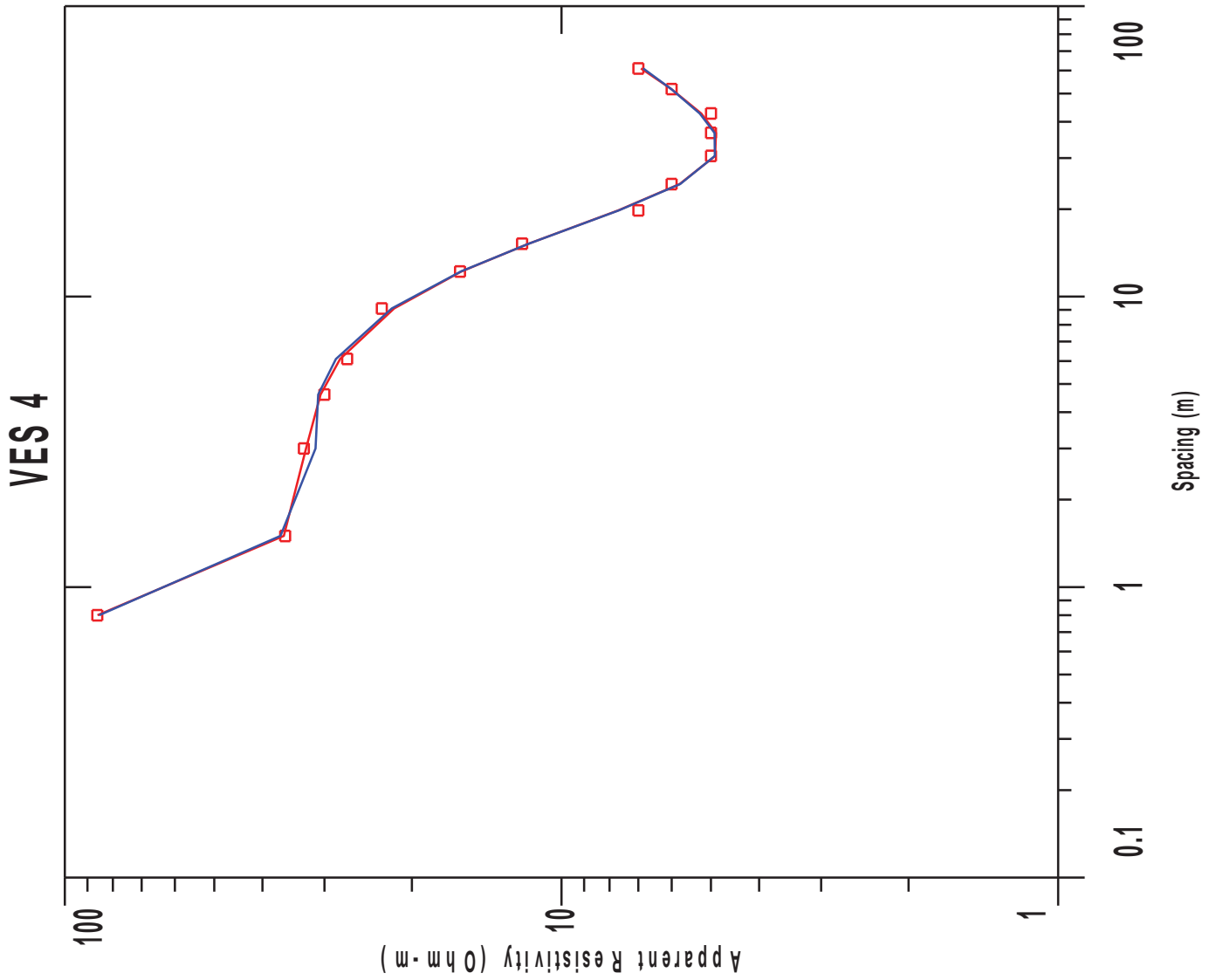
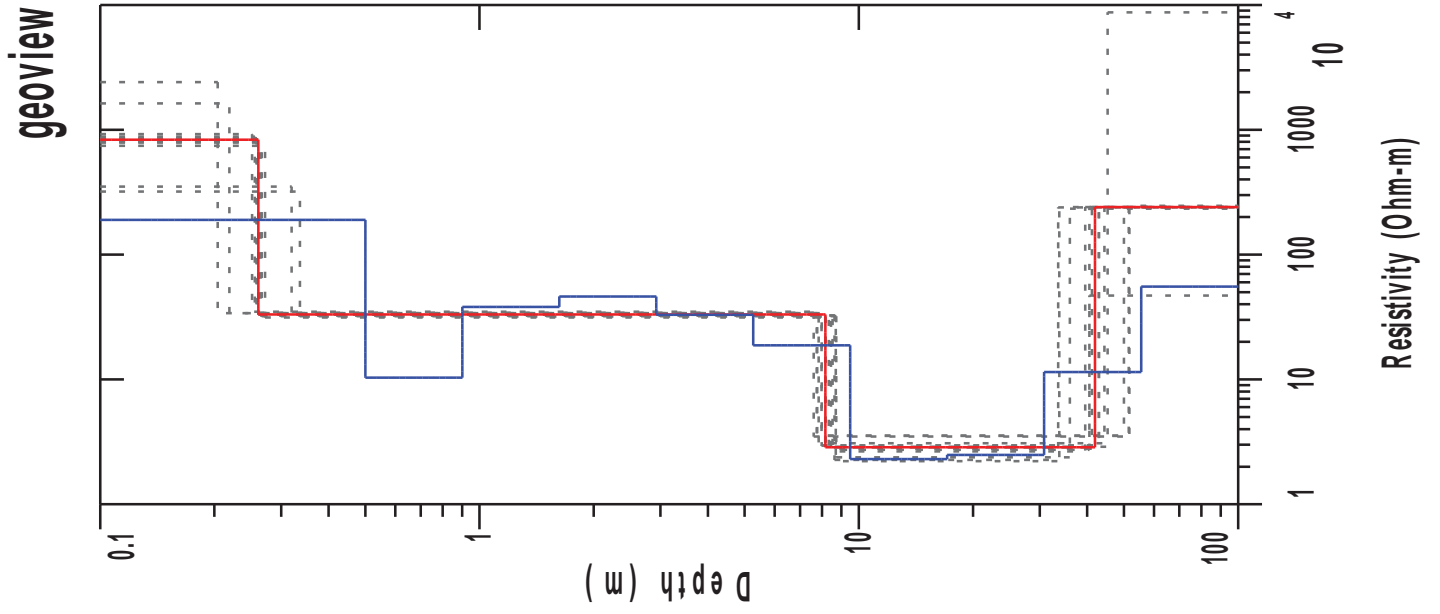
PARAMETER RESOLUTION MATRIX:  
 "FIX" INDICATES FIXED PARAMETER

RHO	1	0.98						
RHO	2	0.00	0.12					
RHO	3	0.01	-0.05	0.67				
RHO	4	0.00	0.02	0.01	0.18			
DEP	1	-0.04	-0.16	0.11	-0.03	0.80		
DEP	2	-0.02	0.26	0.11	-0.03	-0.05	0.86	
DEP	3	0.00	0.00	-0.32	-0.25	0.08	0.07	0.58
	R	1	R	2	R	3	R	4
	D	1	D	2	D	3		

Smooth Model: Ridge Regression

L #	RESISTIVITY	THICKNESS (meters)	DEPTH	ELEVATION (meters)	LONG. COND. (Siemens)	TRANS. RES. (Ohm-m <sup>2</sup> )
				0.0		
1	55.55	0.500	0.500 *	-0.500	0.00900	27.77
2	35.81	0.532	1.03 *	-1.03	0.0148	19.06
3	34.85	1.09	2.13 *	-2.13	0.0315	38.31
4	106.2	2.26	4.40 *	-4.40	0.0213	241.2
5	23.67	4.68	9.08 *	-9.08	0.197	110.9
6	3.80	9.67	18.76 *	-18.76	2.54	36.80
7	8.44	19.98	38.74 *	-38.74	2.36	168.7
8	30.44					

"\*" INDICATES FIXED PARAMETER



# VES 4

## Wenner Array

Northing: 0.0 Easting: 0.0 Elevation: 0.0

No.	Spacing (meters)	Layered Model:			Smooth Model:	
		Data Resistivity	Synthetic Resistivity	DIFFERENCE (percent)	Synthetic Resistivity	DIFFERENCE (percent)
1	0.800	86.00	85.89	0.117	85.26	0.855
2	1.50	36.00	36.22	-0.638	36.78	-2.17
3	3.00	33.00	32.67	0.972	31.27	5.24
4	4.60	30.00	30.54	-1.81	30.88	-2.93
5	6.10	27.00	27.89	-3.31	28.44	-5.36
6	9.10	23.00	21.71	5.57	21.95	4.54
7	12.20	16.00	15.89	0.673	15.93	0.409
8	15.20	12.00	11.65	2.85	11.64	2.92
9	19.80	7.00	7.68	-9.82	7.66	-9.52
10	24.40	6.00	5.77	3.66	5.76	3.89
11	30.50	5.00	4.90	1.94	4.91	1.77
12	36.60	5.00	4.88	2.31	4.91	1.67
13	42.70	5.00	5.22	-4.54	5.26	-5.30
14	51.80	6.00	6.00	-0.0881	6.01	-0.184
15	61.00	7.00	6.91	1.18	6.84	2.24

NO DATA ARE MASKED

### Layered Model

L #	RESISTIVITY	THICKNESS (meters)	DEPTH	ELEVATION (meters)	LONG. COND. (Siemens)	TRANS. RES. (Ohm-m <sup>2</sup> )
				0.0		
1	832.0	0.261	0.261	-0.261	0.0	217.4
2	33.12	7.90	8.16	-8.16	0.238	261.7
3	2.86	33.77	41.93	-41.93	11.79	96.72
4	240.0					

ALL PARAMETERS ARE FREE



Parameter Bounds from Equivalence Analysis

LAYER		MINIMUM	BEST	MAXIMUM
RHO	1	319.96	832.06	2407.69
	2	31.38	33.13	34.87
	3	2.21	2.86	3.55
	4	47.00	240.04	8727.95
THICK	1	0.20	0.26	0.34
	2	7.35	7.90	8.46
	3	24.84	33.77	43.91

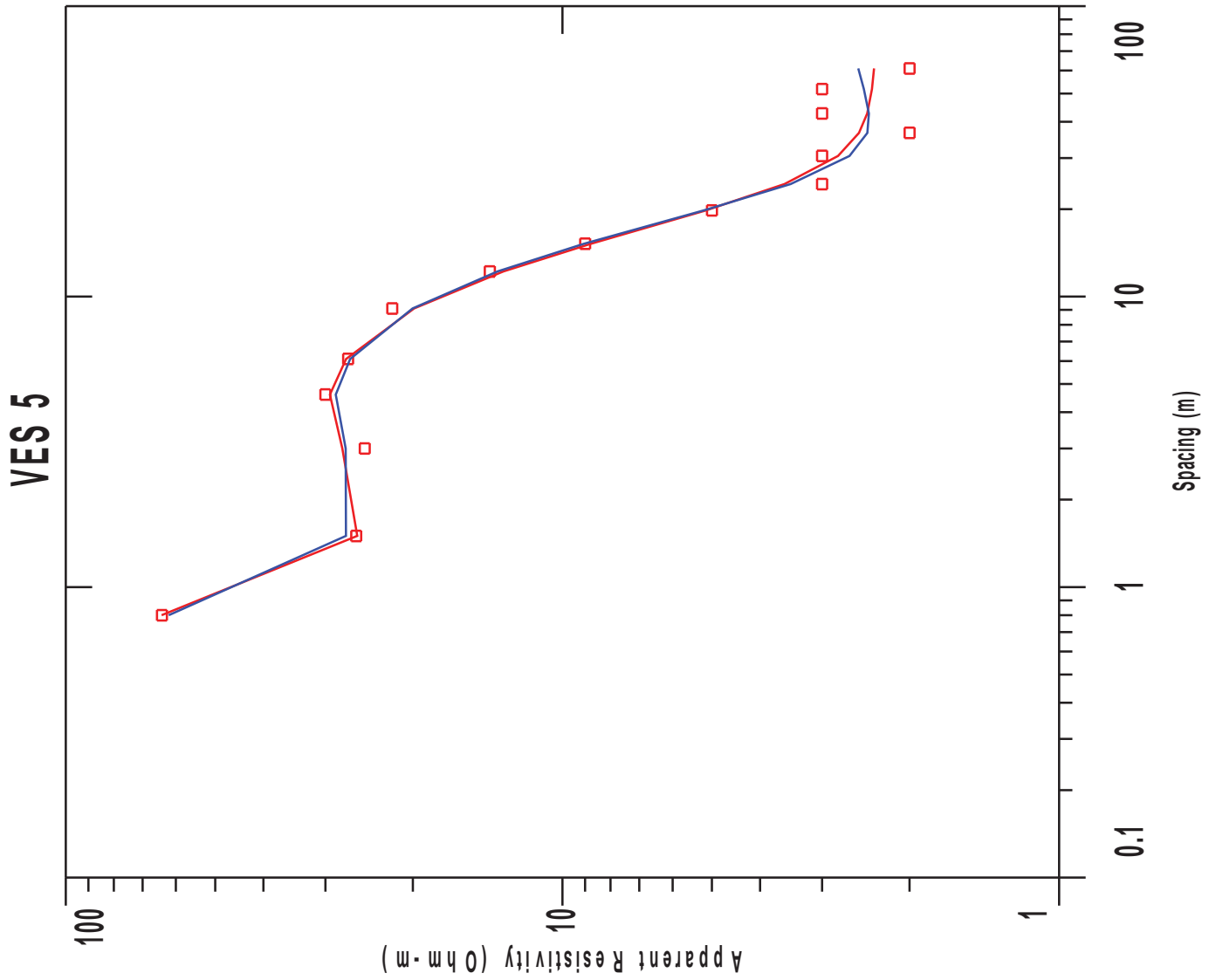
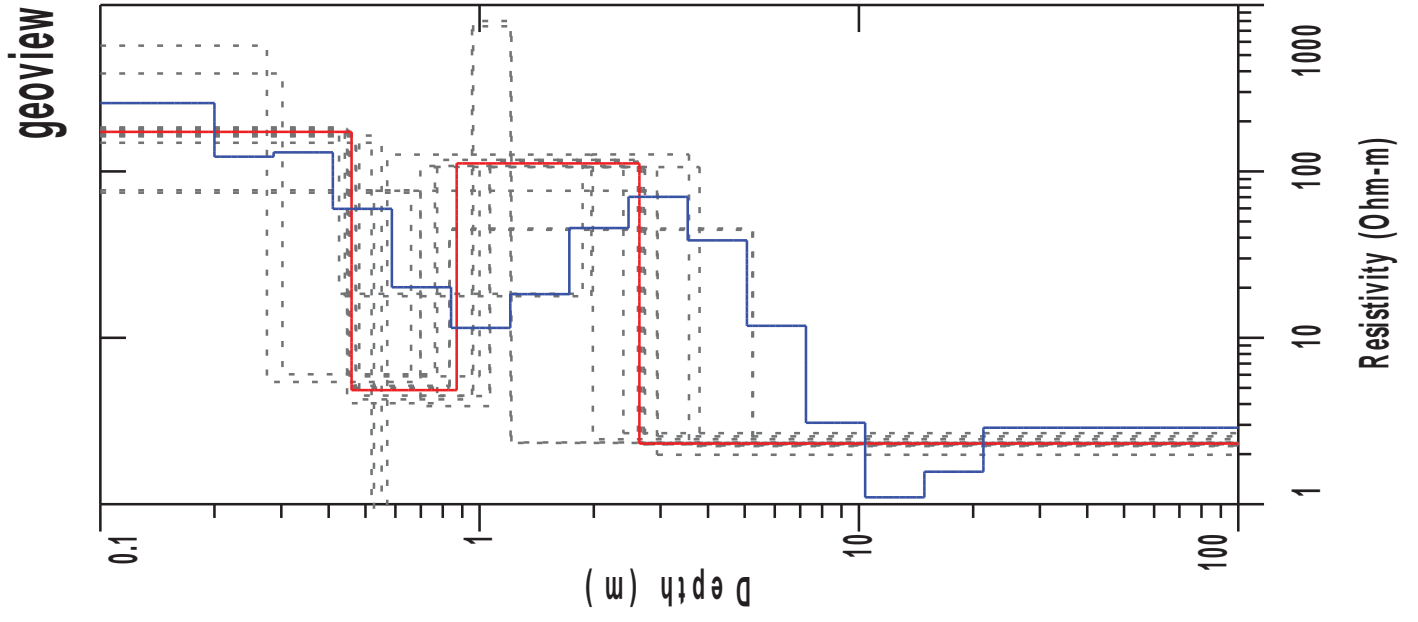
PARAMETER RESOLUTION MATRIX:  
 "FIX" INDICATES FIXED PARAMETER

RHO	1	0.17						
RHO	2	-0.02	0.99					
RHO	3	-0.02	-0.01	0.81				
RHO	4	0.00	0.00	0.00	0.00			
THK	1	0.19	0.01	0.01	0.00	0.95		
THK	2	0.01	0.01	0.05	0.00	-0.01	0.98	
THK	3	-0.03	-0.02	-0.23	-0.03	0.01	0.05	0.72
	R	1	R	2	R	3	R	4
	T	1	T	2	T	3		

Smooth Model: Ridge Regression

L #	RESISTIVITY	THICKNESS (meters)	DEPTH	ELEVATION (meters)	LONG. COND. (Siemens)	TRANS. RES. (Ohm-m <sup>2</sup> )
				0.0		
1	189.6	0.500	0.500 *	-0.500	0.00264	94.82
2	10.32	0.400	0.900 *	-0.900	0.0388	4.14
3	38.09	0.722	1.62 *	-1.62	0.0189	27.50
4	46.14	1.30	2.92 *	-2.92	0.0282	60.03
5	32.92	2.34	5.26 *	-5.26	0.0711	77.17
6	18.75	4.22	9.49 *	-9.49	0.225	79.18
7	2.30	7.60	17.09 *	-17.09	3.30	17.51
8	2.48	13.70	30.80 *	-30.80	5.51	34.08
9	11.46	24.69	55.50 *	-55.50	2.15	283.1
10	55.49					

"\*" INDICATES FIXED PARAMETER



# VES 5

## Wenner Array

Northing: 0.0 Easting: 0.0 Elevation: 0.0

No.	Spacing (meters)	Layered Model:			Smooth Model:	
		Data Resistivity	Synthetic Resistivity	DIFFERENCE (percent)	Synthetic Resistivity	DIFFERENCE (percent)
1	0.800	64.00	64.11	-0.174	62.04	3.06
2	1.50	26.00	25.88	0.449	27.27	-4.89
3	3.00	25.00	27.74	-10.97	27.30	-9.21
4	4.60	30.00	29.39	2.03	28.58	4.70
5	6.10	27.00	27.26	-0.979	26.75	0.920
6	9.10	22.00	19.88	9.60	20.02	8.97
7	12.20	14.00	13.14	6.08	13.51	3.47
8	15.20	9.00	8.76	2.59	9.05	-0.635
9	19.80	5.00	5.14	-2.80	5.19	-3.89
10	24.40	3.00	3.56	-18.99	3.47	-15.66
11	30.50	3.00	2.78	7.13	2.64	11.94
12	36.60	2.00	2.52	-26.39	2.43	-21.64
13	42.70	3.00	2.43	18.88	2.41	19.51
14	51.80	3.00	2.38	20.64	2.47	17.62
15	61.00	2.00	2.35	-17.90	2.53	-26.84

NO DATA ARE MASKED

### Layered Model

L #	RESISTIVITY	THICKNESS (meters)	DEPTH	ELEVATION (meters)	LONG. COND. (Siemens)	TRANS. RES. (Ohm-m <sup>2</sup> )
				0.0		
1	172.6	0.459	0.459	-0.459	0.00266	79.35
2	4.84	0.410	0.870	-0.870	0.0847	1.99
3	111.6	1.76	2.63	-2.63	0.0158	197.2
4	2.31					

ALL PARAMETERS ARE FREE

Parameter Bounds from Equivalence Analysis

LAYER		MINIMUM	BEST	MAXIMUM
RHO	1	74.46	172.70	569.47
	2	0.09	4.85	18.37
	3	44.61	111.63	801.37
	4	1.98	2.31	2.67
THICK	1	0.27	0.46	0.70
	2	0.01	0.41	1.53
	3	0.25	1.77	4.43

PARAMETER RESOLUTION MATRIX:  
 "FIX" INDICATES FIXED PARAMETER

RHO	1	0.76						
RHO	2	-0.02	0.50					
RHO	3	0.01	0.02	0.51				
RHO	4	0.00	0.01	0.00	0.99			
THK	1	0.10	0.03	-0.01	0.00	0.95		
THK	2	-0.01	-0.47	-0.04	0.01	0.01	0.53	
THK	3	-0.02	-0.03	0.49	0.00	0.01	0.04	0.50
	R	1	R	2	R	3	R	4
	T	1	T	2	T	3		

Smooth Model: Ridge Regression

L #	RESISTIVITY	THICKNESS (meters)	DEPTH	ELEVATION (meters)	LONG. COND. (Siemens)	TRANS. RES. (Ohm-m <sup>2</sup> )
				0.0		
1	257.1	0.200	0.200 *	-0.200	0.0	51.43
2	122.5	0.0864	0.286 *	-0.286	0.0	10.58
3	130.2	0.123	0.410 *	-0.410	0.0	16.11
4	59.52	0.177	0.587 *	-0.587	0.00298	10.54
5	20.13	0.253	0.841 *	-0.841	0.0126	5.10
6	11.46	0.363	1.20 *	-1.20	0.0316	4.16
7	18.32	0.520	1.72 *	-1.72	0.0284	9.53
8	45.69	0.745	2.46 *	-2.46	0.0163	34.04
9	70.24	1.06	3.53 *	-3.53	0.0151	74.95
10	38.51	1.52	5.06 *	-5.06	0.0396	58.84
11	11.80	2.18	7.25 *	-7.25	0.185	25.82
12	3.08	3.13	10.38 *	-10.38	1.01	9.66

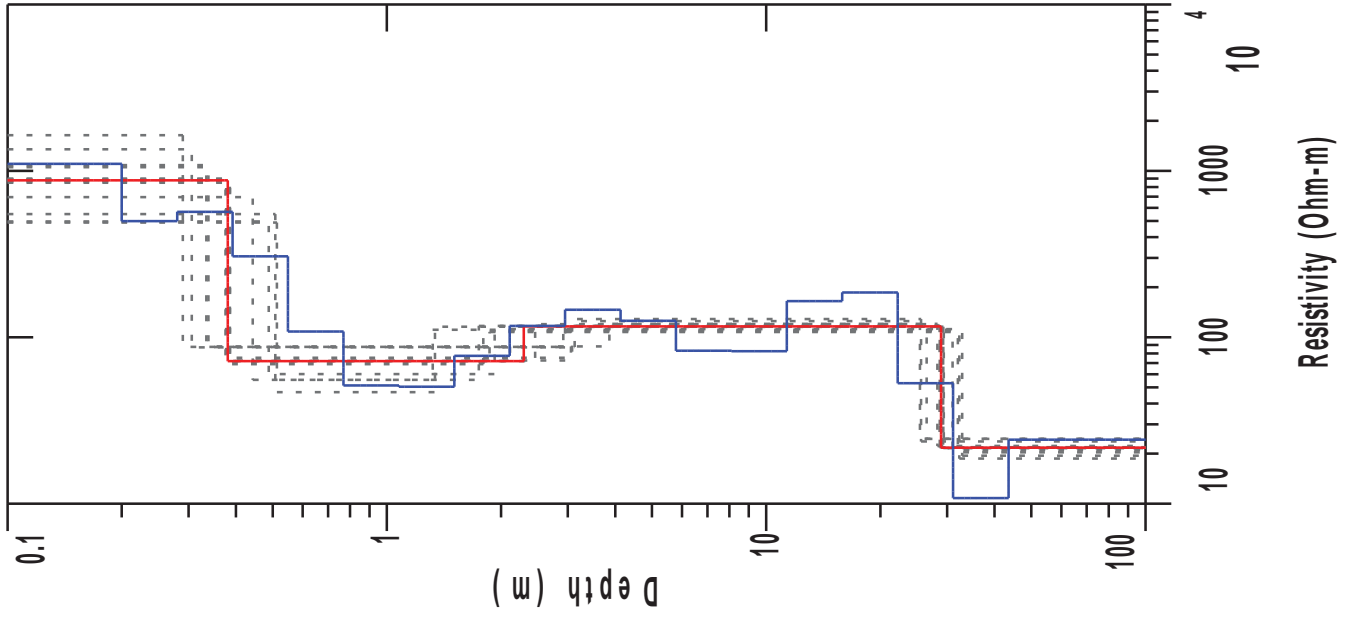
VES 5

Page 3

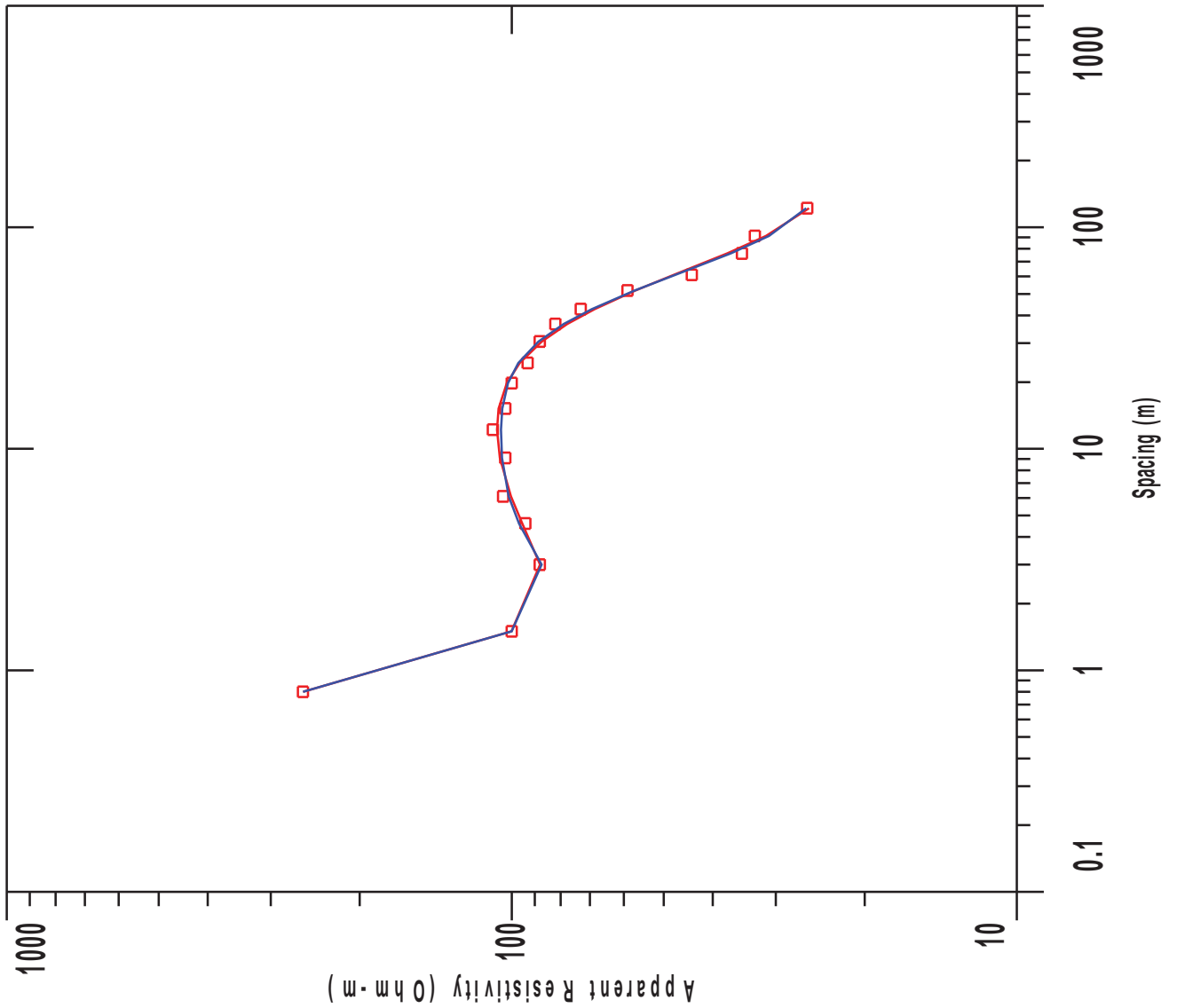
L #	RESISTIVITY	THICKNESS (meters)	DEPTH	ELEVATION (meters)	LONG. COND. (Siemens)	TRANS. RES. (Ohm-m <sup>2</sup> )
13	1.09	4.48	14.87 *	-14.87	4.07	4.93
14	1.56	6.42	21.29 *	-21.29	4.09	10.08
15	2.88					

"\*" INDICATES FIXED PARAMETER

geoview



VES 6





# VES 6

## Wenner Array

Northing: 0.0 Easting: 0.0 Elevation: 0.0

No.	Spacing (meters)	Layered Model:			Smooth Model:	
		Data Resistivity	Synthetic Resistivity	DIFFERENCE (percent)	Synthetic Resistivity	DIFFERENCE (percent)
1	0.800	259.0	258.8	0.0493	258.9	0.00397
2	1.50	100.0	100.0	-0.0821	100.0	-0.0277
3	3.00	88.00	87.86	0.150	87.26	0.830
4	4.60	94.00	95.32	-1.40	96.72	-2.89
5	6.10	104.0	100.3	3.50	101.3	2.50
6	9.10	103.0	105.5	-2.46	104.5	-1.52
7	12.20	109.0	106.9	1.86	104.9	3.67
8	15.20	103.0	106.1	-3.05	104.3	-1.35
9	19.80	100.0	102.2	-2.27	101.7	-1.75
10	24.40	93.00	96.43	-3.69	97.02	-4.33
11	30.50	88.00	87.19	0.913	88.48	-0.554
12	36.60	82.00	77.60	5.35	78.86	3.82
13	42.70	73.00	68.55	6.08	69.42	4.89
14	51.80	59.00	56.94	3.49	57.11	3.18
15	61.00	44.00	47.76	-8.54	47.43	-7.79
16	76.20	35.00	37.44	-6.99	36.83	-5.22
17	91.40	33.00	31.38	4.90	30.93	6.24
18	121.9	26.00	25.78	0.831	26.11	-0.444

NO DATA ARE MASKED

### Layered Model

L #	RESISTIVITY	THICKNESS (meters)	DEPTH	ELEVATION (meters)	LONG. COND. (Siemens)	TRANS. RES. (Ohm-m <sup>2</sup> )
				0.0		
1	877.5	0.380	0.380	-0.380	0.0	334.1
2	71.93	1.91	2.29	-2.29	0.0266	137.8
3	116.3	26.61	28.90	-28.90	0.228	3095.0
4	21.71					

ALL PARAMETERS ARE FREE

Parameter Bounds from Equivalence Analysis

LAYER		MINIMUM	BEST	MAXIMUM
RHO	1	489.02	877.52	1638.84
	2	46.79	71.94	88.09
	3	107.68	116.31	128.77
	4	18.67	21.72	24.57
THICK	1	0.29	0.38	0.51
	2	0.83	1.92	3.52
	3	22.34	26.61	31.07

PARAMETER RESOLUTION MATRIX:  
 "FIX" INDICATES FIXED PARAMETER

RHO	1	0.61						
RHO	2	-0.12	0.89					
RHO	3	0.00	0.00	0.99				
RHO	4	0.00	0.00	-0.01	0.96			
THK	1	0.17	0.07	0.00	0.00	0.91		
THK	2	-0.20	-0.22	-0.04	-0.03	0.13	0.35	
THK	3	0.00	0.01	0.02	0.03	0.00	0.09	0.95
	R	1	R	2	R	3	R	4
	T	1	T	2	T	3		

Smooth Model: Ridge Regression

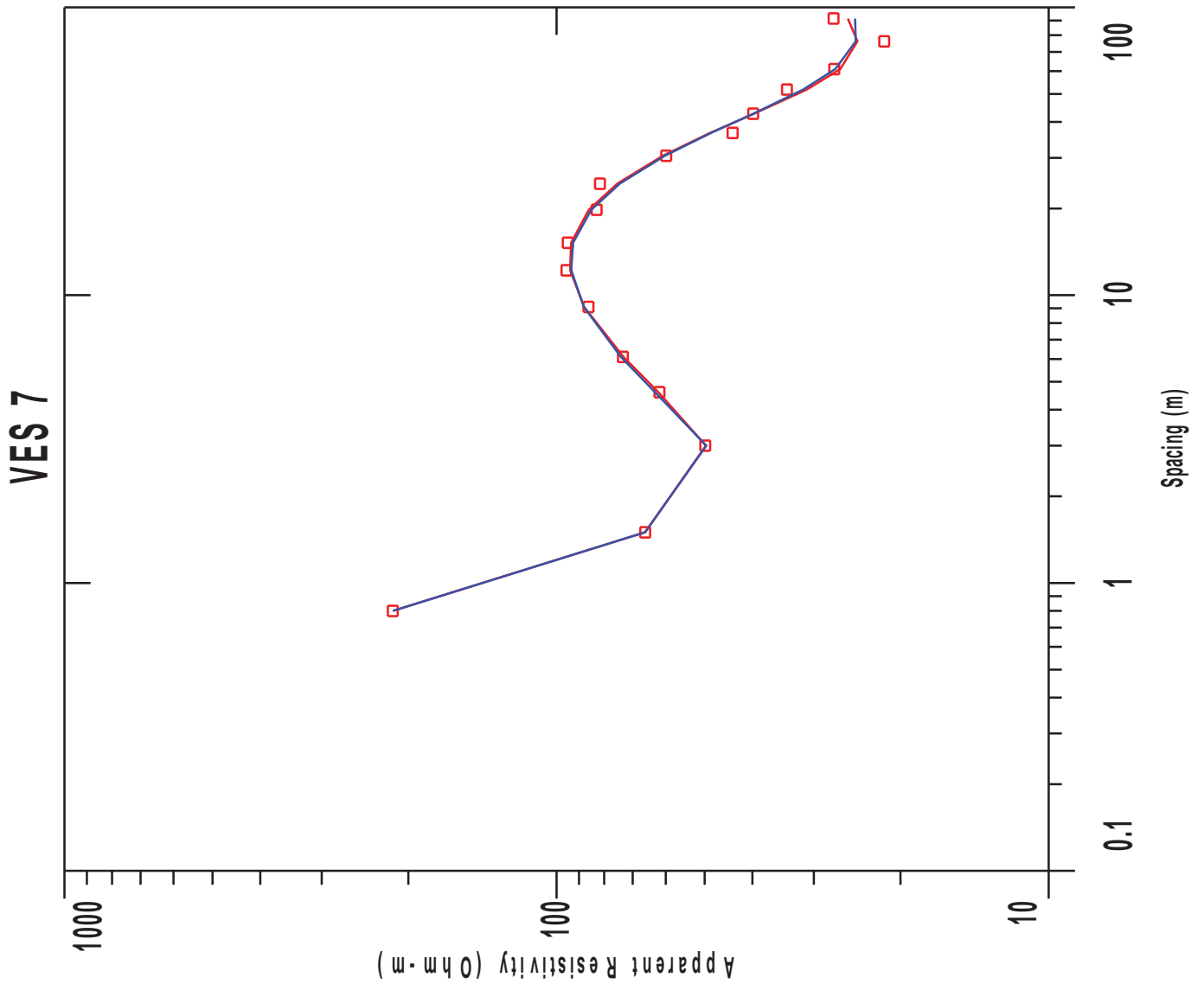
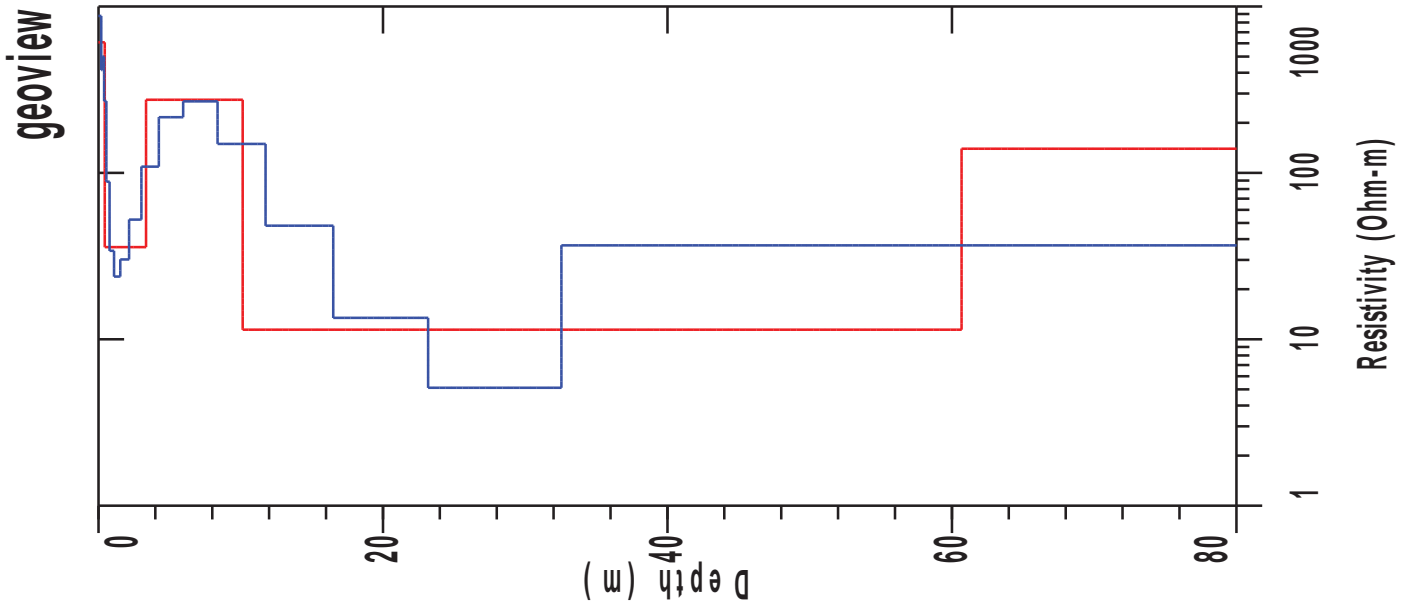
L #	RESISTIVITY	THICKNESS (meters)	DEPTH	ELEVATION (meters)	LONG. COND. (Siemens)	TRANS. RES. (Ohm-m <sup>2</sup> )
				0.0		
1	1102.6	0.200	0.200 *	-0.200	0.0	220.5
2	498.4	0.0799	0.279 *	-0.279	0.0	39.87
3	566.7	0.111	0.391 *	-0.391	0.0	63.46
4	306.9	0.156	0.548 *	-0.548	0.0	48.11
5	108.3	0.219	0.768 *	-0.768	0.00203	23.78
6	51.41	0.307	1.07 *	-1.07	0.00598	15.79
7	50.44	0.430	1.50 *	-1.50	0.00853	21.69
8	77.30	0.602	2.10 *	-2.10	0.00779	46.55
9	117.1	0.843	2.95 *	-2.95	0.00719	98.77
10	146.4	1.18	4.13 *	-4.13	0.00806	172.7
11	125.6	1.65	5.78 *	-5.78	0.0131	207.6
12	83.11	2.31	8.09 *	-8.09	0.0278	192.2

VES 6

Page 3

L #	RESISTIVITY	THICKNESS (meters)	DEPTH	ELEVATION (meters)	LONG. COND. (Siemens)	TRANS. RES. (Ohm-m <sup>2</sup> )
13	82.44	3.23	11.33 *	-11.33	0.0392	266.9
14	165.0	4.53	15.86 *	-15.86	0.0274	748.1
15	185.8	6.34	22.21 *	-22.21	0.0341	1179.2
16	53.02	8.88	31.09 *	-31.09	0.167	471.1
17	10.80	12.43	43.53 *	-43.53	1.15	134.4
18	24.26					

"\*" INDICATES FIXED PARAMETER



# VES 7

## Wenner Array

Northing: 0.0 Easting: 0.0 Elevation: 0.0

No.	Spacing (meters)	Layered Model:			Smooth Model:	
		Data Resistivity	Synthetic Resistivity	DIFFERENCE (percent)	Synthetic Resistivity	DIFFERENCE (percent)
1	0.800	215.1	215.1	0.00131	214.8	0.128
2	1.50	66.03	66.04	-0.0140	66.10	-0.111
3	3.00	49.85	49.72	0.248	49.62	0.461
4	4.60	61.76	62.05	-0.474	63.06	-2.10
5	6.10	73.27	73.08	0.261	73.99	-0.985
6	9.10	86.12	87.86	-2.02	87.99	-2.17
7	12.20	95.44	93.84	1.67	93.35	2.19
8	15.20	94.88	93.38	1.57	92.56	2.44
9	19.80	82.90	85.98	-3.71	84.99	-2.52
10	24.40	81.62	75.25	7.81	74.34	8.92
11	30.50	59.84	60.85	-1.67	60.24	-0.663
12	36.60	43.87	48.78	-11.20	48.55	-10.68
13	42.70	39.84	39.70	0.351	39.83	0.0209
14	51.80	34.02	31.01	8.84	31.52	7.34
15	61.00	27.27	26.51	2.76	27.13	0.487
16	76.20	21.58	24.46	-13.34	24.65	-14.21
17	91.40	27.34	25.58	6.43	24.72	9.58

NO DATA ARE MASKED

### Layered Model

L #	RESISTIVITY	THICKNESS (meters)	DEPTH	ELEVATION (meters)	LONG. COND. (Siemens)	TRANS. RES. (Ohm-m <sup>2</sup> )
				0.0		
1	609.1	0.442	0.442	-0.442	0.0	269.6
2	35.83	2.90	3.34	-3.34	0.0810	104.0
3	274.7	6.79	10.14	-10.14	0.0247	1866.8
4	11.42	50.54	60.68	-60.68	4.42	577.6
5	139.7					

ALL PARAMETERS ARE FREE

PARAMETER RESOLUTION MATRIX:  
 "FIX" INDICATES FIXED PARAMETER

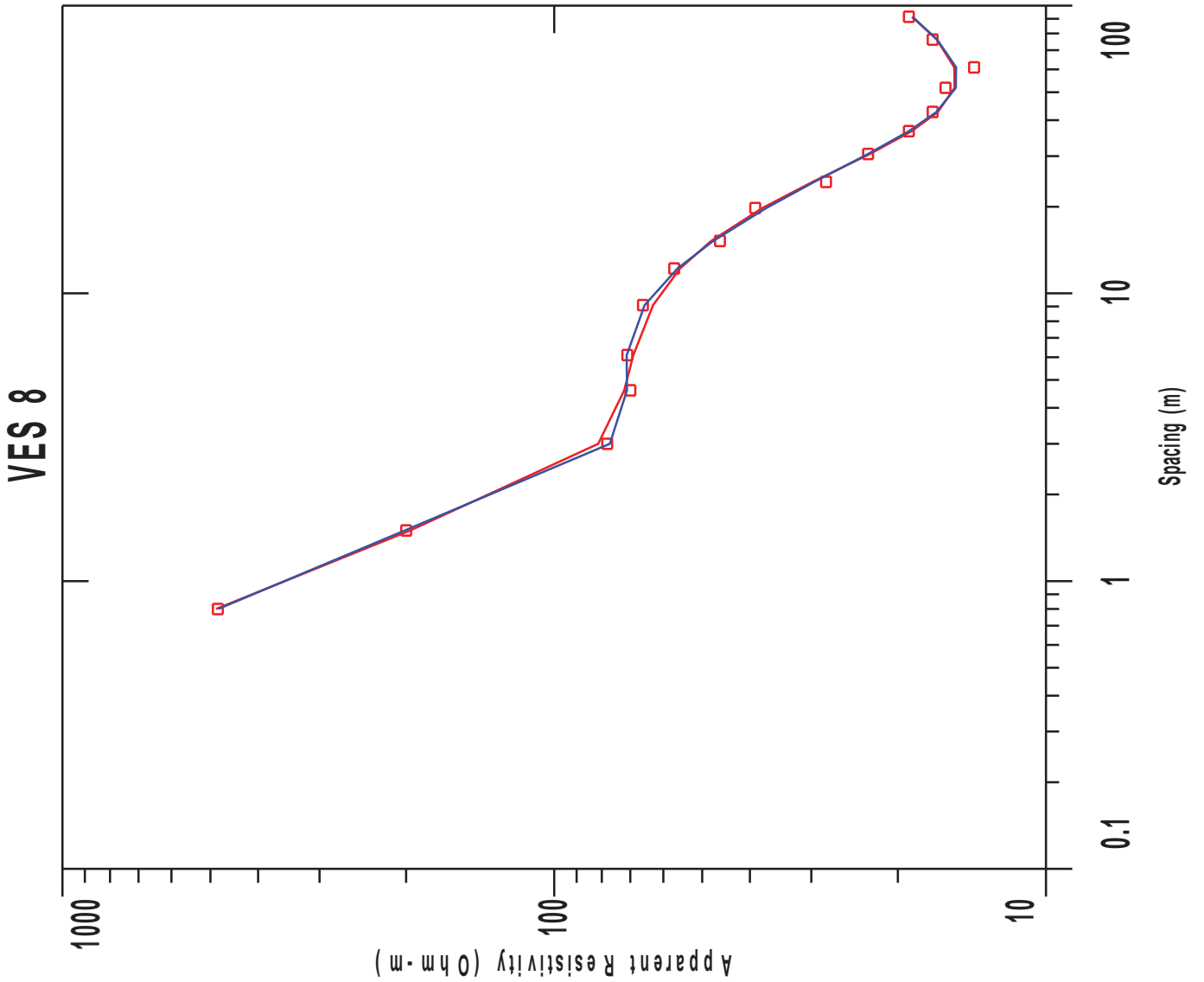
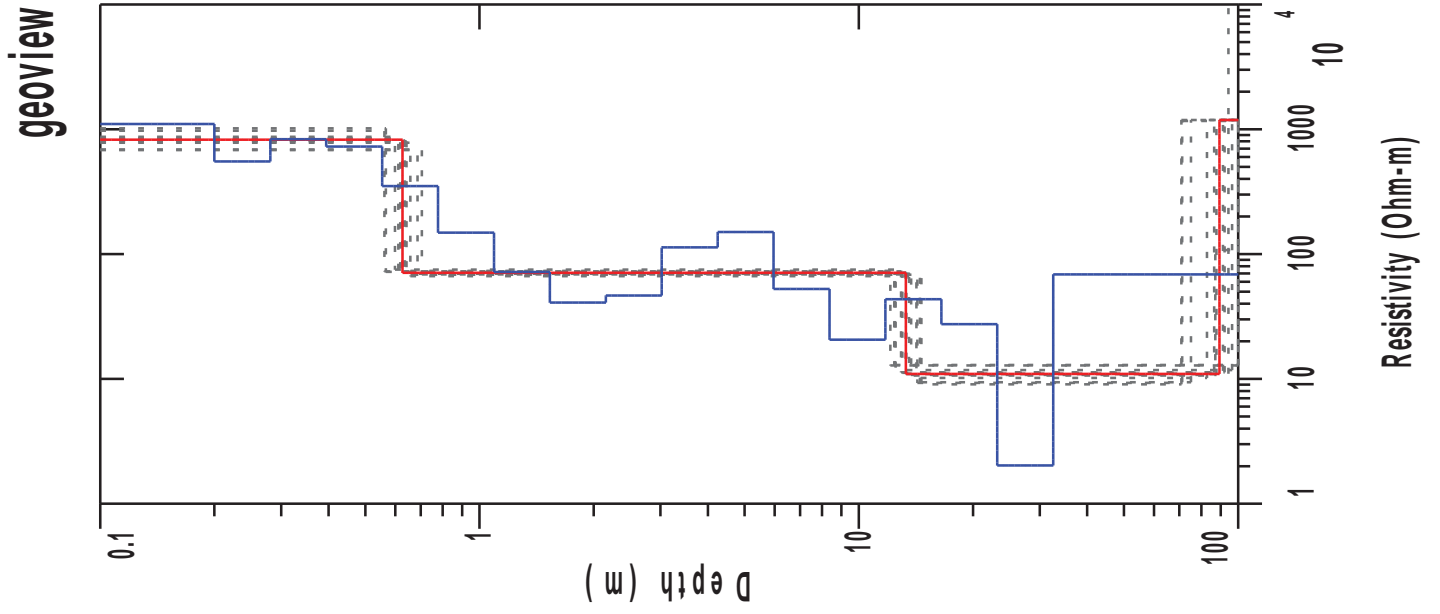
RHO 1 0.79  
 RHO 2 -0.09 0.85  
 RHO 3 0.00 -0.02 0.54  
 RHO 4 0.01 0.03 0.00 0.64  
 RHO 5 0.00 -0.01 0.00 0.05 0.02  
 THK 1 0.09 0.07 0.00 -0.01 0.00 0.95  
 THK 2 -0.10 -0.18 -0.11 0.06 -0.01 0.08 0.75  
 THK 3 0.00 0.02 0.47 0.06 -0.01 0.00 0.11 0.51  
 THK 4 0.01 0.02 0.01 -0.41 -0.09 -0.01 0.05 0.06 0.48  
 R 1 R 2 R 3 R 4 R 5 T 1 T 2 T 3 T 4

Smooth Model: Ridge Regression

L #	RESISTIVITY	THICKNESS (meters)	DEPTH	ELEVATION (meters)	LONG. COND. (Siemens)	TRANS. RES. (Ohm-m <sup>2</sup> )
				0.0		
1	877.1	0.200	0.200 *	-0.200	0.0	175.4
2	415.4	0.0808	0.280 *	-0.280	0.0	33.58
3	500.1	0.113	0.394 *	-0.394	0.0	56.77
4	269.8	0.159	0.553 *	-0.553	0.0	43.00
5	88.43	0.223	0.777 *	-0.777	0.00253	19.79
6	34.05	0.314	1.09 *	-1.09	0.00923	10.70
7	23.84	0.441	1.53 *	-1.53	0.0185	10.52
8	30.21	0.619	2.15 *	-2.15	0.0205	18.72
9	52.43	0.870	3.02 *	-3.02	0.0166	45.62
10	108.9	1.22	4.24 *	-4.24	0.0112	133.0
11	216.0	1.71	5.96 *	-5.96	0.00794	370.7
12	268.9	2.40	8.37 *	-8.37	0.00896	648.0
13	149.2	3.38	11.75 *	-11.75	0.0226	505.0
14	48.14	4.75	16.50 *	-16.50	0.0986	228.7
15	13.46	6.67	23.17 *	-23.17	0.495	89.85
16	5.11	9.36	32.54 *	-32.54	1.83	47.93
17	36.64					

"\*" INDICATES FIXED PARAMETER





# VES 8

## Wenner Array

Northing: 0.0 Easting: 0.0 Elevation: 0.0

No.	Spacing (meters)	Layered Model:			Smooth Model:	
		Data Resistivity	Synthetic Resistivity	DIFFERENCE (percent)	Synthetic Resistivity	DIFFERENCE (percent)
1	0.800	483.0	486.9	-0.827	481.8	0.246
2	1.50	200.0	196.1	1.94	201.0	-0.503
3	3.00	78.00	81.34	-4.28	77.06	1.20
4	4.60	70.00	72.06	-2.94	71.09	-1.56
5	6.10	71.00	69.02	2.78	71.19	-0.268
6	9.10	66.00	62.90	4.68	65.44	0.846
7	12.20	57.00	55.45	2.71	56.09	1.58
8	15.20	46.00	47.97	-4.29	47.49	-3.24
9	19.80	39.00	37.72	3.28	37.02	5.05
10	24.40	28.00	29.81	-6.47	29.58	-5.66
11	30.50	23.00	22.81	0.800	23.02	-0.104
12	36.60	19.00	18.75	1.26	19.00	-0.0440
13	42.70	17.00	16.58	2.44	16.69	1.80
14	51.80	16.00	15.33	4.13	15.25	4.66
15	61.00	14.00	15.35	-9.70	15.23	-8.80
16	76.20	17.00	16.67	1.90	16.64	2.11
17	91.40	19.00	18.72	1.43	18.67	1.73

NO DATA ARE MASKED

### Layered Model

L #	RESISTIVITY	THICKNESS (meters)	DEPTH	ELEVATION (meters)	LONG. COND. (Siemens)	TRANS. RES. (Ohm-m <sup>2</sup> )
				0.0		
1	824.0	0.626	0.626	-0.626	0.0	516.2
2	70.81	12.67	13.30	-13.30	0.179	897.7
3	10.97	76.00	89.30	-89.30	6.92	834.3
4	1185.1					

ALL PARAMETERS ARE FREE

Parameter Bounds from Equivalence Analysis

LAYER		MINIMUM	BEST	MAXIMUM
RHO	1	680.60	824.06	1015.95
	2	66.58	70.81	75.11
	3	9.06	10.98	12.92
	4	107.77	1185.14	176083.55
THICK	1	0.56	0.63	0.70
	2	11.50	12.68	13.98
	3	56.39	76.00	100.80

PARAMETER RESOLUTION MATRIX:  
 "FIX" INDICATES FIXED PARAMETER

RHO	1	0.92												
RHO	2	-0.01	0.99											
RHO	3	-0.01	-0.01	0.91										
RHO	4	0.00	0.00	0.00	0.00									
THK	1	0.04	0.01	0.01	0.00	0.97								
THK	2	0.01	0.01	0.04	0.00	-0.01	0.98							
THK	3	-0.01	-0.01	-0.13	-0.01	0.01	0.06	0.77						
	R	1	R	2	R	3	R	4	T	1	T	2	T	3

Smooth Model: Ridge Regression

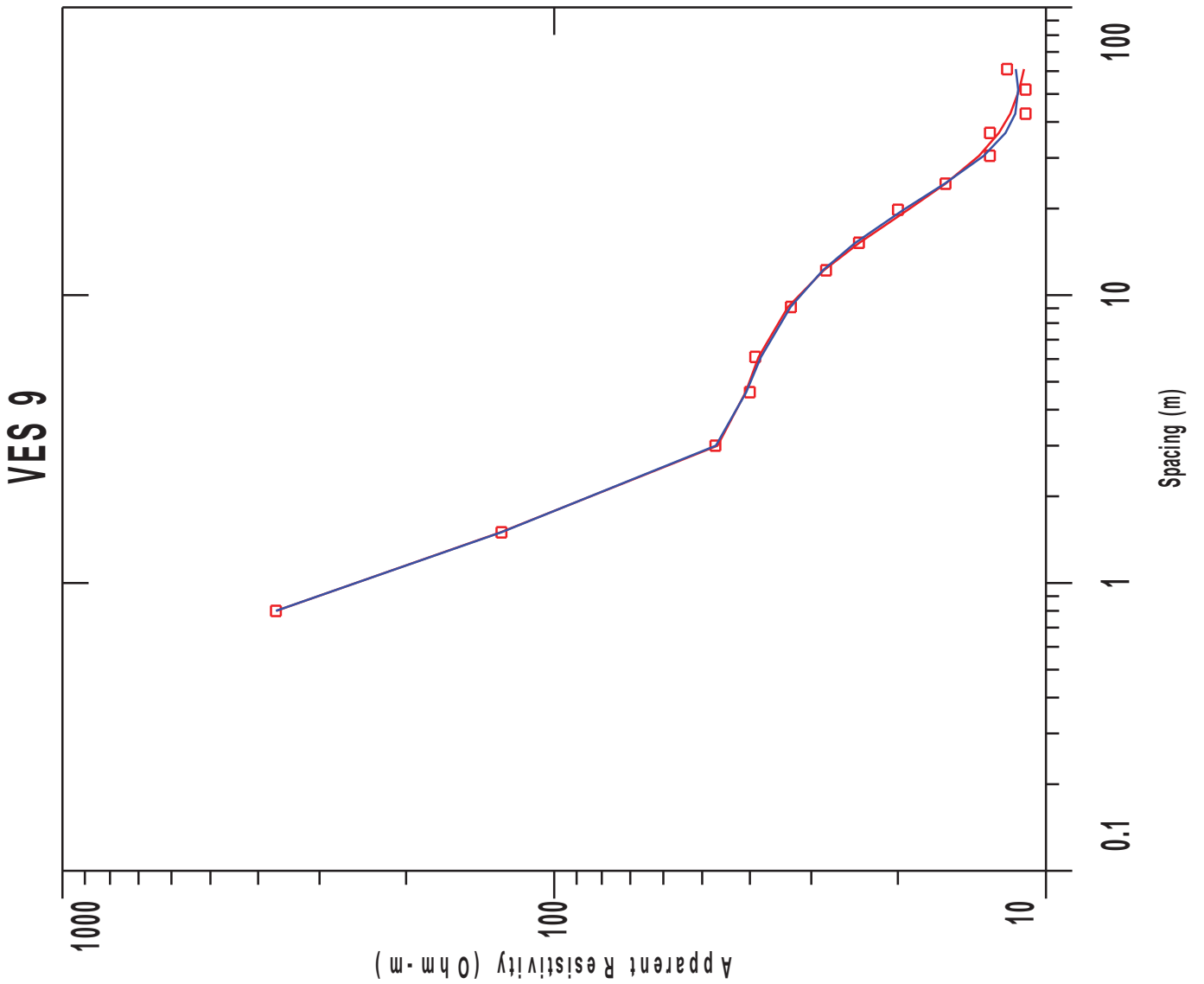
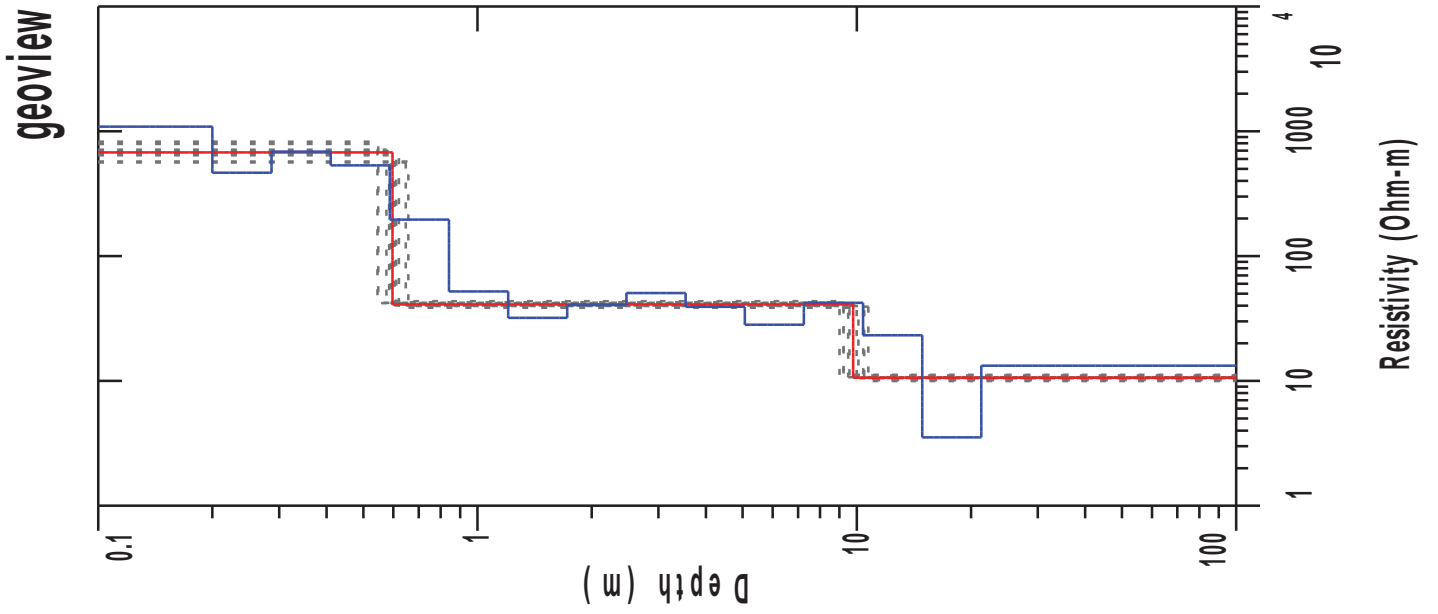
L #	RESISTIVITY	THICKNESS (meters)	DEPTH	ELEVATION (meters)	LONG. COND. (Siemens)	TRANS. RES. (Ohm-m <sup>2</sup> )
				0.0		
1	1102.8	0.200	0.200 *	-0.200	0.0	220.5
2	552.0	0.0808	0.280 *	-0.280	0.0	44.62
3	833.2	0.113	0.394 *	-0.394	0.0	94.59
4	726.7	0.159	0.553 *	-0.553	0.0	115.8
5	350.4	0.223	0.777 *	-0.777	0.0	78.44
6	148.7	0.314	1.09 *	-1.09	0.00211	46.74
7	71.87	0.441	1.53 *	-1.53	0.00614	31.72
8	40.86	0.619	2.15 *	-2.15	0.0151	25.32
9	46.55	0.870	3.02 *	-3.02	0.0186	40.51
10	113.1	1.22	4.24 *	-4.24	0.0108	138.2
11	150.3	1.71	5.96 *	-5.96	0.0114	258.0
12	52.54	2.40	8.37 *	-8.37	0.0458	126.6

VES 8

Page 3

L #	RESISTIVITY	THICKNESS (meters)	DEPTH	ELEVATION (meters)	LONG. COND. (Siemens)	TRANS. RES. (Ohm-m <sup>2</sup> )
13	20.63	3.38	11.75 *	-11.75	0.163	69.83
14	43.55	4.75	16.50 *	-16.50	0.109	206.9
15	27.45	6.67	23.17 *	-23.17	0.242	183.1
16	2.02	9.36	32.54 *	-32.54	4.61	18.99
17	68.84					

"\*" INDICATES FIXED PARAMETER



# VES 9

## Wenner Array

Northing: 0.0 Easting: 0.0 Elevation: 0.0

No.	Spacing (meters)	Layered Model:			Smooth Model:	
		Data Resistivity	Synthetic Resistivity	DIFFERENCE (percent)	Synthetic Resistivity	DIFFERENCE (percent)
1	0.800	368.0	367.3	0.177	367.9	0.00760
2	1.50	128.0	128.4	-0.327	128.0	-0.0154
3	3.00	47.00	46.54	0.968	46.89	0.216
4	4.60	40.00	40.79	-1.98	40.69	-1.73
5	6.10	39.00	38.40	1.52	37.98	2.61
6	9.10	33.00	33.43	-1.33	33.05	-0.172
7	12.20	28.00	28.27	-0.983	28.41	-1.47
8	15.20	24.00	23.95	0.177	24.41	-1.71
9	19.80	20.00	19.08	4.59	19.48	2.59
10	24.40	16.00	15.99	0.0363	16.05	-0.368
11	30.50	13.00	13.67	-5.18	13.38	-2.95
12	36.60	13.00	12.46	4.09	12.08	7.04
13	42.70	11.00	11.81	-7.43	11.54	-4.94
14	51.80	11.00	11.32	-2.96	11.38	-3.50
15	61.00	12.00	11.08	7.63	11.51	4.02

NO DATA ARE MASKED

### Layered Model

L #	RESISTIVITY	THICKNESS (meters)	DEPTH	ELEVATION (meters)	LONG. COND. (Siemens)	TRANS. RES. (Ohm-m <sup>2</sup> )
				0.0		
1	676.8	0.596	0.596	-0.596	0.0	404.0
2	41.04	9.18	9.78	-9.78	0.223	377.0
3	10.60					

ALL PARAMETERS ARE FREE

### Parameter Bounds from Equivalence Analysis

LAYER	MINIMUM	BEST	MAXIMUM
RHO 1	562.46	676.86	824.37

Prepared for geoview



VES 9

Page 2

		LAYER	MINIMUM	BEST	MAXIM
	2	38.59	41.04	43.53	
	3	9.98	10.61	11.20	
THICK	1	0.54	0.60	0.66	
	2	8.42	9.19	10.12	

PARAMETER RESOLUTION MATRIX:  
 "FIX" INDICATES FIXED PARAMETER

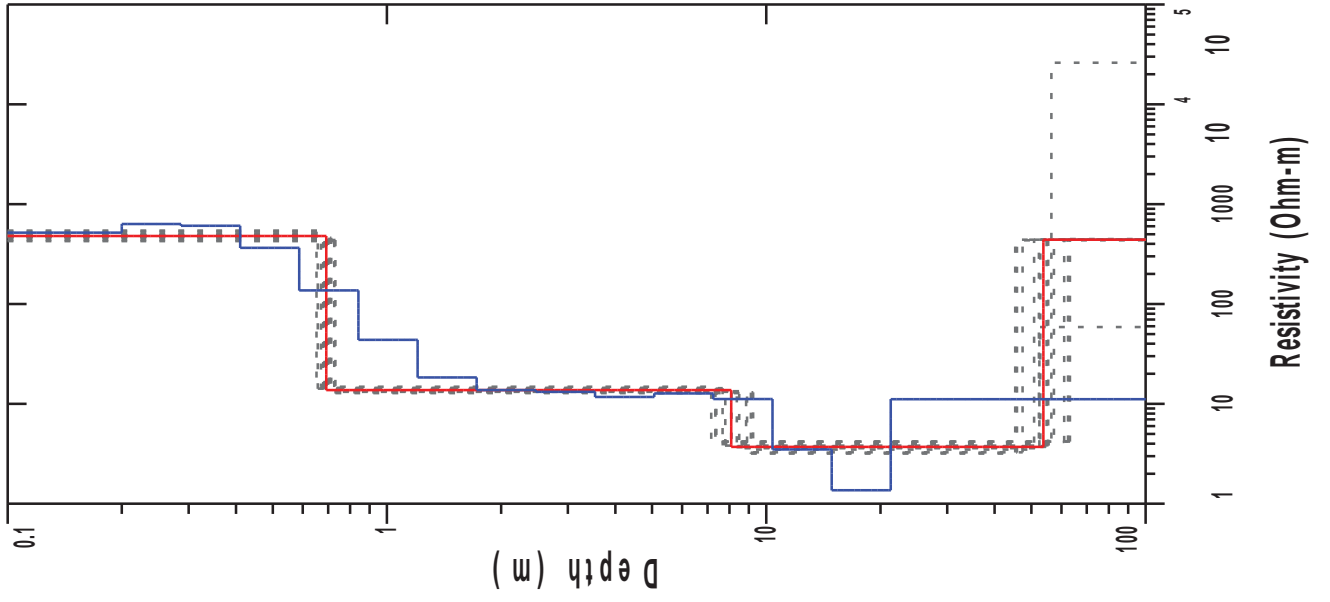
RHO	1	0.93			
RHO	2	-0.01	0.99		
RHO	3	0.00	0.00	0.99	
THK	1	0.03	0.01	0.00	0.98
THK	2	0.01	0.01	0.01	-0.01
	R 1	R 2	R 3	T 1	T 2

Smooth Model: Ridge Regression

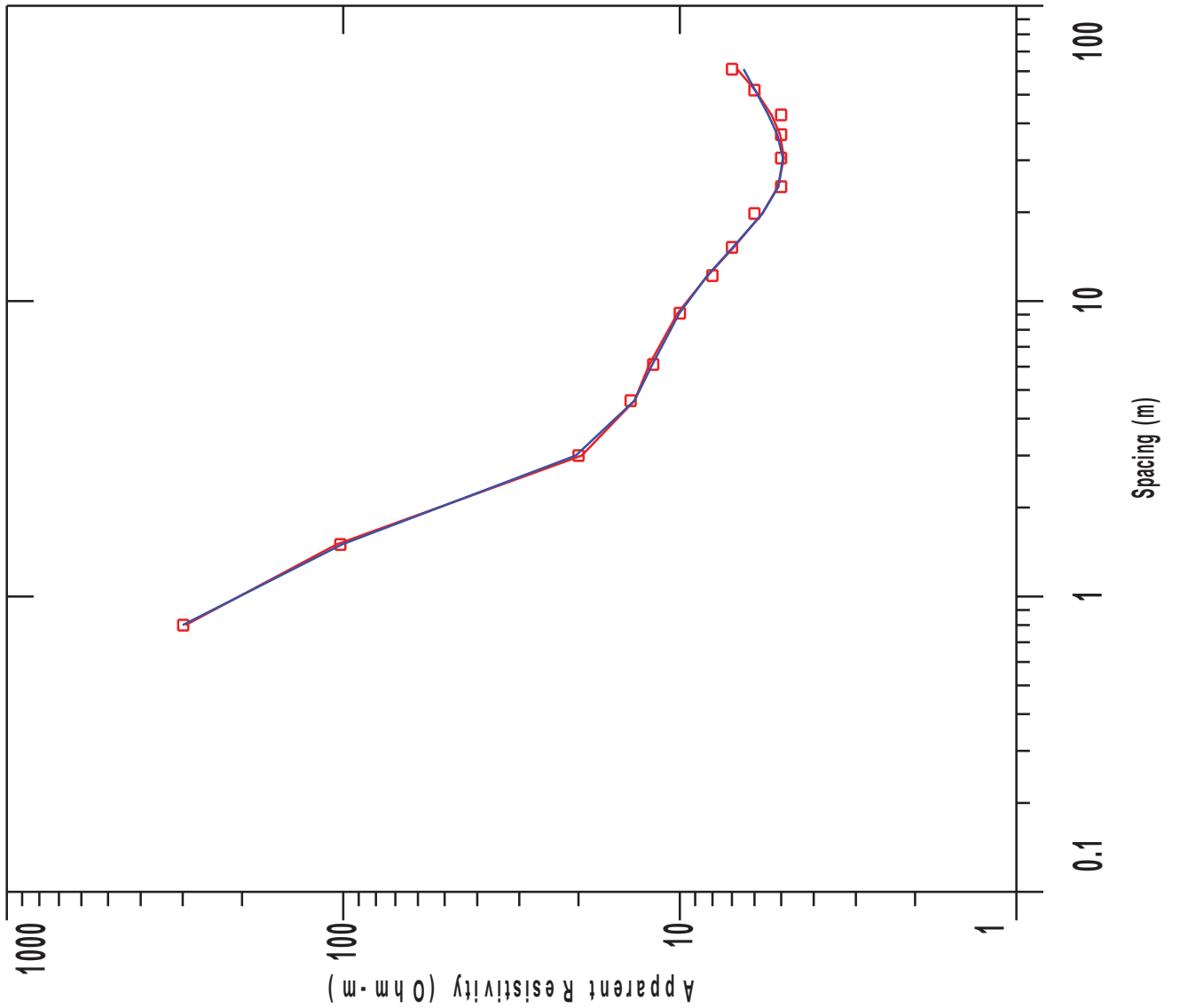
L #	RESISTIVITY	THICKNESS (meters)	DEPTH	ELEVATION (meters)	LONG. COND. (Siemens)	TRANS. RES. (Ohm-m <sup>2</sup> )
				0.0		
1	1088.4	0.200	0.200 *	-0.200	0.0	217.6
2	465.5	0.0864	0.286 *	-0.286	0.0	40.22
3	686.3	0.123	0.410 *	-0.410	0.0	84.91
4	533.3	0.177	0.587 *	-0.587	0.0	94.50
5	195.9	0.253	0.841 *	-0.841	0.00130	49.71
6	52.08	0.363	1.20 *	-1.20	0.00698	18.92
7	32.05	0.520	1.72 *	-1.72	0.0162	16.67
8	40.51	0.745	2.46 *	-2.46	0.0183	30.18
9	50.60	1.06	3.53 *	-3.53	0.0210	53.99
10	39.19	1.52	5.06 *	-5.06	0.0389	59.88
11	28.19	2.18	7.25 *	-7.25	0.0776	61.68
12	42.24	3.13	10.38 *	-10.38	0.0741	132.3
13	23.19	4.48	14.87 *	-14.87	0.193	104.0
14	3.52	6.42	21.29 *	-21.29	1.82	22.67
15	13.24					

"\*" INDICATES FIXED PARAMETER

geoview



VES 10



# VES 10

## Wenner Array

Northing: 0.0 Easting: 0.0 Elevation: 0.0

No.	Spacing (meters)	Layered Model:			Smooth Model:	
		Data Resistivity	Synthetic Resistivity	DIFFERENCE (percent)	Synthetic Resistivity	DIFFERENCE (percent)
1	0.800	299.0	294.3	1.56	300.0	-0.355
2	1.50	102.0	104.6	-2.64	100.8	1.08
3	3.00	20.00	19.56	2.17	20.37	-1.86
4	4.60	14.00	13.63	2.58	13.63	2.57
5	6.10	12.00	12.32	-2.72	12.07	-0.640
6	9.10	10.00	10.14	-1.49	10.02	-0.282
7	12.20	8.00	8.25	-3.22	8.27	-3.49
8	15.20	7.00	6.92	1.10	6.96	0.551
9	19.80	6.00	5.68	5.20	5.68	5.32
10	24.40	5.00	5.11	-2.24	5.09	-1.83
11	30.50	5.00	4.90	1.89	4.93	1.20
12	36.60	5.00	5.03	-0.644	5.13	-2.65
13	42.70	5.00	5.33	-6.73	5.45	-9.04
14	51.80	6.00	5.97	0.380	5.97	0.445
15	61.00	7.00	6.75	3.52	6.46	7.63

NO DATA ARE MASKED

### Layered Model

L #	RESISTIVITY	THICKNESS (meters)	DEPTH	ELEVATION (meters)	LONG. COND. (Siemens)	TRANS. RES. (Ohm-m <sup>2</sup> )
				0.0		
1	480.1	0.691	0.691	-0.691	0.00144	332.2
2	13.76	7.39	8.08	-8.08	0.536	101.7
3	3.70	45.66	53.75	-53.75	12.32	169.2
4	440.7					

ALL PARAMETERS ARE FREE

Parameter Bounds from Equivalence Analysis

LAYER		MINIMUM	BEST	MAXIMUM
RHO	1	426.52	480.14	544.32
	2	12.81	13.77	14.88
	3	3.17	3.71	4.20
	4	58.75	440.77	26058.37
THICK	1	0.65	0.69	0.73
	2	6.48	7.39	8.53
	3	36.24	45.67	55.81

PARAMETER RESOLUTION MATRIX:  
 "FIX" INDICATES FIXED PARAMETER

RHO	1	0.95												
RHO	2	-0.01	0.98											
RHO	3	-0.01	-0.02	0.92										
RHO	4	0.00	0.00	0.00	0.00									
THK	1	0.02	0.01	0.01	0.00	0.99								
THK	2	0.01	0.03	0.06	0.00	-0.01	0.93							
THK	3	-0.01	-0.02	-0.11	-0.01	0.01	0.09	0.81						
	R	1	R	2	R	3	R	4	T	1	T	2	T	3

Smooth Model: Occam's Inversion

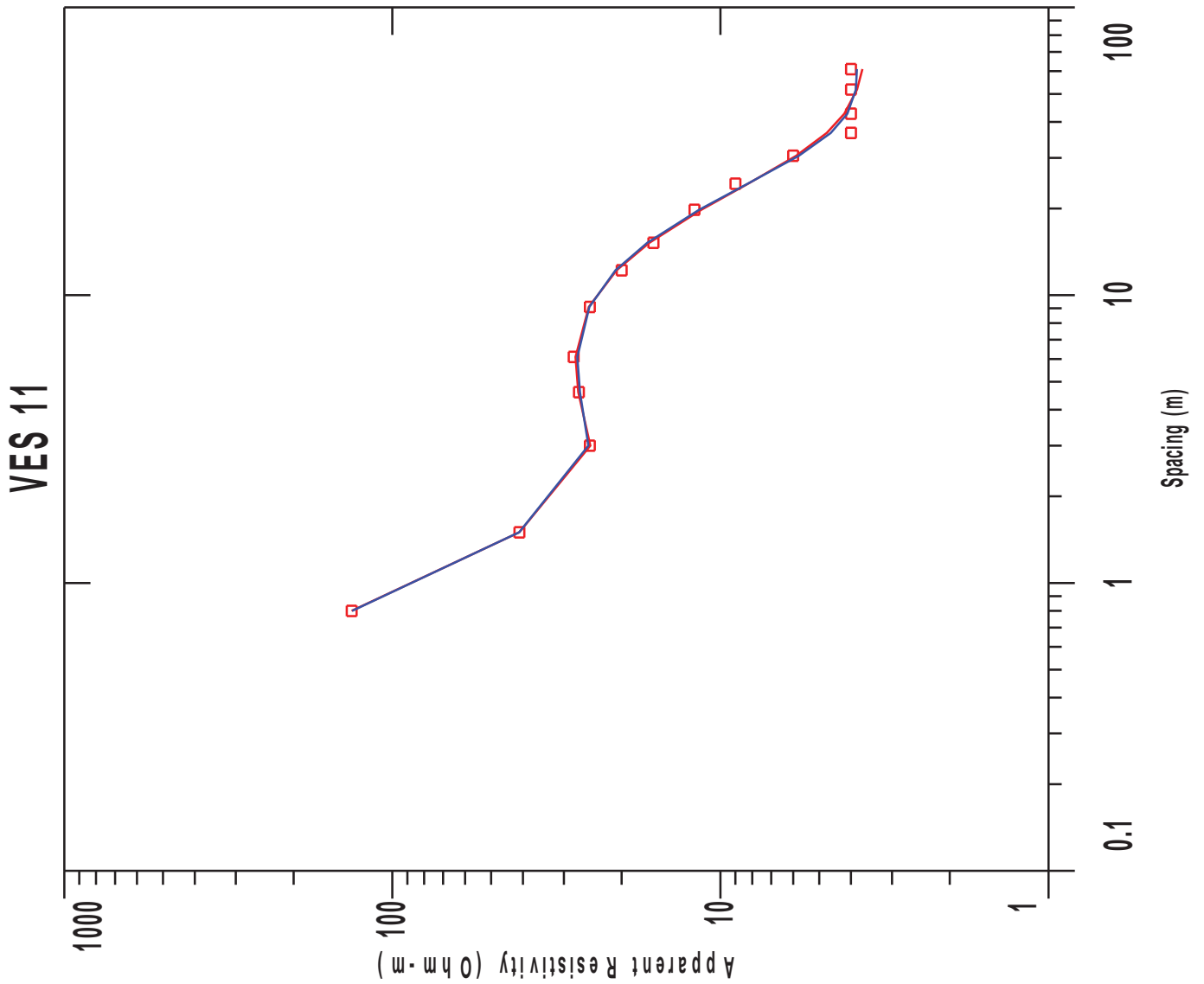
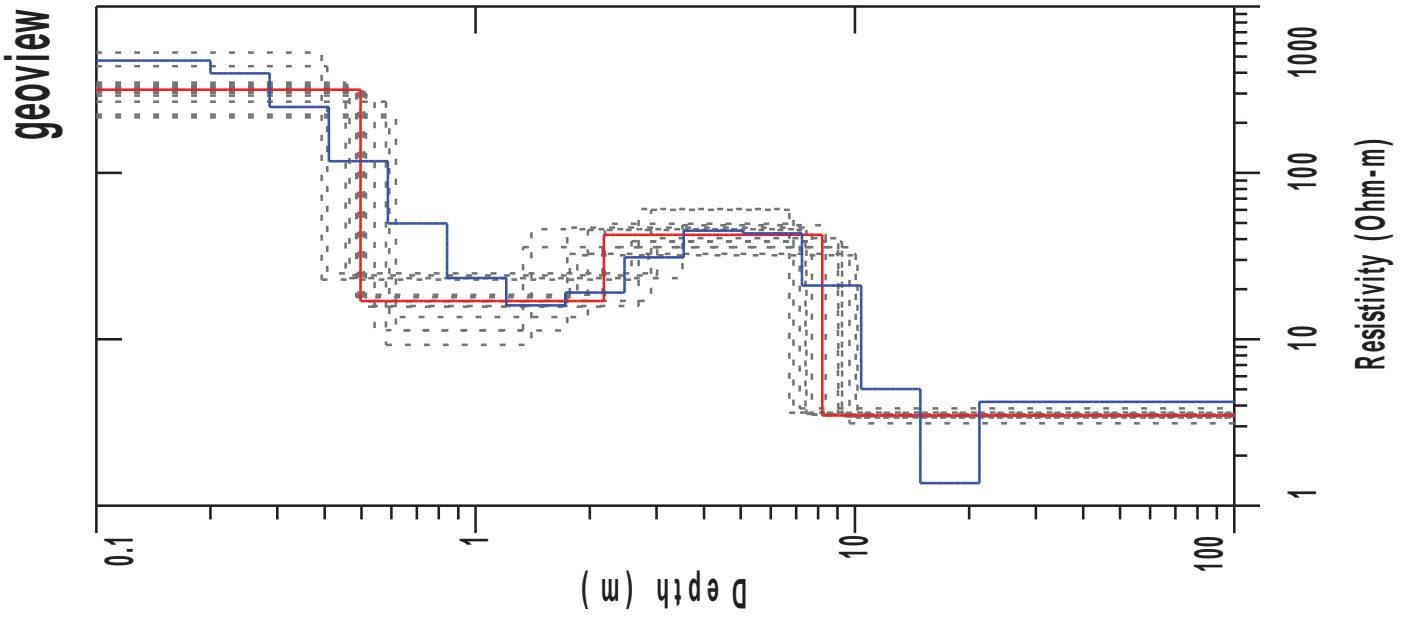
L #	RESISTIVITY	THICKNESS (meters)	DEPTH	ELEVATION (meters)	LONG. COND. (Siemens)	TRANS. RES. (Ohm-m <sup>2</sup> )
				0.0		
1	518.1	0.200	0.200 *	-0.200	0.0	103.6
2	632.4	0.0864	0.286 *	-0.286	0.0	54.64
3	608.0	0.123	0.410 *	-0.410	0.0	75.23
4	365.5	0.177	0.587 *	-0.587	0.0	64.76
5	136.8	0.253	0.841 *	-0.841	0.00185	34.73
6	43.84	0.363	1.20 *	-1.20	0.00829	15.92
7	18.40	0.520	1.72 *	-1.72	0.0282	9.57
8	13.73	0.745	2.46 *	-2.46	0.0542	10.23
9	13.20	1.06	3.53 *	-3.53	0.0808	14.08
10	11.75	1.52	5.06 *	-5.06	0.130	17.95
11	12.72	2.18	7.25 *	-7.25	0.171	27.85
12	11.18	3.13	10.38 *	-10.38	0.280	35.04

VES 10

Page 3

L #	RESISTIVITY	THICKNESS (meters)	DEPTH	ELEVATION (meters)	LONG. COND. (Siemens)	TRANS. RES. (Ohm-m <sup>2</sup> )
13	3.50	4.48	14.87 *	-14.87	1.28	15.71
14	1.36	6.42	21.29 *	-21.29	4.71	8.75
15	11.13					

"\*" INDICATES FIXED PARAMETER



# VES 11

## Wenner Array

Northing: 0.0 Easting: 0.0 Elevation: 0.0

No.	Spacing (meters)	Layered Model:			Smooth Model:	
		Data Resistivity	Synthetic Resistivity	DIFFERENCE (percent)	Synthetic Resistivity	DIFFERENCE (percent)
1	0.800	133.0	133.0	-0.0393	132.6	0.294
2	1.50	41.00	40.99	0.00342	41.05	-0.142
3	3.00	25.00	24.91	0.348	25.24	-0.990
4	4.60	27.00	27.12	-0.450	26.78	0.778
5	6.10	28.00	27.65	1.22	27.28	2.55
6	9.10	25.00	25.17	-0.711	25.08	-0.351
7	12.20	20.00	20.71	-3.57	20.88	-4.40
8	15.20	16.00	16.47	-2.94	16.72	-4.51
9	19.80	12.00	11.43	4.67	11.61	3.22
10	24.40	9.00	8.22	8.59	8.25	8.32
11	30.50	6.00	5.87	2.01	5.77	3.81
12	36.60	4.00	4.74	-18.56	4.60	-15.22
13	42.70	4.00	4.19	-4.79	4.10	-2.55
14	51.80	4.00	3.83	4.13	3.86	3.44
15	61.00	4.00	3.69	7.70	3.83	4.02

NO DATA ARE MASKED

### Layered Model

L #	RESISTIVITY	THICKNESS (meters)	DEPTH	ELEVATION (meters)	LONG. COND. (Siemens)	TRANS. RES. (Ohm-m <sup>2</sup> )
				0.0		
1	316.0	0.497	0.497	-0.497	0.00157	157.1
2	16.96	1.68	2.17	-2.17	0.0991	28.51
3	42.43	6.02	8.20	-8.20	0.142	255.8
4	3.49					

ALL PARAMETERS ARE FREE



Parameter Bounds from Equivalence Analysis

LAYER		MINIMUM	BEST	MAXIMUM
RHO	1	215.69	316.10	528.27
	2	9.25	16.96	24.88
	3	31.98	42.44	60.68
	4	3.13	3.49	3.84
THICK	1	0.39	0.50	0.62
	2	0.79	1.68	3.04
	3	3.99	6.03	8.30

PARAMETER RESOLUTION MATRIX:  
 "FIX" INDICATES FIXED PARAMETER

RHO	1	0.86						
RHO	2	-0.08	0.71					
RHO	3	0.02	0.04	0.80				
RHO	4	0.00	0.01	-0.02	0.99			
THK	1	0.06	0.07	-0.02	0.00	0.96		
THK	2	-0.07	-0.34	-0.15	0.00	0.07	0.35	
THK	3	-0.02	0.00	0.23	0.03	0.01	0.23	0.73
	R	1	R	2	R	3	R	4
	T	1	T	2	T	3		

Smooth Model: Occam's Inversion

L #	RESISTIVITY	THICKNESS (meters)	DEPTH	ELEVATION (meters)	LONG. COND. (Siemens)	TRANS. RES. (Ohm-m <sup>2</sup> )
				0.0		
1	473.0	0.200	0.200 *	-0.200	0.0	94.60
2	396.4	0.0864	0.286 *	-0.286	0.0	34.25
3	248.7	0.123	0.410 *	-0.410	0.0	30.78
4	117.6	0.177	0.587 *	-0.587	0.00151	20.83
5	49.72	0.253	0.841 *	-0.841	0.00510	12.61
6	23.32	0.363	1.20 *	-1.20	0.0155	8.47
7	16.00	0.520	1.72 *	-1.72	0.0325	8.32
8	19.07	0.745	2.46 *	-2.46	0.0390	14.21
9	31.05	1.06	3.53 *	-3.53	0.0343	33.13
10	45.00	1.52	5.06 *	-5.06	0.0339	68.76
11	43.32	2.18	7.25 *	-7.25	0.0505	94.78
12	21.05	3.13	10.38 *	-10.38	0.148	65.95

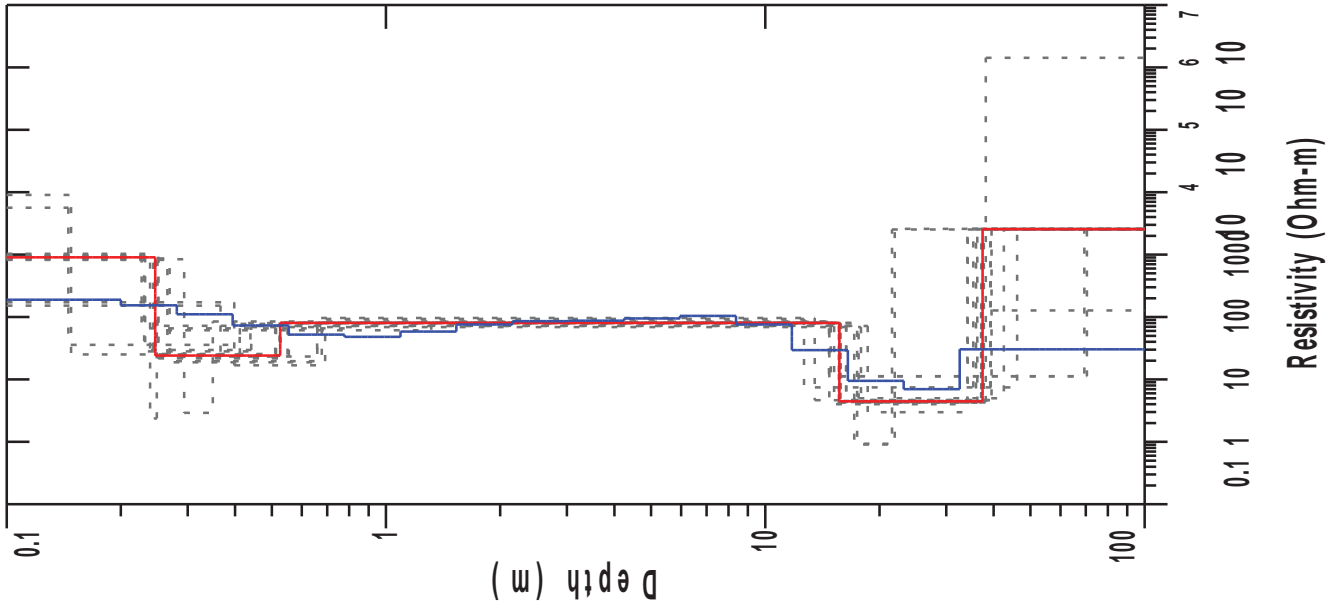
VES 11

Page 3

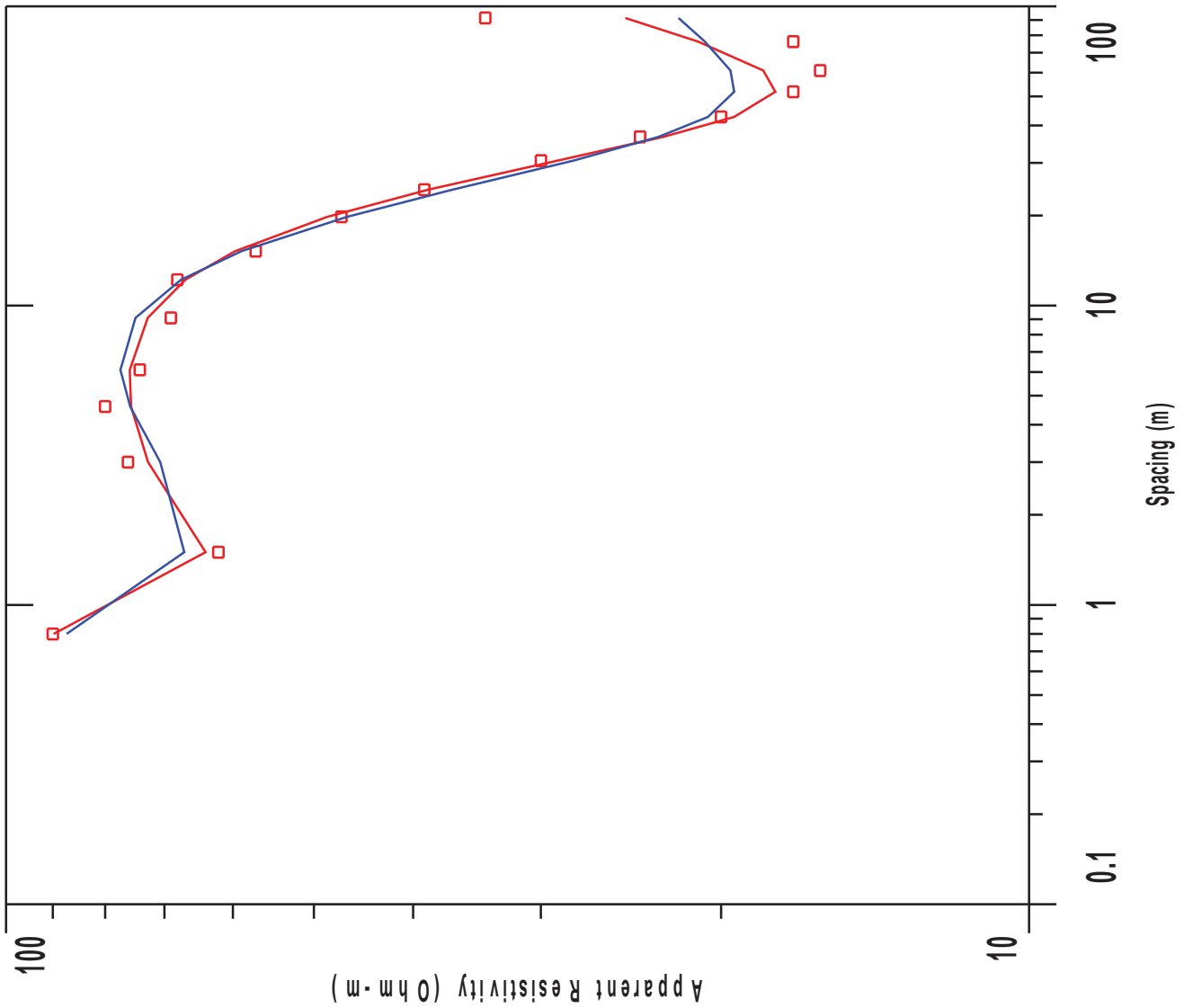
L #	RESISTIVITY	THICKNESS (meters)	DEPTH	ELEVATION (meters)	LONG. COND. (Siemens)	TRANS. RES. (Ohm-m <sup>2</sup> )
13	5.02	4.48	14.87 *	-14.87	0.893	22.53
14	1.36	6.42	21.29 *	-21.29	4.69	8.78
15	4.21					

"\*" INDICATES FIXED PARAMETER

geoview



VES 12



# VES 12

## Wenner Array

Northing: 0.0 Easting: 0.0 Elevation: 0.0

No.	Spacing (meters)	Layered Model:			Smooth Model:	
		Data Resistivity	Synthetic Resistivity	DIFFERENCE (percent)	Synthetic Resistivity	DIFFERENCE (percent)
1	0.800	90.00	89.82	0.199	87.24	3.06
2	1.50	62.00	63.81	-2.93	66.94	-7.97
3	3.00	76.00	72.63	4.43	70.65	7.02
4	4.60	80.00	75.45	5.68	75.61	5.47
5	6.10	74.00	75.68	-2.27	77.30	-4.46
6	9.10	69.00	72.68	-5.34	74.70	-8.27
7	12.20	68.00	66.77	1.80	67.42	0.849
8	15.20	57.00	59.70	-4.75	58.87	-3.28
9	19.80	47.00	48.50	-3.20	46.41	1.25
10	24.40	39.00	38.65	0.890	36.58	6.19
11	30.50	30.00	28.91	3.62	27.90	6.97
12	36.60	24.00	22.78	5.04	23.03	4.01
13	42.70	20.00	19.42	2.87	20.60	-3.00
14	51.80	17.00	17.70	-4.12	19.41	-14.21
15	61.00	16.00	18.18	-13.67	19.58	-22.40
16	76.20	17.00	21.06	-23.88	20.74	-22.02
17	91.40	34.00	24.81	27.02	22.00	35.27

NO DATA ARE MASKED

### Layered Model

L #	RESISTIVITY	THICKNESS (meters)	DEPTH	ELEVATION (meters)	LONG. COND. (Siemens)	TRANS. RES. (Ohm-m <sup>2</sup> )
				0.0		
1	905.5	0.246	0.246	-0.246	0.0	223.2
2	24.08	0.279	0.526	-0.526	0.0116	6.73
3	80.46	15.15	15.68	-15.68	0.188	1219.4
4	4.45	21.72	37.40	-37.40	4.87	96.69
5	2561.6					

ALL PARAMETERS ARE FREE

Parameter Bounds from Equivalence Analysis

LAYER	MINIMUM	BEST	MAXIMUM	
RHO	1	152.54	905.58	9055.83
	2	2.37	24.09	65.89
	3	68.94	80.46	96.56
	4	0.91	4.45	11.26
	5	127.24	2561.61	1425809.50
THICK	1	0.15	0.25	0.40
	2	0.01	0.28	1.07
	3	11.97	15.16	18.19
	4	4.42	21.72	55.61

PARAMETER RESOLUTION MATRIX:  
 "FIX" INDICATES FIXED PARAMETER

RHO	1	0.05									
RHO	2	-0.02	0.45								
RHO	3	0.00	0.01	0.99							
RHO	4	0.01	-0.03	0.00	0.52						
RHO	5	0.00	0.00	0.00	0.00	0.00					
THK	1	0.21	0.05	0.00	0.00	0.00	0.94				
THK	2	0.02	-0.42	-0.02	0.02	0.00	-0.01	0.40			
THK	3	-0.01	-0.01	0.01	0.03	0.00	0.01	0.02	0.98		
THK	4	0.01	-0.03	0.00	-0.48	0.00	0.01	0.02	0.03	0.51	
		R	1 R	2 R	3 R	4 R	5 T	1 T	2 T	3 T	4

Smooth Model: Occam's Inversion

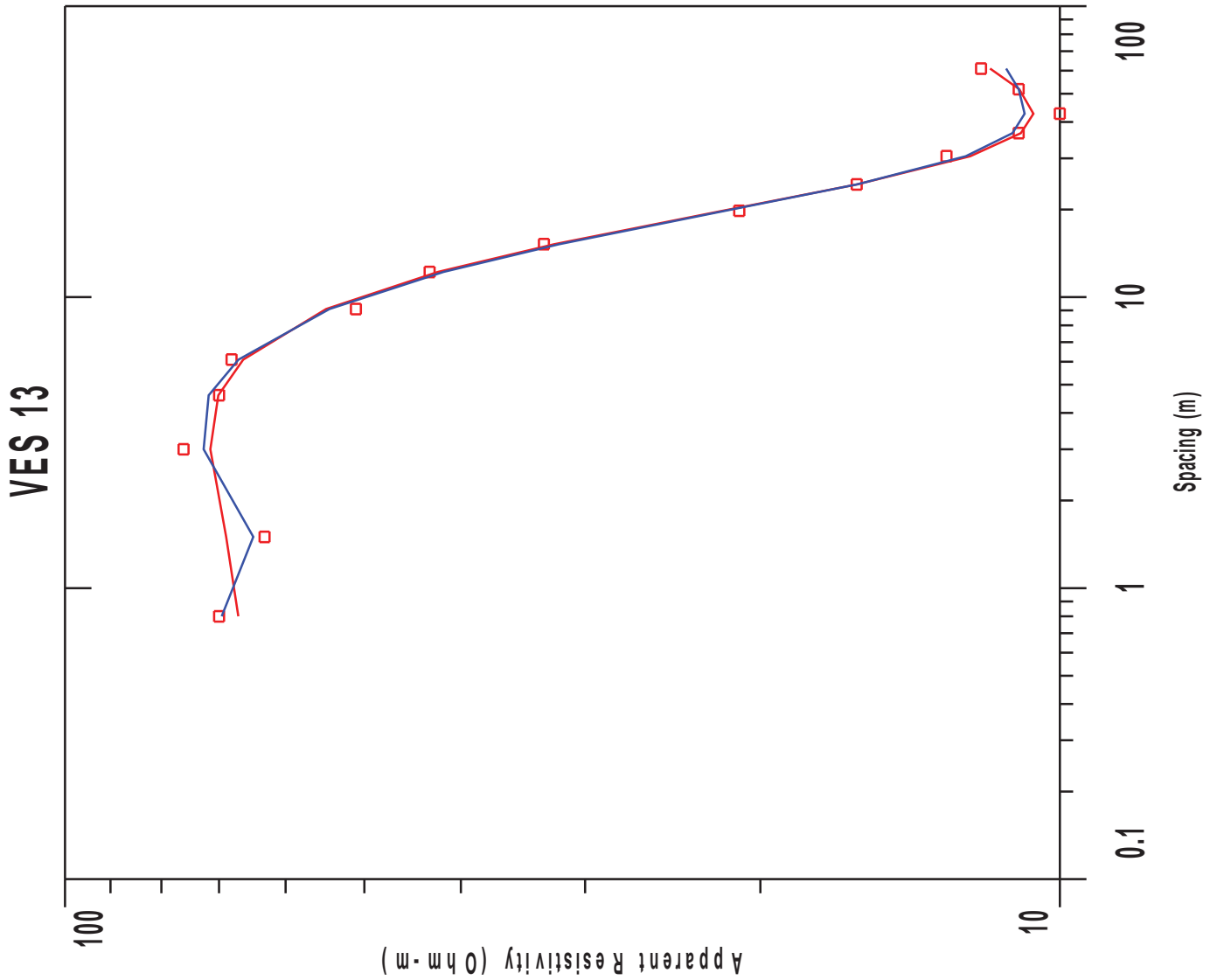
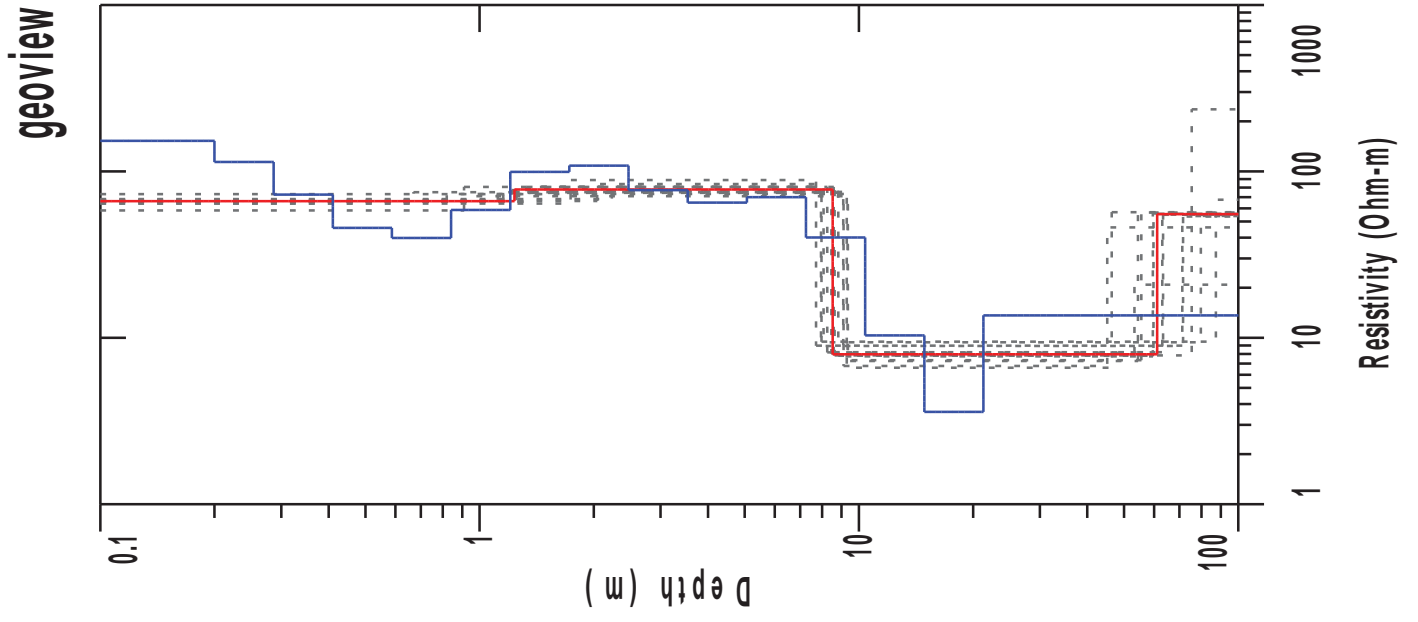
L #	RESISTIVITY	THICKNESS (meters)	DEPTH	ELEVATION (meters)	LONG. COND. (Siemens)	TRANS. RES. (Ohm-m <sup>2</sup> )
				0.0		
1	189.3	0.200	0.200 *	-0.200	0.00106	37.87
2	154.2	0.0808	0.280 *	-0.280	0.0	12.47
3	110.4	0.113	0.394 *	-0.394	0.00103	12.53
4	73.14	0.159	0.553 *	-0.553	0.00218	11.65
5	52.15	0.223	0.777 *	-0.777	0.00429	11.67
6	48.08	0.314	1.09 *	-1.09	0.00654	15.11
7	58.55	0.441	1.53 *	-1.53	0.00754	25.84
8	75.96	0.619	2.15 *	-2.15	0.00816	47.08

VES 12

Page 3

L #	RESISTIVITY	THICKNESS (meters)	DEPTH	ELEVATION (meters)	LONG. COND. (Siemens)	TRANS. RES. (Ohm-m <sup>2</sup> )
9	85.73	0.870	3.02 *	-3.02	0.0101	74.60
10	87.26	1.22	4.24 *	-4.24	0.0140	106.6
11	95.03	1.71	5.96 *	-5.96	0.0180	163.0
12	104.1	2.40	8.37 *	-8.37	0.0231	250.9
13	75.70	3.38	11.75 *	-11.75	0.0446	256.1
14	29.53	4.75	16.50 *	-16.50	0.160	140.3
15	9.49	6.67	23.17 *	-23.17	0.702	63.32
16	6.98	9.36	32.54 *	-32.54	1.34	65.42
17	30.35					

"\*" INDICATES FIXED PARAMETER





# VES 13

## Wenner Array

Northing: 0.0 Easting: 0.0 Elevation: 0.0

No.	Spacing (meters)	Layered Model:			Smooth Model:	
		Data Resistivity	Synthetic Resistivity	DIFFERENCE (percent)	Synthetic Resistivity	DIFFERENCE (percent)
1	0.800	70.00	66.94	4.37	69.58	0.592
2	1.50	63.00	68.86	-9.30	64.65	-2.63
3	3.00	76.00	71.42	6.01	72.53	4.55
4	4.60	70.00	70.11	-0.158	71.71	-2.44
5	6.10	68.00	66.19	2.65	66.91	1.59
6	9.10	51.00	54.63	-7.12	54.20	-6.28
7	12.20	43.00	42.18	1.90	41.63	3.17
8	15.20	33.00	32.22	2.33	31.86	3.44
9	19.80	21.00	21.82	-3.94	21.70	-3.33
10	24.40	16.00	15.98	0.112	15.98	0.0923
11	30.50	13.00	12.30	5.34	12.43	4.35
12	36.60	11.00	10.94	0.498	11.15	-1.45
13	42.70	10.00	10.63	-6.31	10.84	-8.47
14	51.80	11.00	10.98	0.142	10.99	0.0277
15	61.00	12.00	11.75	2.06	11.32	5.64

NO DATA ARE MASKED

### Layered Model

L #	RESISTIVITY	THICKNESS (meters)	DEPTH	ELEVATION (meters)	LONG. COND. (Siemens)	TRANS. RES. (Ohm-m <sup>2</sup> )
				0.0		
1	66.20	1.23	1.23	-1.23	0.0186	81.81
2	77.79	7.29	8.52	-8.52	0.0937	567.3
3	7.96	52.60	61.13	-61.13	6.60	419.1
4	55.35					

ALL PARAMETERS ARE FREE

Parameter Bounds from Equivalence Analysis

LAYER		MINIMUM	BEST	MAXIMUM
RHO	1	58.29	66.21	73.01
	2	71.02	77.80	88.75
	3	6.61	7.97	9.49
	4	20.85	55.35	236.10
THICK	1	0.67	1.24	2.23
	2	5.97	7.29	8.52
	3	36.02	52.60	79.33

PARAMETER RESOLUTION MATRIX:  
 "FIX" INDICATES FIXED PARAMETER

RHO	1	0.98					
RHO	2	0.01	0.98				
RHO	3	0.00	-0.02	0.93			
RHO	4	0.00	0.00	0.01	0.04		
THK	1	-0.04	-0.05	-0.04	0.01	0.15	
THK	2	0.00	0.03	0.05	-0.01	0.20	0.92
THK	3	0.01	-0.03	-0.14	-0.16	-0.06	0.07 0.68
	R	1 R	2 R	3 R	4 T	1 T	2 T 3

Smooth Model: Occam's Inversion

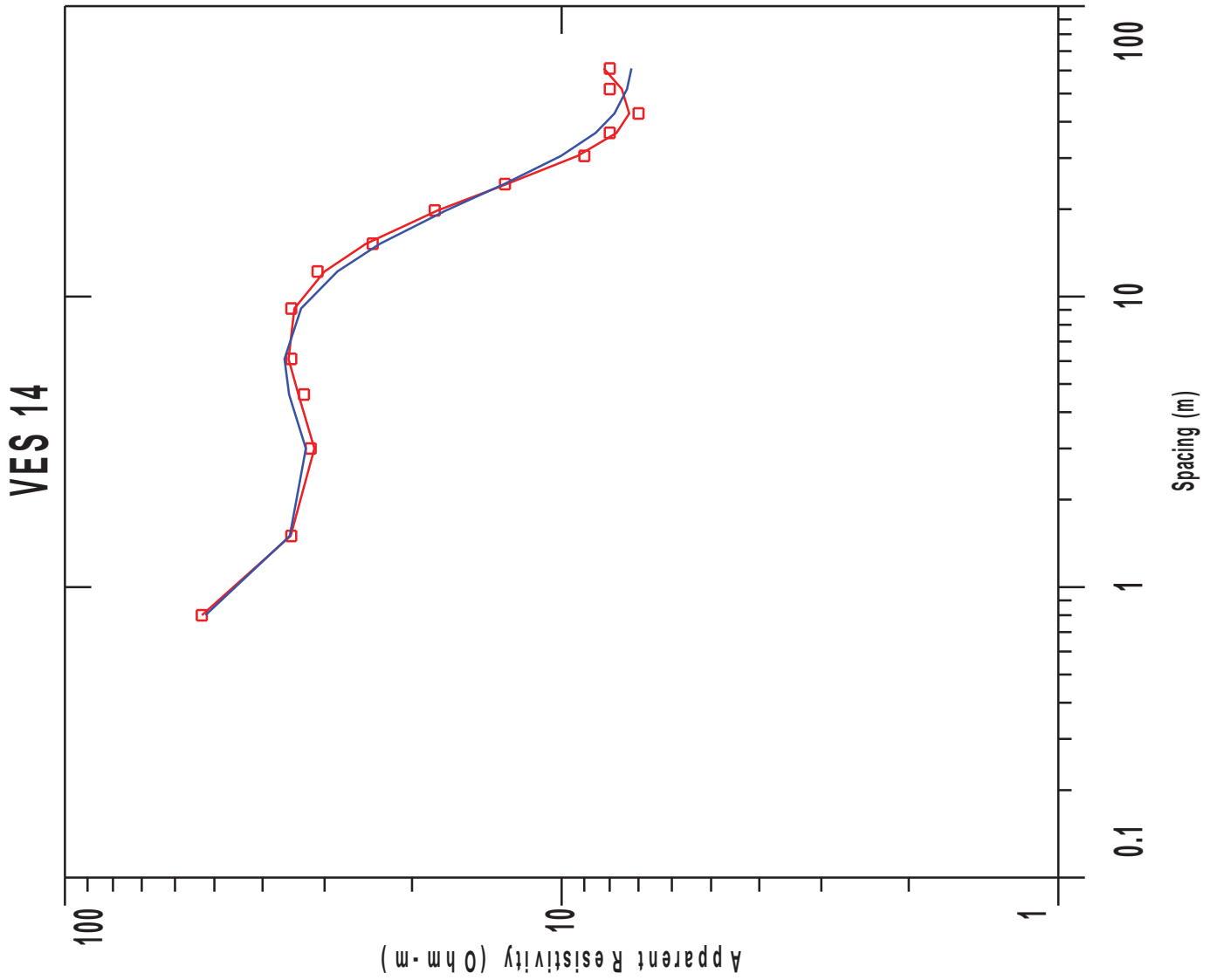
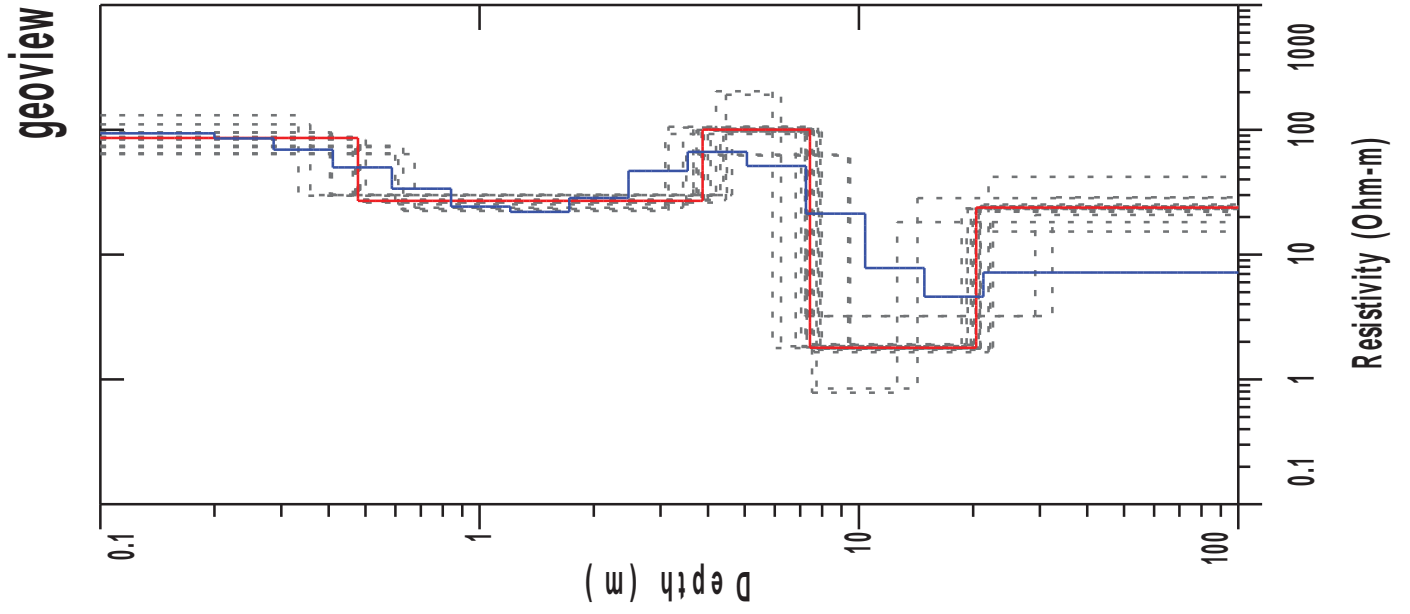
L #	RESISTIVITY	THICKNESS (meters)	DEPTH	ELEVATION (meters)	LONG. COND. (Siemens)	TRANS. RES. (Ohm-m <sup>2</sup> )
				0.0		
1	152.5	0.200	0.200 *	-0.200	0.00131	30.51
2	113.9	0.0864	0.286 *	-0.286	0.0	9.84
3	72.56	0.123	0.410 *	-0.410	0.00171	8.97
4	45.79	0.177	0.587 *	-0.587	0.00387	8.11
5	39.81	0.253	0.841 *	-0.841	0.00637	10.10
6	58.64	0.363	1.20 *	-1.20	0.00620	21.30
7	99.32	0.520	1.72 *	-1.72	0.00524	51.67
8	108.3	0.745	2.46 *	-2.46	0.00687	80.75
9	77.09	1.06	3.53 *	-3.53	0.0138	82.26
10	64.95	1.52	5.06 *	-5.06	0.0235	99.24
11	70.07	2.18	7.25 *	-7.25	0.0312	153.3
12	40.03	3.13	10.38 *	-10.38	0.0782	125.4

VES 13

Page 3

L #	RESISTIVITY	THICKNESS (meters)	DEPTH	ELEVATION (meters)	LONG. COND. (Siemens)	TRANS. RES. (Ohm-m <sup>2</sup> )
13	10.33	4.48	14.87 *	-14.87	0.433	46.39
14	3.58	6.42	21.29 *	-21.29	1.79	23.04
15	13.63					

"\*" INDICATES FIXED PARAMETER



# VES 14

## Wenner Array

Northing: 0.0 Easting: 0.0 Elevation: 0.0

No.	Spacing (meters)	Layered Model:			Smooth Model:	
		Data Resistivity	Synthetic Resistivity	DIFFERENCE (percent)	Synthetic Resistivity	DIFFERENCE (percent)
1	0.800	53.00	52.96	0.0620	52.11	1.66
2	1.50	35.00	35.09	-0.283	35.25	-0.723
3	3.00	32.00	31.44	1.74	32.72	-2.26
4	4.60	33.00	33.86	-2.63	35.36	-7.16
5	6.10	35.00	35.44	-1.26	36.13	-3.23
6	9.10	35.00	34.50	1.42	33.44	4.43
7	12.20	31.00	29.99	3.24	28.26	8.82
8	15.20	24.00	24.76	-3.16	23.21	3.28
9	19.80	18.00	17.75	1.37	17.07	5.14
10	24.40	13.00	12.89	0.787	13.04	-0.349
11	30.50	9.00	9.29	-3.24	10.02	-11.41
12	36.60	8.00	7.74	3.13	8.54	-6.76
13	42.70	7.00	7.30	-4.40	7.82	-11.78
14	51.80	8.00	7.56	5.44	7.38	7.69
15	61.00	8.00	8.22	-2.75	7.23	9.58

NO DATA ARE MASKED

### Layered Model

L #	RESISTIVITY	THICKNESS (meters)	DEPTH	ELEVATION (meters)	LONG. COND. (Siemens)	TRANS. RES. (Ohm-m <sup>2</sup> )
				0.0		
1	85.94	0.478	0.478	-0.478	0.00556	41.08
2	26.94	3.39	3.87	-3.87	0.125	91.43
3	100.1	3.55	7.43	-7.43	0.0355	356.4
4	1.79	12.94	20.37	-20.37	7.21	23.22
5	23.82					

ALL PARAMETERS ARE FREE

Parameter Bounds from Equivalence Analysis

LAYER	MINIMUM	BEST	MAXIMUM	
RHO	1	63.76	85.94	130.65
	2	22.41	26.94	30.21
	3	62.15	100.15	203.29
	4	0.78	1.79	3.22
	5	15.29	23.82	42.00
THICK	1	0.33	0.48	0.67
	2	2.49	3.39	4.22
	3	1.72	3.56	5.86
	4	5.09	12.95	24.98

PARAMETER RESOLUTION MATRIX:  
 "FIX" INDICATES FIXED PARAMETER

RHO	1	0.72								
RHO	2	-0.06	0.93							
RHO	3	0.02	0.02	0.53						
RHO	4	0.01	0.01	0.00	0.48					
RHO	5	-0.01	-0.02	0.01	0.12	0.17				
THK	1	0.24	0.10	-0.03	-0.01	0.02	0.72			
THK	2	-0.10	-0.11	-0.06	0.04	-0.06	0.16	0.77		
THK	3	0.00	0.01	0.48	0.02	-0.02	-0.01	0.12	0.48	
THK	4	0.00	0.00	0.01	-0.47	-0.15	0.00	0.00	0.01	0.47
	R	1 R	2 R	3 R	4 R	5 T	1 T	2 T	3 T	4

Smooth Model: Occam's Inversion

L #	RESISTIVITY	THICKNESS (meters)	DEPTH	ELEVATION (meters)	LONG. COND. (Siemens)	TRANS. RES. (Ohm-m <sup>2</sup> )
				0.0		
1	93.69	0.200	0.200 *	-0.200	0.00213	18.73
2	85.16	0.0864	0.286 *	-0.286	0.00101	7.35
3	69.32	0.123	0.410 *	-0.410	0.00178	8.57
4	49.96	0.177	0.587 *	-0.587	0.00355	8.85
5	33.70	0.253	0.841 *	-0.841	0.00753	8.55
6	24.22	0.363	1.20 *	-1.20	0.0150	8.80
7	22.01	0.520	1.72 *	-1.72	0.0236	11.45
8	28.43	0.745	2.46 *	-2.46	0.0262	21.18

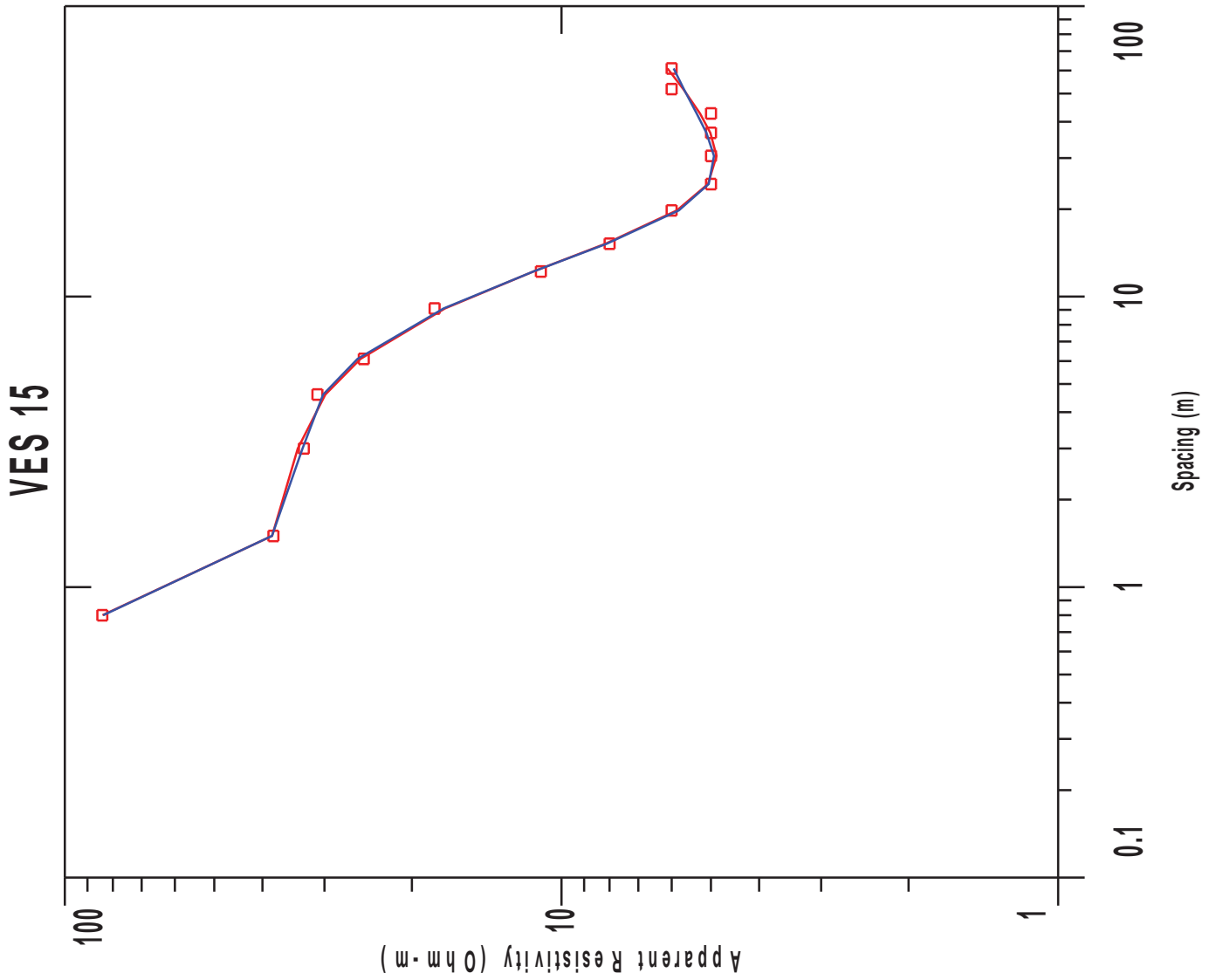
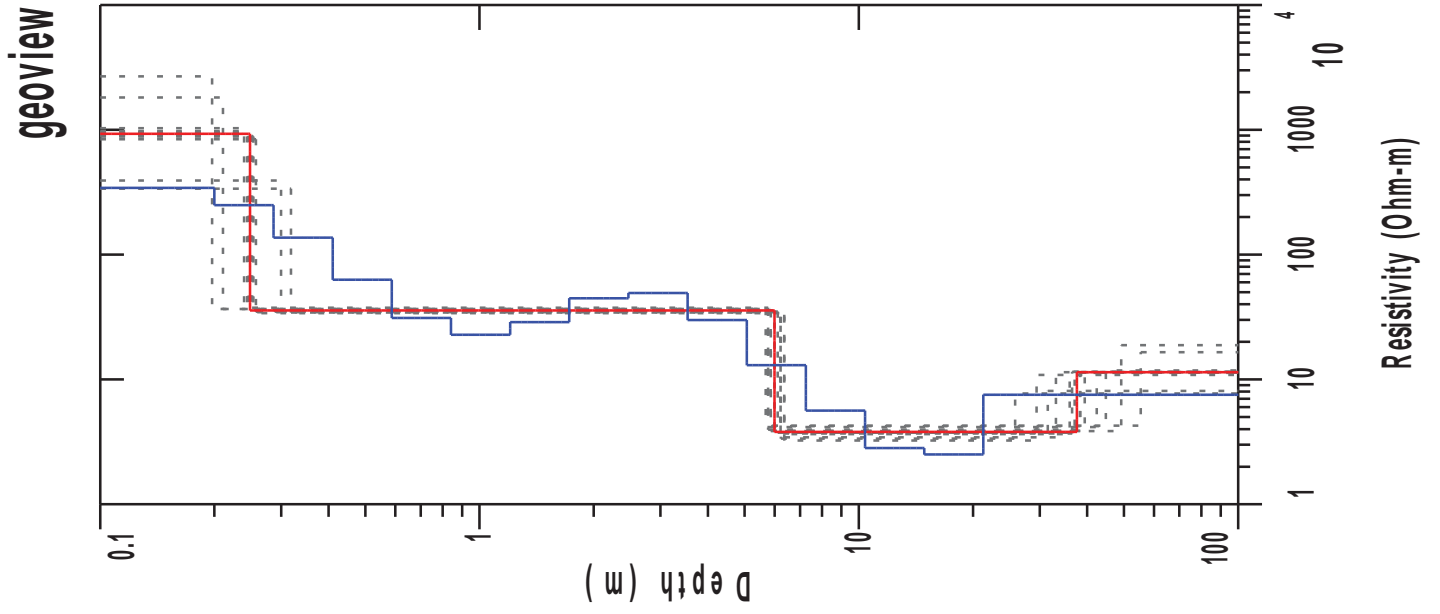
VES 14

Page 3

L #	RESISTIVITY	THICKNESS (meters)	DEPTH	ELEVATION (meters)	LONG. COND. (Siemens)	TRANS. RES. (Ohm-m <sup>2</sup> )
9	46.75	1.06	3.53 *	-3.53	0.0228	49.88
10	66.52	1.52	5.06 *	-5.06	0.0229	101.6
11	51.23	2.18	7.25 *	-7.25	0.0427	112.1
12	21.27	3.13	10.38 *	-10.38	0.147	66.65
13	7.80	4.48	14.87 *	-14.87	0.575	35.00
14	4.60	6.42	21.29 *	-21.29	1.39	29.57
15	7.17					

"\*" INDICATES FIXED PARAMETER





# VES 15

## Wenner Array

Northing: 0.0 Easting: 0.0 Elevation: 0.0

No.	Spacing (meters)	Layered Model:			Smooth Model:	
		Data Resistivity	Synthetic Resistivity	DIFFERENCE (percent)	Synthetic Resistivity	DIFFERENCE (percent)
1	0.800	84.00	83.91	0.104	83.68	0.376
2	1.50	38.00	38.23	-0.614	38.27	-0.725
3	3.00	33.00	33.95	-2.90	33.21	-0.649
4	4.60	31.00	29.88	3.59	30.19	2.58
5	6.10	25.00	25.40	-1.60	25.75	-3.01
6	9.10	18.00	17.15	4.70	17.26	4.09
7	12.20	11.00	11.38	-3.46	11.37	-3.42
8	15.20	8.00	8.15	-1.94	8.10	-1.36
9	19.80	6.00	5.85	2.37	5.80	3.26
10	24.40	5.00	5.06	-1.34	5.05	-1.07
11	30.50	5.00	4.87	2.55	4.92	1.40
12	36.60	5.00	5.01	-0.236	5.10	-2.11
13	42.70	5.00	5.25	-5.19	5.34	-6.80
14	51.80	6.00	5.68	5.23	5.66	5.52
15	61.00	6.00	6.11	-1.92	5.94	0.954

NO DATA ARE MASKED

### Layered Model

L #	RESISTIVITY	THICKNESS (meters)	DEPTH	ELEVATION (meters)	LONG. COND. (Siemens)	TRANS. RES. (Ohm-m <sup>2</sup> )
				0.0		
1	929.4	0.248	0.248	-0.248	0.0	230.8
2	35.70	5.74	5.99	-5.99	0.160	205.1
3	3.79	31.60	37.59	-37.59	8.31	120.0
4	11.42					

ALL PARAMETERS ARE FREE

Parameter Bounds from Equivalence Analysis

LAYER		MINIMUM	BEST	MAXIMUM
RHO	1	337.57	929.46	2680.48
	2	33.97	35.71	37.58
	3	3.24	3.80	4.27
	4	7.72	11.42	18.84
THICK	1	0.20	0.25	0.32
	2	5.44	5.74	6.11
	3	19.60	31.60	49.60

PARAMETER RESOLUTION MATRIX:  
 "FIX" INDICATES FIXED PARAMETER

RHO	1	0.12						
RHO	2	-0.02	0.99					
RHO	3	-0.01	-0.01	0.94				
RHO	4	0.00	0.00	-0.02	0.38			
THK	1	0.19	0.01	0.01	0.00	0.95		
THK	2	0.01	0.01	0.02	0.00	0.00	0.99	
THK	3	-0.02	-0.01	-0.12	-0.38	0.01	0.04	0.53
	R	1	R	2	R	3	R	4
	T	1	T	2	T	3		

Smooth Model: Occam's Inversion

L #	RESISTIVITY	THICKNESS (meters)	DEPTH	ELEVATION (meters)	LONG. COND. (Siemens)	TRANS. RES. (Ohm-m <sup>2</sup> )
				0.0		
1	342.7	0.200	0.200 *	-0.200	0.0	68.54
2	248.8	0.0864	0.286 *	-0.286	0.0	21.49
3	136.6	0.123	0.410 *	-0.410	0.0	16.91
4	62.93	0.177	0.587 *	-0.587	0.00282	11.15
5	31.09	0.253	0.841 *	-0.841	0.00816	7.89
6	22.82	0.363	1.20 *	-1.20	0.0159	8.29
7	28.79	0.520	1.72 *	-1.72	0.0180	14.98
8	44.70	0.745	2.46 *	-2.46	0.0166	33.31
9	49.22	1.06	3.53 *	-3.53	0.0216	52.52
10	29.89	1.52	5.06 *	-5.06	0.0511	45.68
11	13.01	2.18	7.25 *	-7.25	0.168	28.47
12	5.63	3.13	10.38 *	-10.38	0.556	17.64

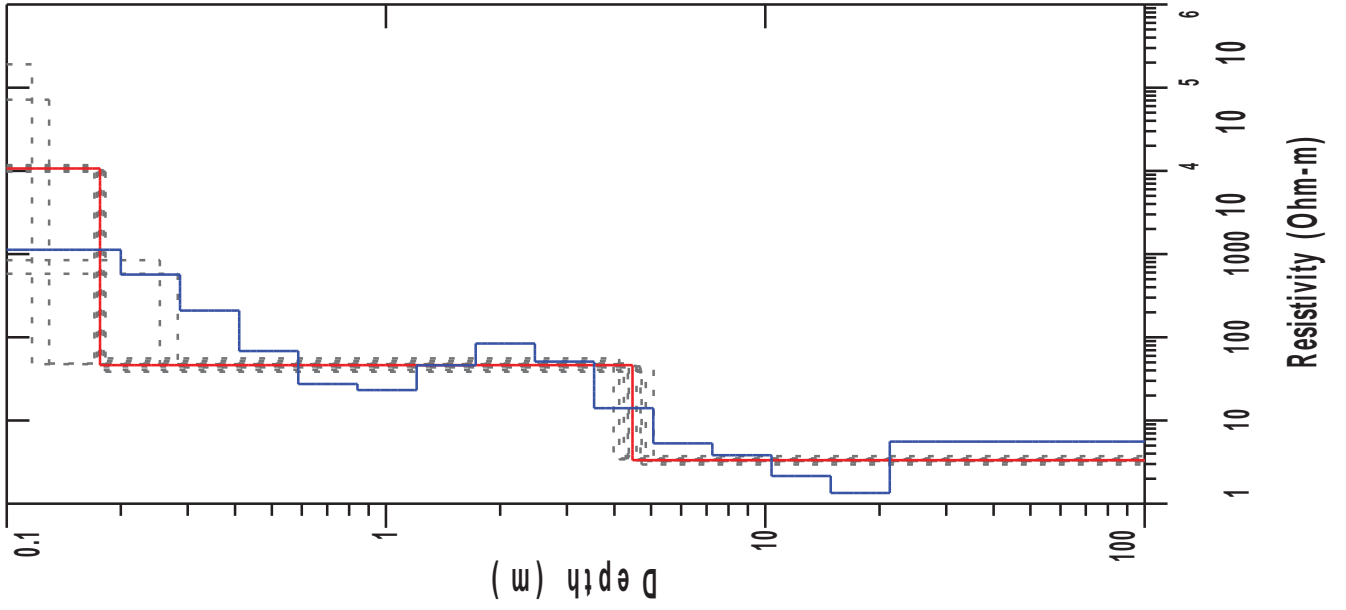
VES 15

Page 3

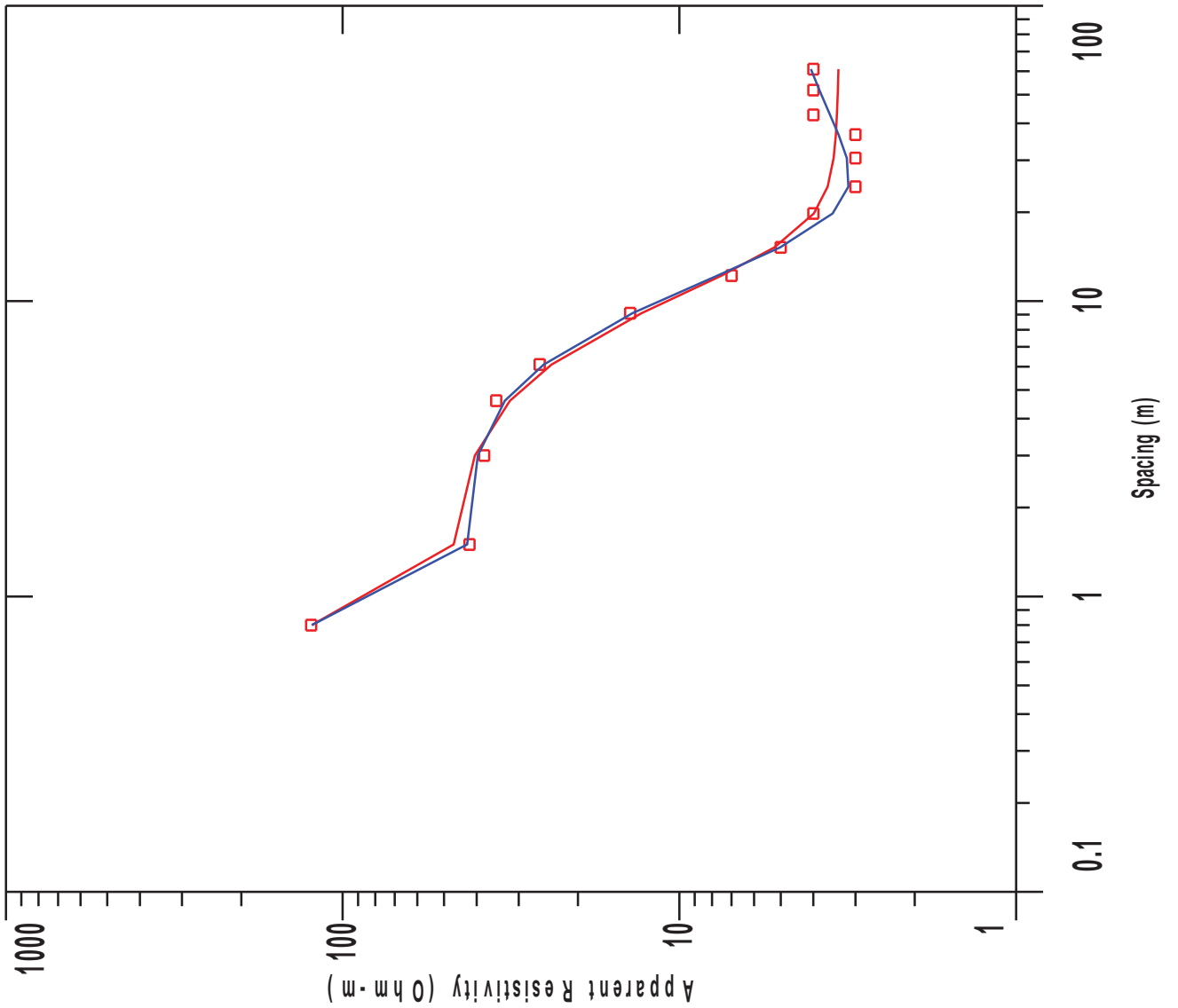
L #	RESISTIVITY	THICKNESS (meters)	DEPTH	ELEVATION (meters)	LONG. COND. (Siemens)	TRANS. RES. (Ohm-m <sup>2</sup> )
13	2.82	4.48	14.87 *	-14.87	1.58	12.66
14	2.51	6.42	21.29 *	-21.29	2.55	16.12
15	7.54					

"\*" INDICATES FIXED PARAMETER

geoview



VES 16



# VES 16

## Wenner Array

Northing: 0.0 Easting: 0.0 Elevation: 0.0

No.	Spacing (meters)	Layered Model:			Smooth Model:	
		Data Resistivity	Synthetic Resistivity	DIFFERENCE (percent)	Synthetic Resistivity	DIFFERENCE (percent)
1	0.800	124.0	123.4	0.447	123.4	0.468
2	1.50	42.00	46.78	-11.39	42.66	-1.57
3	3.00	38.00	40.48	-6.54	39.68	-4.42
4	4.60	35.00	31.85	8.98	32.99	5.73
5	6.10	26.00	23.95	7.86	25.27	2.77
6	9.10	14.00	12.95	7.47	13.77	1.62
7	12.20	7.00	7.48	-6.97	7.70	-10.04
8	15.20	5.00	5.22	-4.46	5.02	-0.405
9	19.80	4.00	3.98	0.313	3.50	12.30
10	24.40	3.00	3.62	-20.96	3.14	-4.96
11	30.50	3.00	3.48	-16.08	3.18	-6.09
12	36.60	3.00	3.42	-14.32	3.36	-12.17
13	42.70	4.00	3.40	14.90	3.56	10.83
14	51.80	4.00	3.38	15.46	3.83	4.02
15	61.00	4.00	3.36	15.75	4.06	-1.73

NO DATA ARE MASKED

### Layered Model

L #	RESISTIVITY	THICKNESS (meters)	DEPTH	ELEVATION (meters)	LONG. COND. (Siemens)	TRANS. RES. (Ohm-m <sup>2</sup> )
				0.0		
1	10703.0	0.176	0.176	-0.176	0.0	1885.7
2	46.39	4.28	4.46	-4.46	0.0924	198.9
3	3.34					

ALL PARAMETERS ARE FREE

### Parameter Bounds from Equivalence Analysis

LAYER	MINIMUM	BEST	MAXIMUM
RHO 1	579.25	10703.09	190793.05

Prepared for geoview

VES 16

Page 2

	LAYER	MINIMUM	BEST	MAXIM
	2	38.66	46.40	55.68
	3	2.97	3.34	3.73
THICK	1	0.12	0.18	0.28
	2	3.81	4.29	4.90

PARAMETER RESOLUTION MATRIX:  
 "FIX" INDICATES FIXED PARAMETER

RHO 1 0.03  
 RHO 2 -0.01 0.98  
 RHO 3 0.00 0.00 0.99  
 THK 1 0.14 0.00 0.00 0.98  
 THK 2 0.00 0.01 0.00 0.00 0.99  
 R 1 R 2 R 3 T 1 T 2

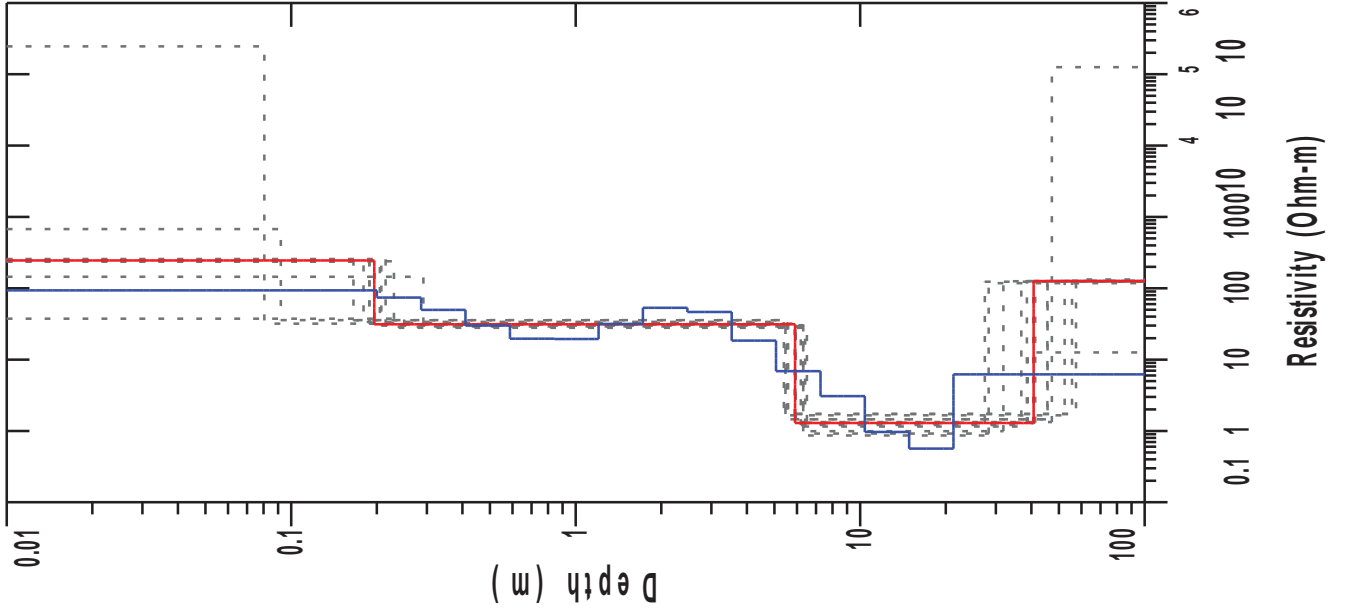
Smooth Model: Occam's Inversion

L #	RESISTIVITY	THICKNESS (meters)	DEPTH	ELEVATION (meters)	LONG. COND. (Siemens)	TRANS. RES. (Ohm-m <sup>2</sup> )
				0.0		
1	1128.9	0.200	0.200 *	-0.200	0.0	225.7
2	568.6	0.0864	0.286 *	-0.286	0.0	49.13
3	209.9	0.123	0.410 *	-0.410	0.0	25.97
4	68.38	0.177	0.587 *	-0.587	0.00259	12.11
5	27.51	0.253	0.841 *	-0.841	0.00922	6.98
6	23.26	0.363	1.20 *	-1.20	0.0156	8.45
7	46.11	0.520	1.72 *	-1.72	0.0112	23.99
8	84.16	0.745	2.46 *	-2.46	0.00885	62.71
9	51.15	1.06	3.53 *	-3.53	0.0208	54.58
10	14.10	1.52	5.06 *	-5.06	0.108	21.55
11	5.30	2.18	7.25 *	-7.25	0.412	11.60
12	3.83	3.13	10.38 *	-10.38	0.816	12.02
13	2.15	4.48	14.87 *	-14.87	2.08	9.66
14	1.35	6.42	21.29 *	-21.29	4.75	8.67
15	5.58					

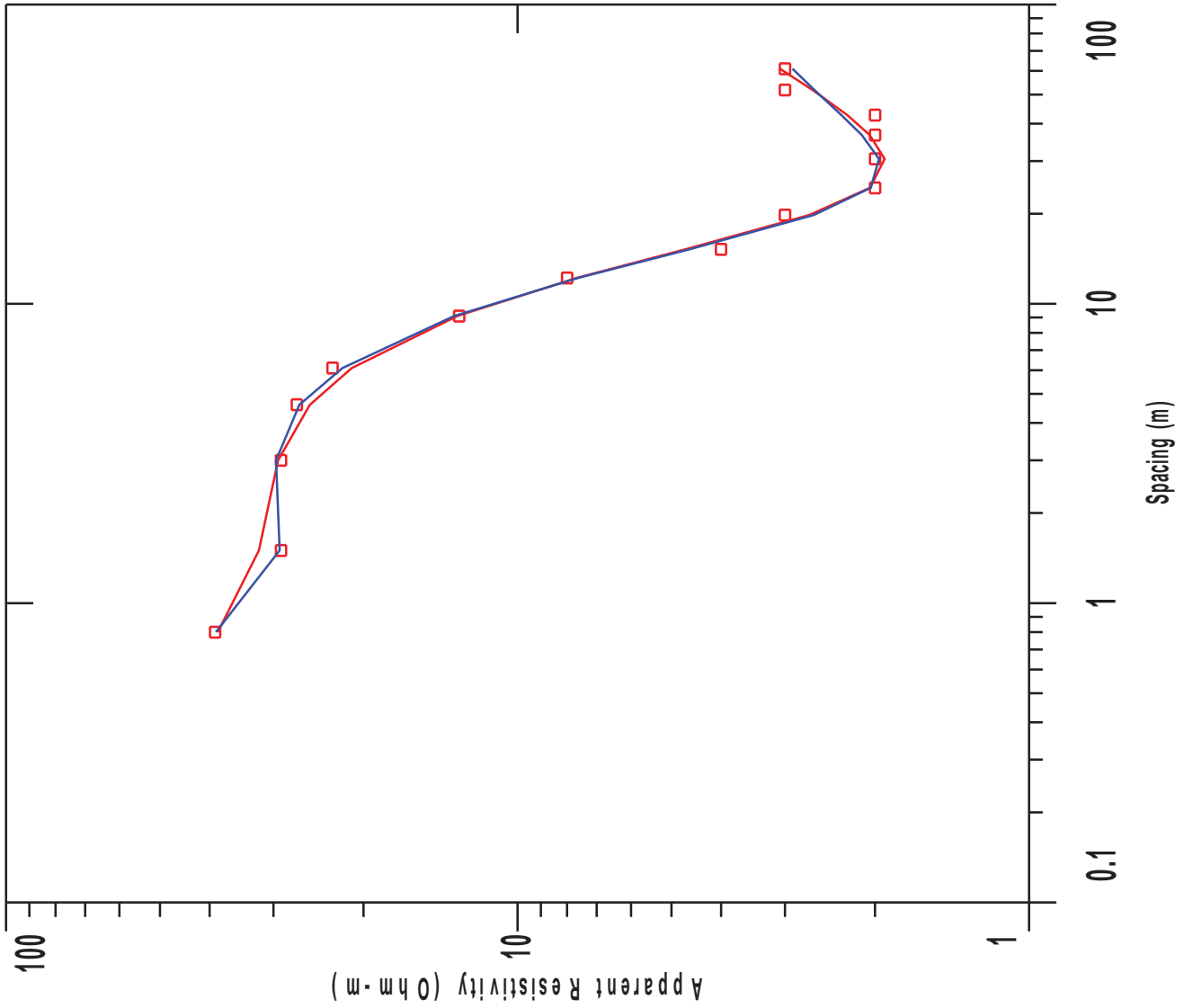
"\*" INDICATES FIXED PARAMETER



geoview



VES 17



# VES 17

## Wenner Array

Northing: 0.0 Easting: 0.0 Elevation: 0.0

No.	Spacing (meters)	Layered Model:			Smooth Model:	
		Data Resistivity	Synthetic Resistivity	DIFFERENCE (percent)	Synthetic Resistivity	DIFFERENCE (percent)
1	0.800	39.00	38.55	1.14	38.86	0.336
2	1.50	29.00	32.01	-10.40	29.17	-0.599
3	3.00	29.00	29.38	-1.31	29.65	-2.24
4	4.60	27.00	25.46	5.67	26.69	1.13
5	6.10	23.00	21.08	8.30	21.99	4.35
6	9.10	13.00	13.11	-0.866	13.30	-2.31
7	12.20	8.00	7.65	4.29	7.60	4.94
8	15.20	4.00	4.70	-17.53	4.61	-15.42
9	19.80	3.00	2.68	10.36	2.63	12.14
10	24.40	2.00	2.04	-2.30	2.03	-1.99
11	30.50	2.00	1.91	4.21	1.96	1.76
12	36.60	2.00	2.04	-2.39	2.12	-6.09
13	42.70	2.00	2.26	-13.26	2.32	-16.32
14	51.80	3.00	2.64	11.67	2.62	12.43
15	61.00	3.00	3.06	-2.27	2.90	3.29

NO DATA ARE MASKED

### Layered Model

L #	RESISTIVITY	THICKNESS (meters)	DEPTH	ELEVATION (meters)	LONG. COND. (Siemens)	TRANS. RES. (Ohm-m <sup>2</sup> )
				0.0		
1	245.8	0.195	0.195	-0.195	0.0	48.18
2	31.33	5.71	5.90	-5.90	0.182	178.9
3	1.29	34.83	40.74	-40.74	26.98	44.97
4	125.8					

ALL PARAMETERS ARE FREE

Parameter Bounds from Equivalence Analysis

LAYER		MINIMUM	BEST	MAXIMUM
RHO	1	37.39	245.87	245871.91
	2	27.85	31.34	35.74
	3	0.86	1.29	1.73
	4	12.58	125.83	125827.03
THICK	1	0.08	0.20	0.29
	2	5.21	5.71	6.29
	3	21.03	34.84	51.80

PARAMETER RESOLUTION MATRIX:  
 "FIX" INDICATES FIXED PARAMETER

RHO	1	0.02						
RHO	2	0.00	0.99					
RHO	3	0.00	-0.01	0.89				
RHO	4	0.00	0.00	0.00	0.00			
THK	1	0.13	0.02	0.01	0.00	0.91		
THK	2	0.00	0.01	0.02	0.00	-0.01	0.99	
THK	3	0.00	-0.01	-0.13	-0.02	0.02	0.03	0.82
	R	1	R	2	R	3	R	4
	T	1	T	2	T	3		

Smooth Model: Occam's Inversion

L #	RESISTIVITY	THICKNESS (meters)	DEPTH	ELEVATION (meters)	LONG. COND. (Siemens)	TRANS. RES. (Ohm-m <sup>2</sup> )
				0.0		
1	93.35	0.200	0.200 *	-0.200	0.00214	18.67
2	74.13	0.0864	0.286 *	-0.286	0.00117	6.40
3	49.77	0.123	0.410 *	-0.410	0.00249	6.15
4	30.04	0.177	0.587 *	-0.587	0.00590	5.32
5	19.65	0.253	0.841 *	-0.841	0.0129	4.98
6	19.44	0.363	1.20 *	-1.20	0.0186	7.06
7	31.52	0.520	1.72 *	-1.72	0.0165	16.40
8	53.35	0.745	2.46 *	-2.46	0.0139	39.75
9	46.61	1.06	3.53 *	-3.53	0.0228	49.73
10	18.49	1.52	5.06 *	-5.06	0.0826	28.25
11	6.88	2.18	7.25 *	-7.25	0.317	15.06
12	3.07	3.13	10.38 *	-10.38	1.01	9.64

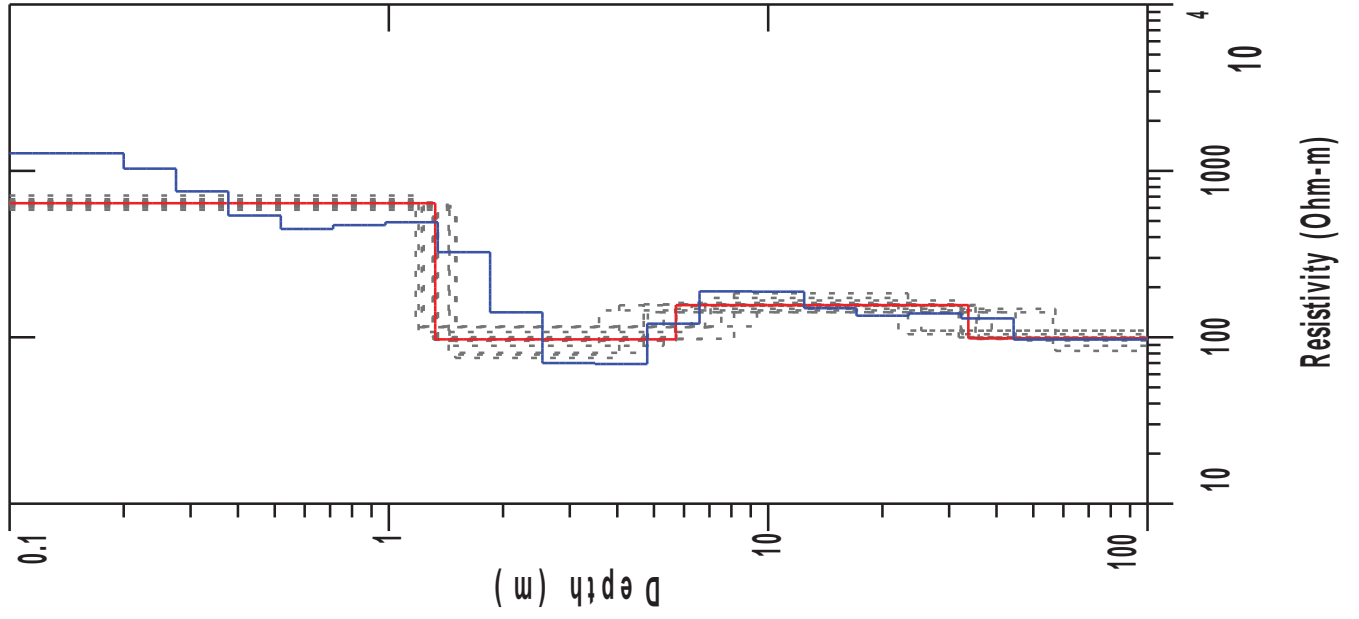
VES 17

Page 3

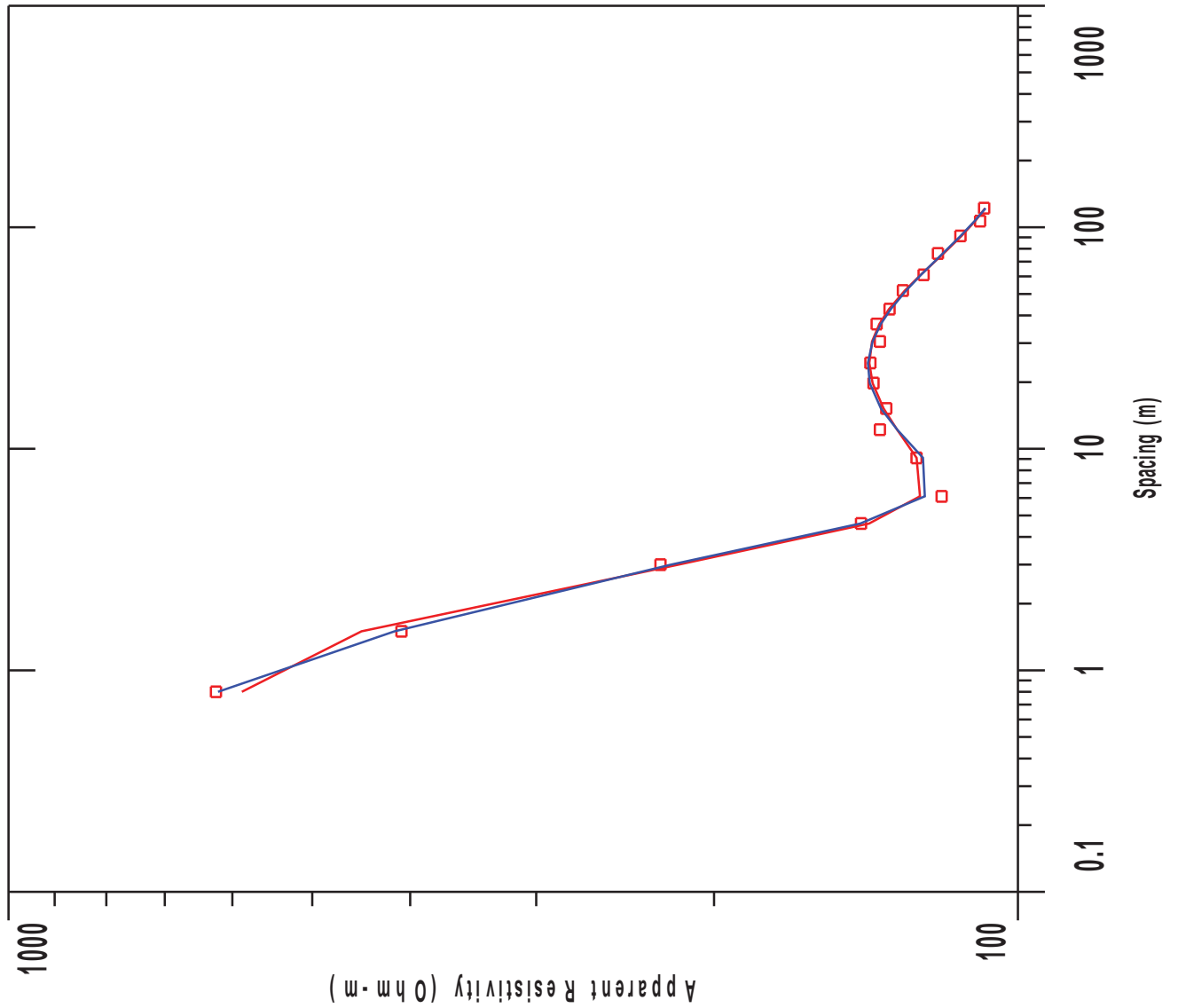
L #	RESISTIVITY	THICKNESS (meters)	DEPTH	ELEVATION (meters)	LONG. COND. (Siemens)	TRANS. RES. (Ohm-m <sup>2</sup> )
13	0.965	4.48	14.87 *	-14.87	4.64	4.33
14	0.565	6.42	21.29 *	-21.29	11.35	3.63
15	6.21					

"\*" INDICATES FIXED PARAMETER

geoview



VES 22



# VES 22

## Wenner Array

Northing: 0.0 Easting: 0.0 Elevation: 0.0

No.	Spacing (meters)	Layered Model:			Smooth Model:	
		Data Resistivity	Synthetic Resistivity	DIFFERENCE (percent)	Synthetic Resistivity	DIFFERENCE (percent)
1	0.800	623.0	587.1	5.75	619.9	0.484
2	1.50	408.0	446.8	-9.53	414.4	-1.58
3	3.00	226.0	216.7	4.08	220.5	2.41
4	4.60	143.0	140.4	1.81	143.2	-0.191
5	6.10	119.0	124.9	-5.04	123.6	-3.90
6	9.10	126.0	125.9	0.0120	124.1	1.44
7	12.20	137.0	131.7	3.85	131.6	3.89
8	15.20	135.0	135.8	-0.610	136.6	-1.22
9	19.80	139.0	139.2	-0.205	140.2	-0.871
10	24.40	140.0	140.3	-0.233	140.7	-0.565
11	30.50	137.0	139.4	-1.79	139.3	-1.68
12	36.60	138.0	137.1	0.609	136.6	0.953
13	42.70	134.0	134.1	-0.135	133.6	0.264
14	51.80	130.0	129.4	0.454	129.0	0.731
15	61.00	124.0	124.8	-0.656	124.7	-0.577
16	76.20	120.0	118.4	1.28	118.6	1.12
17	91.40	114.0	113.6	0.264	113.9	0.0494
18	106.7	109.0	110.2	-1.12	110.3	-1.24
19	121.9	108.0	107.7	0.242	107.6	0.309

NO DATA ARE MASKED

### Layered Model

L #	RESISTIVITY	THICKNESS (meters)	DEPTH	ELEVATION (meters)	LONG. COND. (Siemens)	TRANS. RES. (Ohm-m <sup>2</sup> )
				0.0		
1	639.3	1.32	1.32	-1.32	0.00207	846.9
2	97.15	4.38	5.71	-5.71	0.0451	426.1
3	156.1	28.00	33.71	-33.71	0.179	4372.9
4	98.81					

ALL PARAMETERS ARE FREE

Parameter Bounds from Equivalence Analysis

LAYER	MINIMUM	BEST	MAXIMUM	
RHO	1	583.62	639.32	711.15
	2	75.14	97.15	116.41
	3	141.36	156.14	184.02
	4	82.80	98.81	109.75
THICK	1	1.18	1.32	1.51
	2	2.14	4.39	8.11
	3	15.23	28.01	51.51

PARAMETER RESOLUTION MATRIX:  
 "FIX" INDICATES FIXED PARAMETER

RHO	1	0.99						
RHO	2	-0.01	0.91					
RHO	3	0.00	0.00	0.97				
RHO	4	0.00	0.01	-0.01	0.97			
THK	1	0.01	0.04	0.00	0.00	0.97		
THK	2	-0.02	-0.19	-0.07	0.00	0.07	0.34	
THK	3	0.00	0.00	0.09	0.10	0.01	0.21	0.43
	R	1 R	2 R	3 R	4 T	1 T	2 T	3

Smooth Model: Occam's Inversion

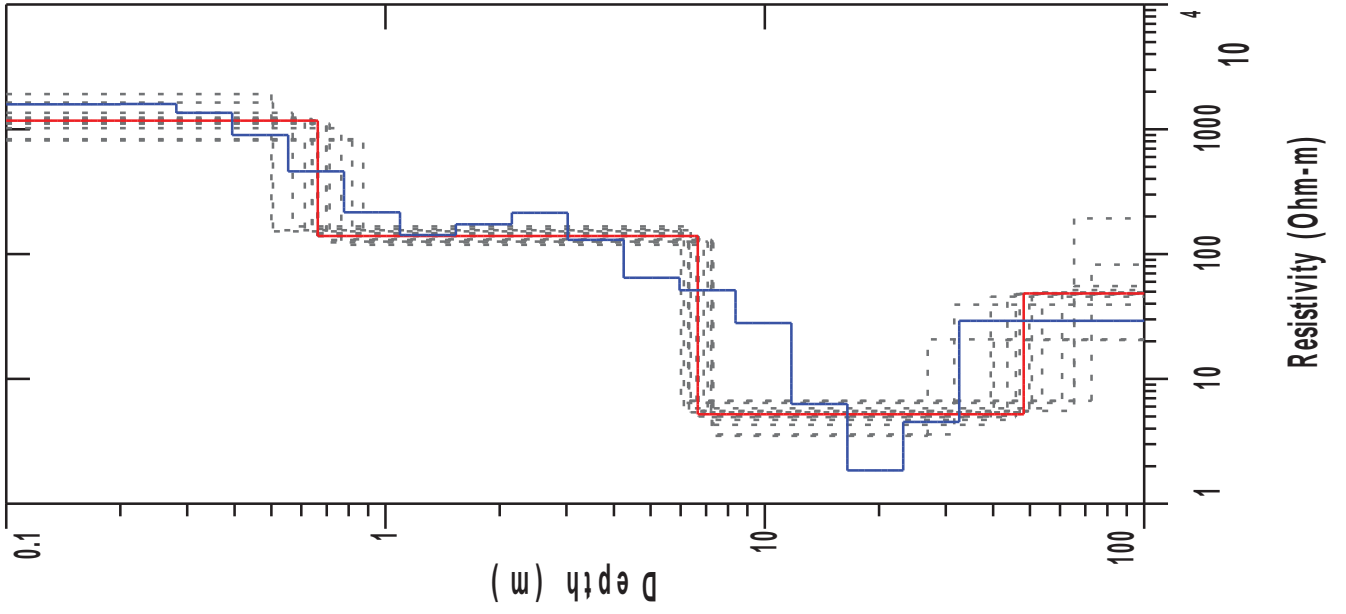
L #	RESISTIVITY	THICKNESS (meters)	DEPTH	ELEVATION (meters)	LONG. COND. (Siemens)	TRANS. RES. (Ohm-m <sup>2</sup> )
				0.0		
1	1274.4	0.200	0.200 *	-0.200	0.0	254.8
2	1030.7	0.0748	0.274 *	-0.274	0.0	77.10
3	753.1	0.102	0.377 *	-0.377	0.0	77.41
4	539.5	0.141	0.518 *	-0.518	0.0	76.20
5	447.4	0.194	0.712 *	-0.712	0.0	86.83
6	472.0	0.266	0.979 *	-0.979	0.0	125.8
7	491.0	0.366	1.34 *	-1.34	0.0	179.9



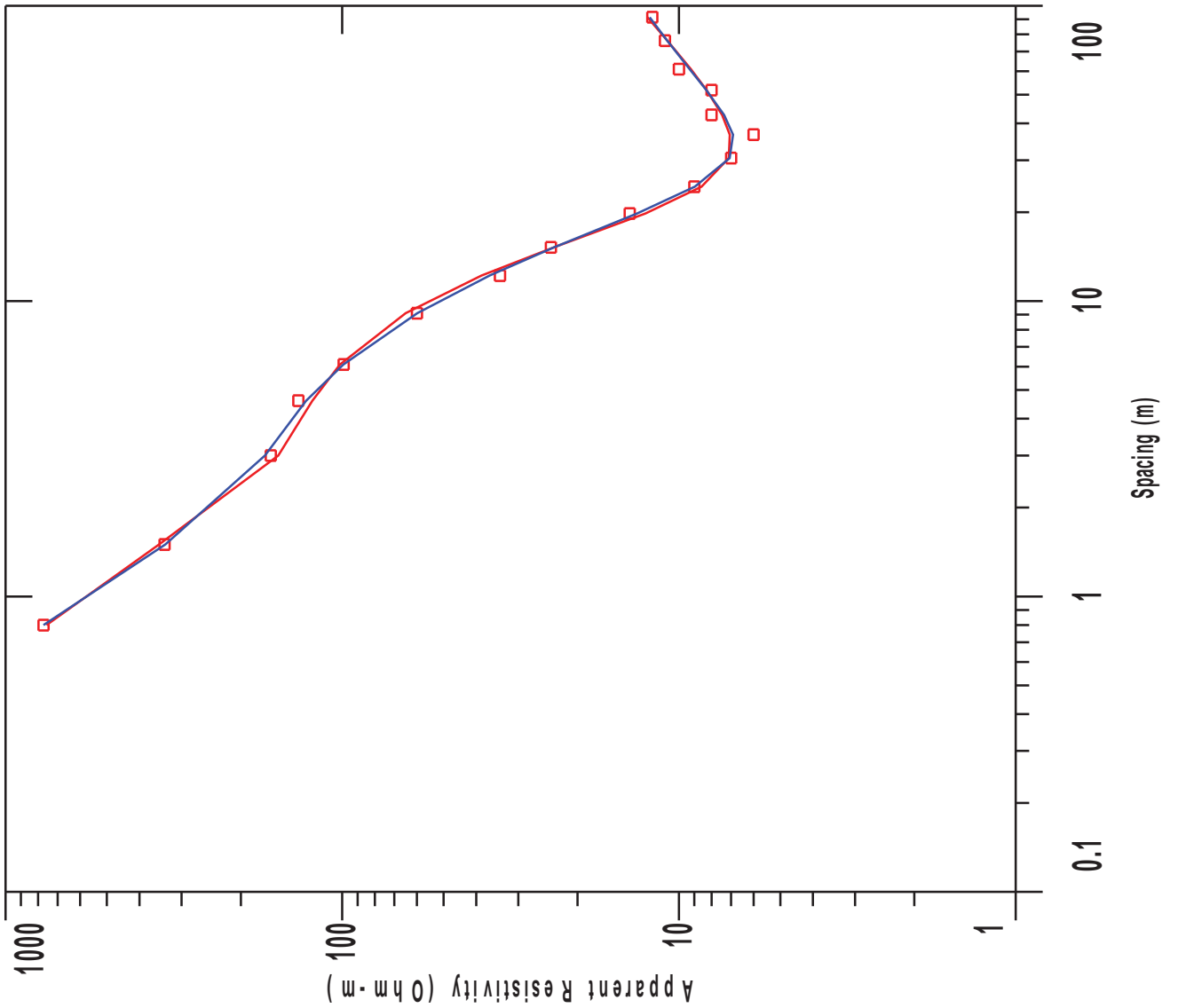
L #	RESISTIVITY	THICKNESS (meters)	DEPTH	ELEVATION (meters)	LONG. COND. (Siemens)	TRANS. RES. (Ohm-m <sup>2</sup> )
8	324.4	0.503	1.84 *	-1.84	0.00155	163.3
9	141.2	0.691	2.54 *	-2.54	0.00490	97.67
10	69.98	0.950	3.49 *	-3.49	0.0135	66.51
11	69.17	1.30	4.79 *	-4.79	0.0188	90.33
12	120.7	1.79	6.59 *	-6.59	0.0148	216.6
13	188.9	2.46	9.05 *	-9.05	0.0130	465.7
14	187.7	3.38	12.44 *	-12.44	0.0180	636.1
15	149.6	4.65	17.09 *	-17.09	0.0311	696.5
16	134.9	6.39	23.49 *	-23.49	0.0473	863.2
17	139.0	8.78	32.28 *	-32.28	0.0632	1221.9
18	129.8	12.07	44.35 *	-44.35	0.0930	1567.8
19	96.90					

"\*" INDICATES FIXED PARAMETER

geoview



VES 23



# VES 23

## Wenner Array

Northing: 0.0 Easting: 0.0 Elevation: 0.0

No.	Spacing (meters)	Layered Model:			Smooth Model:	
		Data Resistivity	Synthetic Resistivity	DIFFERENCE (percent)	Synthetic Resistivity	DIFFERENCE (percent)
1	0.800	771.0	755.9	1.95	771.4	-0.0545
2	1.50	337.0	349.6	-3.74	335.1	0.542
3	3.00	163.0	154.8	5.00	169.5	-4.04
4	4.60	135.0	122.6	9.15	127.9	5.19
5	6.10	99.00	101.6	-2.62	99.28	-0.288
6	9.10	60.00	64.81	-8.02	59.81	0.303
7	12.20	34.00	38.55	-13.40	36.49	-7.34
8	15.20	24.00	23.54	1.89	23.53	1.95
9	19.80	14.00	12.57	10.14	13.31	4.89
10	24.40	9.00	8.57	4.76	8.96	0.370
11	30.50	7.00	7.11	-1.62	7.06	-0.960
12	36.60	6.00	7.06	-17.75	6.90	-15.09
13	42.70	8.00	7.44	6.92	7.34	8.24
14	51.80	8.00	8.27	-3.38	8.29	-3.66
15	61.00	10.00	9.21	7.84	9.29	7.01
16	76.20	11.00	10.83	1.53	10.83	1.46
17	91.40	12.00	12.40	-3.40	12.20	-1.74

NO DATA ARE MASKED

### Layered Model

L #	RESISTIVITY	THICKNESS (meters)	DEPTH	ELEVATION (meters)	LONG. COND. (Siemens)	TRANS. RES. (Ohm-m <sup>2</sup> )
				0.0		
1	1171.0	0.662	0.662	-0.662	0.0	776.1
2	139.7	5.99	6.65	-6.65	0.0428	837.8
3	5.20	41.48	48.14	-48.14	7.97	215.9
4	48.32					

ALL PARAMETERS ARE FREE

Parameter Bounds from Equivalence Analysis

LAYER		MINIMUM	BEST	MAXIMUM
RHO	1	812.09	1171.06	1914.80
	2	118.51	139.77	166.61
	3	3.50	5.20	6.68
	4	20.52	48.32	193.20
THICK	1	0.50	0.66	0.87
	2	5.40	5.99	6.60
	3	19.64	41.49	66.38

PARAMETER RESOLUTION MATRIX:  
 "FIX" INDICATES FIXED PARAMETER

RHO	1	0.88						
RHO	2	-0.02	0.98					
RHO	3	-0.01	-0.02	0.93				
RHO	4	0.00	0.00	-0.04	0.12			
THK	1	0.07	0.02	0.01	0.00	0.94		
THK	2	0.00	0.01	0.02	0.01	-0.01	0.99	
THK	3	-0.01	-0.02	-0.10	-0.22	0.01	0.02	0.80
	R	1	R	2	R	3	R	4
	T	1	T	2	T	3		

Smooth Model: Occam's Inversion

L #	RESISTIVITY	THICKNESS (meters)	DEPTH	ELEVATION (meters)	LONG. COND. (Siemens)	TRANS. RES. (Ohm-m <sup>2</sup> )
				0.0		
1	1585.3	0.200	0.200 *	-0.200	0.0	317.0
2	1591.2	0.0808	0.280 *	-0.280	0.0	128.6
3	1356.3	0.113	0.394 *	-0.394	0.0	153.9
4	899.5	0.159	0.553 *	-0.553	0.0	143.3
5	459.3	0.223	0.777 *	-0.777	0.0	102.8
6	215.8	0.314	1.09 *	-1.09	0.00146	67.85
7	142.1	0.441	1.53 *	-1.53	0.00311	62.73
8	173.2	0.619	2.15 *	-2.15	0.00358	107.3
9	213.8	0.870	3.02 *	-3.02	0.00407	186.1
10	130.1	1.22	4.24 *	-4.24	0.00939	159.0
11	64.64	1.71	5.96 *	-5.96	0.0265	110.9
12	51.32	2.40	8.37 *	-8.37	0.0469	123.6

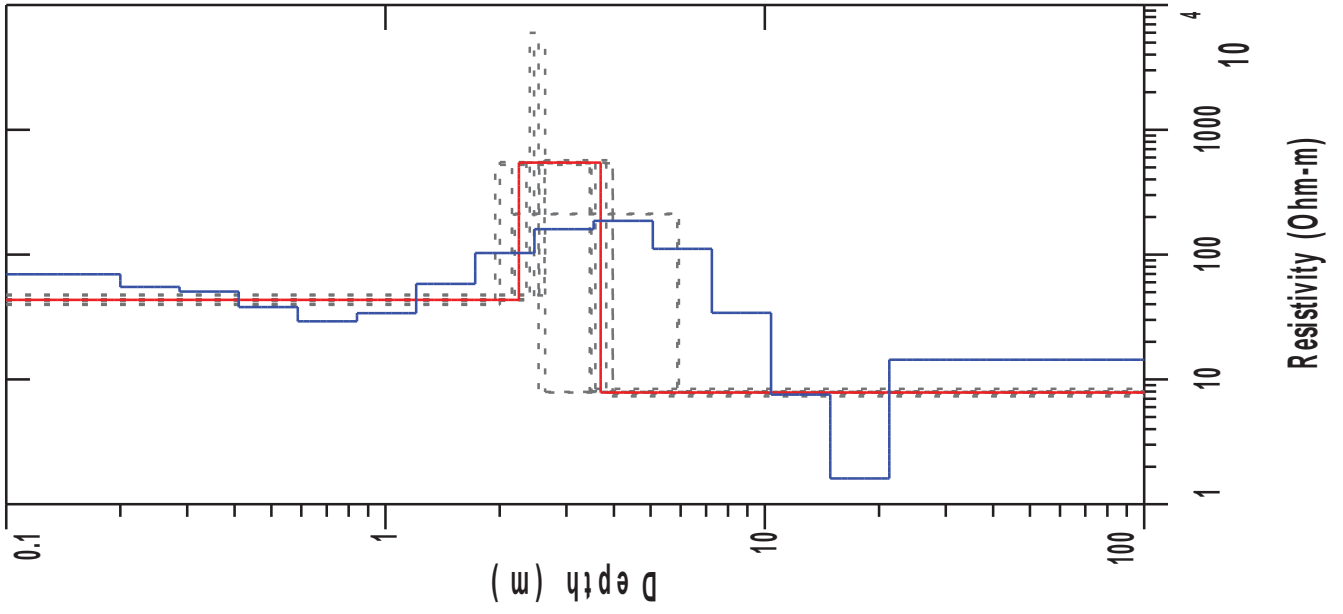
VES 23

Page 3

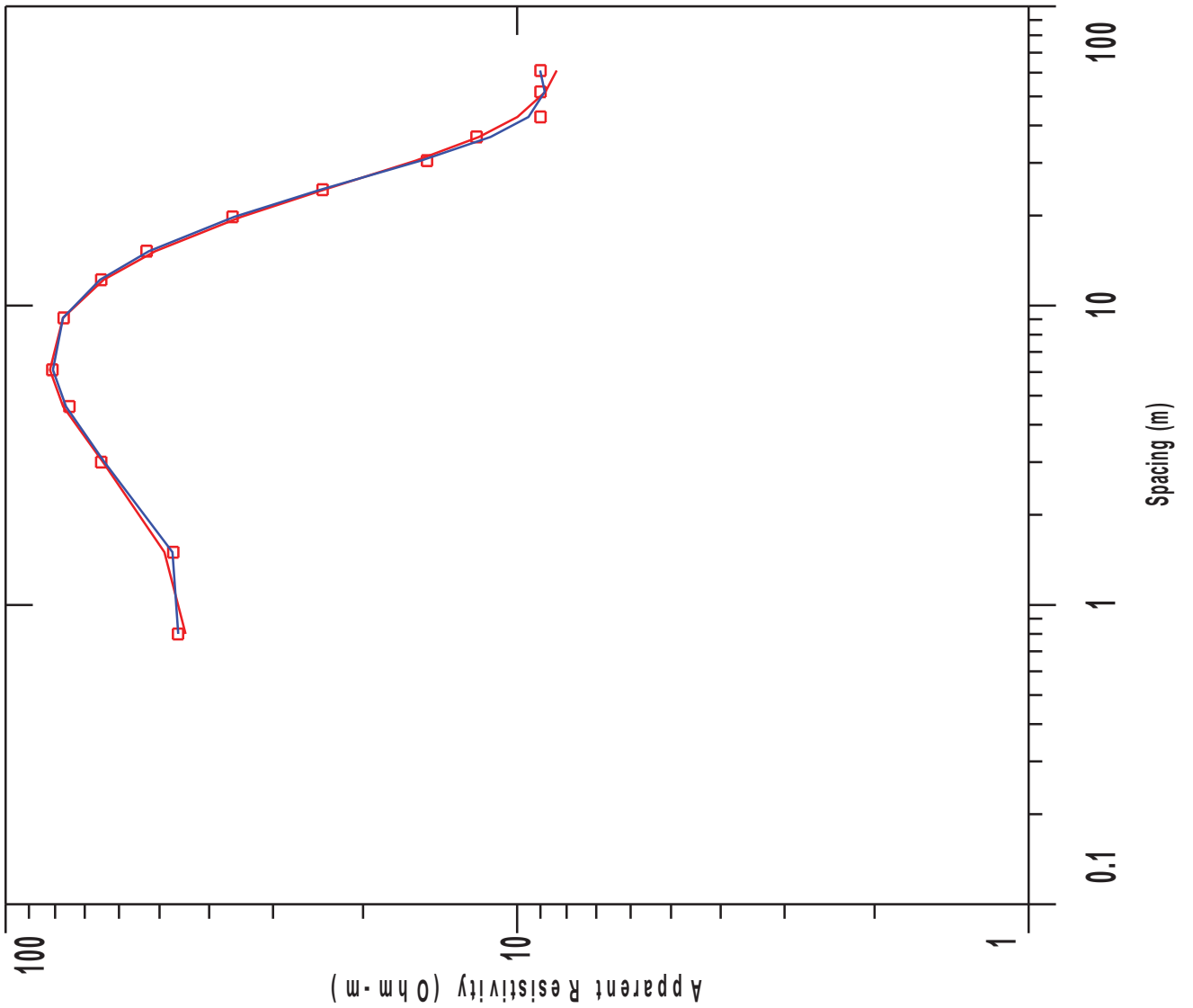
L #	RESISTIVITY	THICKNESS (meters)	DEPTH	ELEVATION (meters)	LONG. COND. (Siemens)	TRANS. RES. (Ohm-m <sup>2</sup> )
13	28.03	3.38	11.75 *	-11.75	0.120	94.86
14	6.29	4.75	16.50 *	-16.50	0.754	29.91
15	1.84	6.67	23.17 *	-23.17	3.61	12.32
16	4.52	9.36	32.54 *	-32.54	2.07	42.35
17	29.18					

"\*" INDICATES FIXED PARAMETER

geoview



VES 24



# VES 24

## Wenner Array

Northing: 0.0 Easting: 0.0 Elevation: 0.0

No.	Spacing (meters)	Layered Model:			Smooth Model:	
		Data Resistivity	Synthetic Resistivity	DIFFERENCE (percent)	Synthetic Resistivity	DIFFERENCE (percent)
1	0.800	46.00	44.48	3.30	45.96	0.0832
2	1.50	47.00	48.90	-4.05	47.17	-0.366
3	3.00	65.00	64.50	0.754	64.05	1.45
4	4.60	75.00	77.17	-2.90	76.18	-1.57
5	6.10	81.00	81.87	-1.08	80.77	0.279
6	9.10	77.00	77.23	-0.301	77.19	-0.259
7	12.20	65.00	64.26	1.12	65.33	-0.520
8	15.20	53.00	50.99	3.78	52.45	1.03
9	19.80	36.00	34.60	3.88	35.70	0.820
10	24.40	24.00	23.82	0.746	24.19	-0.808
11	30.50	15.00	15.79	-5.27	15.43	-2.90
12	36.60	12.00	11.86	1.09	11.26	6.10
13	42.70	9.00	9.98	-10.91	9.49	-5.54
14	51.80	9.00	8.80	2.19	8.82	1.91
15	61.00	9.00	8.36	7.05	9.01	-0.173

NO DATA ARE MASKED

### Layered Model

L #	RESISTIVITY	THICKNESS (meters)	DEPTH	ELEVATION (meters)	LONG. COND. (Siemens)	TRANS. RES. (Ohm-m <sup>2</sup> )
				0.0		
1	43.41	2.24	2.24	-2.24	0.0517	97.61
2	545.3	1.44	3.69	-3.69	0.00264	786.5
3	7.86					

ALL PARAMETERS ARE FREE

### Parameter Bounds from Equivalence Analysis

LAYER	MINIMUM	BEST	MAXIMUM
RHO 1	39.63	43.42	47.82

VES 24

Page 2

	LAYER	MINIMUM	BEST	MAXIM
	2	210.58	545.35	5986.18
	3	7.32	7.87	8.41
THICK	1	1.95	2.25	2.63
	2	0.13	1.44	3.78

PARAMETER RESOLUTION MATRIX:  
 "FIX" INDICATES FIXED PARAMETER

RHO	1	0.98			
RHO	2	0.00	0.50		
RHO	3	0.00	0.00	0.99	
THK	1	-0.02	-0.01	0.01	0.95
THK	2	0.00	0.50	0.00	0.02
		R 1	R 2	R 3	T 1 T 2

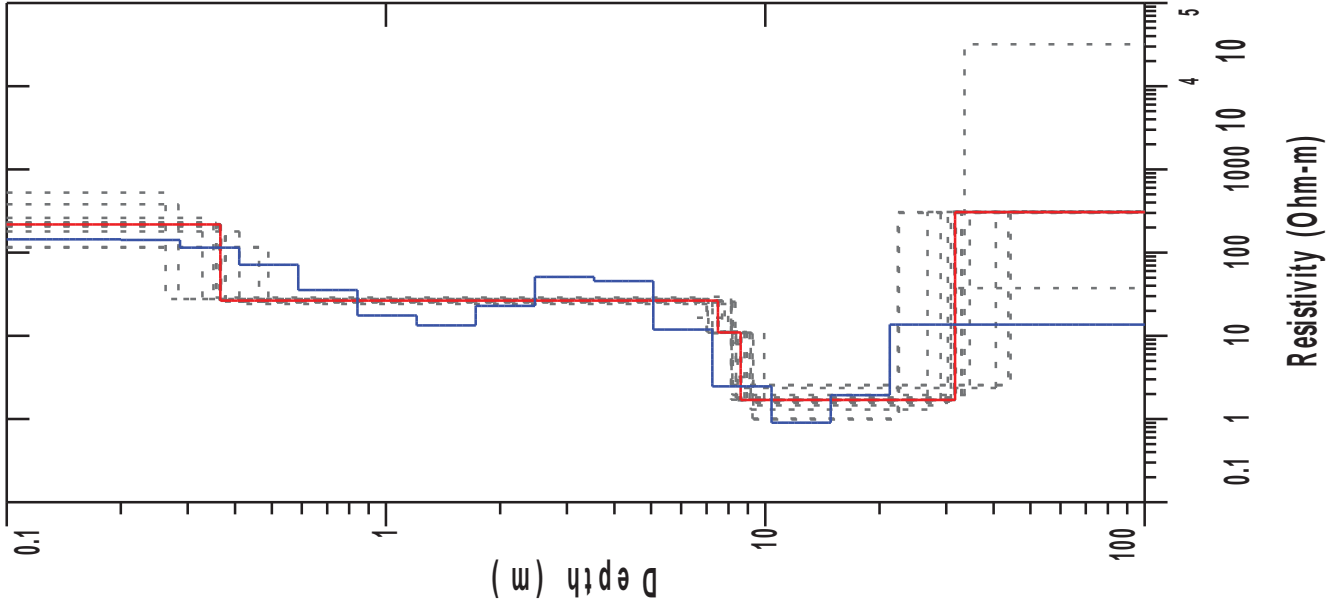
Smooth Model: Ridge Regression

L #	RESISTIVITY	THICKNESS (meters)	DEPTH	ELEVATION (meters)	LONG. COND. (Siemens)	TRANS. RES. (Ohm-m <sup>2</sup> )
				0.0		
1	69.47	0.200	0.200 *	-0.200	0.00288	13.89
2	55.15	0.0864	0.286 *	-0.286	0.00157	4.76
3	50.51	0.123	0.410 *	-0.410	0.00245	6.25
4	37.94	0.177	0.587 *	-0.587	0.00467	6.72
5	29.19	0.253	0.841 *	-0.841	0.00869	7.40
6	33.95	0.363	1.20 *	-1.20	0.0107	12.33
7	58.24	0.520	1.72 *	-1.72	0.00893	30.30
8	103.1	0.745	2.46 *	-2.46	0.00722	76.85
9	159.7	1.06	3.53 *	-3.53	0.00668	170.4
10	186.2	1.52	5.06 *	-5.06	0.00821	284.5
11	111.1	2.18	7.25 *	-7.25	0.0196	243.1
12	34.12	3.13	10.38 *	-10.38	0.0918	106.9
13	7.56	4.48	14.87 *	-14.87	0.593	33.93
14	1.61	6.42	21.29 *	-21.29	3.98	10.35
15	14.38					

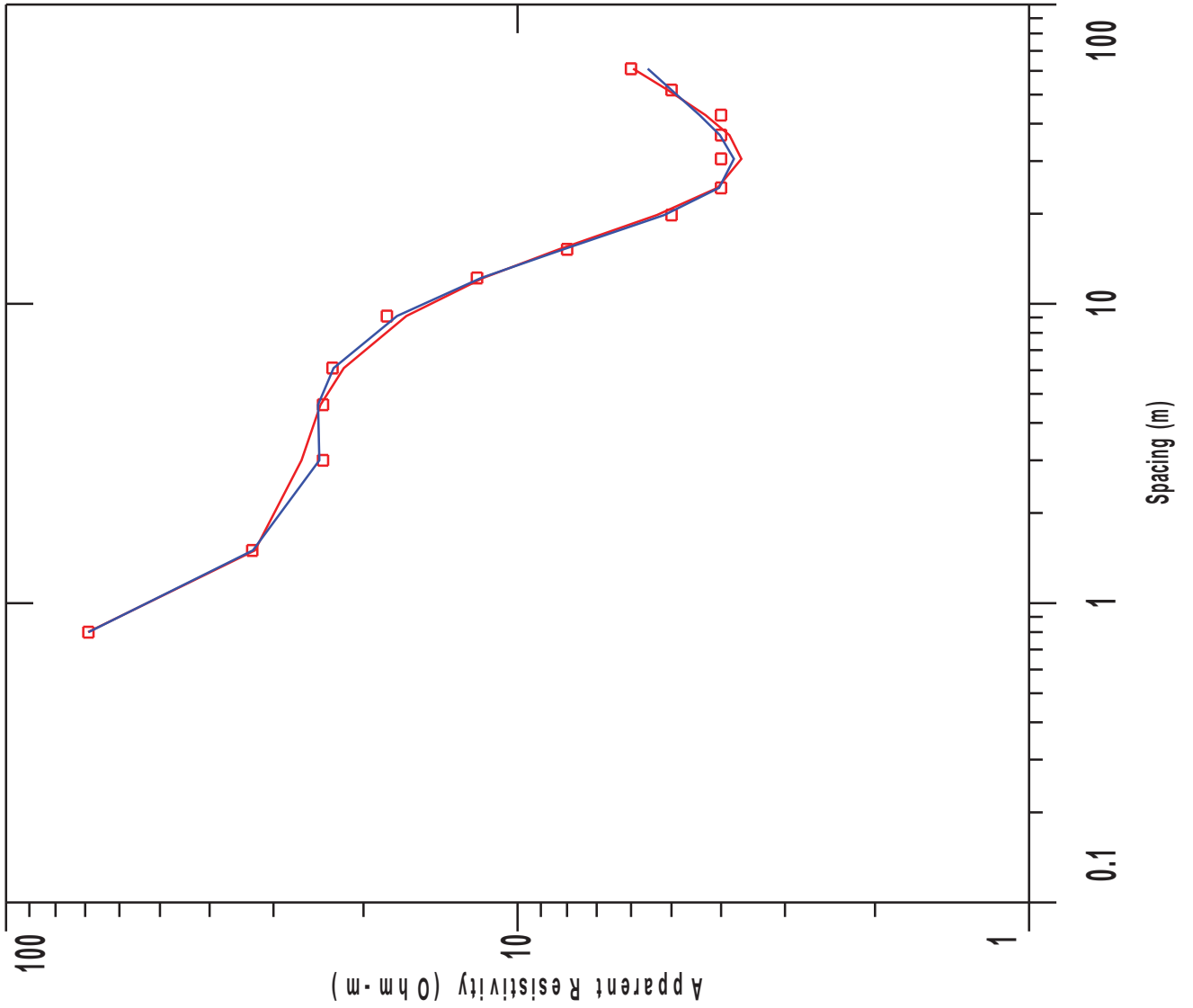
"\*" INDICATES FIXED PARAMETER



geoview



VES 25



# VES 25

## Wenner Array

Northing: 0.0 Easting: 0.0 Elevation: 0.0

No.	Spacing (meters)	Layered Model:			Smooth Model:	
		Data Resistivity	Synthetic Resistivity	DIFFERENCE (percent)	Synthetic Resistivity	DIFFERENCE (percent)
1	0.800	69.00	69.13	-0.192	68.91	0.123
2	1.50	33.00	32.61	1.17	32.90	0.281
3	3.00	24.00	26.43	-10.14	24.39	-1.63
4	4.60	24.00	24.27	-1.14	24.54	-2.27
5	6.10	23.00	21.86	4.95	22.88	0.479
6	9.10	18.00	16.49	8.35	17.20	4.44
7	12.20	12.00	11.66	2.78	11.77	1.90
8	15.20	8.00	8.30	-3.83	8.14	-1.76
9	19.80	5.00	5.33	-6.79	5.16	-3.29
10	24.40	4.00	4.06	-1.62	4.03	-0.882
11	30.50	4.00	3.65	8.74	3.77	5.62
12	36.60	4.00	3.85	3.67	4.02	-0.512
13	42.70	4.00	4.28	-7.23	4.40	-10.07
14	51.80	5.00	5.08	-1.72	5.00	-0.0216
15	61.00	6.00	5.94	0.937	5.56	7.24

NO DATA ARE MASKED

### Layered Model

L #	RESISTIVITY	THICKNESS (meters)	DEPTH	ELEVATION (meters)	LONG. COND. (Siemens)	TRANS. RES. (Ohm-m <sup>2</sup> )
				0.0		
1	218.0	0.365	0.365	-0.365	0.00168	79.76
2	26.50	7.13	7.49	-7.49	0.269	189.0
3	10.98	1.11	8.61	-8.61	0.101	12.25
4	1.69	23.02	31.63	-31.63	13.60	38.96
5	307.0					

ALL PARAMETERS ARE FREE

Parameter Bounds from Equivalence Analysis

LAYER	MINIMUM	BEST	MAXIMUM	
RHO	1	114.81	218.07	525.48
	2	24.20	26.51	28.87
	3	3.21	10.98	29.51
	4	0.99	1.69	2.57
	5	37.39	307.06	31914.03
THICK	1	0.26	0.37	0.49
	2	6.20	7.13	7.96
	3	0.33	1.12	2.89
	4	13.05	23.02	36.21

PARAMETER RESOLUTION MATRIX:  
 "FIX" INDICATES FIXED PARAMETER

RHO	1	0.55									
RHO	2	-0.02	0.99								
RHO	3	0.01	0.00	0.01							
RHO	4	-0.03	-0.02	-0.01	0.66						
RHO	5	0.00	0.00	0.00	0.00	0.00					
THK	1	0.17	0.01	0.00	0.02	0.00	0.92				
THK	2	0.01	0.01	0.07	0.06	0.00	-0.01	0.98			
THK	3	0.00	0.00	0.01	-0.01	0.00	0.00	0.07	0.01		
THK	4	-0.03	-0.02	-0.02	-0.36	-0.02	0.02	0.06	0.00	0.61	
		R	1 R	2 R	3 R	4 R	5 T	1 T	2 T	3 T	4

Smooth Model: Occam's Inversion

L #	RESISTIVITY	THICKNESS (meters)	DEPTH	ELEVATION (meters)	LONG. COND. (Siemens)	TRANS. RES. (Ohm-m <sup>2</sup> )
				0.0		
1	144.2	0.200	0.200 *	-0.200	0.00139	28.84
2	141.6	0.0864	0.286 *	-0.286	0.0	12.23
3	114.9	0.123	0.410 *	-0.410	0.00108	14.22
4	71.43	0.177	0.587 *	-0.587	0.00248	12.65
5	35.45	0.253	0.841 *	-0.841	0.00716	8.99
6	17.52	0.363	1.20 *	-1.20	0.0207	6.36
7	13.35	0.520	1.72 *	-1.72	0.0389	6.94
8	22.88	0.745	2.46 *	-2.46	0.0325	17.05

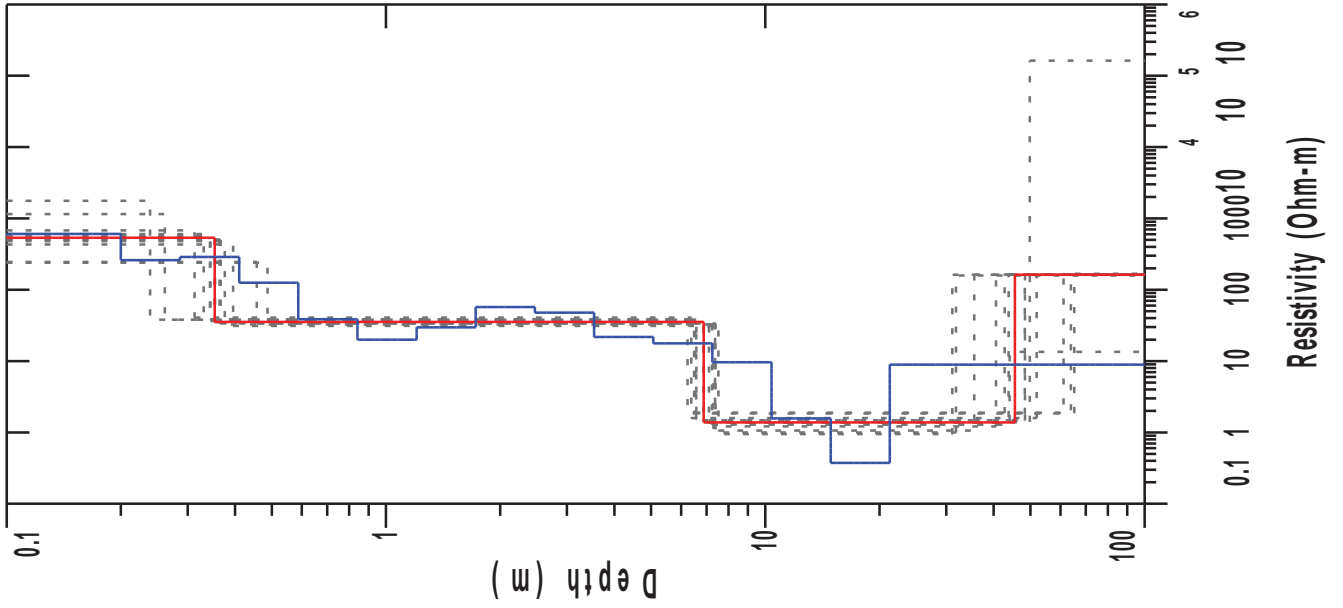
VES 25

Page 3

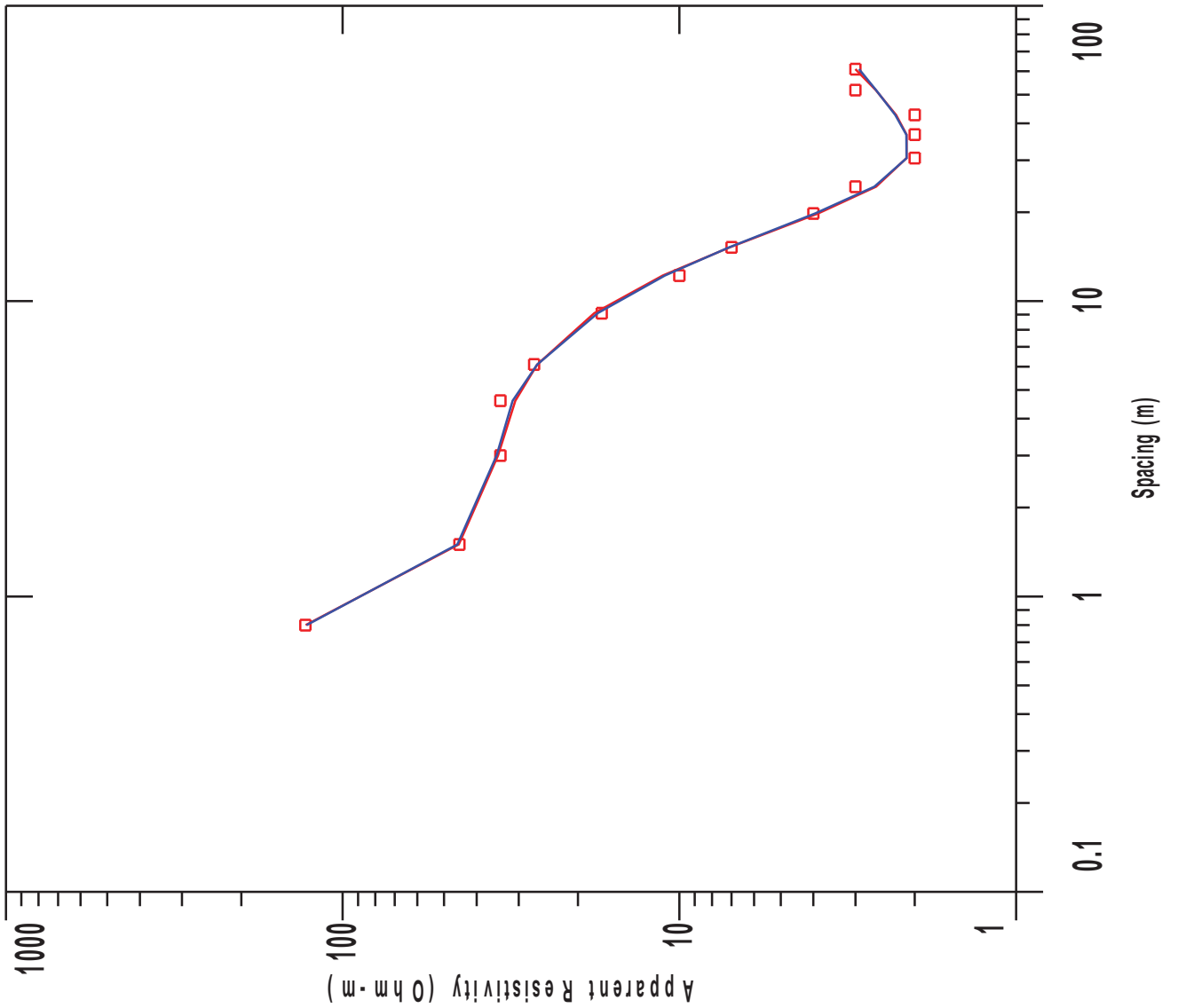
L #	RESISTIVITY	THICKNESS (meters)	DEPTH	ELEVATION (meters)	LONG. COND. (Siemens)	TRANS. RES. (Ohm-m <sup>2</sup> )
9	50.95	1.06	3.53 *	-3.53	0.0209	54.36
10	45.55	1.52	5.06 *	-5.06	0.0335	69.59
11	11.89	2.18	7.25 *	-7.25	0.184	26.01
12	2.47	3.13	10.38 *	-10.38	1.26	7.74
13	0.902	4.48	14.87 *	-14.87	4.97	4.05
14	1.93	6.42	21.29 *	-21.29	3.32	12.42
15	13.65					

"\*" INDICATES FIXED PARAMETER

geoview



VES 26



# VES 26

## Wenner Array

Northing: 0.0 Easting: 0.0 Elevation: 0.0

No.	Spacing (meters)	Layered Model:			Smooth Model:	
		Data Resistivity	Synthetic Resistivity	DIFFERENCE (percent)	Synthetic Resistivity	DIFFERENCE (percent)
1	0.800	129.0	128.7	0.193	127.8	0.880
2	1.50	45.00	45.18	-0.401	45.63	-1.41
3	3.00	34.00	34.55	-1.64	34.91	-2.68
4	4.60	34.00	30.69	9.73	31.27	8.01
5	6.10	27.00	26.42	2.11	26.42	2.11
6	9.10	17.00	17.88	-5.22	17.48	-2.82
7	12.20	10.00	11.20	-12.01	11.03	-10.36
8	15.20	7.00	7.09	-1.35	7.12	-1.79
9	19.80	4.00	3.87	3.16	3.95	1.08
10	24.40	3.00	2.60	13.19	2.63	12.12
11	30.50	2.00	2.11	-5.83	2.11	-5.68
12	36.60	2.00	2.11	-5.70	2.11	-5.86
13	42.70	2.00	2.27	-13.58	2.28	-14.25
14	51.80	3.00	2.61	12.97	2.60	13.17
15	61.00	3.00	3.00	-0.0790	2.92	2.45

NO DATA ARE MASKED

### Layered Model

L #	RESISTIVITY	THICKNESS (meters)	DEPTH	ELEVATION (meters)	LONG. COND. (Siemens)	TRANS. RES. (Ohm-m <sup>2</sup> )
				0.0		
1	535.0	0.353	0.353	-0.353	0.0	189.2
2	35.34	6.52	6.87	-6.87	0.184	230.6
3	1.38	38.62	45.50	-45.50	27.94	53.38
4	162.8					

ALL PARAMETERS ARE FREE

Parameter Bounds from Equivalence Analysis

LAYER		MINIMUM	BEST	MAXIMUM
RHO	1	238.72	535.00	1766.68
	2	31.12	35.35	40.65
	3	0.95	1.38	1.88
	4	13.48	162.85	162854.08
THICK	1	0.24	0.35	0.49
	2	5.90	6.53	7.15
	3	23.73	38.63	58.74

PARAMETER RESOLUTION MATRIX:  
 "FIX" INDICATES FIXED PARAMETER

RHO	1	0.55						
RHO	2	-0.03	0.98					
RHO	3	-0.02	-0.02	0.87				
RHO	4	0.00	0.00	0.00	0.00			
THK	1	0.15	0.01	0.01	0.00	0.94		
THK	2	0.01	0.01	0.03	0.00	-0.01	0.99	
THK	3	-0.03	-0.02	-0.17	-0.02	0.02	0.03	0.76
	R	1	R	2	R	3	R	4
	T	1	T	2	T	3		

Smooth Model: Ridge Regression

L #	RESISTIVITY	THICKNESS (meters)	DEPTH	ELEVATION (meters)	LONG. COND. (Siemens)	TRANS. RES. (Ohm-m <sup>2</sup> )
				0.0		
1	604.8	0.200	0.200 *	-0.200	0.0	120.9
2	259.3	0.0864	0.286 *	-0.286	0.0	22.41
3	287.5	0.123	0.410 *	-0.410	0.0	35.57
4	125.5	0.177	0.587 *	-0.587	0.00141	22.24
5	38.59	0.253	0.841 *	-0.841	0.00657	9.79
6	19.98	0.363	1.20 *	-1.20	0.0181	7.26
7	29.67	0.520	1.72 *	-1.72	0.0175	15.44
8	57.19	0.745	2.46 *	-2.46	0.0130	42.61
9	47.85	1.06	3.53 *	-3.53	0.0223	51.06
10	21.74	1.52	5.06 *	-5.06	0.0702	33.22
11	17.76	2.18	7.25 *	-7.25	0.123	38.86
12	9.61	3.13	10.38 *	-10.38	0.325	30.13

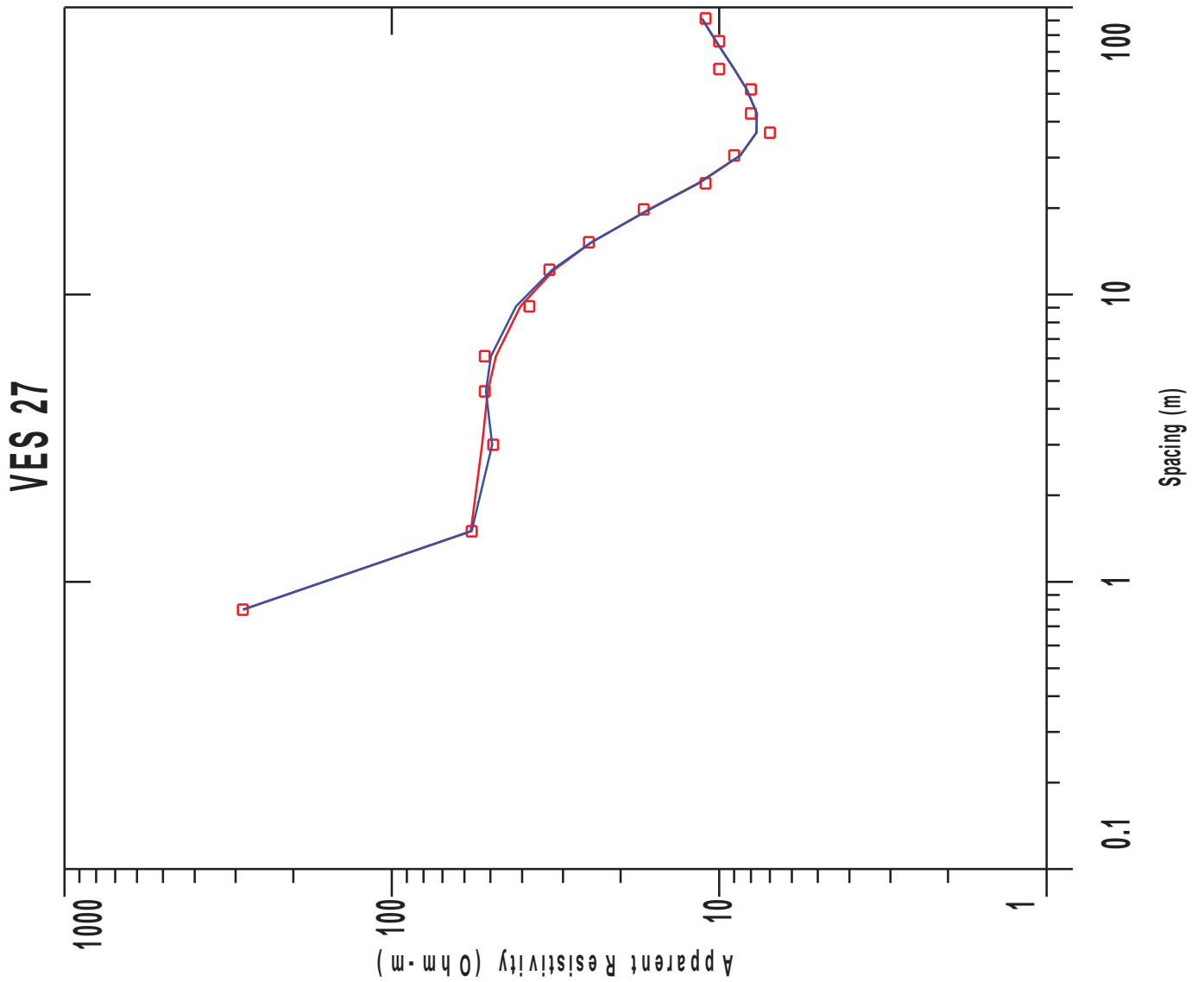
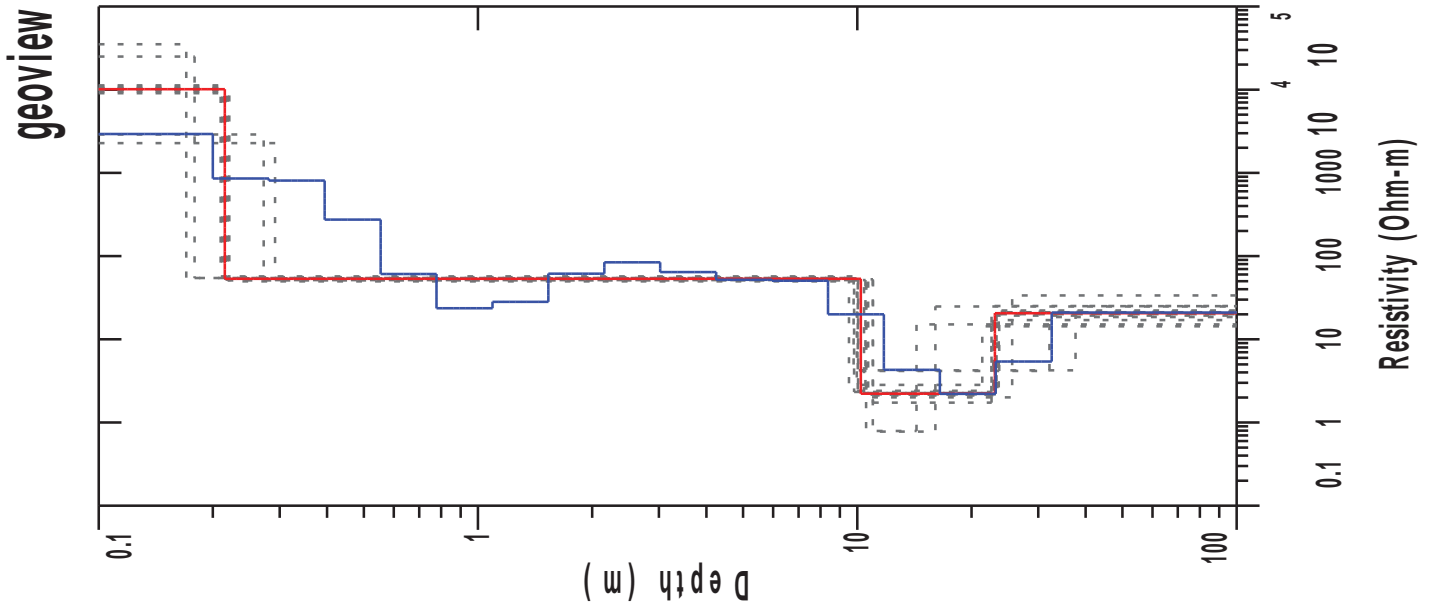
VES 26

Page 3

L #	RESISTIVITY	THICKNESS (meters)	DEPTH	ELEVATION (meters)	LONG. COND. (Siemens)	TRANS. RES. (Ohm-m <sup>2</sup> )
13	1.57	4.48	14.87 *	-14.87	2.84	7.06
14	0.374	6.42	21.29 *	-21.29	17.14	2.40
15	8.90					

"\*" INDICATES FIXED PARAMETER





# VES 27

## Wenner Array

Northing: 0.0 Easting: 0.0 Elevation: 0.0

No.	Spacing (meters)	Layered Model:			Smooth Model:	
		Data Resistivity	Synthetic Resistivity	DIFFERENCE (percent)	Synthetic Resistivity	DIFFERENCE (percent)
1	0.800	285.0	284.5	0.157	284.8	0.0378
2	1.50	57.00	57.41	-0.723	57.07	-0.139
3	3.00	49.00	53.00	-8.17	49.37	-0.769
4	4.60	52.00	50.91	2.08	51.57	0.818
5	6.10	52.00	48.08	7.53	49.79	4.23
6	9.10	38.00	40.45	-6.45	41.71	-9.78
7	12.20	33.00	31.87	3.41	32.32	2.03
8	15.20	25.00	24.54	1.82	24.59	1.61
9	19.80	17.00	16.39	3.54	16.28	4.18
10	24.40	11.00	11.60	-5.53	11.53	-4.83
11	30.50	9.00	8.63	4.08	8.61	4.26
12	36.60	7.00	7.69	-9.89	7.70	-10.00
13	42.70	8.00	7.66	4.16	7.67	4.08
14	51.80	8.00	8.24	-3.03	8.23	-2.96
15	61.00	10.00	9.01	9.85	8.99	10.02
16	76.20	10.00	10.24	-2.40	10.21	-2.18
17	91.40	11.00	11.30	-2.75	11.28	-2.58

NO DATA ARE MASKED

### Layered Model

L #	RESISTIVITY	THICKNESS (meters)	DEPTH	ELEVATION (meters)	LONG. COND. (Siemens)	TRANS. RES. (Ohm-m <sup>2</sup> )
				0.0		
1	10140.4	0.215	0.215	-0.215	0.0	2180.9
2	53.35	9.99	10.21	-10.21	0.187	533.5
3	2.22	12.83	23.05	-23.05	5.77	28.54
4	20.61					

ALL PARAMETERS ARE FREE

Parameter Bounds from Equivalence Analysis

LAYER		MINIMUM	BEST	MAXIMUM
RHO	1	2278.09	10140.42	35158.08
	2	49.62	53.35	57.03
	3	0.78	2.22	4.24
	4	14.30	20.61	33.60
THICK	1	0.17	0.22	0.29
	2	9.30	10.00	10.78
	3	3.78	12.84	27.59

PARAMETER RESOLUTION MATRIX:  
 "FIX" INDICATES FIXED PARAMETER

RHO	1	0.14						
RHO	2	-0.02	0.99					
RHO	3	-0.01	-0.01	0.48				
RHO	4	0.02	0.01	0.09	0.57			
THK	1	0.16	0.00	0.00	0.00	0.97		
THK	2	0.01	0.01	0.04	-0.03	0.00	0.99	
THK	3	0.00	0.00	-0.46	-0.14	0.00	0.01	0.45
	R	1	R	2	R	3	R	4
	T	1	T	2	T	3		

Smooth Model: Ridge Regression

L #	RESISTIVITY	THICKNESS (meters)	DEPTH	ELEVATION (meters)	LONG. COND. (Siemens)	TRANS. RES. (Ohm-m <sup>2</sup> )
				0.0		
1	2937.3	0.200	0.200 *	-0.200	0.0	587.4
2	855.5	0.0808	0.280 *	-0.280	0.0	69.16
3	808.4	0.113	0.394 *	-0.394	0.0	91.77
4	274.8	0.159	0.553 *	-0.553	0.0	43.81
5	61.01	0.223	0.777 *	-0.777	0.00367	13.65
6	23.61	0.314	1.09 *	-1.09	0.0133	7.42
7	28.20	0.441	1.53 *	-1.53	0.0156	12.44
8	61.53	0.619	2.15 *	-2.15	0.0100	38.13
9	84.02	0.870	3.02 *	-3.02	0.0103	73.12
10	64.34	1.22	4.24 *	-4.24	0.0189	78.63
11	51.99	1.71	5.96 *	-5.96	0.0330	89.21
12	50.65	2.40	8.37 *	-8.37	0.0475	122.0

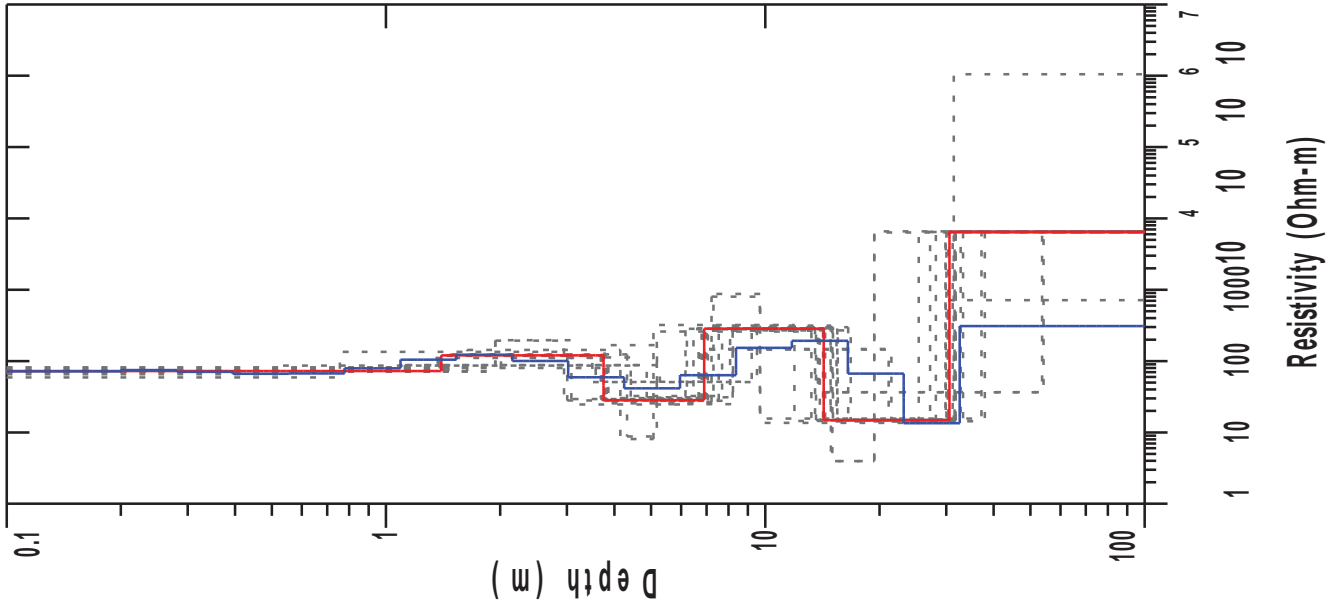
VES 27

Page 3

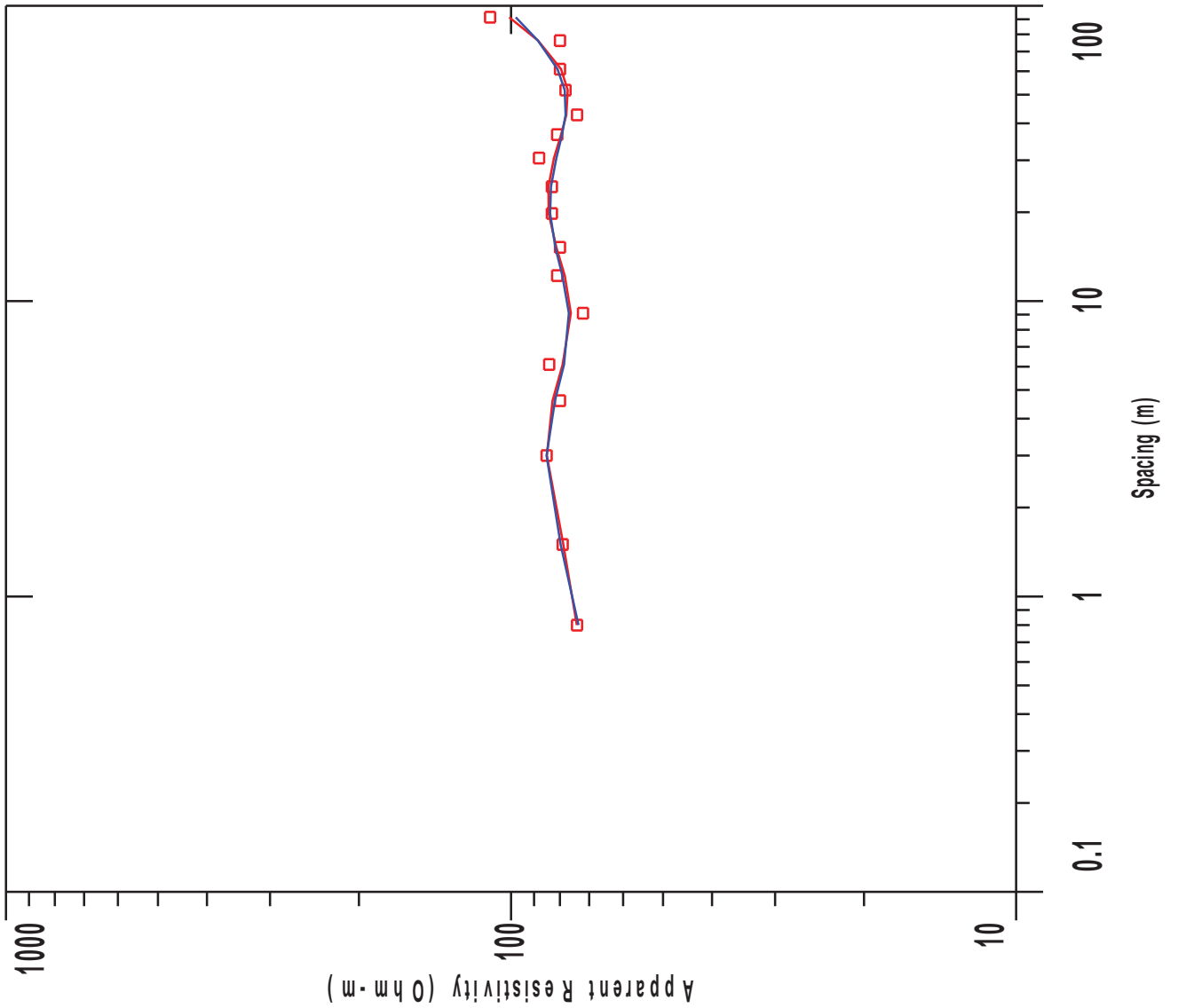
L #	RESISTIVITY	THICKNESS (meters)	DEPTH	ELEVATION (meters)	LONG. COND. (Siemens)	TRANS. RES. (Ohm-m <sup>2</sup> )
13	19.97	3.38	11.75 *	-11.75	0.169	67.59
14	4.29	4.75	16.50 *	-16.50	1.10	20.42
15	2.20	6.67	23.17 *	-23.17	3.02	14.73
16	5.39	9.36	32.54 *	-32.54	1.73	50.58
17	20.94					

"\*" INDICATES FIXED PARAMETER

geoview



VES 28



# VES 28

## Wenner Array

Northing: 0.0 Easting: 0.0 Elevation: 0.0

No.	Spacing (meters)	Layered Model:			Smooth Model:	
		Data Resistivity	Synthetic Resistivity	DIFFERENCE (percent)	Synthetic Resistivity	DIFFERENCE (percent)
1	0.800	74.00	74.08	-0.115	73.51	0.656
2	1.50	79.00	78.76	0.294	79.76	-0.964
3	3.00	85.00	84.90	0.116	85.01	-0.0205
4	4.60	80.00	82.76	-3.45	81.84	-2.31
5	6.10	84.00	79.03	5.91	78.50	6.53
6	9.10	72.00	76.10	-5.70	76.82	-6.70
7	12.20	81.00	78.25	3.38	79.13	2.30
8	15.20	80.00	81.33	-1.66	81.68	-2.11
9	19.80	83.00	84.18	-1.42	83.65	-0.785
10	24.40	83.00	84.33	-1.60	83.35	-0.425
11	30.50	88.00	82.23	6.55	81.32	7.58
12	36.60	81.00	79.60	1.72	79.21	2.20
13	42.70	74.00	77.70	-5.01	77.98	-5.37
14	51.80	78.00	77.22	0.989	78.27	-0.357
15	61.00	80.00	79.62	0.471	80.88	-1.10
16	76.20	80.00	88.38	-10.48	88.43	-10.54
17	91.40	110.0	100.8	8.36	97.87	11.02

NO DATA ARE MASKED

### Layered Model

L #	RESISTIVITY	THICKNESS (meters)	DEPTH	ELEVATION (meters)	LONG. COND. (Siemens)	TRANS. RES. (Ohm-m <sup>2</sup> )
				0.0		
1	72.39	1.39	1.39	-1.39	0.0193	101.2
2	120.3	2.34	3.74	-3.74	0.0195	282.6
3	28.37	3.15	6.90	-6.90	0.111	89.47
4	285.0	7.35	14.25	-14.25	0.0257	2095.4
5	14.82	16.34	30.59	-30.59	1.10	242.4
6	6473.3					

ALL PARAMETERS ARE FREE

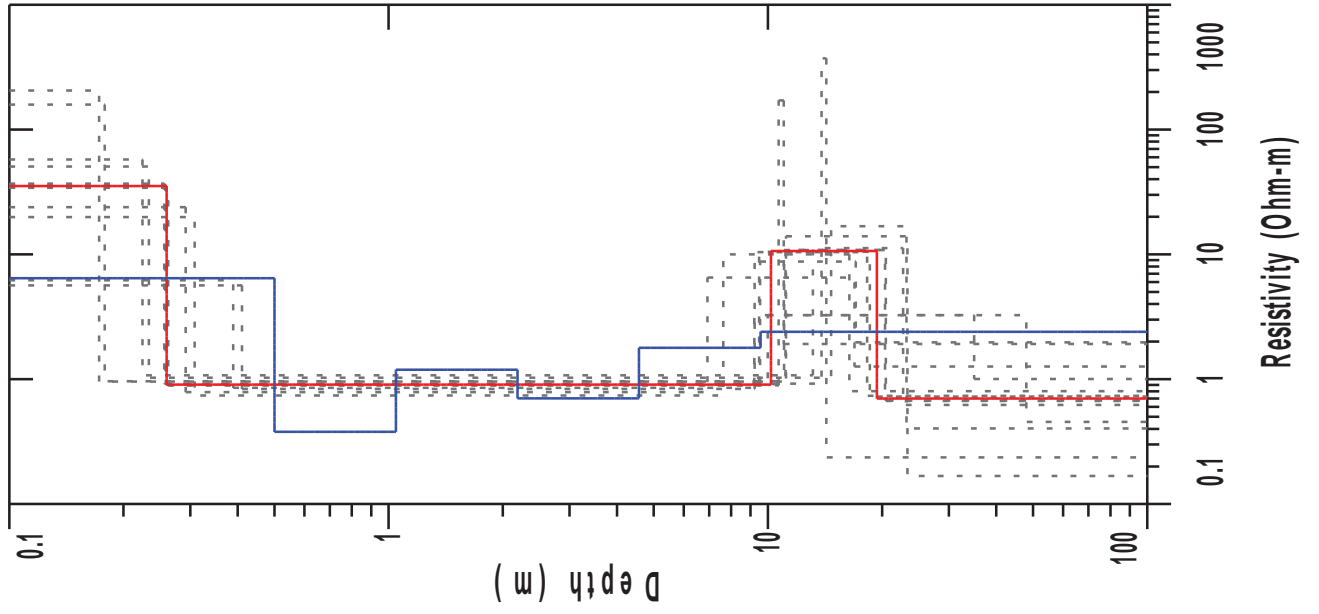


				0.0		
1	71.73	0.200	0.200 *	-0.200	0.00279	14.34
2	74.90	0.0808	0.280 *	-0.280	0.00108	6.05
3	70.49	0.113	0.394 *	-0.394	0.00161	8.00
4	66.33	0.159	0.553 *	-0.553	0.00240	10.57
5	67.08	0.223	0.777 *	-0.777	0.00334	15.01
6	79.19	0.314	1.09 *	-1.09	0.00397	24.89
7	104.4	0.441	1.53 *	-1.53	0.00422	46.11
8	122.9	0.619	2.15 *	-2.15	0.00504	76.18
9	100.2	0.870	3.02 *	-3.02	0.00868	87.23
10	59.32	1.22	4.24 *	-4.24	0.0206	72.49
11	41.55	1.71	5.96 *	-5.96	0.0412	71.30
12	63.27	2.40	8.37 *	-8.37	0.0380	152.4
13	153.5	3.38	11.75 *	-11.75	0.0220	519.6
14	192.3	4.75	16.50 *	-16.50	0.0247	913.8
15	66.71	6.67	23.17 *	-23.17	0.100	445.0
16	13.44	9.36	32.54 *	-32.54	0.696	125.9
17	309.5					

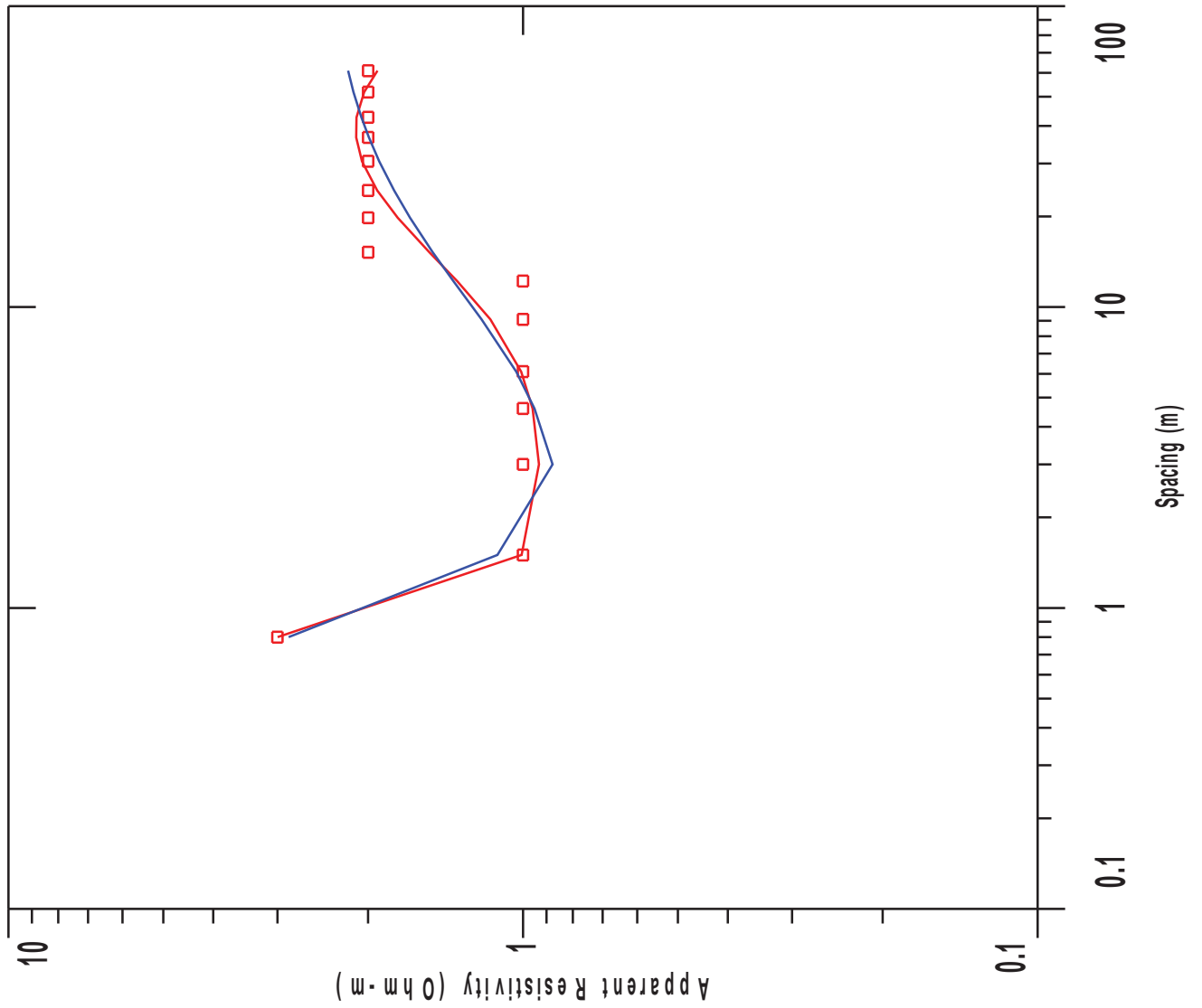
"\*" INDICATES FIXED PARAMETER



geoview



VES 29



# VES 29

## Wenner Array

Northing: 0.0 Easting: 0.0 Elevation: 0.0

No.	Spacing (meters)	Layered Model:			Smooth Model:	
		Data Resistivity	Synthetic Resistivity	DIFFERENCE (percent)	Synthetic Resistivity	DIFFERENCE (percent)
1	0.800	3.00	2.99	0.0478	2.85	4.88
2	1.50	1.00	1.00	-0.600	1.12	-12.11
3	3.00	1.00	0.931	6.88	0.876	12.39
4	4.60	1.00	0.957	4.21	0.949	5.02
5	6.10	1.00	1.00	-0.799	1.03	-3.08
6	9.10	1.00	1.15	-15.75	1.20	-20.36
7	12.20	1.00	1.34	-34.31	1.36	-36.55
8	15.20	2.00	1.52	23.99	1.49	25.13
9	19.80	2.00	1.75	12.45	1.65	17.10
10	24.40	2.00	1.91	4.01	1.78	10.96
11	30.50	2.00	2.05	-2.73	1.90	4.87
12	36.60	2.00	2.10	-5.47	1.99	0.374
13	42.70	2.00	2.10	-5.35	2.06	-3.02
14	51.80	2.00	2.03	-1.76	2.13	-6.73
15	61.00	2.00	1.91	4.12	2.18	-9.38

NO DATA ARE MASKED

### Layered Model

L #	RESISTIVITY	THICKNESS (meters)	DEPTH	ELEVATION (meters)	LONG. COND. (Siemens)	TRANS. RES. (Ohm-m <sup>2</sup> )
				0.0		
1	35.22	0.259	0.259	-0.259	0.00738	9.15
2	0.903	9.93	10.19	-10.19	10.98	8.97
3	10.65	9.19	19.38	-19.38	0.863	97.95
4	0.699					

ALL PARAMETERS ARE FREE

Parameter Bounds from Equivalence Analysis

LAYER	MINIMUM	BEST	MAXIMUM
RHO	1	5.65	35.23
	2	0.74	0.90
	3	3.26	10.65
	4	0.17	0.70
THICK	1	0.17	0.26
	2	6.63	9.93
	3	0.33	9.20

PARAMETER RESOLUTION MATRIX:  
 "FIX" INDICATES FIXED PARAMETER

RHO	1	0.28					
RHO	2	-0.02	0.99				
RHO	3	-0.01	0.00	0.47			
RHO	4	0.02	0.01	0.16	0.15		
THK	1	0.17	0.01	0.00	0.00	0.96	
THK	2	-0.04	-0.01	-0.05	0.06	0.01	0.96
THK	3	-0.01	0.00	0.46	0.17	0.00	0.01
	R	1	R	2	R	3	R
	T	1	T	2	T	3	

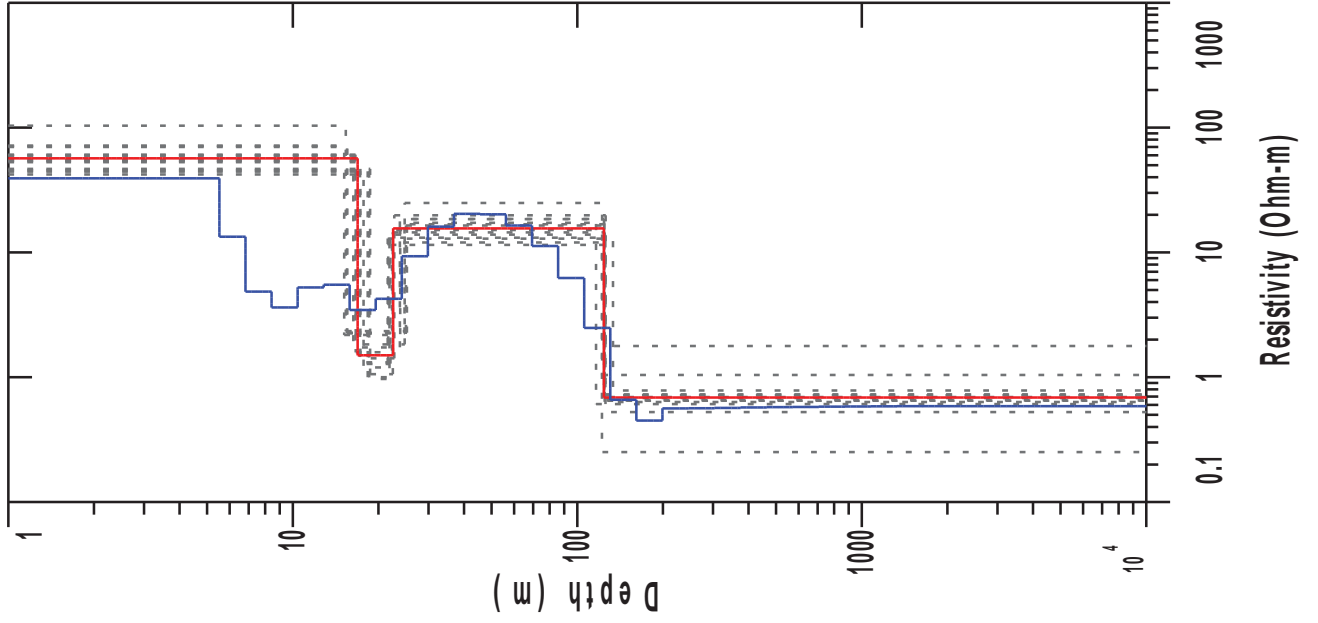
Smooth Model: Ridge Regression

L #	RESISTIVITY	THICKNESS (meters)	DEPTH	ELEVATION (meters)	LONG. COND. (Siemens)	TRANS. RES. (Ohm-m <sup>2</sup> )
				0.0		
1	6.43	0.500	0.500 *	-0.500	0.0776	3.21
2	0.378	0.545	1.04 *	-1.04	1.43	0.206
3	1.19	1.14	2.18 *	-2.18	0.958	1.35
4	0.702	2.38	4.57 *	-4.57	3.39	1.67
5	1.78	4.99	9.56 *	-9.56	2.79	8.91
6	2.39					

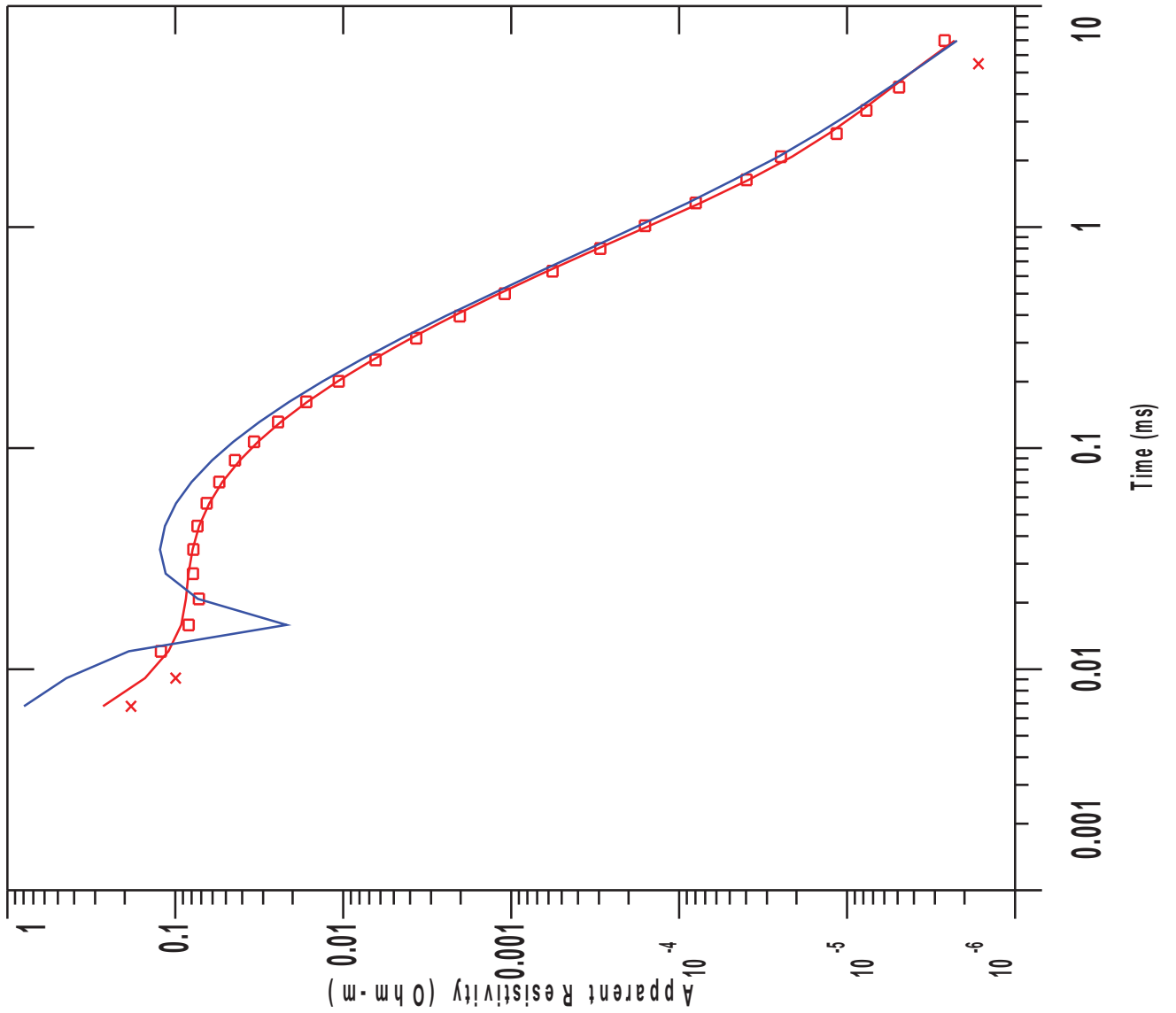
"\*" INDICATES FIXED PARAMETER

( 55,3+ 0< %  
8 6(370, 38 , 1, \* 8 642( .3,80 \* +42(03 8,7 8 03. 6 ,791 87

geoview



TEM 2



# TEM 2

## Fixed Loop TEM

Northing: 0.0 Easting: 0.0 Elevation: 0.0

No.	Time (ms)	Layered Model:			Smooth Model:	
		Data Resistivity (ohm-m)	Synthetic Resistivity (ohm-m)	DIFFERENCE (percent)	Synthetic Resistivity (ohm-m)	DIFFERENCE (percent)
1 *	0.00680	0.183	-0.269	246.6	0.796	-333.8
2 *	0.00911	0.0995	-0.151	252.3	0.445	-347.7
3	0.0120	0.121	-0.109	190.1	0.189	-55.42
4	0.0158	0.0832	-0.0921	210.6	0.0217	73.87
5	0.0208	0.0723	-0.0864	219.4	-0.0733	201.3
6	0.0270	0.0785	-0.0834	206.3	-0.114	245.2
7	0.0348	0.0780	-0.0789	201.1	-0.123	257.8
8	0.0444	0.0737	-0.0721	197.8	-0.115	256.2
9	0.0563	0.0650	-0.0627	196.4	-0.0989	252.0
10	0.0703	0.0546	-0.0524	195.9	-0.0799	246.1
11	0.0881	0.0441	-0.0412	193.5	-0.0602	236.6
12	0.106	0.0339	-0.0321	194.7	-0.0450	232.7
13	0.131	0.0244	-0.0235	196.4	-0.0315	229.3
14	0.161	0.0166	-0.0163	198.6	-0.0210	226.4
15	0.200	0.0106	-0.0107	201.3	-0.0132	224.6
16	0.250	0.00642	-0.00668	204.0	-0.00790	222.9
17	0.314	0.00368	-0.00393	206.9	-0.00449	222.0
18	0.395	0.00202	-0.00221	209.2	-0.00246	221.5
19	0.499	0.00109	-0.00118	208.3	-0.00130	218.7
20	0.631	0.0	0.0	207.8	0.0	218.5
21	0.799	0.0	0.0	203.7	0.0	216.0
22	1.01	0.0	0.0	194.1	0.0	209.2
23	1.28	0.0	0.0	193.1	0.0	211.2
24	1.63	0.0	0.0	196.9	0.0	219.1
25	2.08	0.0	0.0	185.8	0.0	203.3
26	2.64	0.0	0.0	211.3	0.0	229.5
27	3.37	0.0	0.0	206.8	0.0	216.6
28	4.29	0.0	0.0	209.7	0.0	213.6
29 *	5.47	0.0	0.0	314.9	0.0	311.5
30	6.97	0.0	0.0	187.3	0.0	184.5

"\*" INDICATES MASKED DATA POINT

Layered Model

L #	RESISTIVITY (ohm-m)	THICKNESS (m)	DEPTH	ELEVATION (m)	LONG. COND. (Siemens)	TRANS. RES. (Ohm-m <sup>2</sup> )
				0.0		
1	56.75	16.90	16.90	-16.90	0.297	959.5
2	1.49	5.64	22.54	-22.54	3.76	8.44
3	15.55	101.4	123.9	-123.9	6.52	1577.7
4	0.688					

ALL PARAMETERS ARE FREE

Parameter Bounds from Equivalence Analysis

LAYER	MINIMUM	BEST	MAXIMUM
RHO	1 42.05	56.76	103.42
	2 0.97	1.50	2.34
	3 11.49	15.55	24.91
	4 0.25	0.69	1.78
THICK	1 15.16	16.90	18.70
	2 3.32	5.64	9.68
	3 92.60	101.44	111.98

PARAMETER RESOLUTION MATRIX:  
 "FIX" INDICATES FIXED PARAMETER

RHO	1	0.79						
RHO	2	-0.16	0.72					
RHO	3	-0.02	-0.07	0.83				
RHO	4	0.03	0.03	-0.15	0.42			
THK	1	0.03	0.06	0.01	-0.01	0.98		
THK	2	-0.19	-0.34	-0.14	0.01	0.07	0.56	
THK	3	0.01	0.01	0.01	-0.01	0.00	0.02	0.99
	R	1 R	2 R	3 R	4 T	1 T	2 T	3

Smooth Model: Occam's Inversion

TEM 2

Page 3

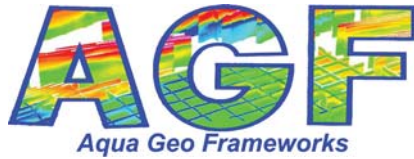
L #	RESISTIVITY (ohm-m)	THICKNESS (m)	DEPTH	ELEVATION (m)	LONG. COND. (Siemens)	TRANS. RES. (Ohm-m <sup>2</sup> )
				0.0		
1	39.24	5.52	5.52 *	-5.52	0.140	216.7
2	13.36	1.29	6.81 *	-6.81	0.0970	17.33
3	4.85	1.60	8.42 *	-8.42	0.329	7.77
4	3.61	1.97	10.39 *	-10.39	0.546	7.15
5	5.23	2.44	12.83 *	-12.83	0.466	12.78
6	5.50	3.01	15.85 *	-15.85	0.547	16.58
7	3.45	3.72	19.57 *	-19.57	1.07	12.85
8	4.24	4.59	24.17 *	-24.17	1.08	19.50
9	9.31	5.67	29.84 *	-29.84	0.609	52.84
10	16.10	7.00	36.85 *	-36.85	0.435	112.8
11	20.36	8.65	45.50 *	-45.50	0.424	176.1
12	20.19	10.68	56.19 *	-56.19	0.529	215.7
13	16.39	13.19	69.38 *	-69.38	0.804	216.3
14	11.26	16.28	85.67 *	-85.67	1.44	183.4
15	6.23	20.11	105.7 *	-105.7	3.22	125.4
16	2.48	24.83	130.6 *	-130.6	10.00	61.63
17	0.659	30.66	161.2 *	-161.2	46.51	20.21
18	0.450	37.86	199.1 *	-199.1	84.13	17.04
19	0.563	46.75	245.9 *	-245.9	83.03	26.33
20	0.564	57.73	303.6 *	-303.6	102.3	32.56
21	0.568	71.29	374.9 *	-374.9	125.4	40.51
22	0.572	88.03	462.9 *	-462.9	153.8	50.37
23	0.575	108.7	571.6 *	-571.6	188.8	62.57
24	0.578	134.2	705.9 *	-705.9	231.9	77.65
25	0.581	165.7	871.6 *	-871.6	285.2	96.29
26	0.583	204.6	1076.2 *	-1076.2	350.9	119.3
27	0.584	252.6	1328.9 *	-1328.9	432.2	147.7
28	0.585	312.0	1641.0 *	-1641.0	532.6	182.7
29	0.586	385.2	2026.2 *	-2026.2	656.8	225.9
30	0.586					

"\*" INDICATES FIXED PARAMETER





APPENDIX B  
AQUA GEO FRAMEWORKS REPORT



April 14, 2016

Report on Advanced Processing and Inversion of AEM Survey Data and Derived Chloride Concentrations near the Turkey Point Power Plant, Southern Florida

Prepared for:

ENERCON Services, Inc.  
12906 Tampa Oaks Blvd., Suite 131  
Temple Terrace, FL 33637  
813-335-4614

Submitted by:

Aqua Geo Frameworks, LLC  
130360 County Road D  
Mitchell, CA 69357  
Phone: (303) 905-6240

Disclaimer:

AGF conducted this project using the current standards of the geophysical industry and used in-house quality control standards to produce this geophysical survey and products. The geophysical methods and procedures described in this report are applicable to the particular project objectives, and these methods have been successfully applied by AGF to investigations and projects of similar size and nature. However, field or subsurface conditions may differ from those anticipated, and the resultant data may not achieve the project objectives. AGF's services were performed consistent with the professional skill and care ordinarily provided by professional geophysicists and geologists under the same or similar circumstances. No other warranty or representation, either expressed or implied, is made by AGF in connection with its services unless in writing and signed by an authorized representative of AGF.

## Executive Summary

Aqua Geo Frameworks (AGF) is pleased to submit this report titled "**Report on Advanced Processing and Inversion of AEM Survey Data and Derived Chloride Concentrations near the Turkey Point Power Plant, Southern Florida**" to ENERCON Services Inc. for a project sponsored by Florida Power and Light. ENERCON required AGF to produce a three-dimensional (3D) data set of chloride concentrations in the area of the January 2016 SkyTEM304M AEM survey of the Turkey Point Power Plant.

The scope of work for this project was as follows:

### 1. SCOPE OF WORK

- 1.1 ENERCON will provide to AGF the final inversions of the SkyTEM304 data collected in January 2016. ENERCON will also provide chloride concentration control points to AGF prior to the beginning of the project.
- 1.2 AGF will produce a 3D map of the estimated salinity of the area of interest (AOI) as provided by ENERCON. The chloride concentrations will be inferred from the resistivity values derived from the AEM data and the process as illustrated in [Fitterman and Prinos \(2011\)](#). The 3D grid (or Voxel) will be created based on the vertical and horizontal discretization of the AEM data and will extend from the land surface to the base of the Biscayne Aquifer ([Fish and Stewart, 1991](#)). Chloride concentration values will only be displayed for those concentrations greater than 19,000, mg/L.
- 1.3 AGF will make a comparison of the voxel of AEM-derived chloride concentrations to the chloride concentration control points provided by ENERCON that are within the project AOI. This comparison will include the chloride concentration control point values at the time of the AEM surveys versus the chloride concentration values derived from the AEM relationships published in [Fitterman and Prinos \(2011\)](#). A detailed analysis of those comparisons will be provided.
- 1.4 AGF will calculate the mass of chloride in the Biscayne Aquifer greater than 19,000 mg/L.
- 1.5 AGF will provide the chloride concentration voxel in a format that is easily readable and importable on or before April 1, 2016.
- 1.6 AGF will provide representative 3D images of the greater than 19,000 mg/L volume.
- 1.7 AGF will provide a summary report that explains the methods and the processes used to create the Voxel and the comparisons of the AEM-derived chloride concentrations versus the chloride concentration control points

### 2. KEY FINDINGS

- 2.1. The acquired AEM data have been processed and inverted. The quality of the AEM data was quite good given the infrastructure in the survey area. Profile and depth slice images are included in the report appendices. Images and data files are presented down to the base of the Biscayne Aquifer ([Fish and Stewart, 1991](#)) and within the AOI.
- 2.2 The chloride concentration control points allowed AGF to calculate a new calibration set for the January 2016 AEM data in addition to analyzing and comparing with the [Fitterman and Prinos \(2011\)](#) calibration. The AEM-derived chloride concentrations compared quite well with the control points of TPGW wells. The chloride concentration images and data are presented down to the base of the Biscayne Aquifer ([Fish and Stewart, 1991](#)).

- 2.3 One issue of note is that the chloride concentration calibration developed is only valid for the range from 20 mg/L to 40,000 mg/L chloride concentration because that is the range of the available data. Note that 1 mg/L equals 1 ppm. These units are used interchangeably throughout this report. The calibration could be expanded with more control points outside of that range, but caution needs to be exercised as the sensitivity of the AEM to the changes outside the above range is problematic due to the fundamental physics of the technique. Fortunately, about 90% of the Turkey Point AEM-derived chloride concentrations lay within the valid range.
- 2.4 The estimated mass of chloride for concentrations greater than 19,000 mg/L is approximately 3,042,471,451 kg.

### 3. RECOMMENDATIONS

Recommendations provided to the client in this section are based on the knowledge and experience of AGF in applying AEM to mapping salinity and hydrogeologic frameworks. There are three recommendations:

- 3.1 A coupled hydrogeophysical inversion approach (CHI) should be implemented using a groundwater transport model of the area and the AEM data ([Herckenrath et al., 2013](#)). In this approach the information that is available with a groundwater flow model is utilized to constrain the ambiguity of the determination of the salinity level of the pore fluid inherent in the Archie approach;
- 3.2 Lithology logs and additional drilling should be acquired and used to construct a hydrogeological framework complementing the AEM resistivity data; and
- 3.3. The resistivity data in this project show a great amount of detail and variety that is related to the geological structure within the survey area. While it was beyond the scope of this study to fully develop a hydrogeological framework, with the use of lithology logs and additional drilling on targets indicated within the AEM, a robust hydrogeological framework could be developed. This would aid in the understanding of the flow paths and ultimate fate of the saline waters within the study area.

#### 4. DELIVERABLES

As mentioned above, project deliverables include data files for the processed and inverted AEM resistivity model and the chloride concentration voxel model and database that was used to calculate the Voxel model. In addition, 2D-profiles of the resistivity and chloride concentration from 0 to 30 meters in depth are provided as well as 2D-layer maps for the first 14 model layers within the 0-30-meter depth range of resistivity and chloride concentrations. The data in these files are presented down to the base of the Biscayne Aquifer as defined by [Fish and Stewart \(1991\)](#).

In particular,

- Data File – Processed and inverted AEM data
- Data File – AEM-derived Chloride concentration data
- Data File – Chloride concentrations in each voxel model cell including identification of cells with greater than 19,000 mg/L and the thickness and volume of those cells.

**Table of Contents**

1 Geophysical Methodology ..... 1

1.1 AEM Methodology, Acquisition, and Inversion ..... 1

1.1.1 AEM Methodology ..... 1

1.1.2 AEM Acquisition ..... 2

1.1.3 Primary Field Compensation ..... 3

1.1.4 Automatic Processing ..... 3

1.1.5 Manual Processing and Laterally-Constrained Inversions ..... 4

1.1.6 Power Line Noise Intensity (PLNI) ..... 4

1.1.7 Total Magnetic Field and Analytic Signal Data ..... 4

1.1.8 In-Field Quality Control ..... 4

1.1.9 Spatially-Constrained Inversion ..... 8

1.2 Resistivity Model Verification and Acceptance ..... 11

1.3 Water Quality Data ..... 18

1.4 Calibration of AEM Resistivity to Chloride Concentration ..... 19

1.5 Producing the Voxel Grid of Chloride Concentration ..... 30

1.6 Comparison of Chloride Concentration from Other Studies ..... 33

1.6.1 Volume and Mass of Chloride Concentration Greater than 19,000 mg/L ..... 37

1.7 Recommendations for Future Studies ..... 38

2 Description of Data Delivered ..... 39

3 References ..... 41

Appendix 1: AEM Resistivity 2D Earth-Model Profiles ..... A1-1

Appendix 2: AEM Chloride Concentration Profiles ..... A3-1

Appendix 3: AEM Chloride Concentration Depth Slices ..... A4-1

## List of Figures

<a href="#">Figure 1-1</a> : Schematic of an AEM survey. ....	1
<a href="#">Figure 1-2</a> : A) Example of a dB/dt sounding curve. B) Corresponding inverted model values. C) Corresponding resistivity earth model. ....	2
<a href="#">Figure 1-3</a> : Power Line Noise Intensity (PLNI) map of the Turkey Point AEM project area.....	5
<a href="#">Figure 1-4</a> : Magnetic Total Field data for the Turkey Point AEM survey area corrected for diurnal drift, with the IGRF removed. ....	6
<a href="#">Figure 1-5</a> : Magnetic Field Analytic Signal plot for the Turkey Point AEM survey area. The Analytic Signal is sensitive to electromagnetic as well as purely magnetic sources.....	7
<a href="#">Figure 1-6</a> : Locations of the decoupled and removed data (blue lines) along the AEM flight lines of the data used in the inversion (red lines) in the Turkey Point project area. Where blue lines are present indicates decoupled (removed) data. ....	9
<a href="#">Figure 1-7</a> : A cut-out example of a Turkey Point AEM resistivity profile illustrating increasing model layer thicknesses with depth – fine near the top, coarser towards the bottom. The dashed grey line indicates what is known as the ‘Depth of Investigation’. ....	10
<a href="#">Figure 1-8</a> : Example Turkey Point AEM SCI inversion result as a 2D profile, profile 14 in this example. The map on the top right shows the position of the profile in the survey area. The top profile on the left shows the profile position in detail. The next profile presents the inversion data residual. The bottom profile is the SCI resistivity model. The resistivity images are presented to the base of the Biscayne Aquifer as determined by <a href="#">Fish and Stewart (1991)</a> . The color scales are on the right of each profile. All 2D resistivity profiles are included in Appendix 1. ....	12
<a href="#">Figure 1-9</a> : Example of 2D depth slice of SCI inversion results, Layer 12 in this example (depths 19.7 m to 22.9 m). Boreholes with induction logs are indicated by black labeled squares. The resistivity color scale is underneath the image.....	13
<a href="#">Figure 1-10</a> : Map of the data residual from the Spatially Constrained Inversion. ....	14
<a href="#">Figure 1-11</a> : Histogram of the data residual from the Spatially Constrained Inversion (red bars). The green line indicates the cumulative histogram.....	15
<a href="#">Figure 1-12</a> : Comparison of Induction Log for TPGW-1 (red line) with the AEM SCI resistivity model (black line). ....	16
<a href="#">Figure 1-13</a> : Comparison of Induction Log for TPGW-4 (red line) with the AEM SCI resistivity model (black line). ....	16
<a href="#">Figure 1-14</a> : Comparison of Induction Log for TPGW-5 (red line) with the AEM SCI resistivity model (black line). ....	17
<a href="#">Figure 1-15</a> : Comparison of Induction Log for TPGW-7 (red line) with the AEM SCI resistivity model (black line). ....	17

[Figure 1-16](#): Cross-plot of AEM and formation water resistivities. The equation that describes the relationship is at the top of the figure. .... 19

[Figure 1-17](#): Cross-plot of formation water resistivities and chloride concentrations. The equation that describes the relationship is at the bottom of the figure. .... 20

[Figure 1-18](#): Cross-plot of AEM-derived and laboratory sample water resistivity. For reference, the black line represents a 1:1 relationship between the two data sets. .... 21

[Figure 1-19](#): Cross-plot of AEM-derived and laboratory sample chloride concentrations. For reference, the black line represents a 1:1 relationship between the two data sets. .... 22

[Figure 1-20](#): Portion of profile 11 and TPGW-1 illustrating the comparison between AEM-derived chloride concentrations and laboratory-determined chloride concentrations. Gray color indicates the location of logged boreholes with the screened intervals colored using the same color scale as the AEM-derived chloride concentrations. TPGW-1 was greater than 200 m from the profile. The bottom of the Biscayne Aquifer is from [Fish and Stewart \(1991\)](#). .... 23

[Figure 1-21](#): Portion of profile 40 and TPGW-2 illustrating the comparison between AEM-derived chloride concentrations and laboratory-determined chloride concentrations. Gray color indicates the location of logged boreholes with the screened intervals colored using the same color scale as the AEM-derived chloride concentrations. TPGW-2 was greater than 200 m from the profile. The bottom of the Biscayne Aquifer is from [Fish and Stewart \(1991\)](#). .... 24

[Figure 1-22](#): Portion of profile 46 and TPGW-4 illustrating the comparison between AEM-derived chloride concentrations and laboratory-determined chloride concentrations. Gray color indicates the location of logged boreholes with the screened intervals colored using the same color scale as the AEM-derived chloride concentrations. TPGW-4 was greater than 200 m from the profile. The bottom of the Biscayne Aquifer is from [Fish and Stewart \(1991\)](#). .... 25

[Figure 1-23](#): Portion of profile 18 and TPGW-5 illustrating the comparison between AEM-derived chloride concentrations and laboratory-determined chloride concentrations. Gray color indicates the location of logged boreholes with the screened intervals colored using the same color scale as the AEM-derived chloride concentrations. TPGW-5 was within 200 m of the profile. The bottom of the Biscayne Aquifer is from [Fish and Stewart \(1991\)](#). .... 26

[Figure 1-24](#): Portion of profile 12 and TPGW-7 illustrating the comparison between AEM-derived chloride concentrations and laboratory-determined chloride concentrations. Gray color indicates the location of logged boreholes with the screened intervals colored using the same color scale as the AEM-derived chloride concentrations. TPGW-7 was within 200 m of the profile. The bottom of the Biscayne Aquifer is from [Fish and Stewart \(1991\)](#). .... 27

[Figure 1-25](#): Portion of profile 24 and TPGW-8 illustrating the comparison between AEM-derived chloride concentrations and laboratory-determined chloride concentrations. Gray color indicates the location of logged boreholes with the screened intervals colored using the same color scale as the AEM-derived chloride concentrations. TPGW-8 was greater than 200 m from the profile. The bottom of the Biscayne Aquifer is from [Fish and Stewart \(1991\)](#). .... 28



[Figure 1-26](#): Portion of profile 4 and TPGW-12 illustrating the comparison between AEM-derived chloride concentrations and laboratory-determined chloride concentrations. Gray color indicates the location of logged boreholes with the screened intervals colored using the same color scale as the AEM-derived chloride concentrations. TPGW-12 was greater than 200 m from the profile. The bottom of the Biscayne Aquifer is from [Fish and Stewart \(1991\)](#)..... 29

[Figure 1-27](#): Example view of Turkey Point AEM chloride concentrations greater than 19,000 mg/L as a 3D voxel. The view is to the northeast. All 3D chloride concentration voxel views are included in Appendix 3A. .... 31

[Figure 1-28](#): Example of 2D depth slice from the voxel of AEM-derived chloride concentrations, Layer 12 in this example (depths 19.7 m to 22.9 m). Boreholes with induction logs are indicated by black labeled squares. All 2D chloride concentration depth slices are in Appendix 2. Note that the color scale is different from that in [Figure 1-27](#) in order to show more variation in the range from 19,000 mg/L to 40,000 mg/L. .... 32

[Figure 1-29](#): Cross-plot of the AEM model resistivity and the September 2015 laboratory measurements of water resistivity (black dots). The black line is the fit determined for the conversion of AEM resistivity to water resistivity. For reference, the [Fitterman and Prinos \(2011\)](#) calibration equation for conversion of formation resistivity to water resistivity is shown as a blue line. Formulas for the lines are at the bottom of the figure. .... 33

[Figure 1-30](#): Cross-plot of the September 2015 laboratory measurements of water resistivity and the September 2015 laboratory measurements of chloride concentration (black dots). The black line is the fit determined for the conversion of September 2015 water resistivity to chloride concentration. For reference, the [Fitterman and Prinos \(2011\)](#) calibration relation for conversion of water resistivity to chloride concentration is shown as a blue line. Formulas for the lines are provided at the bottom of the figure. .... 34

[Figure 1-31](#): Cross-plot of the application of [Fitterman and Prinos \(2011\)](#) calibration and AEM 2016 derived calibration for water resistivity. For reference, the black line represents a 1:1 relationship between the two data sets. .... 35

[Figure 1-32](#): Cross-plot of the application of [Fitterman and Prinos \(2011\)](#) calibration and AEM 2016 derived calibration for chloride concentrations. For reference, the black line represents a 1:1 relationship between the two data sets. .... 36

**List of Tables**

[Table 1-1](#): Thickness and depth to bottom for each layer in the SCI inverted AEM models. The thickness of the model layers increase with depth as the resolution of the AEM technique decreases..... 10

[Table 1-2](#): Induction Logs used to verify the AEM Models ..... 12

[Table 1-3](#): Water Quality Data Used for Calibration (September 2015 Laboratory Measurements)..... 18

[Table 1-4](#): Resistivity Model Layers and Final Voxel Grid Nodes ..... 30

[Table 2-1](#): Channel name, description, and units for *TurkeyPt\_AEM\_Resistivity\_Model\_v1.csv* with the AEM inversion results. Resistivity data are presented down to the base of the Biscayne Aquifer as determined by [Fish and Stewart \(1991\)](#). ..... 39

[Table 2-2](#): Column description for the voxel grid file *TurkeyPt\_Voxel\_Chloride\_Concentrations\_Volume\_Mass\_v1.csv*. Chloride concentrations are presented down to the base of the Biscayne Aquifer as determined by [Fish and Stewart \(1991\)](#). ..... 40

[Table 2-3](#): Channel name, description, and units for *TurkeyPt\_Data\_Chloride\_Concentration\_v1.csv* with X and Y locations, Elevation, and Chloride Concentrations presented down to the base of the Biscayne Aquifer as determined by [Fish and Stewart \(1991\)](#). ..... 40

## List of Abbreviations

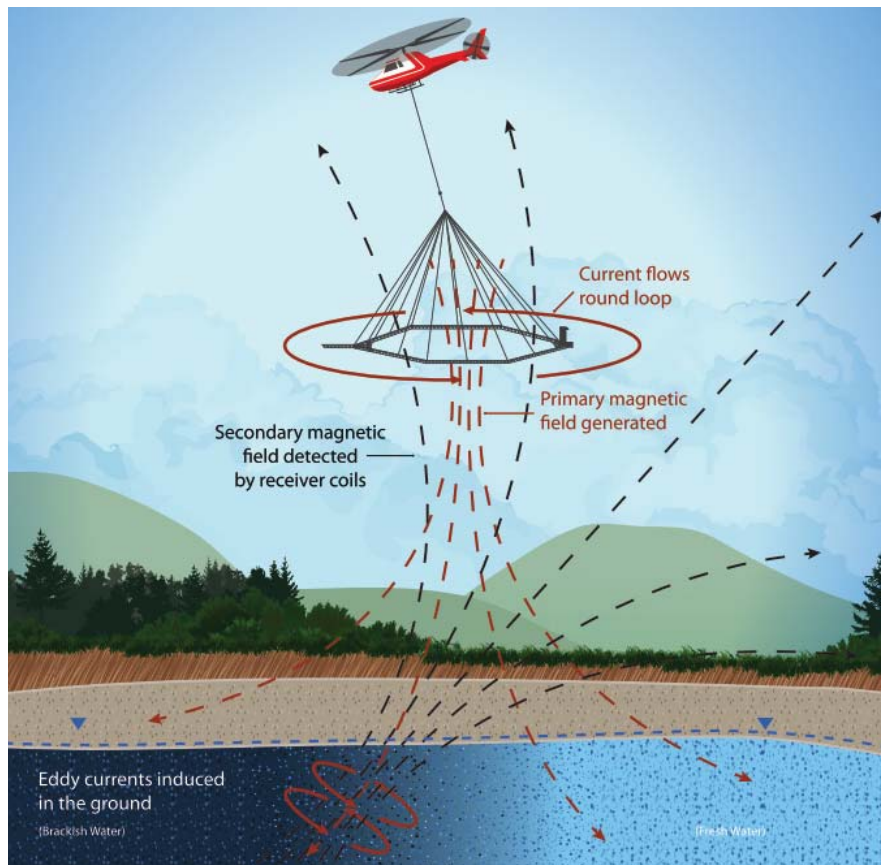
2D	Two-dimensional
3D	Three-dimensional
AEM	Airborne Electromagnetic
AGF	Aqua Geo Frameworks LLC.
B	Magnetic Field
dB/dt	Change in amplitude of magnetic field with time
CHI	Coupled Hydrogeophysical Inversion Approach
cm	Centimeters
em, EM	Electromagnetic
HEM	Helicopter Electromagnetic
m	Meters
mg/L	Milligrams per liter equal to ppm
MSDOS	Microsoft Disk Operating System
μS/cm	Micro Siemens per centimeter
NAD83	North American Datum of 1983
Ohm-m	Ohm meter
PLNI	Power Line Noise Intensity
ppm	parts per million equal to milligrams per liter (mg/L)
PSU	Practical Salinity Units
R <sup>2</sup>	Coefficient of Determination
Rx	Receiver
SCI	Spatially-Constrained Inversion
STD	Standard Deviation
TEM	Transient Electromagnetic
TDS	Total Dissolved Solids
TPGW	Turkey Point Groundwater Well
Tx	Transmitter
USGS	United States Geological Survey
UTM	Universal Transverse Mercator

## 1 Geophysical Methodology

### 1.1 AEM Methodology, Acquisition, and Inversion

#### 1.1.1 AEM Methodology

AEM (Airborne Electromagnetic (AEM)) investigations provide characterization of electrical properties of earth materials from the land surface downward using electromagnetic induction. [Figure 1-1](#) gives a conceptual illustration of the airborne Transient Electromagnetic (TEM) method.

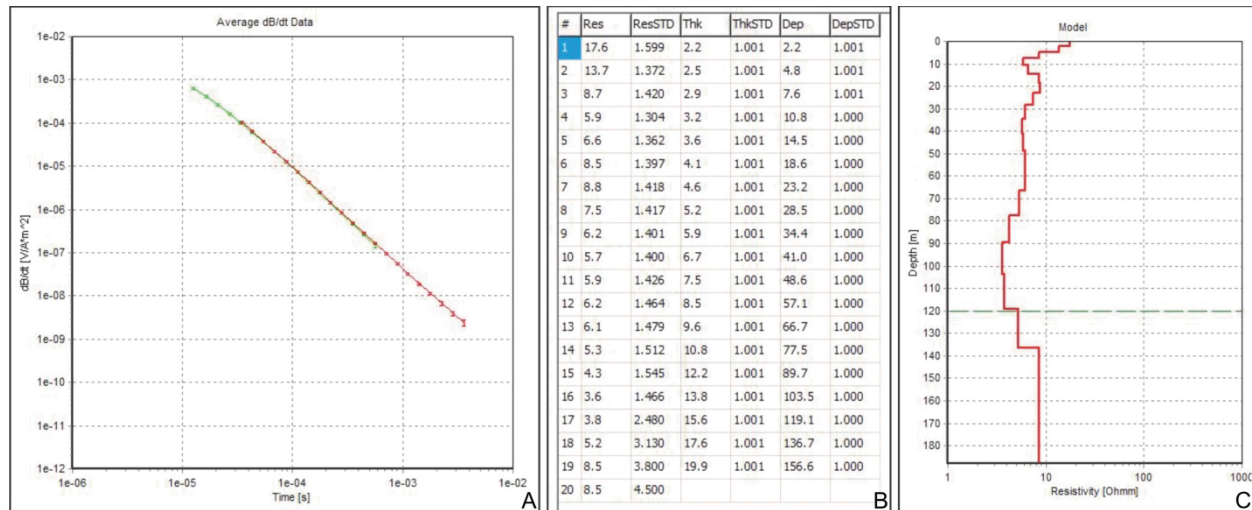


**Figure 1-1: Schematic of an AEM survey.**

To collect TEM data, an electrical current is sent through a large loop of wire consisting of multiple turns which generates an electromagnetic (EM) field. This is called the transmitter (Tx) coil. After the EM field produced by the Tx coil is stable, it is switched off as abruptly as possible. The EM field dissipates and decays with time, traveling deeper and spreading wider into the subsurface. The rate of dissipation is dependent on the electrical properties of the subsurface (controlled by the material composition of the geology including the amount of mineralogical clay, the water content, the presence of dissolved solids, the metallic mineralization, and the percentage of void space). At the moment of turnoff, a secondary EM field, which also begins to decay, is generated within the subsurface. The decaying secondary EM field generates a current in a receiver (Rx) coil, per Ampere's Law. This current is measured at several different moments in time (each moment being within a time band called a "time gate"). From the

induced current, the time rate of decay of the magnetic field,  $B$ , is determined ( $dB/dt$ ). When compiled in time, these measurements constitute a “sounding” at that location. Each AEM measurement produces an EM sounding at one point on the surface.

The sounding curves are numerically inverted to produce a model of subsurface resistivity as a function of depth. Inversion relates the measured geophysical data to probable physical earth properties. [Figure 1-2](#) shows an example of a dual-moment TEM  $dB/dt$  sounding curve and the corresponding inverted electrical resistivity model.



**Figure 1-2: A) Example of a  $dB/dt$  sounding curve. B) Corresponding inverted model values. C) Corresponding resistivity earth model.**

### 1.1.2 AEM Acquisition

AEM data were acquired using the SkyTEM 304M (304) airborne electromagnetic system ([SkyTem Airborne Surveys Worldwide, 2015](#)). The 304 is a rigid frame, dual-magnetic moment (Low and High) transient airborne electromagnetic (TEM) system. The area of the 304 Tx coil is 340.8 m<sup>2</sup> and the coil contains four (4) turns of wire. A peak current of 9 amps is passed through one turn of wire in the Tx for Low Moment measurements and a peak current of 112 amps is passed through the four turns of wire for High Moment measurements. This results in peak Tx Low and High magnetic moments of ~3,000 Ampere-meter-squared (A\*m<sup>2</sup>) and ~150,000 A\*m<sup>2</sup>, respectively.

All SkyTEM systems are calibrated to a ground test site in Lyngby, Denmark prior to being used for production work ([HydroGeophysics Group Aarhus University, 2010](#); [HydroGeophysics Group Aarhus University, 2011](#); [Foged et al., 2013](#)). The calibration process involves acquiring data with the system hovering at different altitudes, from 5 m to 50 m, over the Lyngby site. Acquired data are processed and a scale factor (time and amplitude) is applied so that the inversion process produces the model that approximates the known geology at Lyngby. Details on the calibration can be found in [SkyTEM \(2016\)](#).

Calibration test flights were flown to ensure that the equipment was operating within technical specifications. Survey set-up procedures included measurement of the transmitter waveforms,

verification that the receiver was properly located in a null position, and verification that all positioning instruments were functioning properly. A high altitude test, used to verify system performance, was flown prior to the beginning of the survey's production flights. In the field, visual quality control of the operational parameters for the EM and magnetic field sensors including current levels, positioning sensor dropouts, acquisition speed, and system orientation were conducted with proprietary SkyTEM software following each flight.

Approximately 274 line-miles (444 line-kilometers) of AEM data were acquired over the Turkey Point power plant project area on January 25-27, 2016. The flight planning for these data were carried out by SkyTEM Canada and ENERCON.

### *1.1.3 Primary Field Compensation*

A standard SkyTEM data acquisition procedure involves review of acquired raw data by SkyTEM in Denmark for Primary Field Compensation (PFC) prior to continued data processing by AGF ([Schamper et al., 2014](#)). The primary field of the transmitter affects the recorded early time gates, which in the case of the Low Moment, are helpful in resolving the near surface resistivity structure of the ground. The Low Moment uses a saw tooth waveform which is calculated and then used in the PFC correction to correct the early time gates.

### *1.1.4 Automatic Processing*

The AEM data collected by the 304 were processed using Aarhus Workbench version 5.0.1.0 ([HydroGeophysics Group Aarhus University, 2011](#)).

Automatic processing algorithms provided within the Workbench program are initially applied to the AEM data. GPS locations were filtered using a stepwise, second-order polynomial filter of 5 seconds with a beat time of 0.5 seconds, based on flight acquisition parameters. The AEM data are corrected for tilt deviations from level and so filters were also applied to both of the tilt meter readings with a median filter of 3 seconds and an average filter of 2 seconds. The altitude data were corrected using a series of two polynomial filters. The lengths of both eighth-order polynomial filters were set to 20 seconds with shift lengths of 6 seconds. The lower and upper thresholds were 1 and 100 meters, respectively.

Trapezoidal spatial averaging filters were next applied to the AEM data. The times used to define the trapezoidal filters for the Low Moment were  $1.0 \times 10^{-6}$  sec,  $1.0 \times 10^{-4}$  sec, and  $1.0 \times 10^{-3}$  sec with widths of 2, 5 and 10 seconds. The times used to define the trapezoid for the High Moment were  $1.0 \times 10^{-4}$  sec,  $1.0 \times 10^{-3}$  sec, and  $1.0 \times 10^{-2}$  sec with widths of 5, 10, and 20 seconds. The trapezoid sounding distance was set to 2 seconds and the left/right setting, which requires the trapezoid to be complete on both sides, was turned on. The spike factor and minimum number of gates were both set to 25 percent for both soundings. Lastly, the locations of the averaged soundings were synchronized between the High and Low moments.



### *1.1.5 Manual Processing and Laterally-Constrained Inversions*

After the implementation of the automatic filtering, the AEM data were manually examined using a sliding two-minute time window. The data were examined for possible electromagnetic coupling with surface and buried utilities and metal, as well as for late time-gate noise. Data affected by these were removed. It was determined that the 8<sup>th</sup> time-gate data ( $7.27 \times 10^{-05}$  sec) of the high moment data were precluding adequate data fit, most likely due to it being too close to the “on-time” of the transmitter and looks to be impacted by the Tx turn off ramp. All data from this gate were removed prior to inversion.

### *1.1.6 Power Line Noise Intensity (PLNI)*

The PLNI channel assists in identifying possible sources of noise from power lines. The PLNI is produced by performing a spectral frequency content analysis on the raw received Z-component SkyTEM data. For every Low Moment data block, a Fast Fourier Transform (FFT) is performed on the latest usable time gate data. The FFT is evaluated at the local power line transmission frequency (60 Hz) yielding the amplitude spectral density of the local power line noise. The PLNI data for the Turkey Point project area are presented in [Figure 1-3](#). Pipelines, unless they are cathodically-protected, are not mapped by the PLNI.

### *1.1.7 Total Magnetic Field and Analytic Signal Data*

As discussed above, the SkyTEM 304M includes a Total Field magnetometer. The magnetic field data can yield information about infrastructure as well as geology. [Figure 1-4](#) shows the magnetic Total Field data for the Turkey Point AEM survey area after correcting for diurnal drift and removing the International Geomagnetic Reference Field (IGRF) and [Figure 1-5](#) shows what is known as the Magnetic Field Analytic Signal. The magnetic Analytic Signal data highlights magnetic field sources. These data are used in decoupling efforts.

### *1.1.8 In-Field Quality Control*

As part of the in-field Quality Control program, the AEM data from each day's flight were inverted using a Laterally-Constrained Inversion (LCI) algorithm ([HydroGeophysics Group Aarhus University, 2011](#)). The profile and depth slices were examined, and any remaining electromagnetic couplings were masked out of the data set. Once data acquisition was complete, additional processing was performed on all the acquired data, with more time allocated to data analysis. The result was that a large amount of data were removed in the northwest area of the survey due to above- and below-ground pipelines and power lines.

After final processing, 209 line-miles (338 line-km) of data were retained for the final SCI inversions for the Turkey Point area, a reduction by 106 line-km from the acquired data set. This amounts to a data retention of 76.2% for the Turkey Point area. [Figure 1-6](#) shows the Turkey Point AEM data within the AOI that were decoupled or processed out of the data set with red colors representing data retained for inversion and blue lines data removed due to infrastructure and late time noise.

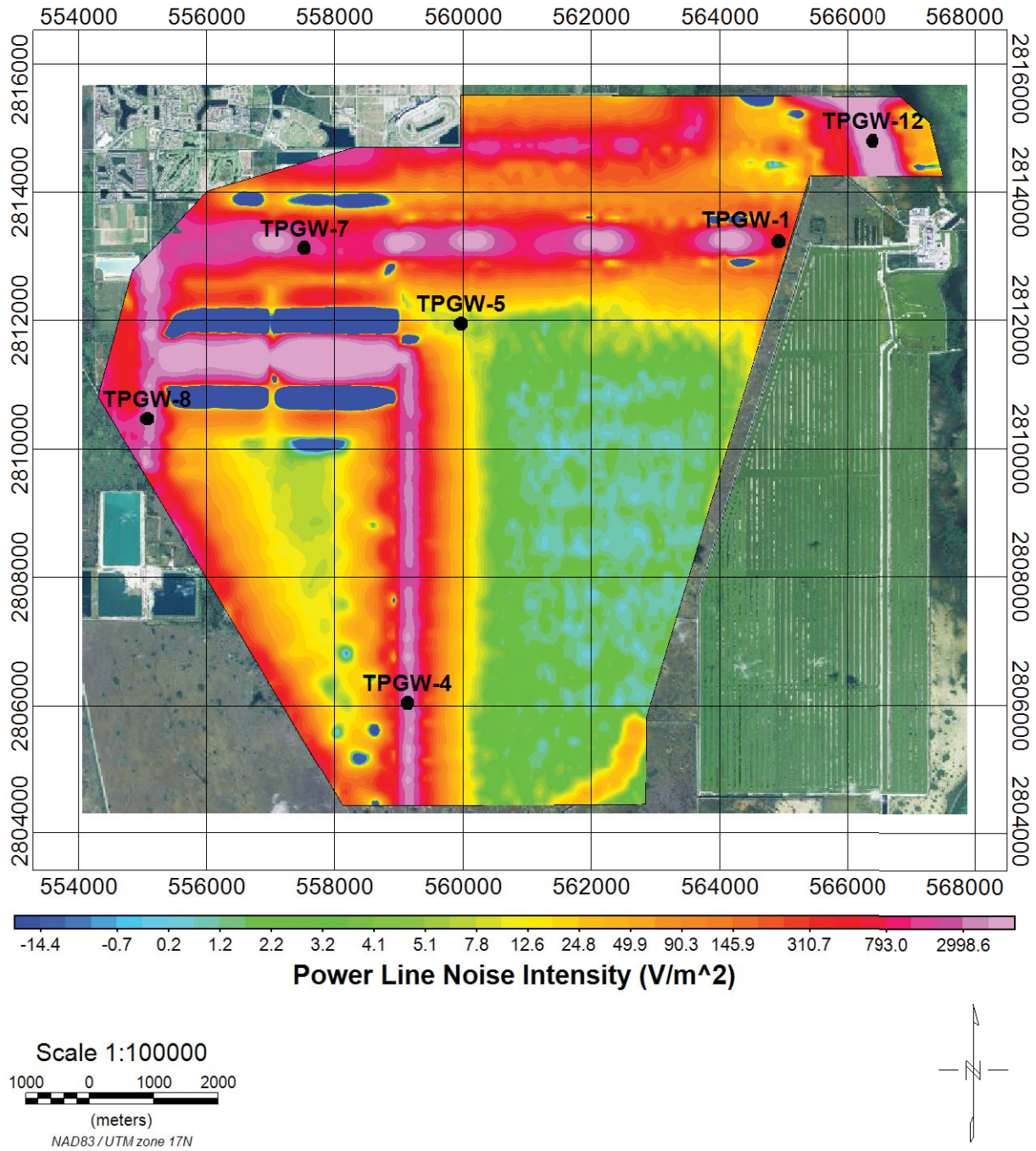
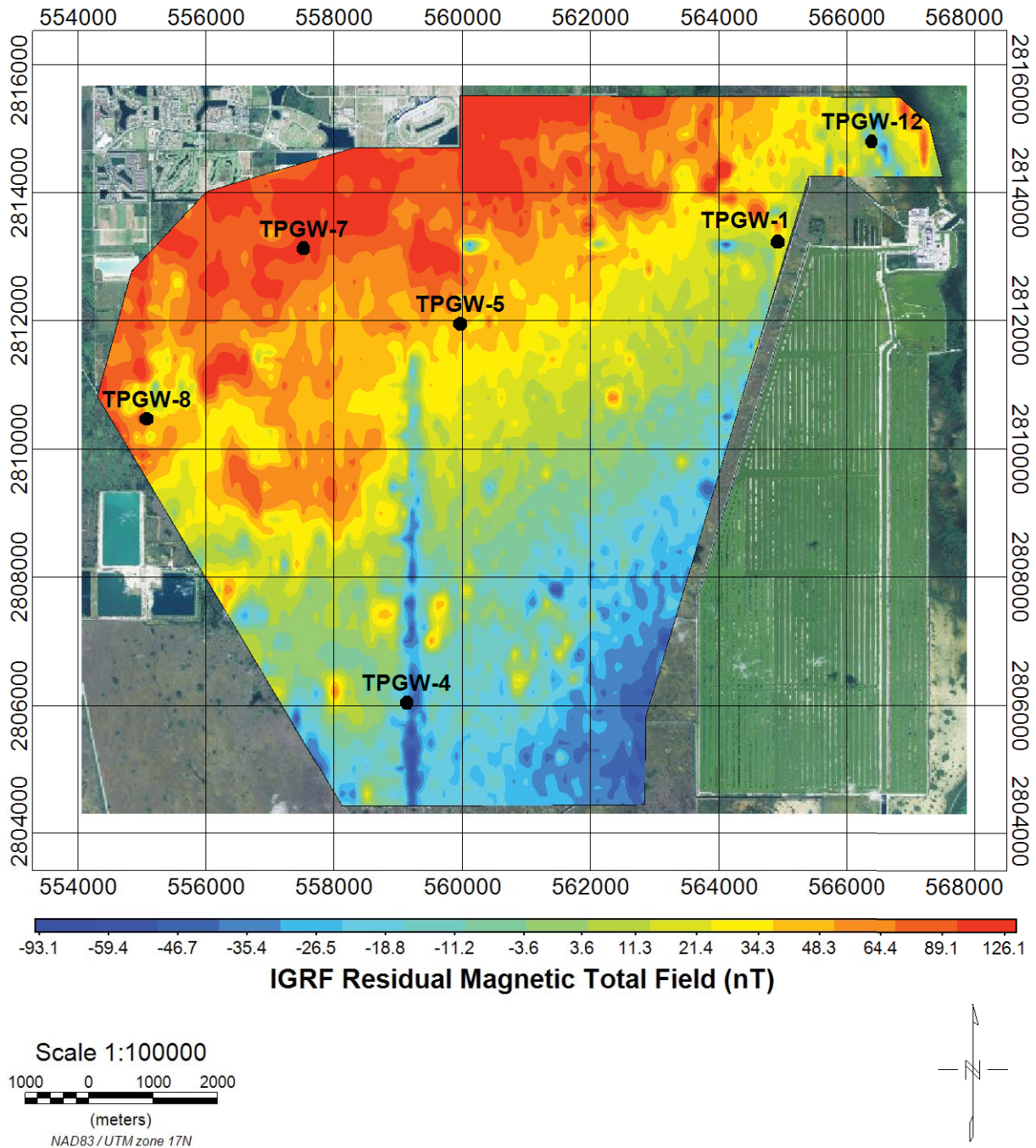
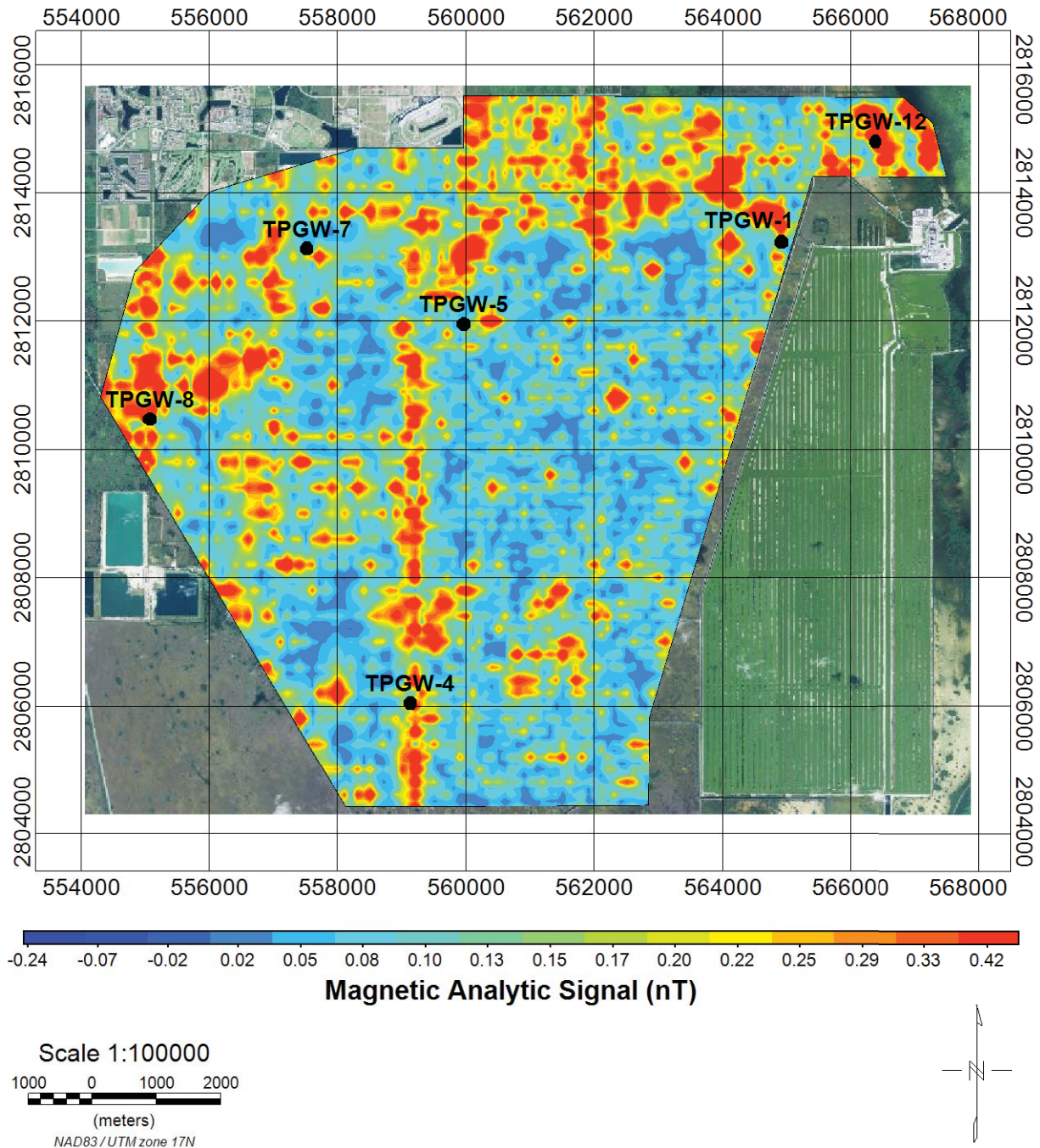


Figure 1-3: Power Line Noise Intensity (PLNI) map of the Turkey Point AEM project area.



**Figure 1-4: Magnetic Total Field data for the Turkey Point AEM survey area corrected for diurnal drift, with the IGRF removed.**





**Figure 1-5: Magnetic Field Analytic Signal plot for the Turkey Point AEM survey area. The Analytic Signal is sensitive to electromagnetic as well as purely magnetic sources.**

### *1.1.9 Spatially-Constrained Inversion*

Following the initial decoupling and LCI analyses, Spatially-Constrained Inversions (SCI) were performed. SCIs use EM data along, and across, flight lines within user-specified distance criteria ([Viezzoli et al., 2008](#)).

The Turkey Point survey data were inverted using SCI smooth models with 30 layers, each with a starting resistivity of 10 ohm-m (equivalent to a 10 ohm-m halfspace). The thicknesses of the first layers of the models were 1 m with the thicknesses of the consecutive layers increasing by a factor of 1.1. The depths to the bottoms of the 30<sup>th</sup> layers were set to 201 m, with thicknesses up to about 21 m. The thicknesses of the layers increase with depth ([Table 1-1](#) and [Figure 1-7](#)) as the resolution of the technique decreases. The spatial reference distance,  $s$ , for the constraints were set to 100 m with power laws of 0.5. The vertical and lateral constraints, ResVerSTD and ResLatStD, were set to 2.0 for all layers.

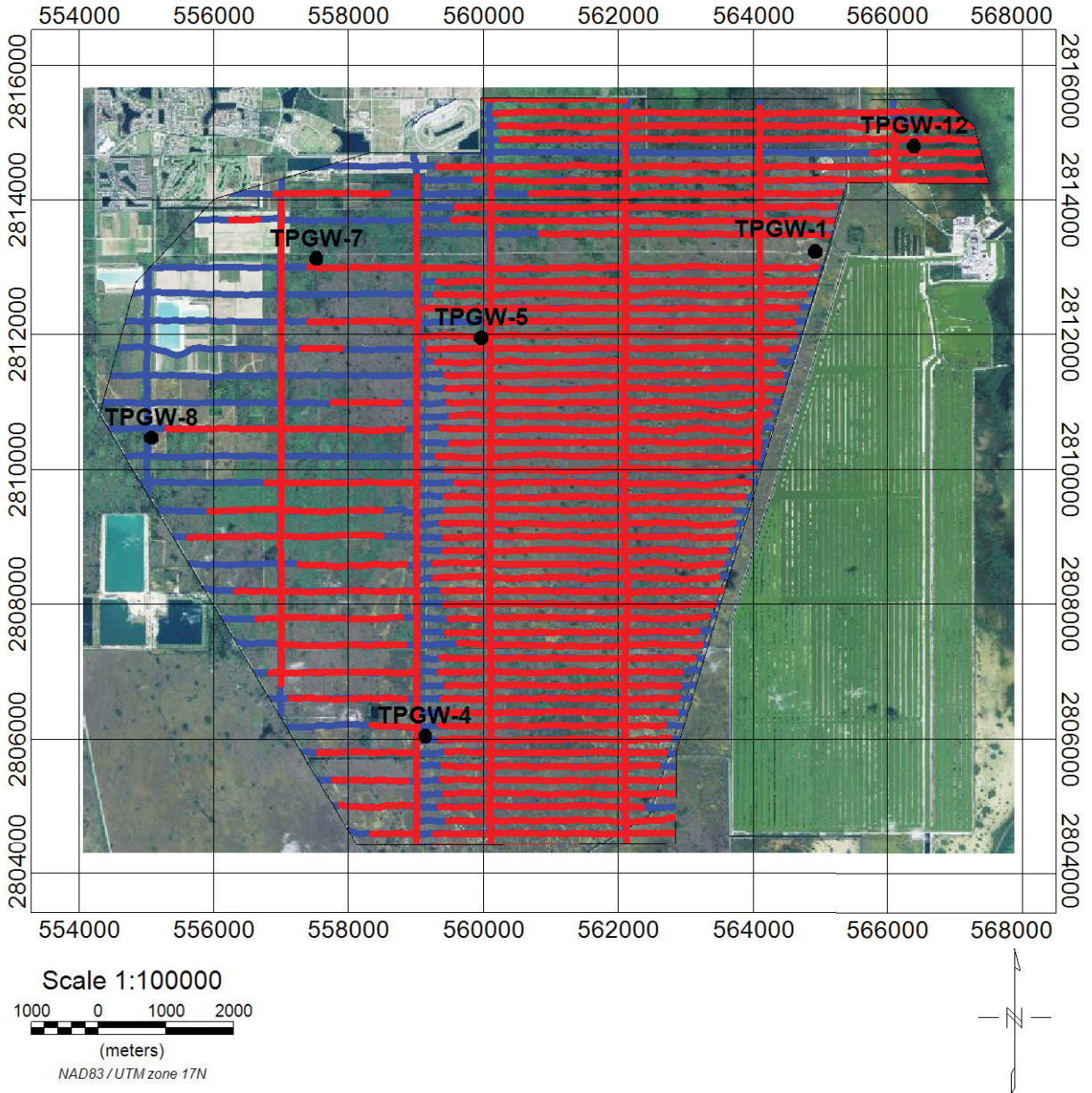
In addition to the recovered resistivity models, the SCI's also produce data residual values (single sounding error residuals), total residual values (total model residual error values), and Depth of Investigation (DOI) estimates. The data residuals compare the measured data with the response of the individual inverted models. The total residual is a weighted average of the data residual and the model residual ([Christensen et al., 2009](#); [SkyTEM Airborne Surveys Worldwide, 2012](#)). The DOI provides a general estimate of the depth to which the AEM data are sensitive to changes in the resistivity distribution at depth ([Christiansen and Auken, 2012](#)). These data are included in the data deliverables described below in Section 2.0.

An example of a full SCI inversion is presented in [Figure 1-8](#). The inset map on the top right of the figure shows the position of the profile within the survey area. The top profile on the left shows the profile position on a detailed map. The next two profiles present the system flight altitude during acquisition and the SCI individual data residuals. The bottom profile is the SCI resistivity earth model. The dashed grey line is a representation of the depth of investigation. The color scales are on the right of each profile.

An example of a 2D map of a depth slice of the SCI earth resistivity model is presented in [Figure 1-9](#).

Note that the data are presented down to the base of the Biscayne Aquifer as determined by [Fish and Stewart \(1991\)](#).

All the 2D resistivity profile representations of the SCI results ([Figure 1-8](#)) are presented in Appendix 1.

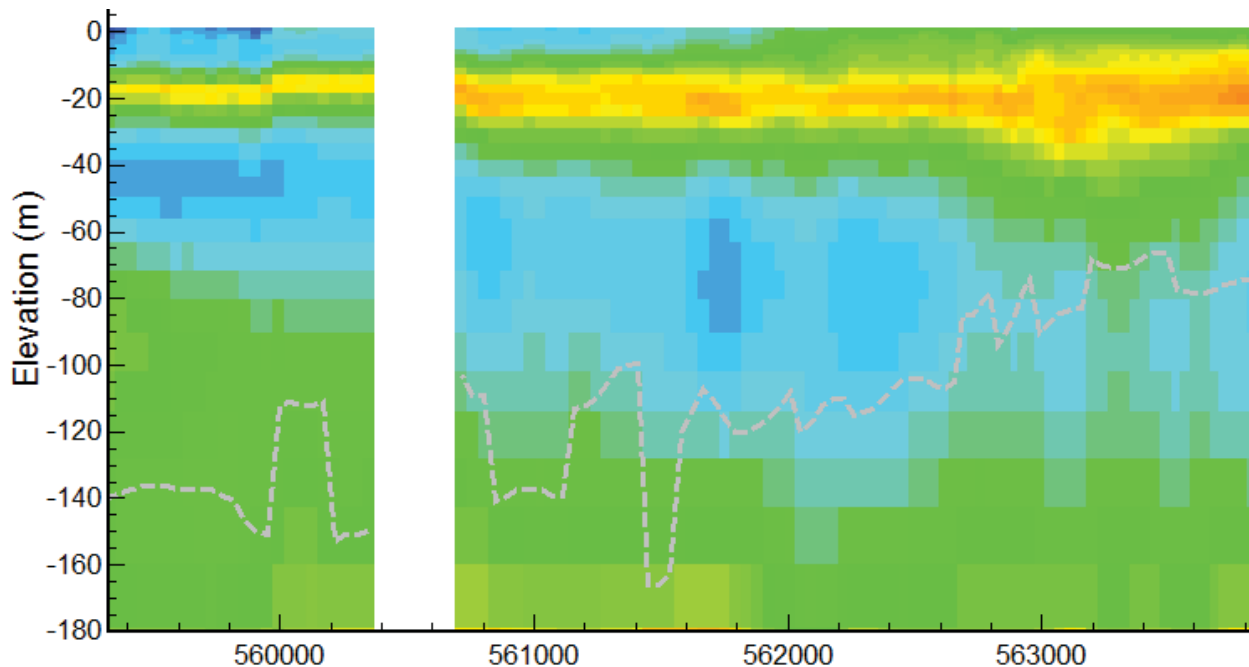


**Figure 1-6: Locations of the decoupled and removed data (blue lines) along the AEM flight lines of the data used in the inversion (red lines) in the Turkey Point project area. Where blue lines are present indicates decoupled (removed) data.**



**Table 1-1: Thickness and depth to bottom for each layer in the SCI inverted AEM models. The thickness of the model layers increase with depth as the resolution of the AEM technique decreases.**

Layer	Depth to Bottom	Thickness	Layer	Depth to Bottom	Thickness
1	1.0	1	16	39.4	4.8
2	2.1	1.1	17	44.7	5.3
3	3.3	1.2	18	50.6	5.9
4	4.7	1.4	19	57.2	6.6
5	6.2	1.5	20	64.5	7.3
6	7.9	1.7	21	72.6	8.1
7	9.8	1.9	22	81.6	9.0
8	11.9	2.1	23	91.6	10.0
9	14.2	2.3	24	103.0	11.1
10	16.8	2.6	25	115.0	12.4
11	19.7	2.9	26	129.0	13.7
12	22.9	3.2	27	144.0	15.3
13	26.4	3.5	28	161.0	16.9
14	30.3	3.9	29	180.0	18.8
15	34.6	4.3	30	201.0	20.7



**Figure 1-7: A cut-out example of a Turkey Point AEM resistivity profile illustrating increasing model layer thicknesses with depth – fine near the top, coarser towards the bottom. The dashed grey line indicates what is known as the 'Depth of Investigation'. The white area represents data that has been cut out during the decoupling process.**

## 1.2 Resistivity Model Verification and Acceptance

One of the key items in 'accepting' the data (i.e. accepting the quality of the data) and verifying the resistivity model is the inspection of the data residuals from the inversion and the comparison of the resistivity structure in the inversion to borehole induction logs. [Figure 1-10](#) is a plot of the data residual from the final Spatially Constrained Inversion and [Figure 1-11](#) is a histogram of the data residuals from the SCI. The distribution is 'normal' around 0.577 indicating that there are no problems with outliers or other biases. A detailed description of the calculation of the residual within the Aarhus Workbench can be found in [Christensen, Reid, and Halkjaer \(2009\)](#).

The next step in verification is to look at the comparison of the induction logs ([Wacker, 2010](#)) (personal communication Craig Oural, ENERCON February 8, 2016) ([Table 1-2](#)) versus the inverted resistivity values. In looking at the induction logs care needs to be taken to understand that the logs are likely not directly on the flight line and may be impacted by the drilling and well completion process, as is common. Another critical component of the analysis is calibration of the well logs ([Ley-Copper and Davis, 2010](#)) – they are usually not very well, if at all, calibrated. However, even with the inherent limitations of borehole measurements, it is important to evaluate the ability of the AEM to reproduce the earth resistivities. Note that this comparison is also dependent on the calibration of the AEM system.

Comparison between some of the available induction logs listed in [Table 1-2](#) and the inverted resistivity models at locations on profiles closest to the boreholes are presented in [Figure 1-12](#) through [Figure 1-15](#). The examination process is to compare how well the borehole log (the red line) and the AEM inversion model (the black line) compare with each other. The results indicate that the AEM resistivity models are reproducing the resistivity structure of the earth in the vicinity of the Turkey Point power plant as indicated by the induction logs within an acceptable range. There are differences at depth that are likely due to small local variations in the subsurface at the location of the borehole versus the AEM flight line.

It should be noted that a qualitative comparison was also made between the available ground-based TEM soundings and HEM survey ([Fitterman et al. 2012](#); [Fitterman and Prinos 2011](#)) and the AEM earth resistivity models. They also compared quite well.

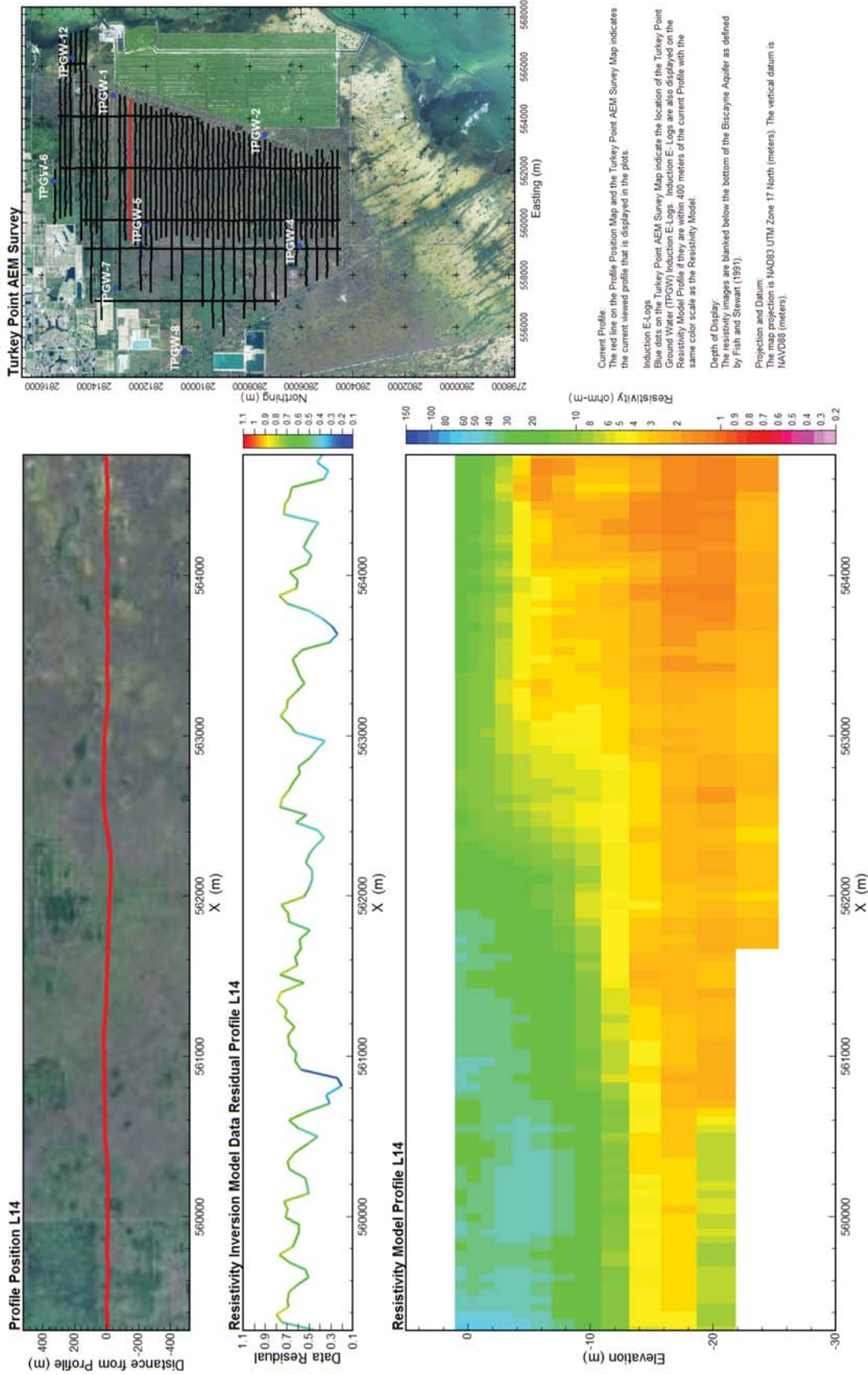


Figure 1-8: Example Turkey Point AEM SCI inversion result as a 2D profile, profile 14 in this example. The map on the top right shows the position of the profile in the survey area. The top profile on the left shows the profile position in detail. The next profile presents the inversion data residual. The bottom profile is the SCI resistivity model. The resistivity images are presented to the base of the Biscayne Aquifer as determined by [Fish and Stewart \(1991\)](#). The color scales are on the right of each profile. All 2D resistivity profiles are included in Appendix 1.

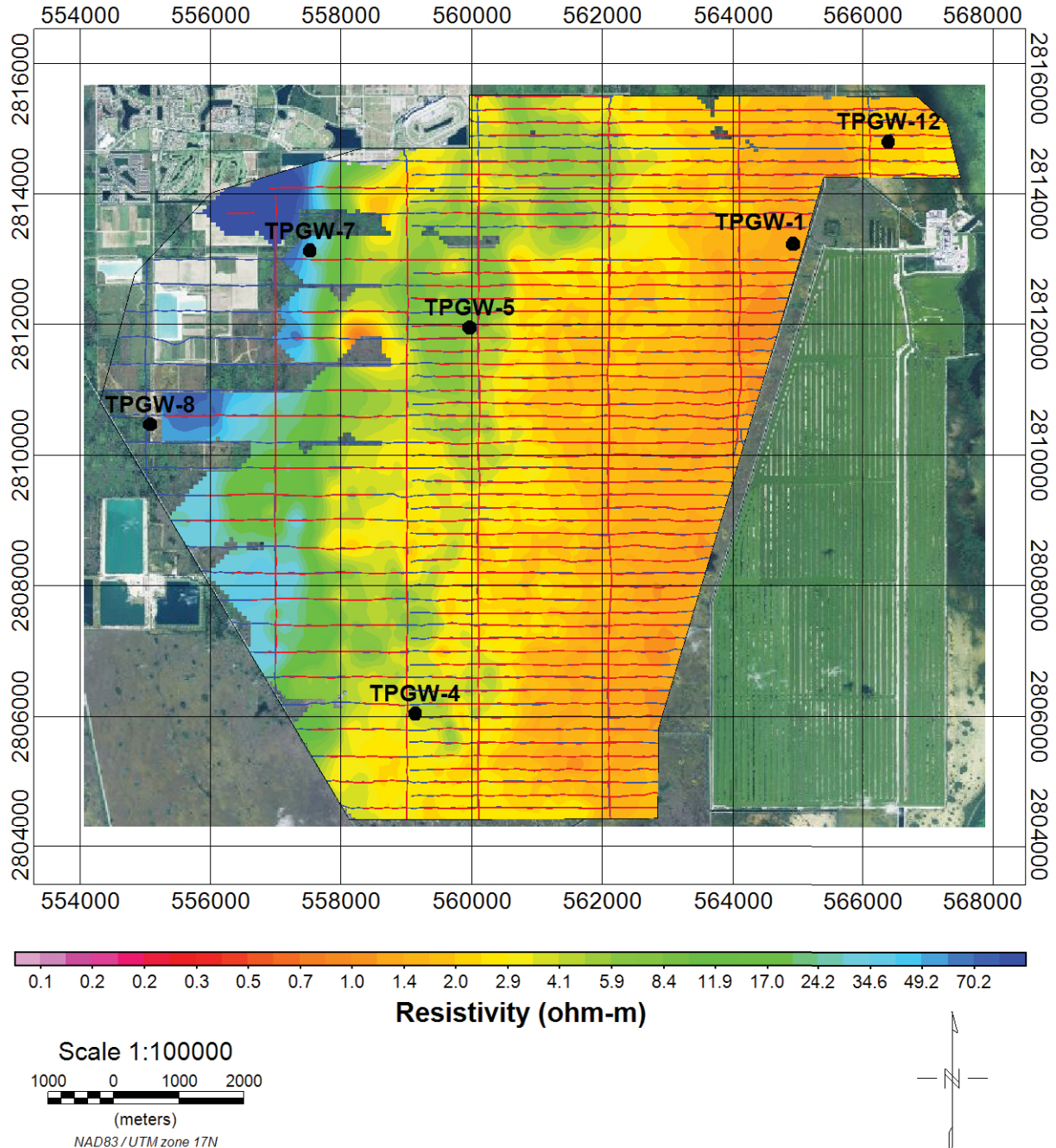


Figure 1-9: Example of 2D depth slice of SCI inversion results, Layer 12 in this example (depths 19.7 m to 22.9 m). Boreholes with induction logs are indicated by black labeled squares. The resistivity color scale is underneath the image.



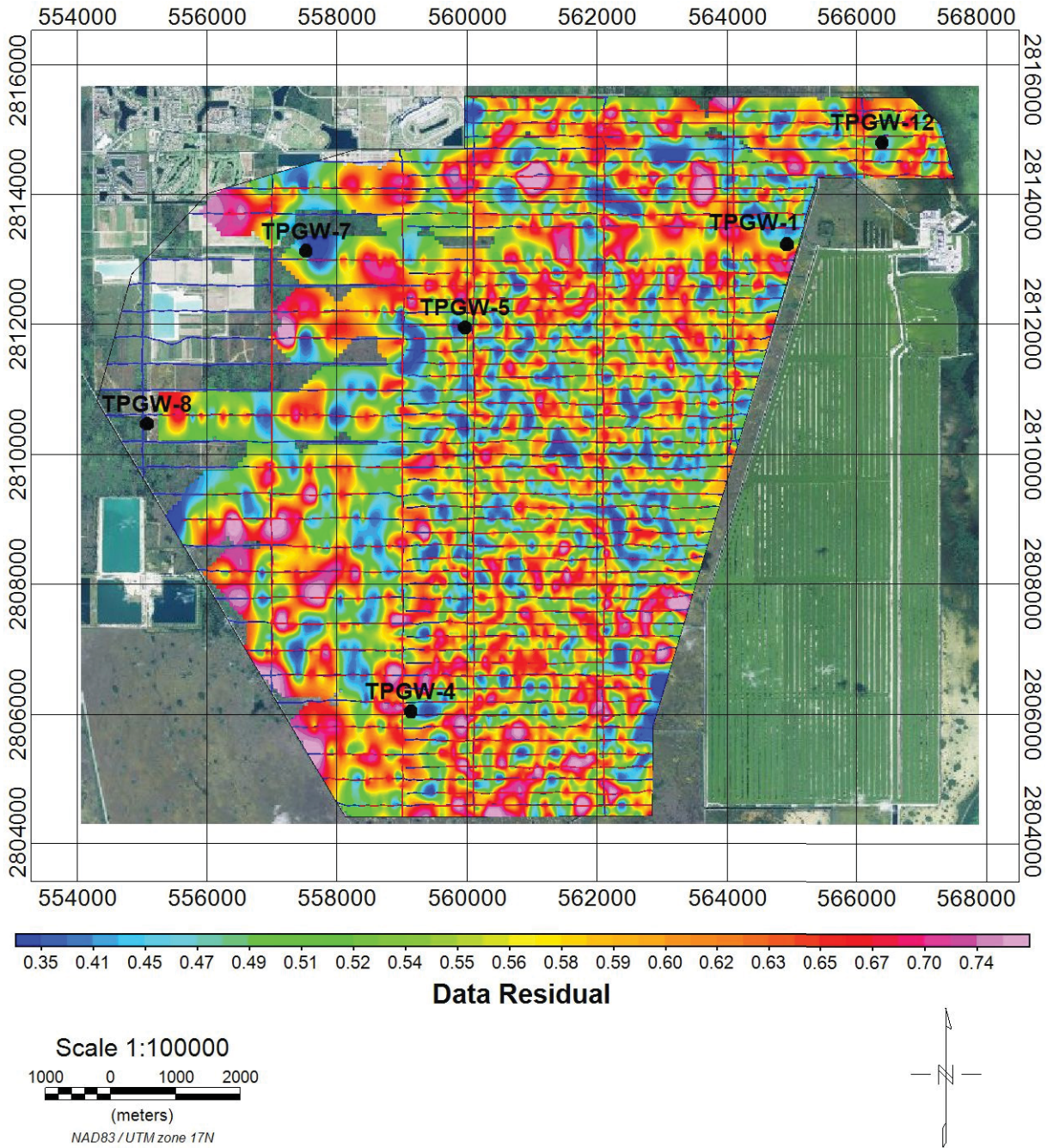


Figure 1-10: Map of the data residual from the Spatially Constrained Inversion.



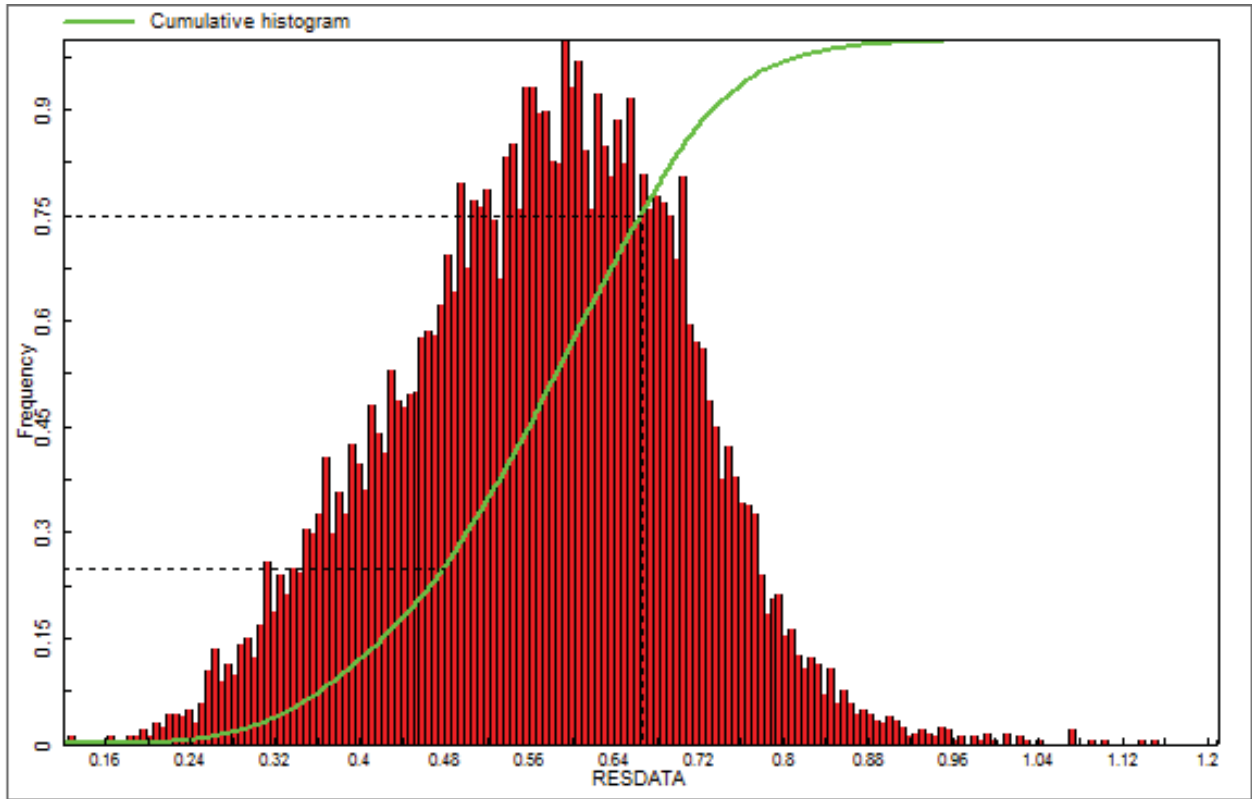


Figure 1-11: Histogram of the data residual from the Spatially Constrained Inversion (red bars). The green line indicates the cumulative histogram.

Table 1-2: Induction Logs used to verify the AEM Models

Well ID	Logging Date	AEM Line	Position of AEM Line in Reference to Well Location
TPGW-1	03-25-2013	101101	Off Line
TPGW-4	03-27-2013	200301	Off Line
TPGW-5	03-26-2013	101701	Within 200 m
TPGW-7	03-26-2013	301201	Within 200 m
TPGW-8	03-26-2013	302401	Off Line
TPGW-12	03-25-2013	100501	Within Line Break due to Coupling

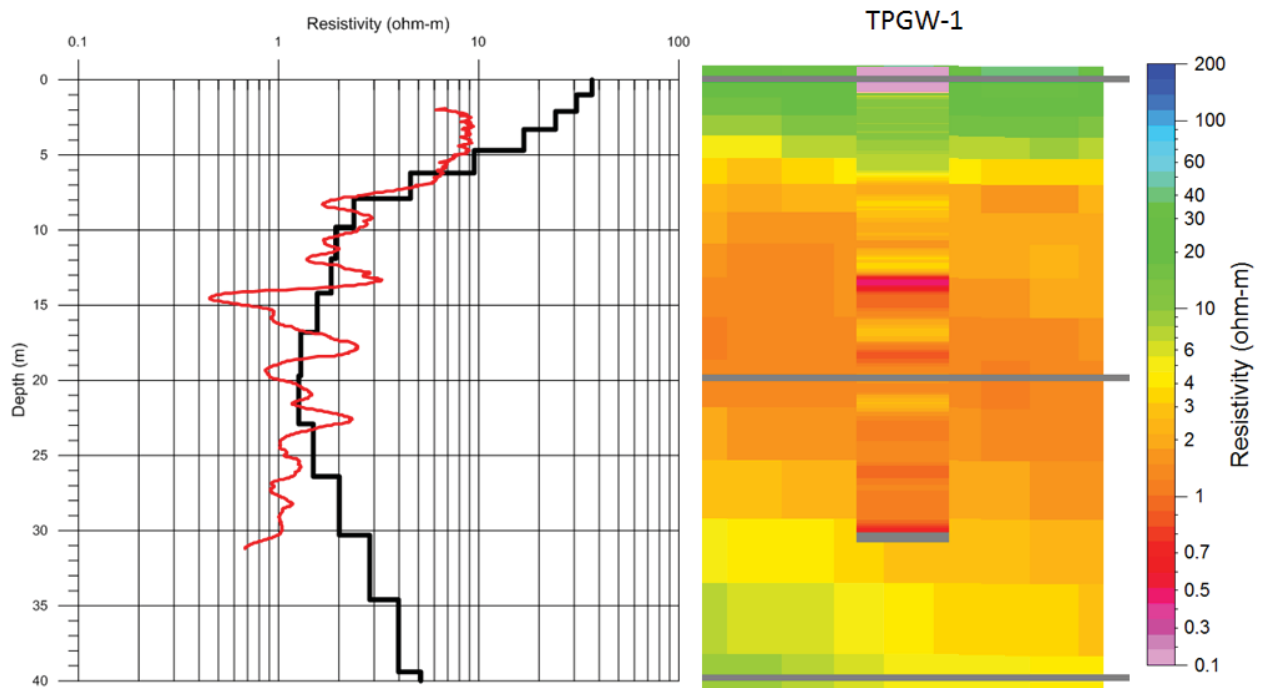


Figure 1-12: Comparison of Induction Log for TPGW-1 (red line) with the AEM SCI resistivity model (black line).

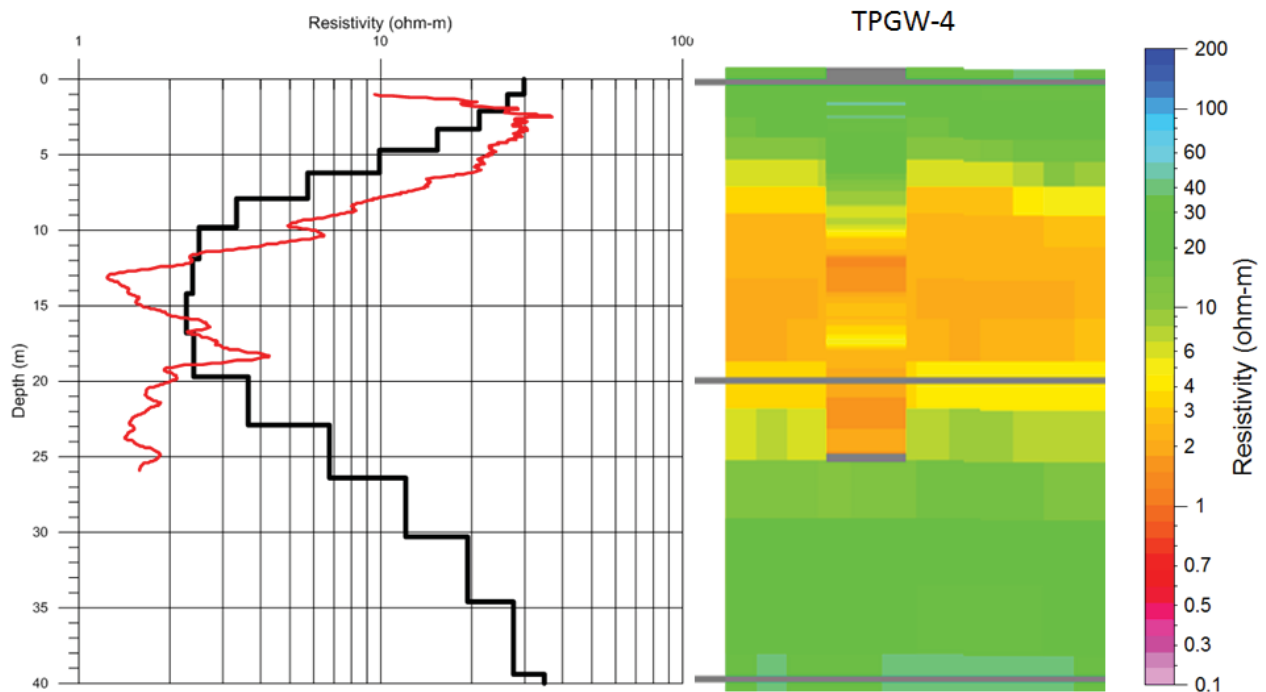


Figure 1-13: Comparison of Induction Log for TPGW-4 (red line) with the AEM SCI resistivity model (black line).

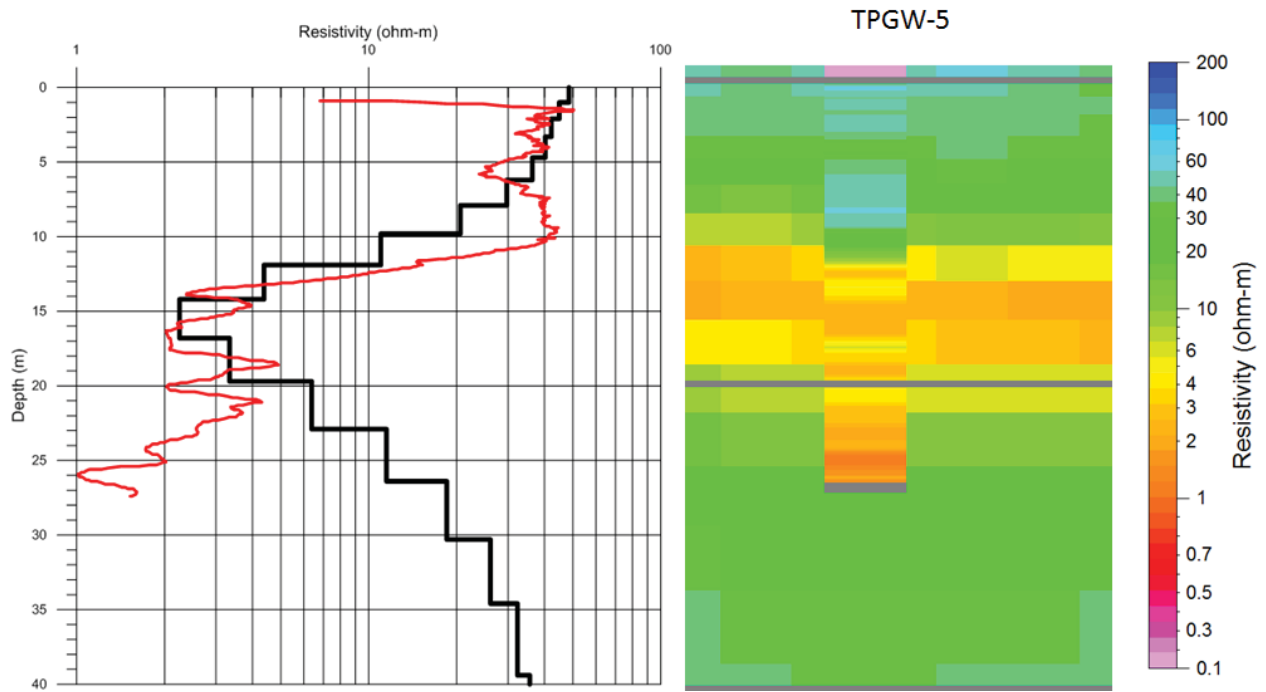


Figure 1-14: Comparison of Induction Log for TPGW-5 (red line) with the AEM SCI resistivity model (black line).

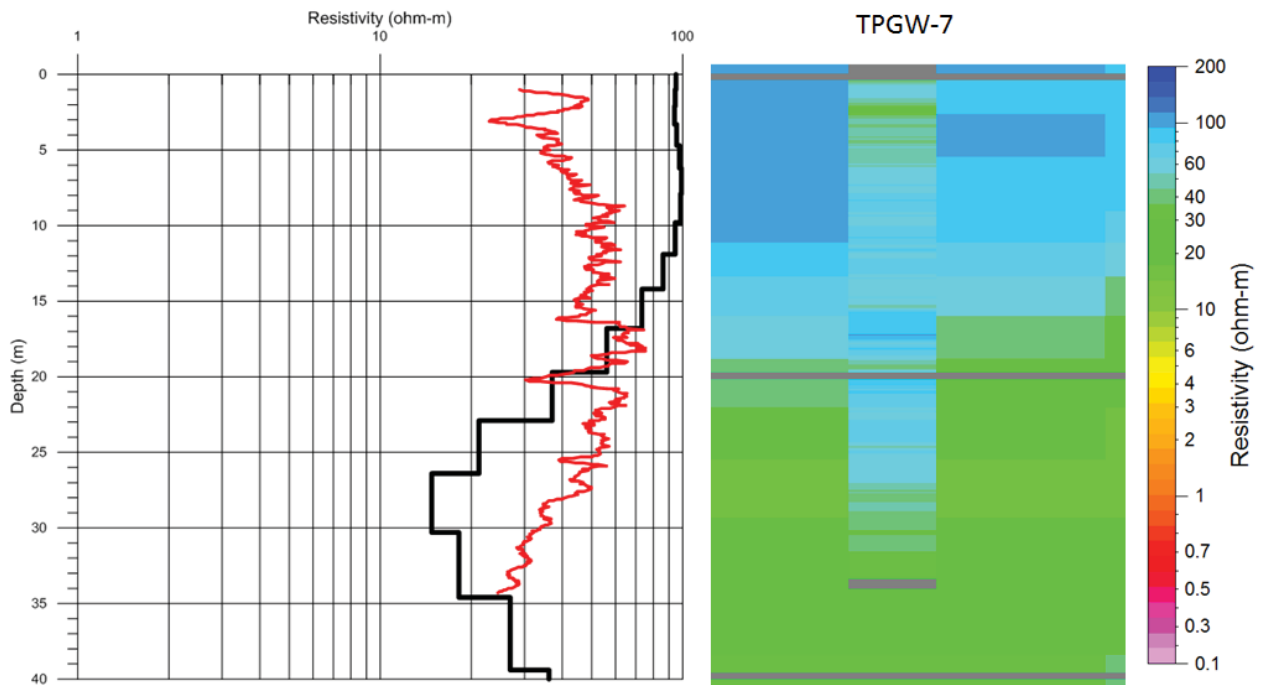


Figure 1-15: Comparison of Induction Log for TPGW-7 (red line) with the AEM SCI resistivity model (black line).

### 1.3 Water Quality Data

Water quality samples from multi-level monitoring wells used by Florida Power and Light to track various parameters over time were used to calibrate the AEM. These samples were analyzed in a laboratory for total dissolved solids (TDS), chloride, sodium, salinity, and several other parameters. Samples taken in September 2015 (personal communication Craig Oural, ENERCON February 24, 2016) from shallow, medium, and deep levels at each well site were used in the calibration of the AEM resistivity models to water conductivity/resistivity and to chloride concentration. [Table 1-3](#) is a list of the parameters that were examined including the specific conductance and the chloride concentrations used in the calibration. Sample analysis for all wells was complete for all parameters and depths. The chloride concentrations levels varied from 31.8 (mg/L) (TPGW-8S) to 28,800 mg/L (TPGW-2D). Information on laboratory methods and analysis, sampling procedures including field parameters, blanks and spikes, chain of custody and related protocols are available from ENERCON (personal communication Craig Oural, ENERCON February 24, 2016).

**Table 1-3: Water Quality Data Used for Calibration (September 2015 Laboratory Measurements)**

Well ID	Screen		CL (mg/L)	NA (mg/L)	TDS (mg/L)	Salinity (PSU)	Specific Conductance (µS/cm)
	From (m)	To (m)					
TPGW-1S	8.23	8.84	21200	11800	37200	38.909	58381
TPGW-1M	14.63	15.24	26700	14500	39600	48.97	71423
TPGW-1D	24.38	25.6	27000	14800	48200	50.08	72806
TPGW-4S	6.86	7.47	487	244	1150	1.12	2195
TPGW-4M	11.58	13.1	12900	7530	24500	25.8	40457
TPGW-4D	18.89	20.12	15500	8250	26600	27.52	42850
TPGW-5S	7.32	8.53	151	74.4	526	0.49	999
TPGW-5M	13.72	15.24	10700	5870	18000	19.7	31646
TPGW-5D	19.05	20.57	11800	6700	21100	22.71	35991
TPGW-7S	6.71	7.92	36.7	21.1	298	0.28	572
TPGW-7M	14.63	15.84	37.799	21.2	314	0.28	584
TPGW-7D	24.38	25.6	2130	876	5100	3.75	6840
TPGW-8S	5.18	6.4	31.8	17.1	216	0.21	444
TPGW-8M	10.67	11.28	31.8	17.6	360	0.31	643
TPGW-8D	15.09	16.31	43	25.2	382	0.34	705
TPGW-12S	6.71	7.31	16300	9480	29200	30.93	47659
TPGW-12M	17.07	18.29	23000	12800	41200	41.99	62472
TPGW-12D	27.43	28.65	23700	14100	41500	44.4	65603